Coordination control of autonomous robotic multi-agent systems under constraints

Esteban Restrepo

université PARIS-SACLAY

Coordination Control of Autonomous Robotic Multi-agent Systems Under Constraints

Commande en coordination de systèmes multi-agents robotiques autonomes sous contraintes

Thèse de doctorat de l'université Paris-Saclay

École doctorale n° 580, Sciences et Technologies de l'Information et de la Communication (STIC)
Spécialité de doctorat : Automatique
Graduate School : Informatique et science du numérique
Référent : Faculté des sciences d'Orsay

Thèse préparée dans le **Laboratoire des signaux et systèmes** (Université Paris-Saclay, CNRS, CentraleSupélec), sous la direction d'**Antonio LORÍA**, Directeur de recherche, la co-direction de **Julien MARZAT**, Ingénieur de recherche (HDR), et le co-encadrement de **Ioannis SARRAS**, Ingénieur de recherche.

Thèse soutenue à Paris-Saclay, le 30 Novembre 2021, par

Esteban RESTREPO

Composition du jury

Dimos V. DIMAROGONAS Professeur, KTH Royal Institute of Technology	Président & Rapporteur
Paolo ROBUFFO GIORDANO Directeur de recherche, CNRS/IRISA et INRIA Bretagne Atlantique	Rapporteur & Examinateur
Magnus EGERSTEDT Professeur, UCI Samueli School of Engineering	Examinateur
Sandra HIRCHE Professeure, Technical University of Munich	Examinatrice
Antonio LORÍA Directeur de recherche, CNRS/L2S	Directeur de thèse

THESE DE DOCTORAT

NNT : 2021UPASG093

ACKNOWLEDGMENTS

The most critical factor leading to the success of my Ph.D. are the people that supported me during the last few years. Let me thank them all, by adopting the appropriate language.

First and foremost I would like to thank my supervisors. I'm grateful to Julien for his readiness and for always being there to help me when I had to "play" with the robots. I would like to address a special thanks to Ioannis for all his effort and his daily follow-up, for his enormous enthusiasm concerning all my results, no matter how small, and for always pushing me to do what was best for me. And an equally special thanks to Antonio for his kindness, his good humor and above all for his high standards and his constructive criticism.

I would like to express my appreciation to Profs. Dimarogonas and Robuffo-Giordano for their constructive reviews that helped me improve this manuscript. Thanks also to Profs. Egerstedt and Hirche for devoting their time and willingness to being part of the jury for my defense. I'm also thankful to Kristin Y. Pettersen and Josef Matouš for their warm welcome in Trondheim and for the great collaboration that followed.

Je remercie tous les doctorants et stagiaires à l'ONERA, sans qui ces trois années de thèse auraient été sans doute beaucoup moins agréables. Commençant par les "anciens" Vincent, Iréna, Nathan (Satan ?), Sergio (el chimboso), Camille S. (j'attends le "R" !), ensuite Julius, Antonello, Etienne, Hannae, Clara, Mathieu et Paul (le duo Welsch), Baptiste E., Jorge, et finalement les nouveaux Romain, Thomas et les 4 fantastiques. Un grand merci à Thomas C. pour son "fact checking" et pour toute son aide. Merci également à Emilien et tous ses "stagiaires" pour les séances de musique absolument magiques

En particulier je tiens à remercier l'Opération Apocalypse qui fut un soutien essentiel lors des confinements. Qu'il s'agisse des "nombreuses" crémaillères, des soirées films, du séjour à Chamonix ou des histoires gênantes, chacun de ces moments restera pour toujours dans ma mémoire. Ainsi je tiens à dire un grand merci en particulier à Alī pour les débats sur les fruits et surtout merci de m'avoir attendu à Massy-Pal lors de cette célèbre soirée. Merci à l'Amiral pour sa connaissance infinie des memes et pour ses rage quit. Merci à Enzo pour ses histoires gênantes et pour toutes les blagues beauf. Merci très particulièrement à ma "vraie-fausse" amie Camille de m'avoir montré les meilleures musiques de l'univers mais surtout d'avoir partagé avec moi tous les bons moments (soirées bar, films, voyages) ainsi que les moins bons (rédaction, soutenances); you are like cinnamon !

Gracias igualmente al grupo de colombianos y especialmente a Daniela y Daniel (con Alicante obviamente), Jean y Carolina, por su compañía en los buenos y malos momentos, por su apoyo constante y por escucharme y aconsejarme cuando lo necesité.

Finalmente, agradezco infinitamente a mi familia, mis padres Gloria y Álvaro y mi hermana Aleja porque, sin duda, sin ustedes nunca habría llegado hasta aquí. Gracias por su ejemplo y educación, por todo su apoyo incondicional (sobre todo en la distancia) y por simpre haberme permitido seguir mis sueños. ¡Gracias por todo!

PREAMBLE

Multi-agent systems are systems composed of multiple plants interacting among themselves, typically, over a communication network. Essentially, in a multi-agent setting, an interconnected agent receives information from a *neighbor*, *e.g.*, the state of the latter, so that the receiving system may compare the neighbor's information against its own and take action accordingly. Systems interacting in such manner are referred to as *cooperative*, since they modify their behavior in function of that of their neighboring agents, in order to achieve a common objective.

Multi-agent cooperative systems offer a great deal of advantages with respect to single-agent systems in terms of versatility, reduced computational loads, robustness to failure, *etc.* Moreover, from a *robotics* perspective, with the significant advances in computing capabilities and the miniaturization of processing units and sensors, networks of autonomous robotic systems have become increasingly pervasive. However, while they bring novel engineering-based solutions to actual socio-economical problems, multi-agent systems are extremely complex to design, to analyze, and, therefore, to make them achieve autonomously and reliably their common mission. Indeed, their complexity imposes the intervention of specialists from a number of disciplines, ranging from computer science, electrical engineering, telecommunications, signal processing, *etc.* In this thesis we address the coordination of multi-agent systems from the perspective of *automatic control*.

From a control perspective, multi-agent systems are commonly modeled as a set of ordinary differential equations, each of which represents the dynamics of a single agent (or system). Each individual model is endowed with a so-called *control input*, which is represented by a function of the actual system's states and those of its neighbors. The network interconnections, in turn, are modeled using a *graph* representation. Graph theory, which essentially relies on tools of linear algebra to manipulate and analyze networks of systems, is particularly useful to address different problems of control of multi-agent systems modeled by linear differential equations. Yet, in many meaningful situations, where the interconnections between the agents are *nonlinear*, the graph-theory and linear-algebra tools may prove insufficient for the analysis of the multi-agent system.

One of the main theoretical contributions of this thesis is to provide a formal analysis of stability and robustness for networks of systems interacting through nonlinear interconnections. For instance, in the context of cooperative autonomous vehicles evolving in physically-constrained environments, the physical restrictions on the system such as collisions to avoid, or network interconnections that are reliable within limited ranges, are modeled via nonlinear interconnections between the agents.

We address and solve several concrete problems of *control* of multi-agent systems under multiple *constraints*. Indeed, in realistic settings, multi-agent systems operate under multiple restrictions that stymie the successful undertaking of the cooperative task. First, the access

to the information of the system is limited. By means of the available communication or measurement devices, each agent can only directly interact with a reduced portion of its neighbors, generally determined by an interaction topology. In turn, such measurement and communication devices, often have limited capabilities *e.g.*, limited bandwidth, limited range or quantization. The latter restrict further the inter-agent exchanges. Other relevant physical limitations are those imposed by the actuators, such as input saturation or minimum activation values, or those resulting from the interaction with the environment, such as potential collisions and bounded workspaces. In addition, physical systems are constantly subject to disturbances in the form of, *e.g.*, external inputs, modeling uncertainties or delays.

From an automatic-control perspective, most of the interactions and coordination tasks of multi-agent systems may be addressed as a problem of *consensus*. Roughly speaking, this problem consists in the convergence of the state variables of all agents to a common value. In the case of autonomous vehicles, this translates into all the agents converging to the same position and, if pertinent, acquiring a common orientation.

The conditions to achieve (or not) consensus vary considerably in function of a number of aspects, such as

(i) the nature of the individual systems' dynamics, which is *e.g.*, linear or nonlinear,
(ii) the nature of the interconnections, which may be perennial and static or may vary and may be linear or nonlinear,
(iii) whether the interconnection topologies change,
(iv) and whether the flow of information is bidirectional or not, to mention a few.

The problem of consensus has been extensively studied in the literature under a number of scenarios, academic or industrial. A review of the pertinent literature is presented in a dedicated chapter, hence here we merely emphasize that the greater effort and bulk of contributions address consensus problems for linear systems. On the other hand, many relaxations are considered in regards to the network's topologies, but considerably less works address consensus for networks of nonlinear systems and even less, with nonlinear interconnections.

We focus on problems of consensus in complex scenarios where the interconnection networks are nonlinear, as such naturally arise due to the incorporation of constraints. In addition, we consider networks both with bidirectional and unidirectional flow of information, that is, modeled by undirected and directed graphs. On the other hand, our work focuses on static interconnections only. Some of our contributions address problems of consensus for linear systems (primarily integrators of any order) and others solve concrete relevant problems involving nonlinear models, such as nonholonomic vehicles or thrust propelled underactuated unmanned autonomous vehicles. Thus, the control problems that we address and their formulation stem from the realm of robotics and more particularly, of control of cooperative autonomous vehicles, both terrestrial and aerial.

ORGANIZATION OF THIS THESIS

The dissertation is organized in four technical chapters, preceded by two introductory ones. The first one gives a brief account of the state of the art prior to this thesis and in the second one we recall some borrowed material that serves as foundation to our work. The contents of the four technical chapters, which contain our original contributions are as follows (the labels of the citations correspond to the list of publications presented in p. 4):

- Chapter 3: We address the problem of consensus with preserved connectivity for first- and second-order integrators. Based on the edge-based representation of the interactions between the agents, we propose a control law that achieves consensus with guaranteed connectivity maintenance. This problem has been solved earlier in the literature with similar controllers. Our contributions, however, consist in providing, for the first time in the literature, strict Lyapunov functions for the consensus-with-connectivity-maintenance problem as well as robustness properties in terms of input-to-state stability.

  These results were originally presented in the following publications: [1], [2], [5]

- Chapter 4: In this chapter we address the problem of full-consensus (in position and orientation) for nonholonomic vehicles. Our contributions consist in presenting novel consensus controllers, based on a polar-coordinates-based model, that are smooth and time-invariant and use only relative variables, making it more suited to practical applications. Then, we extend the latter and solve the full-consensus problem with connectivity maintenance in the case of limited range and limited field-of-view constraints, for which we design a smooth and time-invariant controller based only on relative measurements. In each case, we provide illustrative simulation and experimental results.

  The results presented in this chapter were the object of the following publications: [3], [4], [6]

- Chapter 5: In this chapter we propose a control methodology in order to solve the problem of consensus under inter-agent constraints, mainly connectivity maintenance and collision avoidance, and disturbances for high-order systems in normal form. To this end we build upon the results of Chapter 2. We establish strong stability results: asymptotic convergence of the multi-agent system to the consensus manifold and robustness with respect to bounded disturbances in the sense of practical-input-to-state stability.

  These works correspond to the publication [ii].

- Chapter 6: Finally, in this chapter we solve the rendezvous problem under inter-agent constraints for a group of multiple underactuated UAVs based on the methodology presented in Chapter 5. In a similar way, our contribution is to provide a control law, based on an input transformation and on the controllers designed in Chapter 5, that solve the problem of rendezvous in formation with connectivity maintenance and collision avoidance for multiple thrust-propelled UAVs. Moreover, we establish

asymptotic convergence to the consensus manifold and robustness with respect to bounded disturbances in the sense of practical-input-to-state stability. We provide simulation and experimental results that illustrate the performance of the proposed control algorithms.

The results were presented in the following publications: [ii], [iii]

Some technical appendices are also provided, for ease of reference.
For a detailed Table of contents see p. 11.

PUBLICATIONS

The following is an exhaustive list of publications written during the past three years, that are either published, accepted for publication, or still under review. The material of the publications [i], [7], and [iv] is not included in this thesis but these references are listed since they were produced during the three-year period of the PhD.

- The publication [i] is a collaboration with E. Nuño, A. Loría and E. Panteley, where an output-feedback control based on a persistency of excitation property was proposed to solve the full-consensus problem without velocity measurement for multiple nonholonomic vehicles.
- In [7], with I. Sarras, A. Loría, and J. Marzat, a controller was proposed and validated experimentally for the safe navigation of nonholonomic vehicles in a 3D environment in the presence of dynamic obstacles.
- In the collaboration [iv] with J. Matouš and K. Y. Pettersen, a control strategy was proposed to solve the tracking-in-formation problem of multiple Autonomous Marine Vehicles under proximity and collision-avoidance constraints.

Articles under review

[i] E. Nuño, A. Loría, E. Panteley, and E. Restrepo, "Rendezvous of nonholonomic robots via output-feedback control under time-varying delays," *IEEE Transactions on Control Systems Technology*, 2021, Submitted as a brief paper in November 2021.

[ii] E. Restrepo, A. Loría, I. Sarras, and J. Marzat, "Robust consensus of high-order systems under output constraints: Application to rendezvous of underactuated UAVs," *IEEE Transactions on Automatic Control*, 2021, Submitted as a regular paper in April 2021.

[iii] E. Restrepo, A. Loría, I. Sarras, and J. Marzat, "Robust rendezvous control of UAVs with collision avoidance and connectivity maintenance," *2022 American Control Conference (ACC)*, 2022, Submitted for presentation.

[iv] E. Restrepo, J. Matouš, and K. Y. Pettersen, "Tracking-in-formation of multiple autonomous marine vehicles under proximity and collision-avoidance constraints," *2022 European Control Conference (ECC)*, 2022, Submitted for presentation.

Journal articles

[1] E. Restrepo, A. Loría, I. Sarras, and J. Marzat, "Edge-based strict Lyapunov functions for consensus with connectivity preservation over directed graphs," *Automatica*, vol. 132, p. 109 812, 2021.

[2] E. Restrepo, A. Loría, I. Sarras, and J. Marzat, "Stability and robustness of edge-agreement-based consensus protocols for undirected proximity graphs," *International Journal of Control*, pp. 1–9, 2020.

[3] E. Restrepo, A. Loría, I. Sarras, and J. Marzat, "Leader-follower consensus of unicycles with communication range constraints via smooth time-invariant feedback," *IEEE Control Systems Letters*, vol. 5, no. 2, pp. 737–742, 2020.

Conference proceedings

[4] E. Restrepo, A. Loría, I. Sarras, and J. Marzat, "Distributed full-consensus control of multi-robot systems with range and field-of-view constraints," *In Proceedings of the IEEE International Conference on Robotics and Automation*, 2021, To appear.

[5] E. Restrepo, A. Loría, I. Sarras, and J. Marzat, "Robust consensus and connectivity-maintenance under edge-agreement-based protocols for directed spanning tree graphs," *IFAC-PapersOnLine*, vol. 53, no. 2, pp. 2988–2993, 2020, Presented at the IFAC World Congress 2020.

[6] E. Restrepo, I. Sarras, A. Loría, and J. Marzat, "Leader-follower consensus of unicycle-type vehicles via smooth time-invariant feedback," *In Proceedings of the European Control Conference*, pp. 917–922, 2020.

[7] E. Restrepo, I. Sarras, A. Loría, and J. Marzat, "3D UAV navigation with moving-obstacle avoidance using barrier Lyapunov functions," *IFAC-PapersOnLine*, vol. 52, no. 12, pp. 49–54, 2019, Presented at the 21st IFAC Symposium on Automatic Control in Aerospace.

RÉSUMÉ ÉTENDU EN FRANÇAIS

Les systèmes multi-agents sont composés de plusieurs systèmes dynamiques qui interagissent entre eux, généralement, à travers un réseau de communication. Essentiellement, dans un cadre multi-agent, un agent interconnecté reçoit des informations d'un voisin, par exemple l'état de ce dernier, de sorte à ce que le système récepteur puisse comparer les informations du voisin aux siennes et agisse en conséquence. Les systèmes interagissant de cette manière sont appelés *coopératifs*, car ils modifient leur comportement en fonction de celui de leurs agents voisins, afin d'atteindre un objectif commun.

Les systèmes multi-agents coopératifs offrent de nombreux avantages par rapport aux systèmes mono-agent en termes de polyvalence, d'une réduction des charges de calcul, de robustesse en cas de défaillance, *etc.* En outre, d'un point de vue de la robotique, avec l'accroissement de la puissance de calcul embarquée et la miniaturisation des capteurs et des unités de traitement, les réseaux de systèmes robotiques autonomes gagnent de plus en plus de terrain. Cependant, bien qu'ils apportent des nouvelles solutions à des problèmes socio-économiques réels, les systèmes multi-agent sont extrêmement complexes à concevoir, à analyser, et donc à les faire réaliser de manière autonome et fiable leur mission commune. En effet, leur complexité exige l'intervention de spécialistes en plusieurs disciplines, allant de l'informatique à la génie électrique, les télécommunications, le traitement du signal, *etc.* Dans cette thèse, nous approchons la coordination des systèmes multi-agents du point de vue de *l'automatique*.

Du point de vue de l'automatique, les systèmes multi-agents sont généralement modélisés par un ensemble d'équations différentielles dont chacune représente la dynamique d'un seul agent (ou système). Chaque modèle est doté d'une *entrée* dite de commande, représentée par une fonction de l'état du système et de celui de ses voisins. Le réseau d'interconnexions, à son tour, est modélisé à l'aide d'un *graphe*. La théorie des graphes, qui repose essentiellement sur des outils de l'algèbre linéaire pour la manipulation et l'analyse des réseaux de systèmes, est particulièrement utile pour traiter des problèmes de commande de systèmes multi-agents modélisés par des équations différentielles linéaires. Pourtant, dans des nombreuses situations les interconnexions entre les agents sont *non linéaires* et donc les outils de la théorie des graphes et de l'algèbre linéaire peuvent s'avérer insuffisants pour l'analyse du système.

L'une des principales contributions de cette thèse est de fournir une analyse formelle de la stabilité et de la robustesse des réseaux de systèmes avec des interconnexions non linéaires. Par exemple, dans le contexte des véhicules autonomes coopératifs évoluant dans des environnements contraints, les restrictions imposées sur les systèmes, telles que des interconnexions à portée limitée ou des collisions à éviter, sont modélisées par des interconnexions non linéaires entre les agents.

Nous abordons et résolvons plusieurs problèmes concrets de *commande* de systèmes multi-agents sous des *contraintes* multiples. En effet, dans des scénarios réalistes, les systèmes

multi-agents sont soumis à des multiples restrictions qui entravent l'accomplissement de la tâche coopérative. D'abord l'accès à l'information est limité. Chaque agent ne peut interagir directement qu'avec une partie réduite de ses voisins, généralement déterminée par une topologie d'interaction, au moyen des dispositifs de communication ou de mesure disponibles. Or, de tels dispositifs ont souvent des capacités limitées, par exemple une bande passante limitée, une portée limitée ou des signaux quantifiés. Ces dernières restrictions restreignent d'avantage les échanges inter-agents. D'autres limitations physiques viennent des actionneurs, telles que des saturations des entrées et de seuils d'activation, ou de l'interaction entre les agents et l'environnement, telles que des risques de collision et des espaces de travail délimités. En outre, les systèmes physiques sont constamment soumis à des perturbations sous la forme, par exemple, d'entrées externes, d'incertitudes des modèles ou de retards.

D'un point de vue de l'automatique, la plupart des interactions et des tâches de coordination des systèmes multi-agents peuvent être abordées comme un problème de *consensus*. En gros, ce problème consiste en la convergence des variables d'état de tous les agents vers une valeur commune. Dans le cas des véhicules autonomes, cela se traduit par la convergence de tous les agents vers la même position avec, le cas échéant, la même orientation.

Les conditions pour atteindre (ou non) consensus varient considérablement en fonction d'un certain nombre d'aspects, tels que

(i) la nature de la dynamique de chaque système, qui peut être, par exemple, linéaire ou non linéaire,
(ii) la nature des interconnexions, qui peut être pérenne et statique ou variable et peut être linéaire ou non linéaire,
(iii) si les topologies d'interconnexion varient dans le temps
(iv) et si la flux d'information est bidirectionnel ou non, pour n'en citer que quelques-uns.

Le problème de consensus a été largement étudié dans la littérature pour un nombre important de scénarios, académiques et industriels. Une revue de la littérature pertinente à ce problème est présentée dans un chapitre dédié, c'est pourquoi nous nous limitions ici a souligner que la plupart des contributions se concentrent sur des problèmes de consensus pour des systèmes linéaires. Par ailleurs, des nombreuses simplifications sont faites en ce qui concerne les topologies du réseau, mais beaucoup moins de travaux abordent le problèmes de consensus pour des réseaux de systèmes non linéaires et encore moins, avec des interconnexions non linéaires.

Nous nous concentrons sur les problèmes de consensus dans des scénarios complexes où les interconnexion entre les agents sont non linéaires, ce qui survient naturellement en présence de contraintes. De surcroît, nous considérons que le flux de l'information au sein du réseau peut être unidirectionnel ou bidirectionnel, c'est-à-dire, il peut être modélisé par des graphes orientés et non orientés. En revanche, nos travaux portent uniquement sur des interconnexions statiques. Une partie des contributions consiste à résoudre des problèmes de consensus pour des systèmes linéaires (principalement des intégrateurs de tout ordre) et une autre partie pour des modèles non-linéaires, tels que des véhicules non-holonomes ou des drones autonomes sous-actionnés, en considérant des interconnexions non-linéaires. Ainsi, les problèmes de commande que nous abordons et leur formulation relèvent du domaine de

la robotique et plus particulièrement de la commande des véhicules autonomes coopératifs terrestres et aériens.

ORGANISATION DE CETTE THÈSE

Ce mémoire est organisé en quatre chapitres techniques, précédés de deux chapitres introductifs. Le premier rend compte brièvement de l'état de l'art avant cette thèse et dans le second, nous rappelons quelques concepts emprunté qui servent de base à notre travail. Les contenus des quatre chapitres techniques, qui contiennent les contributions originales, sont présentés ci-dessous (les libellés des citations correspondent à la liste des publications présentée en page 4):

- Chapitre 3 : Nous traitons le problème de consensus avec maintien de la connectivité pour des intégrateurs de premier et second ordre. Sur la base d'une représentation des interactions entre les agents basée sur les arêtes, nous proposons une loi de commande pour atteindre le consensus et garantir le maintien de la connectivité. Ce problème a déjà été résolu dans la littérature avec des lois de commande similaires. Cependant, nos contributions consistent à fournir, pour la première fois dans la littérature, des fonctions de Lyapunov strictes pour le problème de consensus avec maintien de la connectivité ainsi qu'à établir des propriétés de robustesse en termes de stabilité entrée-état.

  Ces résultats ont été initialement présentés dans les publications suivantes : [1], [2], [5]

- Chapitre 4 : Dans ce chapitre, nous traitons le problème de consensus complet (en position et en orientation) pour des véhicules non holonomes. Les contributions consistent à concevoir des nouvelles lois de commande, basées sur un modèle en coordonnées polaires, qui sont lisses et invariantes dans le temps et qui n'utilisent que des variables relatives, ce qui les rend plus adaptées aux applications pratiques. Ensuite, ces résultats sont étendus afin de résoudre le problème de consensus complet avec maintien de la connectivité pour des véhicules avec des portées de communication limitées et de champs de vue réduits, à l'aide de lois de commande lisses et invariantes dans le temps basées sur des mesures relatives. Dans chaque cas, nous illustrons les résultats à l'aide de simulations et d'essais expérimentaux.

  Les résultats présentés dans ce chapitre ont fait l'objet des publications suivantes : [3], [4], [6]

- Chapitre 5 : Dans ce chapitre nous proposons une méthodologie de commande qui permet de résoudre le problème de consensus pour des systèmes d'ordre supérieur en forme normale sous des contraintes inter-agents, particulièrement du maintien de la connectivité et de l'évitement des collisions, et sous l'action des perturbations. A cette fin, nous nous appuyons sur les résultats du Chapitre 2. Nous établissons des résultats de stabilité forts : convergence asymptotique du système multi-agents vers la variété de consensus et robustesse vis-à-vis des perturbations bornées au sens pratique de la stabilité entrée-état.

Ces travaux correspondent à la publication [ii].

- Chapitre 6 : Enfin, dans ce chapitre, nous résolvons le problème de rendez-vous sous contraintes inter-agents pour un groupe de plusieurs drones sous-actionnés sur la base de la méthodologie présentée dans le Chapitre 5. La contribution consiste à concevoir une loi de commande, basée sur une transformation des entrées du systèmes et sur les lois de commande conçues dans le Chapitre 5, afin de résoudre le problème de rendez-vous en formation avec maintien de la connectivité et évitement des collisions pour un groupe de drones sous-actionnés. De plus, nous établissons une convergence asymptotique vers la variété de consensus et de la robustesse par rapport aux perturbations bornées au sens pratique de la stabilité entrée-état. Les performances des algorithmes de commande sont illustrées par des simulations numériques et des résultats expérimentaux.

  Ces résultats ont été présentés dans les publications suivantes : [ii], [iii]

Des annexes techniques sont également fournies pour faciliter la consultation.
Pour une table des matières détaillée, voir la page 11.

CONTENTS

LIST OF FIGURES

LIST OF TABLES

NOTATIONS

$\mathbb{R}$	Set of real numbers.
$\mathbb{R}_{\geq 0}$	Set of positive real numbers.
$\mathbb{R}^n$	Linear space of real vectors of dimension n.
$\mathbb{R}^{n\times m}$	Set of matrices of size $n \times m$.
$\mathrm{E}(n)$	Euclidean group of dimension n.
$\mathrm{SO}(n)$	Special orthogonal group in $\mathbb{R}^n$.
x_i	The i-th element of vector x.
I_n	The identity matrix of size $n \times n$.
$\mathbf{1}$	Column vector of ones.
$0_{n\times m}$	Matrix of zeros of dimension $n \times m$.
$\mathrm{diag}\{\cdot\}$	Diagonal matrix of the input arguments.
$\mathrm{blockdiag}\{\cdot\}$	Block diagonal matrix of the input matrix arguments.
$\lvert x\rvert$	For a vector x denote, its Euclidean norm; for a scalar x denote, its absolute value.
$\lvert x\rvert_{\mathcal{A}}$	For a set $\mathcal{A} \subset \mathbb{R}^n$ denote, $\inf_{y\in\mathcal{A}} \lvert x - y\rvert$.
$\lvert\lvert x\rvert\rvert_\infty$	For a function $x : \mathbb{R}_{\geq 0} \to \mathbb{R}^n$, it denotes, $\operatorname{ess\,sup}_{t\geq 0}\lvert x(t)\rvert$.
$A^\top$	The transpose of matrix A.
$A^\dagger$	The pseudo-inverse of matrix A.
$[A]_{ij}$	The element of matrix A in the ij-th position.
$\lambda_{min}(A)$	The minimal eigenvalue of matrix A.
$\lambda_{max}(A)$	The maximal eigenvalue of matrix A.
$\otimes$	The Kronecker product.
$\lvert\mathcal{A}\rvert$	The cardinality of set $\mathcal{A}$.
$\partial\mathcal{A}$	The boundary of set $\mathcal{A}$.
$\mathcal{K}$	Class of positive continuous and strictly increasing functions $f : \mathbb{R}_{\geq 0} \to \mathbb{R}_{\geq 0}$, with $f(0) = 0$.
$\mathcal{K}_\infty$	Class of $f \in \mathcal{K}$, with $f(s) \to \infty$ as $s \to \infty$.
$\mathcal{L}$	Class of positive continuous and strictly decreasing functions $f : \mathbb{R}_{\geq 0} \to \mathbb{R}_{\geq 0}$, with $f(s) \to 0$ as $s \to \infty$.
$\mathcal{KL}$	Class of positive and continuous functions $f : \mathbb{R}_{\geq 0} \times \mathbb{R}_{\geq 0} \to \mathbb{R}_{\geq 0}$, with $f(\cdot, y) \in \mathcal{K}_\infty$ and $f(x, \cdot) \in \mathcal{L}$.

1

GENERAL OVERVIEW AND CONTEXT

1.1 MOTIVATION

The recent advances in embedded computing and sensing as well as in telecommunication technology with the popularization of the Internet of Things (IoT) are enabling the application of a wide range of systems where large numbers of autonomous agents interact among themselves, typically over a communication network, and work cooperatively towards a common objective. Such multi-agent system is composed of autonomous interconnected agents that, based on the information received or obtained from their local neighbors, *e.g.*, the neighbors' states, modify their behavior in order to achieve a global objective. Compared to single agent systems, multi-agent systems offer a great deal of advantages in terms of versatility, reduced computational loads, robustness to failure, *etc.* Such advantages have encouraged the use of multi-agent systems in numerous relevant engineering applications such as power systems, social networks, or multi-robot systems [1]. In this thesis we focus on the cooperative coordination of multi-agent robotic systems from the perspective of automatic control. Therefore, the objective consists in designing cooperative control strategies for such systems.

In general, cooperative coordination control of multiple vehicle systems consists in designing the control input for each agent in order to accomplish a particular common task. While they enable to find novel solutions to actual engineering problems, cooperative control strategies are extremely complex to design and to analyze. Arguably, the biggest challenge regarding the cooperative control of multi-robot systems is to achieve the desired global behavior of the system by means of local interaction rules. As a matter of fact, in many multi-vehicle applications, an interconnected agent has access only to local information from a limited set of neighbors, as determined by an interaction network modeled using a graph representation. Therefore, centralized approaches, in which each vehicle receives global information consisting in its reference behavior, are generally ruled out for the cooperative coordination setting. Therefore, distributed approaches that exploit only the local knowledge available to each agent have to be implemented.

Distributed cooperative control of multiple vehicle systems has known a rapid development in recent years. However, there are still some major technical challenges that stymie the use of such systems in realistic applications. Such relevant challenges, which have been accurately

listed in [2], are presented hereafter loosely adapted to the problem of cooperative control of multiple robotic vehicles.

- *Nonlinear agent dynamics.* Robotic vehicles, such as ground, aerial and underwater vehicles, are usually modeled via nonlinear dynamic equations. Most existing cooperative control methodologies, based on graph theory, are focused on single integrator or simple linear dynamics, which are not adequate for realistic applications where the performance of the designed control system can deviate greatly from the performance suggested by these simpler system models.
- *Nonlinear agent interconnections.* In multiple scenarios the interconnections betwe of dimension *n*en the agents are nonlinear. For example, in order to avoid collisions two agents may need to apply a very large control input (approaching infinity) as they get close to each other. Similarly, when the distance between them is greater than a threshold, the capability of exchanging information with one another may either fail or become very limited. Most existing cooperative control frameworks address linear agent interactions, while in many real-world multi-agent scenarios such interactions have to be modeled via nonlinear functions.
- *Robustness.* Due to disturbances and uncertainties in agent dynamics, communication links, and operating environments, robustness has to be considered for a successful system design. For example, aerial robotic vehicles are constantly subject to aerodynamics disturbances. Such uncertainties and disturbances can lead to unexpected or even unstable behaviors. Robustness consideration has been discussed in the existing literature for the basic cooperative control problems, but general robust cooperative control for complex systems with nonlinear interconnections has not been addressed.
- *Diversity of real-world problems and application domains.* Numerous problems of cooperative control of autonomous vehicle systems have been successfully solved via a variety of analysis methods and synthesis tools. Nonetheless, networked systems are becoming increasingly ubiquitous and depending on the domain of applications, the control objectives and constraints are inherently different. Hence, beyond the domain of autonomous vehicles, new relevant problems and application domains pose new challenges for nonlinear cooperative control design.

From an automatic-control perspective most of the interactions and coordination tasks of multi-agent systems are based on the problem of *consensus*. Roughly speaking, this problem consists in the state variables of all agents converging to a common value. In the case of autonomous vehicles, this translates into all the agents converging to the same state, that is, reaching the same position, acquiring the same velocity or, if pertinent, achieving a common orientation. The problem of consensus has been extensively studied in the literature under a number of scenarios, motivated by academic or industrial problems. Yet, several open questions on consensus-based control are yet to be answered, specifically when (simultaneously) considering the meaningful realistic challenges evoked above. Indeed, the greater effort and bulk of contributions address consensus problems for linear systems, but considerably less works address consensus considering the technical difficulties mentioned above, that is nonlinear systems with nonlinear interconnections.

In light of the above, we address and solve several concrete problems of *control* of multi-agent systems under multiple *constraints*. In realistic settings, multi-agent systems operate under multiple restrictions that stymie the successful undertaking of the cooperative task and render the interconnections between the agents *nonlinear*. On one hand, the access to the information of the system is limited. By means of the available communication or measurement devices, each agent can only directly interact with a reduced portion of its neighbors, generally determined by an interaction topology. Moreover, in sensor-based approaches, the use of embedded measurement devices naturally leads to *directed* topologies since information exchange among the agents is not possible. In turn, such devices, often have limited capabilities *e.g.*, limited bandwidth, limited range or quantization. The latter restrict further the inter-agent exchanges. Other relevant physical limitations are those imposed by the actuators, such as input saturation or minimum activation values, or those resulting from the interaction with the environment, such as potential collisions and bounded workspaces. On the other hand, physical systems are constantly subject to disturbances in the form of, *e.g.*, external inputs and modeling uncertainties. Therefore, with the purpose of rendering our analytical contributions potentially useful, *e.g.*, in robotics applications, our work focuses on control of multi-agent systems under the constraints mentioned above.

Some preliminary, but original, contributions in Chapter 3 apply to relatively simple systems, such as first- and second-order integrators, but they also serve as a building block for the consensus-based control design and analysis of more complex systems. We consider generalizations in two directions. The first consists in the control of robotic systems modeled by nonlinear dynamic equations; in particular, of nonholonomic mobile terrestrial robots in Chapter 4 and underactuated unmanned aerial vehicles (UAV) in Chapter 6. The second, presented in Chapter 5, consists in exploring the consensus problem, under various meaningful constraints, for systems in normal form (chains of integrators) of arbitrary relative degree. Actually, it is this contribution that allows us to solve a pertinent problem of formation control under connectivity and collision-avoidance constraints, for underactuated aerial vehicles in Chapter 6.

In the remainder of this chapter we present a non-exhaustive review of some pertinent works in the literature concerning the different problems of consensus-based control of multi-agent systems addressed in this thesis.

1.2 ON CONSENSUS CONTROL

Consensus control constitutes the basis of distributed cooperative interactions for multi-agent systems [1]–[4]. Indeed, this consensus objective is fundamental to achieve complex formation maneuvering tasks that are at the core of cooperative coordination applications [5] for multi-agent systems.

The problem of consensus has been extensively studied in the literature for a variety of dynamical systems, such as linear systems [4], [6], [7], relative-degree-one nonholonomic vehicles [8], [9], or second-order Euler-Lagrange systems [10], [11], to mention a few. However, we emphasize, again, that most of the existing contributions address this problem for linear

systems with linear interconnections. Considerably less works address consensus for networks of nonlinear systems with nonlinear interconnections.

In the study of large-scale interconnected dynamical systems, it is typical to turn to graph theory for a mathematical representation of the neighbor-to-neighbor interactions. Such graph-based abstraction plays a fundamental role in the design and analysis of consensus control algorithms. Indeed, it has been well established in the literature that the convergence of the consensus protocols depends greatly on the nature of the network topology describing the information exchange between the agents [1], [3]. In consequence, the analysis of consensus protocols is based on the algebraic properties of the graph encoding the interaction topology.

A common approach for the analysis of multi-agent systems under consensus-based controllers is to consider the dynamic equations of each agent as the state of the system. In terms of the graph representing the network topology, this translates into studying the evolution of the nodes. In this setting, the control design and analysis of the multi-agent system with linear interconnections heavily rely on linear algebra and other tools tailored for, and limited to, linear time-invariant systems [3], [6], [12]–[15]. Moreover, when analyzing the systems from a stability oriented perspective using Lyapunov's method, the proofs of stability are usually performed via non strict Lyapunov functions[1] and the invariance principle [16]. Hence, only convergence to consensus can be established. Furthermore, in realistic settings, the agents' models and the interconnections are modeled via nonlinear equations. In these situations, when analyzing the system in the nodes' perspective, the common tools from linear algebra used in the literature fail at ensuring strong stability and robustness properties, such as *e.g.*, uniform asymptotic stability or input-to-state statbility, which often rely on the design of strict Lyapunov functions [17], [18]. Yet such stronger closed-loop properties are needed for successful deployment in practical applications.

Besides the common node-based approach, some alternative representations of the networked systems have been proposed in the literature to address the consensus problem. Moreover, some works provide strict Lyapunov functions. In [19], so-called star and line transformations are proposed in order to analyze the closed-loop system, and asymptotic stability of the agreement set is established by means of a strict Lyapunov function for first- and second-order systems over static and time-varying directed graphs containing a spanning tree. These transformations, however, do not represent the real interconnections between the agents as given by the graph topology. The approach presented in [20] uses synchronization errors and emergent dynamics in order to establish asymptotic stability of the synchronization manifold. A strict Lyapunov function is provided based on the eigenvectors of the Laplacian matrix of a directed graph containing a spanning tree. However, the transformation into the emergent dynamics requires the use of similar linear algebra tools as in the case of the node-based analyses, and may prove limiting in certain scenarios.

Another alternative representation of the consensus problem for a multi-agent system is the *edge-based* perspective introduced in [21] and further developed in [7], [22]–[26] and some of the references therein. In this framework, the consensus problem is analyzed using the dynamics of the relative state between neighboring agents, that is, the edges of the graph, as

1 See Appendix A.1 for a definition.

opposed to analyzing the evolution of the nodes. This representation has the advantage of using the real interconnections between the agents as the state of the multi-agent system, which constitutes a more natural setting for the consideration of inter-agent constraints. Moreover, in this framework the consensus problem is recast as one of stabilization of the origin, making it well-suited for Lyapunov-based control and Lyapunov's direct method of analysis. Therefore, this thesis strongly relies on the edge-based framework. Remarkably, using this framework, the analysis of consensus is reduced to that of a minimal configuration. The latter allows to establish asymptotic stability of the consensus manifold via strict Lyapunov functions [1], [27]. This property cannot be underestimated; it is stronger than mere convergence, which is more commonly established in the literature —see, e.g., [13]–[15], [28], [29]. Indeed, the property of asymptotic stability through strict Lyapunov functions implies other strong results in terms of convergence rates and robustness, which cannot be ascertained if it is only known that the consensus errors converge.

1.3 ON CONNECTIVITY MAINTENANCE

A necessary and sufficient condition to achieve consensus in a multi-agent system, and which is recurrent in the literature, is that the graph topology representing the agents' interconnections must be connected [1], [3]. However, In many realistic settings, the interconnections between the agents depend on their relative positions and on other environmental factors, and are therefore nonlinear and dynamically changing. For instance, in the cases where the measurement or communication capabilities of each agent are limited in range (as is the case for autonomous vehicles), the link between any two interconnected agents may be lost if they drift too far away from each other. Therefore, although necessary, the connectivity property of the graph topology cannot be assumed but has to be ensured by the control law.

Several works in the literature address the problem of consensus with connectivity preservation. This problem is typically addressed using gradient-type consensus algorithms, relying on so-called barrier functions. Loosely speaking, the control may be assimilated to a force field that "explodes" near the connectivity limits. That is, the control input, as a function of the state, grows unboundedly as the vehicle approaches a specified region. This technique is also reminiscent of potential/navigation functions used in robot control [30], [31]. For undirected graphs several works in the literature address the problem of connectivity maintenance. In [32], barrier functions are used to guarantee that all agents remain inside a given region, but considering an all-to-all communication topology. In [33] barrier functions, as well as properties of the graph Laplacian matrix, are used to show consensus and preservation of connectivity. A general framework for connectivity maintenance in the nodes' perspective is proposed in [34] for both static and dynamic graphs. In [35], [36] a potential function in terms of the algebraic connectivity of the graph is used to guarantee global connectivity maintenance. However, a distributed estimation algorithm has to be implemented so that all the agents have access to the algebraic connectivity, which is a global parameter. Using a nonlinear transformation of the consensus errors, in [37] connectivity is guaranteed via a nonlinear interconnection protocol. Similar barrier-function-based protocols are proposed

in [38]–[40], for second-order systems. A projection-based consensus protocol is designed in [41] that achieves convergence to the consensus manifold while guaranteeing that each agent remains inside a constraint set.

For systems interacting over directed graphs, however, there are far fewer works. In [42], consensus is achieved while guaranteeing that each agent stays inside a given set; however the results only apply to first-order integrators and the communication graph is required to be strongly connected. In [36], [43], [44] connectivity is achieved, but under somewhat conservative assumptions; it is assumed that the directed graph is strongly-connected and, moreover, the controllers proposed therein also rely on the estimation of the algebraic connectivity.

In all the works mentioned above, the consensus problem is studied relying on the node-based representation. Therefore, in general, only convergence to the agreement manifold is established by means of non-strict Lyapunov functions. As evoked above, however, the alternative edge-based representation, in which the consensus problem is recast as a problem of attractivity of the origin, has been used in the literature to establish some stronger stability and robustness properties via strict Lyapunov functions.

Works on edge-based consensus include diverse scenarios and contributions: in [45] a consensus controller in the presence of disturbances and uncertainties is designed –see also [13] for an optimal controller design; in [46] finite-time agreement is achieved for second order systems using edge-based notions and in [47] convergence rates are given for edge-Laplacian-based consensus of first-order multi-agent systems with time-varying interconnections. Notably, in the latter a strict Lyapunov function is constructed, which leads to estimating the convergence rate. In [7] the edge agreement protocol is extended to second-order systems over directed graphs and robustness with respect to edge-weight disturbances is established. A strict Lyapunov function is provided in [24] for consensus over directed graphs. However, the control is designed based on the small-gain theorem, which greatly restricts the control and hence prevents the direct extension of this methodology for connectivity maintenance. In [48] consensus is established for the elementary directed-cycle topology, but under the assumption that it switches and the interconnections are time-varying.

State-dependent constrained consensus, however, has received limited attention so far using the edges' framework. Indeed, none of the edge-based works mentioned above address the connectivity-maintenance problem. A notable exception is [49] where connectivity maintenance is guaranteed under state saturation constraints using an edge-based approach, albeit only for first-order integrators interacting over undirected graphs.

1.4 ON NONHOLONOMIC VEHICLES

For the cooperative coordination of multi-agent systems of nonholonomic vehicles, two main consensus problems are addressed in the literature: position consensus [50], [51] and full consensus [52], [53]. In the first case, all agents converge to the same position with an

arbitrary or predetermined orientation. In the second case, agreement on both position and orientation is sought.

For the consensus control of multiple nonholonomic vehicles, most of the works in the literature use a Cartesian-coordinates-based model. However, for these kinds of nonlinear systems the origin is not stabilizable via smooth invariant feedback. The latter is a well-known result that stems from the seminal paper [54], where necessary conditions for asymptotic stabilization of nonlinear systems via smooth time-invariant feedback are laid. Similar conditions for set-point consensus of multi-agent nonholonomic systems are given in [55]. Therefore, considerable attention has been paid to the problem of designing time-varying or non-smooth controllers for set-point stabilization of nonholonomic systems. For instance, the controllers proposed in [51], [56] are time-varying and they guarantee position consensus. Time-varying feedback is also used in [50], [52], [53], but for full-consensus-based formation control. In [8], on the other hand, a time-invariant non-smooth feedback controller is reported for position-consensus over undirected graphs.

These protocols are normally implemented using absolute position and orientation values. In most practical scenarios, however, protocols using absolute measurements may not be implementable since only the relative measurements from embedded sensing devices are available to the vehicles. Moreover, time-varying and non-smooth controllers add a degree of complexity to the control design problem and to the stability analysis. These drawbacks may be overcome via an alternative representation based on a polar-coordinates transformation [57], [58]. In this representation, the system is singular precisely at the origin, implying that smooth time-invariant controllers may be designed without contradicting [54], [55]. Based on the polar-coordinates model, a smooth time-invariant controller is presented in [59] for consensus of nonholonomic agents over a directed spanning tree, albeit for a linearized system, hence, achieving only position consensus. In [60] a continuous time-invariant feedback for position consensus is proposed for multi-agent systems over undirected graphs. However, time delays have to be considered in order to avoid algebraic loops in the control. In [61] a smooth time-invariant controller is designed to achieve consensus, albeit only in position, for a system communicating over a directed graph containing a directed spanning tree.

Now, in these references, as in many other works, it is assumed that the communication graph is connected at all times. Hence, each agent has permanent access to its neighbors' data, either by transmission or by sensing. However, in realistic settings, as we mentioned above, the communication or embedded sensing devices often have a limited range or a limited field of view. Therefore, in such scenarios assuming that each agent has access to its neighbors' information at all times, although necessary from a theoretical viewpoint, might be conservative in practice.

Consequently, considerable attention has been focused on the study of coordination strategies of multi-agent systems subject to distance and/or field-of-view constraints. In [62]–[64] coordination protocols with field-of-view-based connectivity are considered, albeit for linear integrator models. In [65] using relative information, a navigation-function-based controller with distance-based connectivity maintenance is proposed for multi-agent systems interconnected over directed graphs; nevertheless, the controller is non-smooth and it presents

some problems inherent to the navigation-function framework such as local minima and the need to have a bounded workspace. In [66] distance constraints are considered for leader-follower topologies based on barrier functions. However, only position consensus is achieved and the controller requires the knowledge of absolute positions. In [67] distance constraints are addressed and practical stability of a position-consensus-based formation is achieved, but the estimation of global parameters is required. In [68], [69] the authors develop time-varying control laws with prescribed performance considering both distance and field-of-view constraints. Nevertheless, full consensus is not achieved and only the platooning problem, with interaction topologies consisting of single directed chains, is addressed.

1.5 ON UNDERACTUATED UNMANNED AERIAL VEHICLES

The problem of rendezvous of underactuated thrust-propelled UAVs is an underlying part of more complex maneuvering tasks in which, also, the vehicles may be required to move in formation. This is a good example of a scenario of cooperative systems in which a plethora of difficulties appear naturally. First, the systems' dynamics are clearly nonlinear and underactuated [70]. Therefore, the literature on consensus tailored for linear low-order systems [3], [36] does not apply. Second, the measurements usually come from embedded relative-measurement sensors, such as cameras, LiDAR, ultrasound, *etc.* The use of such devices naturally imposes directed network topologies [63], which add difficulty to the consensus-control design. Third, autonomous vehicles moving "freely" in the workspace are prone to undesired collisions among themselves; therefore, guaranteeing the safety of the system in the sense of inter-agent collision avoidance is a restriction that must be considered as well. A fourth difficulty stems from the use of on-board relative-measurement devices, which are reliable only if used within a limited range. This translates into guaranteeing that the UAVs do not drift too far apart from their neighbors. Finally, UAVs are constantly subject to external undesired forces and they may also be affected by modeling uncertainties, *etc.*; these constitute external disturbances at different levels in the dynamic model. Under such constraints, the objective of rendezvous for thrust-propelled UAVs coins a relevant problem in the aerospace industry motivated by the increasing interest for safety-aware fleet deployment.

From the aforementionned difficulties, tackling the nonlinear and underactuated nature of the UAVs model is particularly essential. Indeed, the UAVs have six degrees of freedom (three-dimensional displacements and three rotations), but only four dimensions can be directly actuated using the actual inputs of the vehicle. To address this difficulty, some hierarchical approaches have been reported in the literature, using the natural cascaded structure of the UAVs' dynamics [70]–[73]. Such designs have been used to solve the formation problem of swarms of UAVs interconnected through undirected and directed communication topologies —*cf.* [71], [72], [74]–[77]. Nonetheless, none of these works address the problem under inter-agent constraints.

In addition, only a handful of works in the literature consider the rendezvous problem of UAVs under a set of realistic assumptions and constraints while not at the expense of formal

analysis. A distributed controller is proposed in [78] based on prescribed-performance control that achieves formation tracking with collision avoidance for multiple UAVs. Nonetheless, the results therein apply only to undirected topologies. Based on the attitude and thrust extraction algorithm, the authors in [79] solve the formation problem for multiple UAVs subject to connectivity constraints, but only undirected topologies are considered and collision-avoidance constraints are not addressed. In [10], [11], and [31], robust formation controllers are proposed based on the prescribed-performance-control [80] and edge-agreement frameworks [1], [21], guaranteeing, also, collision avoidance and connectivity maintenance. However, in these references only fully-actuated Lagrangian systems interconnected over undirected-tree topologies are considered.

1.6 ON HIGH-ORDER SYSTEMS

As it was mentioned previously, the literature is rife with works addressing diverse consensus problems for different types of low-order systems, see *e.g.*, [4], [6]–[11]. However, low-order models may fall short at representing many meaningful and complex engineering problems in which the input-output relationship imposes a high relative degree (with respect to an output of interest) model. A good example of high-order systems is that of certain autonomous vehicles —see [1]–[3], and Chapter 6 in this thesis.

Moreover, in realistic settings, physical systems operate under multiple restrictions in the form of output or state constraints such as limited range measurements/communication. The latter limitations are at the origin of connectivity constraints, as we explained above. Besides such range constraints, the systems are subject to other physical limitations imposed by the actuators or by the environment, such as input saturation or minimal safety distances. In addition, such systems are constantly subject to disturbances such as external inputs, modeling uncertainties, delays, *etc.* Thus, for consensus control laws to be of practical use, multiple inter-agent constraints must be considered in the control design and robustness with respect to disturbances must be guaranteed.

The difficulties described above coin a realistic scenario of automatic control of multi-agent systems. Consensus under such conditions has been addressed in the literature, but to the best of our knowledge never simultaneously.

Many works in the literature address the constrained consensus problem, mainly in the nodes' perspective, for low-order systems interconnected over, both, undirected and directed topologies. Fewer works, however, address this problem for high-order systems. For instance, consensus of high-order systems has been addressed in [81]–[84], albeit without considering inter-agent constraints. In [85] a tracking consensus controller is proposed for networked systems over undirected graphs, but the constraints are considered on the synchronization error and not directly on the inter-agent relative states. This may prove conservative in some situations and fail to capture relevant inter-agent constraints as safety minimal distances. In [86] a synchronization control is designed using an adaptation of the prescribed performance framework in order to achieve consensus over directed graphs with desired bounds on the transient response. Nevertheless, as in [85], the prescribed-performance constraints are

imposed on the consensus error and not on the inter-agent relative states. A consensus control for high-order systems with constraints and interacting over strongly connected directed graphs is presented in [28]. Yet, the constraints considered therein weigh on each individual agent's states (*e.g.*, constraints on the velocity, the acceleration, *etc.*) and, similarly, do not reflect the inter-agent restrictions that stymie the cooperative coordination objectives in multi-agent systems.

2

CONSENSUS PROTOCOLS FOR MULTI-AGENT SYSTEMS

As explained earlier, the consensus objective constitutes the basis of most distributed cooperative tasks for multi-agent systems. With the purpose of exposing its limitations, in this chapter we revisit a classical consensus algorithm through simple examples, as well as its analysis using linear algebra and Lyapunov stability tools, from the perspective of the nodes composing the interaction topology. We show that physical restrictions encountered in realistic settings usually impose nonlinearities to the agents' models or to the interconnections. In these situations, when analyzing the system in the nodes' perspective, the common tools from linear algebra used in the literature fail at ensuring strong stability and robustness results. Yet such stronger results are needed for successful deployment in practical applications.

In light of the previous statement, we reformulate the consensus algorithm by recalling the alternative edge-based representation. In this alternative representation, which is not an original contribution of this thesis, the consensus problem is recast as the stabilization of the origin, rather than the stability of a set as in the node-based perspective. Furthermore, in the edges' perspective, the evolution of the system may be studied via a reduced-order representation. Both of these advantages make the edge-based representation more suited to the problem at hand. The novelty of this work resides in demonstrating how stronger stability properties can be established. The latter is a founding block for our contributions in the context of consensus under constraints presented in the subsequent chapters.

2.1 ELEMENTS OF GRAPH THEORY

In the analysis of multi-agent systems it is natural to consider that each agent has access only to a part of the information of the complete system, normally via neighbor-to-neighbor interactions. Therefore, it is typical to turn to graph theory for a representation of the interaction topology of the network. As the graph representation of multi-agent networks is fundamental for the control design and the analysis of multi-agent systems, we present here some well-known notions and notations on graph theory, mostly taken from [1], [3] and adapted for the purpose of this thesis.

A *graph* is a set-theoretic structure that describes the interaction between the elements of a given set. For a group of N *agents* the graph abstraction is used to encode the communication topology, that is, how the information is exchanged within the group.

A graph is denoted by $\mathcal{G} = (\mathcal{V}, \mathcal{E})$ where the set of nodes $\mathcal{V} = \{1, 2, \ldots, N\}$, corresponds to the labels of the agents, and the set of edges $\mathcal{E} \subseteq \mathcal{V}^2$ of cardinality M characterizes the information exchange between pairs of agents. A *subgraph* $\mathcal{H} = (\mathcal{V}_\mathcal{H}, \mathcal{E}_\mathcal{H}) \subset \mathcal{G}$ is a graph such that $\mathcal{V}_\mathcal{H} \subset \mathcal{V}$ and $\mathcal{E}_\mathcal{H} \subset \mathcal{E}$. A *spanning* subgraph is a subgraph containing all nodes $\mathcal{V}$ —see Figure 2.1 for an example.

An edge $e_k := (i, j) \in \mathcal{E}$, $k \leq M$ is an ordered pair which indicates that a connection exists "starting" at node i and "ending" at node j. In other words, the ith node provides information to the node j or, more generally the behavior of the ith node influences that of the jth node. Hence, given an agent i, we denote as $\mathcal{N}_i = \{j \leq N, j \neq i : (i, j) \in \mathcal{E}\}$ the set of neighbors of i, *i.e.*, the set of agents adjacent to agent i. Besides representing the nodes that interact with each other, the edges of a graph also represent the direction of the flow of information in the system. Indeed, if the information flow is bidirectional, that is, if the edges in a graph have the property that $(i, j) \in \mathcal{E}$ implies $(j, i) \in \mathcal{E}$, the graph is said to be *undirected* and the edge can also be viewed as an unordered pair, *i.e.*, $e_k = (i, j) = (j, i)$ —*cf.* graph on the left in Figure 2.1. Otherwise, if the information flows in a single direction, the graph is said to be *directed* —see *e.g.*, the graph on the right in Figure 2.1. For an undirected graph it is useful to define an *orientation*, consisting in the assignment of directions to its edges.

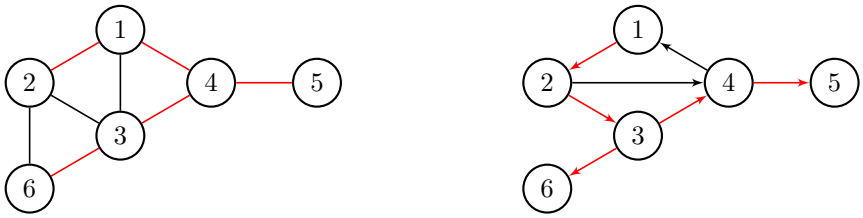

Figure 2.1: Example of a connected undirected graph (left) and a directed graph containing a spanning tree (right). The edges of the spanning tree are colored in red.

A graph is said to be *complete* if there is an undirected edge joining every pair of agents composing the system. A *directed path* is a sequence of edges in a directed graph of the form $(i_1, i_2), (i_2, i_3), \ldots, (i_{N-1}, i_N)$. An *undirected path*, or simply a path, in an undirected graph is defined analogously. The distance $d(i, j)$ between nodes $i, j \in \mathcal{V}$ is the number of edges in the shortest path from i to j.

A directed graph is said to be *strongly connected* if there is a directed path from every node to every other node. An undirected graph is said to be *connected* if there is an undirected path between every pair of distinct nodes. A (directed) *tree* of a (directed) graph is a subgraph in which every node has exactly one parent except for one node, called the root, which has no parent and which has a (directed) path to every other node. A (directed) *spanning tree* is a tree subgraph containing all nodes in $\mathcal{V}$. Note that, by definition, an undirected graph is connected if and only if it contains a spanning tree. The spanning trees in the graphs of Figure 2.1 are colored in red. A (directed) cycle is a (directed) path where the initial and final nodes are the same.

2.2 THE CONSENSUS CONTROL PROBLEM

In Chapter 1, it was suggested that the consensus problem constitutes the basis of cooperative interaction for multi-agent systems [2], [3], [5]. Essentially, the consensus problem consists in finding distributed control laws that make all the agents achieve convergence of a particular variable to a common value using only information of a subset of agents. Both, the control design and the analysis of the closed-loop system are normally carried out considering the dynamics of each individual node (agent) composing the graph representation of the system. Hereafter, to better put the contributions of this thesis inperspective, we revisit some classical control designs for consensus of multi-agent systems. The elements presented in this section are mostly adapted from [1], [3].

For illustration, let us consider first a two-agent system interacting via the graph in Figure 2.2, and composed of two agents described by

$$\dot{x}_1 = -a(x_1 - x_2), \quad a > 0 \tag{2.1a}$$
$$\dot{x}_2 = -a(x_2 - x_1), \tag{2.1b}$$

where, for $i \in \{1, 2\}$, $x_i \in \mathbb{R}^n$ is the state of each agent. The equations in (2.1) can be interpreted as two single-integrator agents with a proportional control law where, for each agent, the reference is taken to be the state of its neighbor.

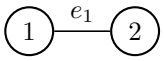

Figure 2.2: Undirected graph for a two-agent system.

Now, rearranging (2.1) we have

$$\dot{x}_1 = -a\,x_1 + a\,x_2 \tag{2.2a}$$
$$\dot{x}_2 = -a\,x_2 + a\,x_1. \tag{2.2b}$$

We see from (2.2) that the system consists in an interconnection of two exponentially stable systems. Indeed, the systems in (2.2) may be equivalently represented by first-order filters as in the figure below with $i = 1$ and $j = 2$ for (2.2a), and $i = 2$ and $j = 1$ for (2.2b).

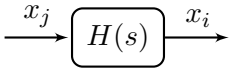

$$H(s) := \frac{1}{s + a}$$

Figure 2.3: Bloc-diagram equivalence of Equations (2.2).

Therefore, for both subsystems in (2.2), the output x_i of the first-order system, corresponding to the state of the agents, tends to track the input x_j (up to a DC-gain factor), which corresponds to the state of its neighbor. Hence we have that $x_1(t) \to x_2(t)$ and $x_2(t) \to x_1(t)$.

To see this more clearly let us define the Lyapunov function $V(x_1 - x_2) = (x_1 - x_2)^2$. Its derivative along (2.1) gives

$$\begin{aligned}\dot{V}(x_1 - x_2) =& 2a\,[-a(x_1 - x_2) + a(x_2 - x_1)]\,(x_1 - x_2)\\ =& -4a^2\,(x_1 - x_2)^2 \leq 0.\end{aligned} \tag{2.3}$$

Then, invoking LaSalle's invariance principle [16], it is clear that the system converges to the invariant set $\{x_1, x_2 \in \mathbb{R}^n : \dot{V} = 0\}$, that is, $\{x_1 = x_2\}$, thus achieving consensus.

Consider now a three-agent system interconnected through a complete graph as in Figure 2.4. Following the same idea as for system (2.1), that is, to use a proportional term for

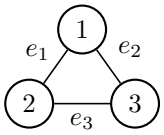

Figure 2.4: Undirected graph for a three-agent system.

the difference between the state x_i and that of each neighbor, we obtain the system

$$\dot{x}_1 = -a_{12}(x_1 - x_2) - a_{13}(x_1 - x_3), \quad a_{ij} > 0 \tag{2.4a}$$
$$\dot{x}_2 = -a_{21}(x_2 - x_1) - a_{23}(x_2 - x_3) \tag{2.4b}$$
$$\dot{x}_3 = -a_{31}(x_3 - x_1) - a_{32}(x_3 - x_2). \tag{2.4c}$$

In a similar way as for the two-agent system, let us define the Lyapunov function

$$V(x) = (a_{12} + a_{21})(x_1 - x_2)^2 + (a_{13} + a_{31})(x_1 - x_3)^2 + (a_{23} + a_{32})(x_2 - x_3)^2. \tag{2.5}$$

The time-derivative of V in this case is given by the cumbersome expression

$$\begin{aligned}\dot{V}(x) =& -2(a_{12} + a_{21})^2(x_1 - x_2)^2 - 2(a_{13} + a_{31})^2(x_1 - x_3)^2 - 2(a_{23} + a_{32})^2(x_2 - x_3)^2\\ &- 2(2a_{12}a_{13} + a_{13}a_{21} + a_{12}a_{31})(x_1 - x_2)(x_1 - x_3)\\ &+ 2(2a_{23}a_{21} + a_{21}a_{32} + a_{23}a_{12})(x_1 - x_2)(x_2 - x_3)\\ &- 2(2a_{31}a_{32} + a_{31}a_{23} + a_{32}a_{13})(x_1 - x_3)(x_2 - x_3),\end{aligned} \tag{2.6}$$

which is even more so for networked systems of dimension $N > 3$. Therefore, we shall use the more compact notation that consists in setting $x^\top := \begin{bmatrix} x_1^\top & x_2^\top & x_3^\top \end{bmatrix} \in \mathbb{R}^{3n}$ and, assuming that $a_{ij} = a_{ji}$, we rewrite the system (2.4) in the compact form

$$\dot{x} = -[L \otimes I_n]\, x, \tag{2.7}$$

where

$$L := \begin{bmatrix} a_{12} + a_{13} & -a_{12} & -a_{13} \\ -a_{12} & a_{12} + a_{23} & -a_{23} \\ -a_{13} & -a_{23} & a_{13} + a_{23} \end{bmatrix}. \tag{2.8}$$

The matrix L is called the Laplacian matrix associated to the graph representing the interconnection between the agents [1]. The Laplacian matrix plays a fundamental role in the analysis of the consensus problem. Indeed, note that, by construction, L has zero row sums. Hence, the null space of L is span$\{\mathbf{1}\}$. Consequently, we have that

$$[L \otimes I_n]x = 0 \iff x_1 = x_2 = x_3,$$

that is, $[L \otimes I_n]x = 0$ at consensus.

In this compact notation, the Lyapunov function defined in (2.5) may now be written as

$$V(x) = x^\top [L \otimes I_n]\, x \tag{2.9}$$

and its derivative along the trajectories of (2.7) yields

$$\begin{aligned}\dot{V}(x) &= -2\, x^\top \left[L^\top L \otimes I_n\right] x \\ &= -2 \left| [L \otimes I_n]\; x\right|^2 \leq 0.\end{aligned} \tag{2.10}$$

Invoking, again, LaSalle's invariance principle [16], we may also establish that, from (2.10) the system converges to the invariant set $\{x \in \mathbb{R}^{3n} : [L \otimes I_n]x = 0\}$, that is, $\{x_1 = x_2 = x_3\}$.

From the latter, we can see that in a more general case just driving the state of each agent to follow that of its neighbors, as done for the two-agents system, might not be enough to reach consensus. Indeed, it is clear that the structure of the Laplacian matrix, hence, of the interconnections among the agents via the graph representation, plays a determinant role in the achievement of consensus. For the three-agent example, the graph in Figure 2.4 is complete. That is, every agent interacts with all the other agents in the system. In general, however, this is not the case so, the achievement of consensus is determined by the structure of the topology and the properties of the Laplacian, as we explain next.

Let us consider a network composed of N agents with an interaction topology described by a graph $\mathcal{G} = (\mathcal{V}, \mathcal{E})$. Consider that each agent is modeled by a first-order integrator given by

$$\dot{x}_i = u_i, \quad i \leq N, \tag{2.11}$$

where $x_i \in \mathbb{R}^n$ is the state of each agent and $u_i \in \mathbb{R}^n$ is the control input. For this system the consensus problem is formulated as follows.

Consensus problem. Consider a multi-agent system of N agents (2.11), interacting over a graph $\mathcal{G} = (\mathcal{V}, \mathcal{E})$. Under these conditions, find a distributed controller u_i, $i \leq N$, such that

$$\lim_{t\to\infty} x_i(t) - x_j(t) = 0, \quad \forall i, j \in \mathcal{V} \tag{2.12}$$

is achieved. •

Now, following a similar reasoning as for the two-agent and three-agent networks, the consensus protocol that solves the consensus problem formulated above is typically given by the inputs —*cf.* [1], [3], [6] and references therein—

$$u_i = -c \sum_{j=1}^{N} a_{ij}(x_i - x_j), \quad c > 0, \tag{2.13}$$

where the coefficients $a_{ij} > 0$ if and only if $(j, i) \in \mathcal{E}$ and $a_{ij} = 0$ otherwise. The protocol (2.13) drives the state of agent i towards the states of its neighbors $j \in \mathcal{N}_i$, converging at the so-called consensus point. In general, the consensus point is unspecified and depends on the initial conditions of the system.

Let the matrix $A = [a_{ij}] \in \mathbb{R}^{N\times N}$ denote the so-called *adjacency matrix* of the graph, and let the diagonal matrix $D \in \mathbb{R}^{N\times N}$ with entries $d_{ii} = \sum_j a_{ij}$ denote the so-called *degree matrix* of a graph. Then, collecting the states of all the agents as $x := \begin{bmatrix} x_1^\top & \cdots & x_N^\top \end{bmatrix}^\top \in \mathbb{R}^{nN}$ and replacing (2.13) into (2.11), the consensus problem boils down to study the behavior of the closed-loop system

$$\dot{x} = -c\,[L \otimes I_n]\,x, \tag{2.14}$$

where $L \in \mathbb{R}^{N\times N}$ is the Laplacian matrix associated with graph $\mathcal{G}$, given by

$$L := D - A = \begin{bmatrix} \sum_{i=2}^{N} a_{1i} & -a_{12} & \cdots & -a_{1N} \\ -a_{21} & \sum_{i=1,i\neq 2}^{N} a_{2i} & \cdots & -a_{2N} \\ \vdots & \vdots & \ddots & \vdots \\ -a_{N1} & -a_{N2} & \cdots & \sum_{i=1}^{N-1} a_{Ni} \end{bmatrix}. \tag{2.15}$$

As for the three-agent system (2.4), the structure of the network's topology, represented by the Laplacian matrix, plays a fundamental role in establishing consensus for the system (2.14). Indeed, as before, note that L has zero row sums by construction. Therefore, zero is an eigenvalue of L with the associated eigenvector $\mathbf{1}$ and the eigenvalues of the Laplacian matrix can be ordered as

$$0 = \lambda_1 \leq \lambda_2 \leq \cdots \leq \lambda_N,$$

with $\lambda_1 = 0$. Moreover, using well-known statements of linear algebra it follows that for an undirected graph, L is a symmetric positive semi-definite matrix and 0 is a simple eigenvalue of L if and only if the undirected graph is connected [87]. For a directed graph, all non-zero eigenvalues of L have positive real parts and 0 is a simple eigenvalue if and only if the directed graph contains a directed spanning tree [1].

Thus, for systems interconnected via static undirected graphs and with constant linear interconnections, a necessary and sufficient condition for the consensus protocol (2.14) to converge to agreement is that the graph is connected. Alternatively, in the case of directed graphs consensus is achieved if the underlying graph contains a directed spanning tree. To see this, akin to (2.5), consider the candidate Lyapunov function

$$V(x) = x^\top\,[L \otimes I_n]\,x. \tag{2.16}$$

The time-derivative of V (2.16) along (2.14) is given by

$$\begin{aligned} \dot{V}(x) &= -\,2\,c\,x^\top \Big[L^\top L \otimes I_n\Big]\,x \\ &= -\,2\,c\,\big|\,[L \otimes I_n]\;x\big|^2 \leq 0. \end{aligned} \tag{2.17}$$

The function V is not a strict Lyapunov function[1]. However, if the graph $\mathcal{G}$ is undirected and connected or directed containing a directed spanning tree, L is a positive semi-definite matrix with a single zero eigenvalue associated to the eigenvector $\mathbf{1}$ [1]. Then, since the null space of L is given by span$\{\mathbf{1}\}$, the largest invariant set contained in the set

$$\{x \in \mathbb{R}^{nN} \,:\, \dot{V}(x) = 0\}$$

corresponds to the consensus manifold

$$\mathcal{S} := \{x_1 = x_2 = \cdots = x_N\}. \tag{2.18}$$

Thus, convergence to the consensus manifold (2.18) follows from LaSalle's invariance principle [16].

The previous development allows us to establish *convergence* to the consensus manifold for networks of linear systems with linear time-invariant interconnections. In such cases, the achievement of consensus depends exclusively on the nature of the network topology; this, however, is no longer true in the case of networks with nonlinear interconnections or systems with nonlinear dynamics. Moreover, note that, even in the cases of linear systems and linear interconnections, the analysis of the consensus problem via Lyapunov's first method with a non-strict Lyapunov function poses considerable limitations. Indeed, in general when considering the agreement agreement protocol in (2.13), using LaSalle's invariance principle, only convergence to the consensus manifold is established. In contrast, via the construction of strict Lyapunov functions tailored for set-stability analysis and with the right properties, stronger results such as (global) asymptotic stability or robustness of the agreement set may be established —see Remark 2.1 on the next page.

Therefore, it is appealing to use an alternative representation based on the edges of the graph, rather than the nodes, that is useful for a stability-based analysis of the consensus problem via strict Lyapunov functions.

2.3 THE EDGE-BASED FORMULATION

In this thesis we choose to study the consensus problem using the alternative edge-based representation of networked systems [7], [21]–[26]. As previously explained, this representation uses the dynamics of the *edges* of the underlying graph, as opposed to that of the *nodes*. Hence, the agreement problem is reformulated as one of stabilization of the origin, rendering it well-suited for standard Lyapunov-based control and Lyapunov's direct method of analysis.

The concepts of edge-based agreement, which are presented next, are mainly borrowed from [7], [21], [22] and adapted here for the purpose of this thesis. They constitute the mathematical basis for the contributions presented in the following chapters.

1 See Appendix A.1 for a definition.

2.3.1 *The edge transformation*

The edge-based representation of a graph focuses on the difference between any two nodes' states. For illustration, consider the two-agents system described by (2.1), but let us study the dynamics of the edge e_1 in Figure 2.2 rather than those of the nodes x_1 and x_2. To that end, define the *edge* variable

$$z_1 := x_1 - x_2, \tag{2.19}$$

which literally stands for the difference between the states of the two interconnected systems. That is, they are in consensus if $z_1 = 0$. Now, differentiating with respect to time and using (2.1), we obtain

$$\begin{aligned} \dot{z}_1 &= -a(x_1 - x_2) + a(x_2 - x_1) \\ &= -2\,a\,z_1. \end{aligned} \tag{2.20}$$

Hence, under the edge-based perspective, the consensus objective, that $x_1(t) - x_2(t) \to 0$, is transformed into $z_1(t) \to 0$. Moreover, the interconnected system (2.1) is transformed into the single exponentially stable system (2.20). Indeed, taking the Lyapunov function $V(z_1) = |z_1|^2$, its total derivative reads

$$\dot{V}(z_1) = -2\,a\,|z_1|^2 < 0. \tag{2.21}$$

From (2.21), $V(z_1)$ is a strict Lyapunov function for the system (2.20), implying exponential stability at the origin $\{z_1 = 0\}$ and, equivalently, of the consensus manifold $\{x_1 = x_2\}$.

Remark 2.1. *As evident as it may appear for this very simple example, exponential stability of the origin $\{z_1 = 0\}$, or equivalently of $\{x_1 = x_2\}$, is not the same as reaching consensus. More precisely the former implies the latter, but not vice-versa. This is because consensus, defined as the mere convergence of $x_1 \to x_2$ is a much weaker property than asymptotic (let alone exponential) stability. The difference becomes more important when the systems are nonlinear or time-varying. In such cases, it is crucial to dispose of strict Lyapunov functions to guarantee uniform (in the initial conditions) asymptotic stability, and in certain cases as we shall see, robust stability in the sense of input-to-state stability.* •

Now, in the case of the three-agent system described by the equations (2.4), akin to (2.19), for the edges in Figure 2.4 the edge states are given by

$$z_1 = x_1 - x_2, \quad z_2 = x_1 - x_3, \quad z_3 = x_2 - x_3. \tag{2.22}$$

Note that, defining $z^\top = \begin{bmatrix} z_1^\top & z_2^\top & z_3^\top \end{bmatrix}$ and $x^\top = \begin{bmatrix} x_1^\top & x_2^\top & x_3^\top \end{bmatrix}$, the edge states are given by

$$z = \left(\begin{bmatrix} 1 & -1 & 0 \\ 1 & 0 & -1 \\ 0 & 1 & -1 \end{bmatrix} \otimes I_n \right) x \tag{2.23}$$

which may also be written in the compact form

$$z = \left[E^\top \otimes I_n\right] x, \tag{2.24}$$

where the matrix E that we just introduced is the so-called *incidence* matrix of graph $\mathcal{G}$. Its rows are indexed by the nodes and its columns are indexed by the edges. The incidence matrix represents the edges connected at each node. In general, for a network composed of N agents, given an oriented undirected graph or a directed graph, the incidence matrix $E \in \mathbb{R}^{N\times M}$ of the graph is defined such that its ikth element

$$[E]_{ik} := \begin{cases} +1, & \text{if } i \text{ is the initial node of edge } e_k \\ -1, & \text{if } i \text{ is the terminal node of edge } e_k \\ 0, & \text{otherwise.} \end{cases} \tag{2.25}$$

Now, let us again consider a system composed of N agents described by the first-order integrator in compact form

$$\dot{x} = u, \tag{2.26}$$

where $x^\top = \begin{bmatrix} x_1^\top & \cdots & x_N^\top \end{bmatrix}$ and $u^\top = \begin{bmatrix} u_1^\top & \cdots & u_N^\top \end{bmatrix}$. Then, akin to (2.22), define the states of the edges in the underlying graph as

$$z_k := x_i - x_j \quad \forall k \leq M, \quad (i,j) \in \mathcal{E}. \tag{2.27}$$

From (2.25), similarly to (2.24), the edge states in compact form are obtained using the transformation

$$z = \left[E^\top \otimes I_n\right] x, \quad z \in \mathbb{R}^{nM}. \tag{2.28}$$

Then, in the edge coordinates the networked system's dynamics (2.26) is transformed into

$$\dot{z} = \left[E^\top \otimes I_n\right] u. \tag{2.29}$$

Equation (2.29) is significant because it allows us to recast the consensus problem as one of stabilization of an equilibrium point, exactly as we did for the system (2.1) —*cf.* (2.20). To better see this, let us recall that the consensus problem consists in driving the states of all the agents to a common value. Mathematically this translates into making $x_i - x_j \to 0$ for all $(i,j) \in \mathcal{V}^2$. Equivalently, recalling (2.27), the consensus objective is to drive $z_k \to 0$ for all $k \leq M$. More precisely, the control problem is transformed from rendering the agreement manifold (2.18) attractive to the stabilization of the origin for system (2.29). Hence, from a control-systems viewpoint this alternative edges' perspective is well-suited for Lyapunov-based control and Lyapunov's direct method of analysis.

Note, moreover, that the formulation in (2.29) is valid both for directed and undirected graphs. In the edge coordinates, if the graph is undirected, the consensus protocol (2.13) for a single agent becomes

$$u_i = -c\sum_{k=1}^{M}[E]_{ik}z_k, \quad c > 0, \tag{2.30}$$

and, for the multi-agent system in compact form, we have

$$u = -c\,[E \otimes I_n]\,z. \tag{2.31}$$

Then, replacing (2.31) into (2.29), we obtain the closed-loop system

$$\begin{aligned}\dot{z} =& -c\,\left[E^\top E \otimes I_n\right] z \\ =& -c\,[L_e \otimes I_n]\,z.\end{aligned} \tag{2.32}$$

The control law (2.31) is valid for undirected graphs. For directed graphs, however, $a_{ij} \neq a_{ji}$ and the control design is less direct. In this case note first that the incidence matrix may be expressed as the sum of two matrices —*cf.* [22]—:

$$E = E_\odot + E_\otimes \tag{2.33}$$

where $E_\odot \in \mathbb{R}^{N\times M}$ corresponds to the so-called *in-incidence* matrix, whose elements are defined as

$$[E_\odot]_{ik} := \begin{cases} -1 & \text{if } i \text{ is the terminal node of edge } e_k \\ 0 & \text{otherwise} \end{cases} \tag{2.34}$$

and $E_\otimes \in \mathbb{R}^{N\times M}$ is the so-called *out-incidence* matrix, with elements are defined as

$$[E_\otimes]_{ik} := \begin{cases} 1 & \text{if } i \text{ is the initial node of edge } e_k \\ 0 & \text{otherwise.} \end{cases} \tag{2.35}$$

The in-incidence matrix $E_\odot$ represents the edges coming in to a node, whereas the out-incidence matrix $E_\otimes$ represents the edges stemming out from a node. Then, if the graph is directed, the consensus protocol (2.13), in compact form, is given by

$$u = -c\,[E_\odot \otimes I_n]\,z. \tag{2.36}$$

Similarly, but with a slight abuse of notation, we obtain the closed-loop system

$$\begin{aligned}\dot{z} =& -c\,\left[E^\top E_\odot \otimes I_n\right] z \\ =& -c\,[L_e \otimes I_n]\,z.\end{aligned} \tag{2.37}$$

Now, considering the closed-loop systems (2.32) and (2.37) let us define the matrix $L_e \in \mathbb{R}^{M\times M}$, given by

$$L_e = E^\top E, \tag{2.38}$$

for undirected graphs and by

$$L_e = E^\top E_\odot, \tag{2.39}$$

for directed graphs. The latter is named the *edge Laplacian* matrix of the graph. Indeed, note that (2.32) and (2.37) have a similar structure to the equivalent system (2.14) in the nodes' perspective, albeit, with the matrix L_e, instead of the graph Laplacian L.

In the nodes' framework, for linear static interconnections, the properties of the graph, and more precisely the properties of the matrix representation of the graph in the form of the Laplacian L, play an important role in the stability analysis of the consensus protocol. Moreover, note that, alluding to (2.14), the Laplacian matrix of an oriented undirected graph can be alternatively defined in terms of the incidence matrix as

$$L = EE^\top. \tag{2.40}$$

For directed graphs, the Laplacian can be defined in terms of the incidence and in-incidence matrices as

$$L = E_\odot E^\top. \tag{2.41}$$

Therefore, the edge Laplacian L_e can be considered as an "edge dual" of the graph Laplacian L. In that sense, in the edge framework, the properties of the edge Laplacian matrix play a similar role as those of the graph Laplacian L in the nodes' framework. Indeed, L_e has the following properties [7], [22]:

- the non-zero eigenvalues of L_e are equal to the non-zero eigenvalues of L,
- $\text{rank}(L_e) = \text{rank}(L) = N - 1$,
- for a (directed) graph containing a (directed) spanning tree, the algebraic multiplicity of the zero eigenvalue of L_e is equal to $M - N + 1$.

Remark 2.2. *Note that as a direct consequence of the previous properties, if the graph is a (directed) spanning tree, then all the eigenvalues of the edge Laplacian L_e have positive real parts. Indeed, any spanning tree is composed of exactly $N - 1$ edges. Therefore, since the eigenvalues of L_e are exactly the $N - 1$ non-zero eigenvalues of the graph Laplacian L and rank$(L_e) = N - 1$, the claim follows.* •

From the properties of the edge Laplacian listed above, it is clear that the edge Laplacian, as the graph Laplacian, is a positive semi-definite matrix. Hence, recalling the Lyapunov analysis exposed in the previous section for the consensus algorithm in the node-based representation, the same conclusions in terms of non-strict Lyapunov functions are obtained for the edge-based systems (2.32) and (2.37).

A particular case, however, is that of a graph that consists of a single spanning tree. To see this, suppose that the network is interconnected over a (directed) spanning tree. Then, as evoked in Remark 2.2, all the eigenvalues of the edge Laplacian $L_e \in \mathbb{R}^{(N-1)\times(N-1)}$ of a (directed) spanning tree have strictly positive real part. Hence, in this case, the matrix $-[L_e \otimes I_n]$ in (2.32) and (2.37) is Hurwitz. Consequently, from standard arguments from linear systems' theory, the origin $\{z = 0\}$ for systems (2.32) and (2.37) is exponentially stable. Consequently, consensus is achieved exponentially. Moreover, letting $\Gamma \in \mathbb{R}^{(N-1)\times(N-1)}$ be a symmetric positive definite matrix satisfying the Lyapunov equation

$$\Gamma L_e + L_e^\top \Gamma = Q,$$

with, $Q \in \mathbb{R}^{(N-1)\times(N-1)}$ a symmetric positive definite matrix, the Lyapunov function

$$V(z) = z^\top [\Gamma \otimes I_n] z \tag{2.42}$$

is a strict Lyapunov function for systems (2.32) and (2.37).

Now, a well-known necessary and sufficient condition for consensus is that the (directed) graph $\mathcal{G}$ representing the network topology contains at least one (directed) spanning tree [3]. The latter and the exponential stability of the consensus manifold in the case of a (directed) spanning tree, suggests that the system dynamics may be studied by concentrating on that of a reduced-order system, whose states, in the edges' framework, correspond exclusively to those of the edges in a tree. Indeed, using a particular labeling of the graph, it is possible to obtain such a reduced-order representation as proposed in [7], [21]. This is explained hereafter.

2.3.2 *A reduced-order edge-based model*

To better understand how one can obtain a reduced representation, it is convenient to remark that if a graph contains a spanning tree it can be represented as the sum of two subgraphs: one consisting of a spanning tree $\mathcal{G}_t = (\mathcal{V}, \mathcal{E}_t)$ where $\mathcal{E}_t \subset \mathcal{E}$ and $|\mathcal{E}_t| = N - 1$, and one containing the rest of the edges that complete the "cycles" $\mathcal{G}_c = (\mathcal{V}, \mathcal{E}_c)$ where $\mathcal{E}_c := \mathcal{E} \backslash \mathcal{E}_t$ and $|\mathcal{E}_c| = M - N + 1$ —see Figure 2.5.

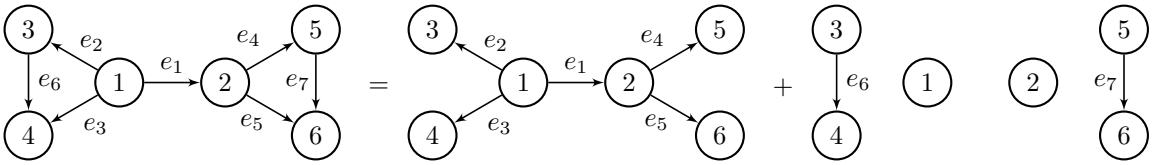

Figure 2.5: Partition of a graph into a spanning tree and the remaining edges.

Note that the graph in Figure 2.5 has been labeled. In the context of the edge-agreement framework, the right labeling ensures that the incidence and Laplacian matrices associated to the underlying (directed or oriented undirected) graph have certain properties and structures which are fundamental for stability analysis of the consensus protocol. For this purpose, it is convenient to follow the labeling algorithm proposed in [7]:

1. Choose an arbitrary directed spanning tree contained in $\mathcal{G}$ and label the root as node "1".
2. For any two nodes i and j belonging to a branch of the tree, label them such that if the path length from the root to i is smaller than the path length from the root to j, then $i < j$.
3. Label the $n-1$ edges belonging to the tree such that for any edge e_k with terminal node j, one has $j > k$.
4. Freely label the rest of the edges.

Remark 2.3. *Although the edges that do not belong to the tree, $\mathcal{E}_c$, may be freely labeled, for consistency with the literature (and specially in the case of acyclic directed graphs) it is recommended to follow the following labeling: for any two edges $e_f, e_g \in \mathcal{E}_c$ that have the same terminal nodes as edges $e_i, e_j \in \mathcal{E}_t$ respectively, label them such that if $i < j$, one has $f < g$. Note that this rule is contradictory for edges completing directed cycles, in consequence, only the edges in $\mathcal{E}_c$ that do not complete directed cycles (if they exist) should be labeled in such a way, while the other edges can be labeled freely.* •

Then, using the labeling of the edges described above, it is possible to partition the incidence matrix into

$$E = [\, E_t \quad E_c \,] \tag{2.43}$$

where $E_t \in \mathbb{R}^{N\times(N-1)}$ denotes the full-column-rank incidence matrix corresponding to a spanning tree $\mathcal{G}_t$ and $E_c \in \mathbb{R}^{N\times(M-N+1)}$ represents the incidence matrix corresponding to the remaining edges not contained in $\mathcal{G}_t$. Moreover, the columns of E_c are linearly dependent on the columns of E_t. The latter can be expressed in terms of the existence of a matrix T such that

$$E_c = E_t T. \tag{2.44}$$

Left-multiplying both sides of (2.44) by $E_t^\top$, we have

$$E_t^\top E_c = E_t^\top E_t T. \tag{2.45}$$

Therefore, since E_t has full column rank, its Moore-Penrose pseudo-inverse exists and we can define

$$T := \left(E_t^\top E_t\right)^{-1} E_t^\top E_c, \tag{2.46}$$

so that (2.45) is satisfied. Now, defining

$$R := [\, I_{N-1} \quad T \,], \tag{2.47}$$

and using (2.43), one obtains an alternative representation of the incidence matrix of the graph in terms of the incidence matrix of a spanning tree. This is given by

$$E = E_t R. \tag{2.48}$$

The identity (2.48) is useful to derive a reduced-order dynamic model —*cf.* [7], [21]. Indeed, following the reasoning as for the incidence matrix, the edges' states may be split as

$$z = \begin{bmatrix} z_t^\top & z_c^\top \end{bmatrix}^\top, \quad z_t \in \mathbb{R}^{n(N-1)}, \; z_c \in \mathbb{R}^{n(M-N+1)} \tag{2.49}$$

where z_t are the states corresponding to the edges of an arbitrary spanning tree $\mathcal{G}_t$ and z_c denote the states of the remaining edges in $\mathcal{G}_c$. Then, after (2.28) and (2.48), we obtain the following identity

$$z = \left[R^\top \otimes I_n\right] z_t. \tag{2.50}$$

Now, for systems interacting over undirected connected graphs, using the identity (2.50) in both sides of (2.32), we obtain

$$\left[R^\top \otimes I_n\right] \dot{z}_t = -c \left[L_e R^\top \otimes I_n\right] z_t. \tag{2.51}$$

Then, recalling (2.38) and using (2.48), we have

$$\left[R^\top \otimes I_n\right] \dot{z}_t = -c \left[R^\top E_t^\top E_t R R^\top \otimes I_n\right] z_t, \tag{2.52}$$

and since R is full-row-rank, we obtain the reduced-order system

$$\dot{z}_t = -c \left[E_t^\top E_t R R^\top \otimes I_n\right] z_t, \tag{2.53}$$

by premultiplicating by $\left[\left(R^\top\right)^\dagger \otimes I_n\right]$ and using the properties of the Kronecker product. Similarly, for systems interacting over directed graphs containing a spanning tree, from (2.39), we obtain

$$\dot{z}_t = -c \left[E_t^\top E_\odot R^\top \otimes I_n\right] z_t. \tag{2.54}$$

Equations (2.53) and (2.54) are remarkable because, even though they are of reduced dimension ($z_t \in \mathbb{R}^{N-1}$), they completely capture the synchronization behavior of the whole system. In particular, consensus for (2.26) holds if and only if the origin $\{z_t = 0\}$ is attractive for the solutions of (2.53) for undirected graphs or (2.54) for directed ones. Therefore, the consensus problem becomes a problem of stabilization of the origin for a reduced-order multi-agent system that represents the evolution of the edges in a (directed) spanning tree.

For the purpose of the stability analysis of the multi-agent system in the reduced-order edge representation, let us first state the following Lemmata from [7], [23]:

Lemma 2.1 ([23])**.** *The edge Laplacian L_e associated to a connected undirected graph with cycles is similar*[2] *to the matrix*

$$\begin{bmatrix} E_t^\top E_t R R^\top & 0_{(N-1)\times(M-N+1)} \\ 0_{(M-N+1)\times(N-1)} & 0_{(M-N+1)\times(M-N+1)} \end{bmatrix}. \tag{2.55}$$

□

2 Recall that two matrices A, $B \in \mathbb{R}^{n\times n}$ are *similar* if there exists an invertible matrix $P \in \mathbb{R}^{n\times n}$ such that $B = P^{-1}AP$ [88].

Lemma 2.2 ([7]). *The edge Laplacian L_e associated to a directed graph containing a directed spanning tree is similar to the matrix*

$$\begin{bmatrix} E_t^\top E_\odot R^\top & E_t^\top E_\odot N_t \\ 0_{(M-N+1)\times(N-1)} & 0_{(M-N+1)\times(M-N+1)} \end{bmatrix}, \tag{2.56}$$

where the columns of the matrix $N_t \in \mathbb{R}^{M\times(M-N+1)}$ form the orthonormal basis for the null space of R. □

Since the edge Laplacian L_e of a connected undirected graph has exactly $M-N+1$ zero eigenvalues, a direct consequence of Lemma 2.1 is that the matrix $E_t^\top E_t R R^\top$ is symmetric positive definite, and its eigenvalues are precisely the non-zero eigenvalues of the graph Laplacian L. In a similar way, it may be concluded from Lemma 2.2 that, all the eigenvalues of the matrix $E_t^\top E_\odot R^\top$ in (2.54) lie in the complex right half-plane.

In light of the previous facts, let us denote

$$L_{eR} := \begin{cases} E_t^\top E_t R R^\top & \text{if the graph is undirected} \\ \\ E_t^\top E_\odot R^\top & \text{if the graph is directed.} \end{cases} \tag{2.57}$$

Let $Q \in \mathbb{R}^{(N-1)\times(N-1)}$ be an arbitrarily given positive definite matrix. Then, there exists a unique solution $\Gamma \in \mathbb{R}^{(N-1)\times(N-1)}$ to the Lyapunov equation

$$\Gamma L_{eR} + L_{eR}^\top \Gamma = Q$$

such that Γ is positive definite and, therefore, the function $V : \mathbb{R}^{n(N-1)} \to \mathbb{R}_{\geq 0}$

$$V(z_t) = z_t^\top \left[\Gamma \otimes I_n\right] z_t, \tag{2.58}$$

is positive definite. Moreover, from (2.53) and (2.53), it follows that the time-derivative of V (2.58) is given by

$$\begin{aligned} \dot{V}(z_t) &= -\,2c\, z_t^\top \left[\Gamma L_{eR} \otimes I_n\right] z_t \\ &= -\,c\, z_t^\top \left[\Gamma L_{eR} + L_{eR}^\top \Gamma \otimes I_n\right] z_t \\ &= -\,c\, z_t^\top \left[Q \otimes I_n\right] z_t < 0. \end{aligned} \tag{2.59}$$

Note that, contrary to the Lyapunov function (2.16) in the nodes' perspective, V in (2.58) is a strict Lyapunov function for (2.53) and (2.54). Therefore, from (2.59) and the fact that V is quadratic, the origin $\{z_t = 0\}$ is exponentially stable. Furthermore, as we mentioned above, recalling the identity (2.50), the latter implies that $\{z = 0\}$ is exponentially stable. The exponential stability of $\{z_t = 0\}$, in turn, implies exponential stability of the agreement manifold, which is a stronger result than mere convergence established with non-strict Lyapunov functions and LaSalle's invariance principle. Indeed, exponential stability and the construction of a strict Lyapunov function directly imply other properties of robustness and convergence rates that cannot be ascertained if only convergence is established.

2.4 A GLIMPSE ON GRAPHS WITH NONLINEAR INTERCONNECTIONS

In anticipation of the main contributions of this thesis on consensus under constraints, we emphasize that another important advantage of the edge-based representation, relative to the more classical node-based approach is its direct applicability in the analysis of graphs with nonlinear interconnections.

This is important to us because in this thesis we deal with the coordination of multi-agent systems in realistic scenarios. In many meaningful cases, such as in the presence of inter-agent constraints, or state- or time-dependent communication, the interconnections between the agents become nonlinear or time-varying. This further motivates the choice to use the edge-agreement approach of [21] to study consensus under constraints, which is the main focus of this thesis.

The analysis provided in Section 2.2 to prove the achievement of consensus using inputs of the form (2.13) in the nodes' perspective is valid in the case of networks of linear systems under linear interconnections. However, when the interconnections are nonlinear, the analysis based on tools from linear algebra may fail to establish consensus.

To better see this let us consider that the interconnections between the agents are state or time-dependent. Then, the consensus protocol (2.13) becomes

$$u_i = -c\sum_{j=1}^{N} a_{ij}(t,x)(x_i - x_j), \quad c > 0, \tag{2.60}$$

where $a_{ij} : \mathbb{R}_{\geq 0} \times \mathbb{R}^{nN} \to \mathbb{R}_{\geq 0}$ are functions denoting the interconnection through the arc (i,j). Under (2.60), the closed-loop system becomes

$$\dot{x} = -c\,[L(t,x) \otimes I_n]\,x. \tag{2.61}$$

Therefore, in this case, the linear-algebra-based argumentation that relies on the nature of the eigenvalues of the Laplacian matrix, no longer holds.

In contrast to this, let us consider again the consensus protocol with state- or time-dependent interconnections (2.60) analyzed through the edge-based perspective. To that end, for each edge z_k, $k \leq M$, let $\rho_k(t, z_k)$ denote the nonlinear "weight" of the edge. Then, in the edge coordinates the protocol (2.60) is equivalent to

$$u_i = -c\sum_{k=1}^{M} [E]_{ik}\rho_k(t,z_k)z_k, \quad c > 0. \tag{2.62}$$

Equation (2.62) highlights an important perk of using the edge-based representation when considering nonlinear interconnections. Note that the closed-loop system is given by

$$\dot{z} = -c_1\left[L_e P(t,z) \otimes I_N\right]z,$$

where $P(t,z) := \mathrm{diag}\{\rho_k(t,z_k)\} \in \mathbb{R}^{M\times M}$, whereas, in the nodes' representation, recalling (2.40) and with an abuse of notation, the closed-loop system (2.61) is equivalent to

$$\dot{x} = -c_1\left[EP(t,[E^\top \otimes I_N]x)E^\top \otimes I_N\right]x,$$

but, one cannot rely on the properties of the eigenvalues of the graph Laplacian $L(t,x) = EP(t,[E^\top \otimes I_N]x)E^\top$ —for each fixed t and x— to assess the stability properties of $\{x_1 = \cdots = x_N\}$ of $\{z = 0\}$. In contrast to this, using the edge-based representation it is possible to dissociate the interaction topology, represented by the (unweighted) edge Laplacian L_e and the nonlinear interconnections given by the diagonal matrix $P(t,z)$. Hence, despite the nonlinear interconnections, it is possible to use the eigenvalue analysis of the edge Laplacian in order to prove asymptotic stability of the consensus manifold for graphs with nonlinear interconnections by means of a strict Lyapunov function. This will be explained in more detail in subsequent chapters. In the context of limited-range interactions it is an original contribution of this thesis and it is presented in Chapter 3. Furthermore, we show that such strict Lyapunov functions are fundamental for the Lyapunov-based design developed in Chapters 5 and 6.

2.5 CONCLUSION

We presented a brief introduction to the fundamental agreement protocol that lies at the basis of most interactions in a multi-agent coordination scenario. The achievement of consensus is in general determined by the underlying graph representing the network's topology. In the nodes' perspective the stability analysis relies on the algebraic properties of the graph Laplacian. However, using Lyapunov's direct method, only a non-strict Lyapunov function is provided. The latter, besides complicating the robustness analysis, may prove limiting when considering more complex (*e.g.*, high-order, nonlinear, underactuated) systems with (possibly) nonlinear interconnections between the agents.

In contrast, the alternative representation based on the edges of the graph poses some advantages with respect to the node-based one: the state of the system is composed of relative quantities (*e.g.*, relative positions) which may prove convenient in actual application scenarios; the behavior of the system may be studied via a reduced-order representation in terms of the edges of a spanning tree contained in the graph; in the case of nonlinear interconnections, the effects of the interaction topology and of the nonlinearities may be decoupled, facilitating the stability analysis using the properties of the edge Laplacian and Lyapunov's first method.

In the succeeding chapters we build on the edge-based representation in order to establish consensus of multi-agent systems subject to state restrictions and, therefore, nonlinear interconnections. Although for first- and second-order systems, modulo a transformation to the edge coordinates, some of the proposed controllers are reminiscent of others appearing in the literature, our contributions lie in establishing stronger properties such as asymptotic stability and robustness in terms of input-to-state (multi-)stability, which are possible since we provide strict Lyapunov functions.

3

CONSENSUS WITH CONNECTIVITY MAINTENANCE

As we saw in Chapter 2, the existence of a rooted (directed) spanning tree is a necessary and sufficient condition for consensus over (directed) graphs [89]. Yet, although necessary, this condition may as well be conservative in various robotics applications. For instance, for networks of autonomous multi-vehicle systems that (can) communicate only if they are within range of each other at a given instant, the interconnections between the agents depend on their relative positions and on other environmental factors and are therefore nonlinear and dynamically changing. In such scenarios, the connectivity properties of the underlying graph cannot be assumed in general. In consequence, the proofs of convergence of the agreement protocol that rely on the assumption that the graph contains a spanning tree at every time instant no longer hold. Moreover, the arguments of stability based on the algebraic properties of the matrices modeling the network topology, tailored for linear systems with linear interconnections, no longer hold either.

A primary goal of the present chapter is to establish strong stability and robustness results for the consensus-with-preserved-connectivity algorithm for first- and second-order integrators, presented respectively in Section 3.2 and Section 3.3. For this purpose in Section 3.1.3, we first encode the constraints using so-called *barrier Lyapunov functions* [90], [91]. These are functions that may be assimilated to a potential field with unbounded maxima. Then, the distributed control laws are derived as a gradient of such functions and, consequently, grow unboundedly as the state approaches the boundary of the set where the constraints hold. In other words, the control input is such that an infinite control effort is required to violate a constraint. We stress that neither the method nor the concept described above are original of this thesis.

The original contributions presented in this chapter consist in providing, for the first time in the literature, strict Lyapunov functions for the first- and second-order consensus-with-preserved-connectivity problem when considering both undirected and directed interaction topologies, in the edge-based representation framework. A significant byproduct is to establish asymptotic stability of the consensus manifold and, more importantly, robustness in terms of input-to-state stability, as presented in Sections 3.2.3 and 3.3.3. These properties are stronger than the non-uniform convergence usually established in the literature —see, *e.g.*, [13]–[15], [28], [29]. Indeed, for the considered problem, input-to-state stability implies boundedness of the systems' state trajectories and the satisfaction of the constraints, even in the presence

of external disturbances. The same cannot be ascertained if it is only known that, in the absence of disturbances, the system converges to the consensus manifold.

Now, even though strict Lyapunov functions have been proposed earlier for consensus problems of both first and second-order systems over undirected and directed network topologies, this is done without addressing the connectivity-preservation requirement, or vice-versa. For instance, in [92], a non-strict Lyapunov function is provided for first-order systems with field-of-view constraints; however, only boundedness of the trajectories is guaranteed. The difficulty of constructing a strict Lyapunov function is stressed therein.

3.1 PROBLEM FORMULATION AND MATHEMATICAL PRELIMINARIES

3.1.1 *Motivational case-study*

As a means of illustration, we start with a simple case-study to motivate the problem of connectivity maintenance. Consider a system composed of six agents described by a single-integrator model

$$\dot{x}_i = u_i, \quad x_i,\, u_i \in \mathbb{R}^n$$

and interconnected over the undirected graph presented in Figure 3.1. Moreover, suppose that each agent can only exchange information with its neighbors if they are within a limited circular region centered at each agent's position —see Figure 3.2.

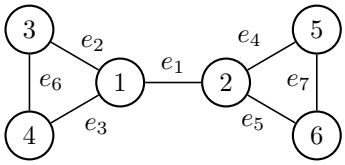

Figure 3.1: Case-study: undirected connected graph.

As we recalled in Chapter 2, the connectivity of the network topology (*i.e.*, the existence of a spanning tree) is a necessary and sufficient condition for reaching consensus. In this case-study the graph in Figure 3.1 is connected. However, despite the latter, since the interactions between the agents are limited in range, the linear consensus algorithm (in the edge-based representation)

$$u_i = -\sum_{k \leq M} [E]_{ik}\, z_k, \quad z_k \in \mathbb{R}^n \tag{3.1}$$

does not guarantee that the agents converge to the consensus manifold. Indeed, under the consensus control law (3.1), the trajectories of some of the agents may be so that they leave the interaction zones of their neighbors, hence loosing connectivity. This is illustrated in Figure 3.2 where two snapshots of a simulation are presented for an example in which the inputs are defined as in the classical consensus protocol (2.13). Note that, at $t = 0$ s the

interaction graph in connected, hence, were the graph to remain connected, the agents would reach consensus. However, as evidenced by the right-hand side figure, at some time instant $t > 0$, the graph becomes disconnected and consensus is not achieved.

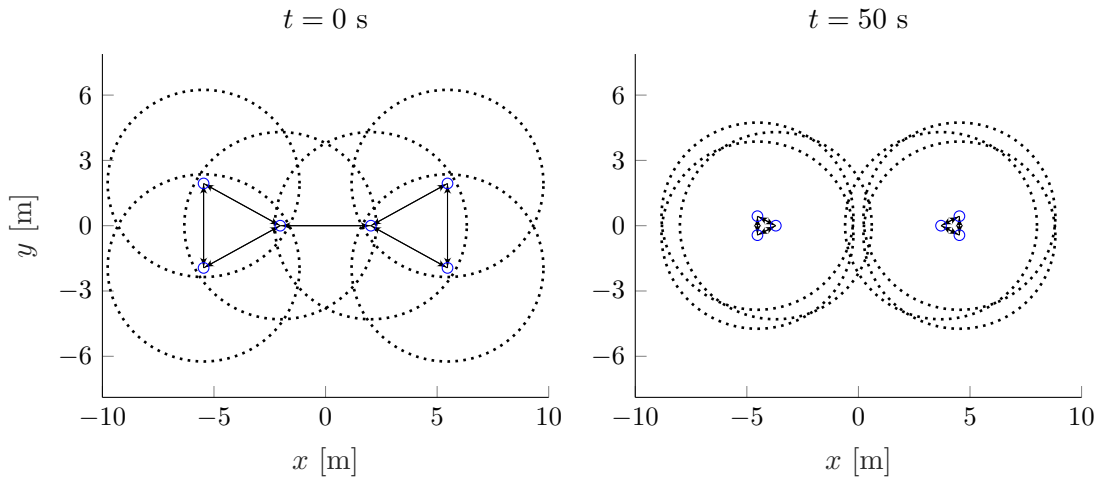

Figure 3.2: Example of connectivity loss under the classical agreement protocol for agents with limited sensing ranges (dotted circles).

For the purpose of illustration, in this numerical example the initial conditions are set so that the network becomes disconnected. However, in the case of autonomous vehicles this may occur due to a number of reasons at non-predefined moments. Indeed, even though for some initial conditions it is possible for the agents to reach consensus even with limited-range interconnections, this is not true in general, *e.g.*, if the agents are subject to disturbances. Indeed, such disturbances may also drive an agent to leave the sensing zone of its neighbors, thereby losing connectivity.

It is then evident that in order to reach consensus in a more realistic scenario where agents have limited sensing zones and are subject to disturbances, a different agreement protocol must be proposed; one that allows to guarantee connectivity maintenance, rather than assuming it. For instance, in the case of autonomous vehicles with limited-range interconnections φ_k may be defined as a function that grows non-linearly as the error z_k grows so that the agents do not steer too far away from each other and lose connectivity. More generally, in such scenarios, the consensus algorithm has to be replaced by a control law of the form

$$u_i = -\sum_{k \leq M} [E]_{ik} \varphi_k(t, z_k)$$

where φ_k is a function representing the *nonlinear* interconnections between the agents and may be defined in various manners.

In the literature various approaches have been proposed that define φ_k as the gradient of a nonlinear function. Indeed, note that in the linear consensus algorithm (3.1) we have $\varphi_k = z_k$,

which may be seen as the gradient of a quadratic function. Therefore, by constructing a nonlinear function with some desired properties that encode the inter-agent constraints, φ_k can be set as the gradient of such function in order to guarantee consensus with preserved connectivity. For this purpose, multiple types of functions have been proposed including barrier functions [93], potential functions [94], navigation functions [95] or a barrier Lyapunov functions [32]. In this thesis we use the design based on the gradient of barrier Lyapunov functions, as we shall explain in more detail farther below and in the subsequent chapters.

3.1.2 *Problem formulation*

For clarity of exposition, let us start with the consensus problem for first-order systems. Although relatively simple, the results presented in this first part of the present chapter are interesting on their own and are a foundation block for most of the results of this thesis. Hence, let us consider a system composed of N agents evolving in an n-dimensional workspace and described by a first-order integrator of the form

$$\dot{p}_i = u_i \tag{3.2}$$

where $p_i \in \mathbb{R}^n$ is the position of agent $i \leq N$, and $u_i \in \mathbb{R}^n$ is the control input.

Remark 3.1. *In the sequel we use the notation p_i to denote the position, as opposed to a more generic choice, to recall that autonomous vehicles take a special part in this work.* •

In this chapter we consider that the graph $\mathcal{G} = (\mathcal{V}, \mathcal{E})$ is either undirected or of one of two classes of directed graphs: spanning-trees or cycles. Each of the two directed topologies presents difficulties and practical interests of its own, notably in formation control of autonomous vehicles using a leader-follower configuration [96], [97] and in the context of cyclic pursuit [98]. Furthermore, to address the consensus problem under constraints we use the edge-based representation presented in Chapter 2 —*cf.* [21]—, since it is fundamental for establishing the desired stability and robustness properties via the construction of strict Lyapunov functions.

Let the relative positions between two interconnected agents be denoted

$$z_k := p_i - p_j \quad \forall k \leq M, \quad (i,j) \in \mathcal{E}. \tag{3.3}$$

Hence, akin to the edge transformation in (2.28), note that the relative positions (3.3) correspond to the elements of the edge state of the underlying graph, and are given by

$$z = \left[E^\top \otimes I_n\right] p, \quad z \in \mathbb{R}^{nM}, \tag{3.4}$$

where $z := \begin{bmatrix} z_1^\top & \cdots & z_M^\top \end{bmatrix}^\top \in \mathbb{R}^{nM}$, $p = \begin{bmatrix} p_1^\top & \cdots & p_N^\top \end{bmatrix}^\top \in \mathbb{R}^{nN}$ and E is the incidence matrix of the graph, defined in (2.25). Denote $u = \begin{bmatrix} u_1^\top & \cdots & u_N^\top \end{bmatrix}^\top \in \mathbb{R}^{nN}$. Then, the multi-agent system (3.2) is transformed into

$$\dot{z} = \left[E^\top \otimes I_n\right] u. \tag{3.5}$$

The control goal is for the agents' positions to satisfy $p_i - p_j \to 0$ for all $(i,j) \in \mathcal{V}^2$ and $p_i \to p_c$ for all $i \in \mathcal{V}$ with p_c a non-predefined constant. Equivalently, in the edge coordinates we want $z_k \to 0$ for all $k \leq M$. More precisely, the consensus objective is that

$$\lim_{t\to\infty} z(t) = 0. \tag{3.6}$$

Furthermore, we consider that each agent can only sense or communicate with its neighbors if they are within a limited range centered at their position. As we presented above, in situations where the exchange of information is limited to a determined area, the linear consensus protocol (2.13) does not guarantee that the graph remains connected, therefore stymieing the achievement of consensus. Hence, the connectivity of the graph is a property that has to be ensured via the control. Indeed, under these sensing-range limitations, the topology of the network depends on the relative states of the agents at each time instant.

Multiple connectivity-maintenance strategies exist in the literature [99]. In general, these strategies may be classified into two categories: those concerned with global connectivity maintenance [100], [101] and those considering local connectivity preservation [33]. In essence, *global* connectivity-maintenance strategies seek to guarantee that the algebraic connectivity of the graph, denoted $\lambda_2(\mathcal{G}(t))$ and corresponding to the second smallest eigenvalue of the graph Laplacian L[1], has a positive real part, that is, that $Re\,(\lambda_2(\mathcal{G}(t))) > 0$ for all time[2] t. These strategies, however, require that the agents composing the system have knowledge of the value of the algebraic connectivity, which is a global parameter. Therefore, additional computations have to be implemented, such as a distributed estimation algorithm [100], in order to successfully implement the control strategy in a distributed way. Moreover, such distributed estimation algorithms often need the *transmission* of information among agents, which is not possible when using sensor-based interactions. On the other hand, *local* strategies, also known as edge-preservation strategies, consist in maintaining (and possibly increasing) the individual existing edges in the graph $\mathcal{G}$. Therefore, in these strategies, only the local relative states are needed for the connectivity maintenance, which does not rely neither on global knowledge of the network nor on estimations of the latter. The main drawback of the local strategies with respect to the global ones is the lack of flexibility that they impose on the system. Indeed, the necessity of maintaining all the initial edges of the graph may prevent the achievement of the desired objective in certain cases where it would be pertinent to add/remove edges, *e.g.*, in cluttered environments. Nonetheless, with aims at solving the consensus problem relying only on the available embedded sensors, that is, without communication between the agents, in this thesis, we adopt a local strategy for the connectivity maintenance.

For the purpose of defining the local connectivity maintenance objective, we refer to an *initial graph* as the graph corresponding to the existing edges at $t = t_0$, where t_0 is the initial time. Then, we assume the following:

1 Here we denote $\lambda_2(\mathcal{G}(t))$ to emphasize that the algebraic connectivity is dependent of the graph topology, which may vary in the case of limited interactions between the agents.

2 Recall that for a connected undirected graph, or for a directed graph containing a directed spanning tree, the Laplacian matrix L has a single zero eigenvalue denoted $\lambda_1 = 0$ —see Chapter 2. Therefore, the condition $Re\,(\lambda_2(\mathcal{G}(t))) > 0$ for all time t, guarantees that the graph remains connected.

Assumption 3.1. *The initial undirected graph contains a spanning tree.*

In other words, Assumption 3.1 imposes that the graph contains a spanning tree only at the initial time of the *motion*. Such initial graph is determined by the initial relative positions of the agents. For directed graphs, we focus on two directed topologies with difficulties and practical interests of their own: directed spanning trees and directed cycles. Indeed, each of the two directed topologies are found, respectively, in formation control of autonomous vehicles using a leader-follower configuration [96], [97] and in the context of cyclic pursuit [98]. Therefore, when considering directed graphs, we assume the following:

Assumption 3.2. *The initial directed graph is either a directed spanning tree or a directed cycle.*

Now, mathematically, the sensing-range limitations mean that $(i, j) \in \mathcal{E}$ if and only if $|p_i - p_j| < \Delta_k$, where Δ_k denotes the maximum distance between agents i and j such that the communication/sensing through the arc e_k is reliable, for each $k \leq M$. For the multi-agent system in edge coordinates, the latter is encoded via an inter-agent constraints set defined as

$$\mathcal{J} := \big\{ z \in \mathbb{R}^{nM} : |z_k| < \Delta_k,\ \forall\, k \leq M \big\}. \tag{3.7}$$

Then, the connectivity maintenance objective is to render the constraints set (3.7) forward invariant, *i.e.*, $z(t_0) \in \mathcal{J}$ implies that $z(t) \in \mathcal{J}$ for all $t \geq t_0$. Since in this thesis we deal only with autonomous systems, for simplicity in the rest of this document we assume, without loss of generality, that $t_0 \equiv 0$.

As we recalled previously, in the case of linear time-invariant interconnections, the consensus objective (3.6) can be established in the node-based representation commonly used in the literature by means of non-strict Lyapunov functions. Moreover, in the case of connectivity constraints similar convergence results can be established as well in the node-based perspective [33], [34]. However, the convergence result (3.6) established under the node-based representation does not imply stronger results in terms of robustness and convergence rates. Hence the importance of studying the consensus-with-connectivity-maintenance problem in the edge-based framework. Indeed, as we highlighted in Chapter 2, when the interconnections are linear and time-invariant, asymptotic stability of the consensus manifold is established employing *strict* Lyapunov functions.

Therefore, beyond the convergence objective (3.6), a part of the contributions presented in this chapter is to establish asymptotic stability of the consensus manifold while guaranteeing the respect of the connectivity constraints (forward invariance of the set $\mathcal{J}$ in (3.7)), by means of the construction of strict Lyapunov functions. This implies other important properties in terms of uniformity and robustness, as we also show.

More precisely, recalling the reduced-order edge representation in Section 2.3.2, and using the identities (2.48) and (2.50), the multi-agent system (3.5) may be transformed into the reduced-order system

$$\dot{z}_t = \big[E_t^\top \otimes I_n\big] u, \tag{3.8}$$

where z_t denotes the spanning-tree edge states and E_t is the corresponding incidence matrix. Then, in these coordinates, the objective is to render the reduced-order system (3.8) asymptotically stable at the origin and the constraints set (3.7) forward invariant, along the closed-loop trajectories.

In order to account for the connectivity constraints, the design of the control law solving the position consensus problem is based on the gradient of a so-called *barrier Lyapunov function*. Therefore, before presenting our controllers for consensus with connectivity maintenance for first-order systems (see Section 3.2), we first revisit the concept of barrier Lyapunov functions.

3.1.3 *Barrier Lyapunov functions in edge coordinates*

Barrier Lyapunov functions are reminiscent of Lyapunov functions, so they are positive definite, but their domain of definition is restricted by design to open subsets of the Euclidean space [90], [91], [102]. Furthermore, they grow unbounded as the state approaches the boundary of its domain —see Figure 3.3. The latter property is fundamental for the control design when considering state constraints. Indeed, the stabilization problem under state constraints may be addressed using gradient-type control laws, relying on the gradient of such barrier Lyapunov functions. Loosely speaking, such gradient-based controllers may be assimilated to a force field that "explodes" at the boundary of the constraints set (3.7). That is, the control input as a function of the state grows unboundedly as the system approaches a specified region. This technique is also reminiscent of potential/navigation functions used in robot control [30], [103].

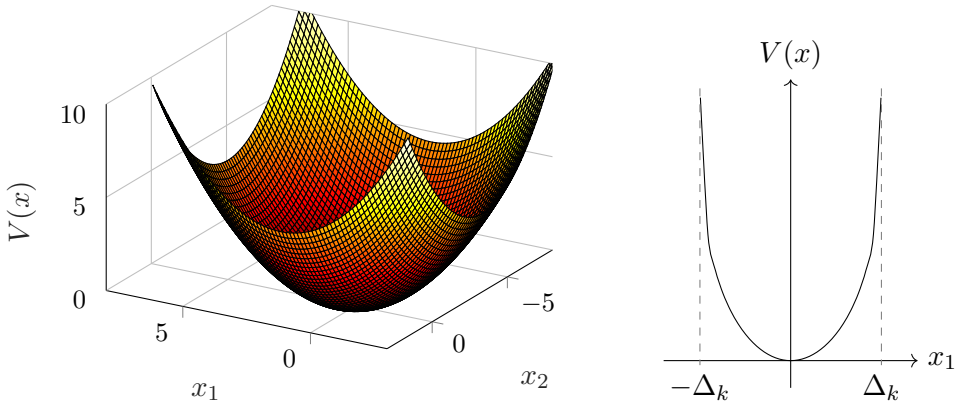

Figure 3.3: Example of a barrier Lyapunov function for a 2-dimensional state $x = [x_1\, x_2]^\top$ (left) and its level curve for $x_2 = 0$ (right).

The following definition is adapted from the one given in [90] for the purposes of this thesis.

Definition 3.1 (Barrier Lyapunov function)**.** *Consider the system $\dot{x} = f(x)$ and let $\mathcal{A}$ be an open set containing the origin. A Barrier Lyapunov function is a positive definite, function $V : \mathcal{A} \to \mathbb{R}_{\geq 0}$, $x \mapsto V(x)$, that is $\mathcal{C}^1$, satisfies*

$$\nabla V(x)^\top f(x) := \frac{\partial V(x)}{\partial x}^\top f(x) \leq 0,$$

and has the property that $V(x) \to \infty$ and $|\nabla V(x)| \to \infty$ as $x \to \partial\mathcal{A}$. □

Now, akin to (3.7), for each $k \leq M$, the inter-agent constraints in terms of the edge coordinates are given by the sets

$$\mathcal{J}_k := \{z_k \in \mathbb{R}^n \, : \, |z_k| < \Delta_k\}. \tag{3.9}$$

Then, in this chapter[3], for each $k \leq M$, we encode the limit-range constraints by a barrier Lyapunov function candidate $W_k : \mathcal{J}_k \to \mathbb{R}_{\geq 0}$, of the form

$$W_k(z_k) = \frac{1}{2}\left[|z_k|^2 + B_k(z_k)\right], \tag{3.10}$$

where B_k is a non-negative function that satisfies: $B_k(0) = 0$, $\nabla B_k(0) = 0$, and $B_k(z_k) \to \infty$ as $|z_k| \to \Delta_k$. Therefore, the barrier Lyapunov function candidate (3.10) satisfies: $W_k(0) = 0$, $\nabla W_k(0) = 0$, and $W_k(z_k) \to \infty$ as $|z_k| \to \Delta_k$. Moreover, we assume that the following holds.

Assumption 3.3. *The barrier Lyapunov function $z_k \mapsto W_k(z_k)$ in (3.10) satisfies*

$$\frac{\kappa_1}{2}|z_k|^2 \leq W_k(z_k) \leq \kappa_2 |\nabla W(z_k)|^2 =: h_k(|z_k|), \tag{3.11}$$

where κ_1 and κ_2 are positive constants and $h_k(\cdot)$ is strictly increasing for all $z_k \in \mathcal{J}_k$ and satisfies $h_k(s) > s$ for all $s > 0$, $h(0) = 0$, and $h_k(s) \to \infty$ as $s \to \partial\mathcal{J}_k$.

Remark 3.2. *Modulo performing a change of coordinates to the node space, examples of functions satisfying the properties of B_k (and of W_k) in (3.10) and Assumption 3.3 are the so-called "edge tension" functions —cf.* [33], [104]*— defined as*

$$B_k(z_k) = \frac{|z_k|^2}{\Delta_k - |z_k|}. \tag{3.12}$$

Other examples are the logarithmic and tangent functions used in [90] *and* [91] *defined, respectively, as*

$$B_k(z_k) = \ln\left(\frac{\Delta_k^2}{\Delta_k^2 - |z_k|^2}\right), \tag{3.13}$$

and

$$B_k(z_k) = \frac{\Delta_k}{\pi}\tan^2\left(\frac{\pi z_k}{2\Delta_k}\right). \tag{3.14}$$

•

3 The specific form of the barrier Lyapunov function changes depending on the problem of interest —*cf.* Chapters 4 and 5.

Now, a barrier Lyapunov function for the multi-agent system is defined as the sum of the barrier Lyapunov functions (3.10) for each $k \leq M$, *i.e.*,

$$W(z) = \sum_{k \leq M} W_k(z_k). \tag{3.15}$$

The latter encodes the connectivity constraints in terms of the state of each edge present in the initial graph, and is used to design gradient-based control laws, as we show next.

3.2 FIRST-ORDER SYSTEMS

3.2.1 *Undirected graphs*

Consider a group of first-order systems interconnected over an undirected graph, as in (3.8). In the absence of inter-agent constraints, we know that under a control law of the form

$$u := -\left[E \otimes I_n\right] z,$$

which is equivalent to the classical consensus algorithm (2.13) in the node-based representation, the origin of the system (3.8) is asymptotically stable. However, since the system is subject to the sensing-range limitations encoded by the set $\mathcal{J}$ in (3.7), the control law is defined as

$$u := -c_1 \left[E \otimes I_n\right] \nabla W(z), \tag{3.16}$$

where $c_1 > 0$ is a design gain and $\nabla W(z)$ is the gradient of the barrier Lyapunov function in (3.15) encoding the state constraints. This is reminiscent of the potential-function-based control used in robotics, where the control law is taken as the gradient of a potential function encoding the constraints in the environment [30]. We emphasize that the gradient-based control input as defined in (3.16) is distributed. Indeed, in the undirected case the columns of E represent the edges at each node, that is, the available information to each agent as defined by the graph.

The control law (3.16) is defined in terms of the edge states of the whole graph z. However, recall that, from the identity (2.50), the edge states z are a function of the edges of a spanning tree contained in the graph, *i.e.*, $z = \left[R^\top \otimes I_n\right] z_t$. Therefore, $W(z) = W\left(\left[R^\top \otimes I_n\right] z_t\right)$. In what follows, and with a slight abuse of notation, we use the same symbol W to denote a function $z_t \mapsto W(z_t)$, defined as

$$W(z_t) := W\left(\left[R^\top \otimes I_n\right] z_t\right). \tag{3.17}$$

Note that $W(z_t)$ corresponds to the same quantity as $W(z)$ defined in (3.15). Indeed, the barrier Lyapunov function in (3.15) is defined as the sum of the functions (3.10) for all the edges $e_k \in \mathcal{E}$, $k \leq M$. Furthermore, again with a slight abuse of notation, using the chain rule, the derivative of the function defined in (3.17), with respect to z_t, yields

$$\nabla W(z_t) := \left[\frac{\partial z}{\partial z_t}\right]^\top \frac{\partial W(z)}{\partial z},$$

from which we obtain the identity

$$\nabla W(z_t) = \big[R \otimes I_n\big] \nabla W(z), \quad \nabla W(z) := \left[\frac{\partial W_1}{\partial z_1}^\top \cdots \frac{\partial W_M}{\partial z_M}^\top \right]^\top. \tag{3.18}$$

Now, using (2.48), in the reduced-order edge coordinates the control (3.16) becomes

$$u = -c_1 \big[E_t \otimes I_n\big] \nabla W(z_t). \tag{3.19}$$

Then, replacing (3.19) into (3.8), the closed-loop system reads

$$\dot{z}_t = -c_1 \big[E_t^\top E_t \otimes I_n\big] \nabla W(z_t), \tag{3.20}$$

or in expanded form

$$\dot{z}_t = -c_1 \big[E_t^\top E_t \otimes I_n\big] \big[R \otimes I_n\big] \nabla W(z), \tag{3.21}$$

For this system we have the following.

Proposition 3.1 ([105]). *Consider the system (3.20). Under Assumption 3.1, the controller (3.19) guarantees consensus with connectivity maintenance, i.e., (3.6) holds and the constraints set $\mathcal{J}$ defined in (3.7) is rendered forward invariant along closed-loop solutions. Furthermore the function $z_t \mapsto W(z_t)$ in (3.17) is a strict Lyapunov function for the closed-loop system (3.20).* □

Proof. For consistency in the notation, we redefine the constraint set (3.7) in terms of the edges of the spanning tree z_t as

$$\mathcal{J}_t := \left\{ z_t \in \mathbb{R}^{n(N-1)} : \left| \left[r_k^\top \otimes I_n \right] z_k \right| \in [0, \Delta_k) \,, \; \forall\, k \leq M \right\} \tag{3.22}$$

where r_k is the kth column of the matrix R in (2.47). Assume first that $\mathcal{J}$ (equivalently $\mathcal{J}_t$) is forward invariant; this hypothesis is relaxed below. Then, for all $z_t \in \mathcal{J}_t$, the derivative of $W(z_t)$ satisfies

$$\dot{W}(z_t) = -c_1 \nabla W(z_t)^\top \left[E_t^\top E_t \otimes I_n \right] \nabla W(z_t). \tag{3.23}$$

The matrix $E_t^\top E_t$ corresponds to the edge Laplacian of a spanning tree $\mathcal{G}_t \subset \mathcal{G}$ and, recalling Remark 2.2, it is symmetric positive definite. Therefore, denoting $c_1' = c_1 \lambda_{min}(E_t^\top E_t) > 0$, we have

$$\dot{W}(z_t) \leq -c_1' |\nabla W(z_t)|^2. \tag{3.24}$$

Thus, from the definition of (3.15) —see also (3.10)— $\dot{W}(z_t) < 0$ for all $z_t \in \mathcal{J}_t \backslash \{0\}$ and $z_t \mapsto W(z_t)$ is a strict Lyapunov function for the closed-loop system (3.20).

Now we establish connectivity maintenance, or equivalently forward invariance of the set $\mathcal{J}$. To that end, we remark that $z_t \in \mathcal{J}_t$ implies that $z \in \mathcal{J}$ and we show that $\mathcal{J}_t$ is forward

invariant. We proceed by contradiction. Assume that there exists $T > 0$ such that for all $t \in [0, T)$, $z_t(t) \in \mathcal{J}_t$ and $z_t(T) \notin \mathcal{J}_t$. More precisely, we have $|z_k(t)| \to \Delta_k$ as $t \to T$ for at least one $k \leq M$. From the definition of W, this implies that $W(z_t(t)) \to \infty$ as $t \to T$. However, the latter is in contradiction with (3.24) which implies that $W(z_t(t))$ is bounded. Therefore, we conclude that $W(z_t(t))$ is bounded for all the trajectories starting inside $\mathcal{J}_t$, *i.e.*, $W(z_t(t)) \leq W(z_t(0)) < \infty$ for all $z_t(0) \in \mathcal{J}_t$ and all $t \geq 0$. Connectivity preservation follows.

It is left to show that the set $\mathcal{J}$ corresponds to the domain of attraction for the closed-loop system. This follows by showing that all solutions of (3.20) starting in $\mathcal{J}_t$ converge to the origin. To that end, for any $\varepsilon \in (0, \Delta_k)$, consider a subset $\mathcal{J}_{\varepsilon t} \subset \mathcal{J}_t$ defined as

$$\mathcal{J}_{\varepsilon t} := \left\{ z_t \in \mathbb{R}^{n(N-1)} \,:\, |z_k| < \Delta_k - \varepsilon, \, \forall\, k \leq M \right\}$$

and let $\bar{\mathcal{J}}_{\varepsilon t}$, denote the closure of $\mathcal{J}_{\varepsilon t}$. From Definition 3.1, (3.10), and Assumption 3.3, $W(z_t)$ is positive definite on $\bar{\mathcal{J}}_{\varepsilon t}$ and it satisfies the bounds

$$\frac{\kappa_1}{2}|z_t|^2 \leq W(z_t) \leq h(|z_t|),$$

where $h(\cdot)$ is defined and strictly increasing everywhere in $\bar{\mathcal{J}}_{\varepsilon t}$, $h(s) > 0$ for all $s > 0$, and $h(0) = 0$. This means that $W(z_t) \to 0$ as $z_t \to 0$. Therefore, from (3.24), and standard Lyapunov theory, *e.g.*, [17, Chapter 3] it follows that all the trajectories of (3.20) starting in $\mathcal{J}_{\varepsilon t}$ converge to the origin. The previous arguments hold for any $\varepsilon \to 0$, so the origin is attractive for all trajectories $z_t(t)$ starting in $\mathcal{J}_t$, that is, for all trajectories $z(t)$ starting in $\mathcal{J}$. ■

Remark 3.3. *Proposition 3.1 is an original contribution of this thesis. It was presented in [105]. Similar statements may be found in [33], [34], but in the latter, only convergence is showed and no strict Lyapunov functions are proposed.* •

3.2.2 *Directed graphs*

In the case of directed topologies, the analysis of stability of the multi-agent systems in closed-loop with the consensus protocol with connectivity maintenance is not as straightforward as in the previous case. The difficulty comes from the fact that for directed graphs the edge Laplacian matrix $L_e = E^\top E_\odot$ is non-symmetric. As we shall see, the interaction topology and the properties of the edge Laplacian play fundamental roles in the stability analysis.

Now, akin to (3.16), the gradient control law is given by

$$u := -c_1 \left[E_\odot \otimes I_n \right] \nabla W(z). \tag{3.25}$$

Note that in this case $E_\odot$ represents the incoming edges on each node, which is, again, the available information to each agent as defined by the directed graph. Then, replacing (3.25) into (3.8), the closed-loop system reads

$$\dot{z}_t = -c_1 \left[E_t^\top E_\odot \otimes I_n \right] \nabla W(z) \tag{3.26}$$

and we have the following.

Proposition 3.2 ([106]). *Consider the system (3.26). If the initial directed graph satisfies Assumption 3.2, the controller (3.25) guarantees consensus with connectivity maintenance, i.e., (3.6) holds and the constraints set $\mathcal{J}$ defined in (3.7) is rendered forward invariant along closed-loop solutions. Furthermore the function $\tilde{W} : \mathcal{J} \to \mathbb{R}_{\geq 0}$, defined as*

$$\tilde{W}(z) = \sum_{k \leq M} \gamma_k W_k(z_k), \quad \gamma_k > 0, \quad \forall k \leq M \tag{3.27}$$

where W_k is defined in (3.10), is a strict Lyapunov function for the closed-loop system (3.26). □

Proof. First, note that we defined the barrier Lyapunov function in (3.27) as a function of z. Indeed, it encodes the connectivity constraints for all the edges present in the initial graph. However, recalling the identity $z = \left[R^\top \otimes I_n\right] z_t$, akin to (3.17), with a slight abuse of notation we use the same symbol $\tilde{W}$ to denote both functions $z \mapsto \tilde{W}(z)$ in (3.27) and

$$\tilde{W}(z_t) := \tilde{W}\left(\left[R^\top \otimes I_n\right] z_t\right). \tag{3.28}$$

Then, akin to (3.18), it holds that

$$\nabla \tilde{W}(z_t) = \left[R \otimes I_n\right] \nabla \tilde{W}(z), \quad \nabla \tilde{W}(z) := \begin{bmatrix} \gamma_1 \dfrac{\partial W_1}{\partial z_1}^\top & \cdots & \gamma_M \dfrac{\partial W_M}{\partial z_M}^\top \end{bmatrix}^\top. \tag{3.29}$$

Furthermore, recalling the barrier Lyapunov function W defined in (3.15) and defining $\Gamma := \operatorname{diag}\{\gamma_k\} \in \mathbb{R}^{M \times M}$, it holds that

$$\nabla \tilde{W}(z) = \left[\Gamma \otimes I_n\right] \nabla W(z). \tag{3.30}$$

Now, the derivative of $\tilde{W}$, along the trajectories of (3.26), is given by

$$\begin{aligned} \dot{\tilde{W}}(z_t) &= -c_1 \nabla \tilde{W}(z_t)^\top \left[E_t^\top E_\odot \otimes I_n\right] \nabla W(z) \\ &= -c_1 \nabla \tilde{W}(z)^\top \left[R^\top E_t^\top E_\odot \otimes I_n\right] \nabla W(z) \\ &= -c_1 \nabla W(z)^\top \left[\Gamma R^\top E_t^\top E_\odot \otimes I_n\right] \nabla W(z), \end{aligned} \tag{3.31}$$

and this equation holds regardless of the directed graph topology.

Next, we analyze separately the two considered cases: directed spanning trees and directed cycles.

Case 1 (Directed spanning tree). In this case we have $\mathcal{G} = \mathcal{G}_t$. Therefore, $z = z_t$, $E = E_t$, and $E_\odot = E_{\odot t}$, where $E_{\odot t}$ corresponds to the in-incidence matrix of a spanning tree —*cf.* (2.34). In turn, from the latter and the identity $E = E_t R$, we have $R = I_{N-1}$. Now, akin to (2.39), albeit with an abuse of notation, we denote the edge-Laplacian matrix of a directed spanning tree as $L_{et} := E_t^\top E_{\odot t} \in \mathbb{R}^{(N-1)\times(N-1)}$. Hence, (3.31) becomes

$$\dot{\tilde{W}}(z_t) = -\frac{c_1}{2} \nabla W(z_t)^\top \left[\Gamma L_{et} + L_{et}^\top \Gamma \otimes I_n\right] \nabla W(z_t). \tag{3.32}$$

Next, we show that the right hand side of (3.32) is negative definite. For that purpose, recalling the labeling of the edges suggested in Chapter 2 borrowed from [7] —see Figure 2.5, we have that the in-incidence matrix is given by

$$E_{\odot t} = \begin{bmatrix} 0_{N-1\times 1} & -I_{N-1} \end{bmatrix}^\top. \tag{3.33}$$

Then, using (2.33) and defining $B := -E_{\otimes t}^\top E_{\odot t}$, the edge Laplacian of a directed spanning tree satisfies

$$L_{et} = E_t^\top E_{\odot t} = E_{\odot t}^\top E_{\odot t} + E_{\otimes t}^\top E_{\odot t} = I_{N-1} - B. \tag{3.34}$$

Note that (3.34) holds since $E_{\odot t}^\top E_{\odot t} = I_{N-1}$ from (3.33).

Now, since $[E_{\otimes t}]_{ij} = 1$ implies that $[E_{\odot t}]_{ij} = 0$ and in view of the previously mentioned labeling $[E_{\otimes t}^\top]_{ij} = 0$ for $i < j$, it follows that B is a lower triangular matrix with zero diagonal and all other elements either equal to 0 or 1. Moreover, for a directed spanning tree, $\text{rank}(L_{et}) = N - 1$ and all the eigenvalues of L_{et} lie on the open right-hand complex plane; indeed, they coincide with the eigenvalues of the graph's Laplacian L. Thus, from the latter and (3.34), we conclude that L_{et} is a non-singular M-matrix [107], that is, a real matrix with positive diagonal, non-positive off-diagonal elements, and eigenvalues with strictly positive real parts. Then, after [107], every non-singular M-matrix is diagonally stable, that is, for any $Q = Q^\top > 0$, L_{et} admits a diagonal solution $\Gamma := \text{diag}\big[\gamma_k\big]$, to the Lyapunov inequality

$$\Gamma L_{e_t} + L_{e_t}^\top \Gamma \geq Q. \tag{3.35}$$

Therefore, redefining γ_k in (3.27), if necessary, so that (3.35) holds, we have

$$\dot{\tilde{W}}(z_t) \leq -c_1' \left|\nabla W(z_t)\right|^2, \tag{3.36}$$

where $c_1' := c_1\, \lambda_{min}(Q)$.

Case 2 (Directed cycle). Using the identity (2.48) in (3.31), and setting $\Gamma = I_M$ we have

$$\begin{aligned} \dot{\tilde{W}}(z_t) &= -\, c_1\, \nabla W(z)^\top \big[E^\top E_\odot \otimes I_n\big] \nabla W(z) \\ &= -\, \frac{c_1}{2}\, \nabla W(z)^\top \big[\big(E^\top E_\odot + E_\odot^\top E\big) \otimes I_n\big] \nabla W(z). \end{aligned} \tag{3.37}$$

Then, using again (2.33), we have that

$$E^\top E_\odot + E_\odot^\top E = E^\top E + E_\odot^\top E_\odot - E_\otimes^\top E_\otimes \tag{3.38}$$

Now, note that, following the same labeling rules mentioned above, the in-incidence and out-incidence matrices for a directed cycle are given by

$$E_\odot = \begin{bmatrix} 0_{1\times N-1} & -1 \\ -I_{N-1} & 0_{N-1\times 1} \end{bmatrix}, \quad E_\otimes = I_N.$$

Hence, we have $E_{\odot}^{\top}E_{\odot} = I_N$ and $E_{\otimes}^{\top}E_{\otimes} = I_N$. Consequently, using (3.38), (3.18) and (2.48), again, (3.37) becomes

$$\dot{\tilde{W}}(z_t) = -c_1\, \nabla W(z_t)^{\top}\left[E_t^{\top}E_t \otimes I_n\right]\nabla W(z_t), \tag{3.39}$$

where $E_t^{\top}E_t$, corresponds to the edge Laplacian of an undirected tree, which is symmetric positive definite —*cf.* Remark 2.2. Then, we have

$$\dot{\tilde{W}}(z_t) \leq -c_1'\left|\nabla W(z_t)\right|^2, \tag{3.40}$$

where, with a slight abuse of notation, $c_1' := c_1\, \lambda_{min}(E_t^{\top}E_t)$.

Hence, we see from (3.36) and (3.40) that $\dot{\tilde{W}}(z_t)$ is negative definite on $\mathcal{J}_t\backslash\{0\}$ for both of the considered directed topologies. Therefore, $\tilde{W}$ in (3.27) is a strict Lyapunov function for the closed-loop system (3.26).

Remark 3.4. *Note that for generic connected directed graphs the symmetric part of the directed edge Laplacian $E^{\top}E_{\odot}$ is not positive semi-definite. Indeed, in such cases, contrary to the case of a directed cycle, the identity $E^{\top}E_{\odot} + E_{\odot}^{\top}E = E^{\top}E$ does not hold —cf. (3.38). Moreover, for the in-incidence matrix of a general directed graph there does not exist an equivalent identity to $E = E_tR$ (2.48). Hence, unlike for connected undirected graphs, the directed edge Laplacian of a general directed graph cannot be transformed into the directed edge Laplacian of a spanning tree $E_t^{\top}E_{\odot t}$, which has a positive-definite symmetric part. Thus, the analysis of the constrained-consensus problem in edge coordinates over general directed graphs, via strict and input-to-state Lyapunov functions, is still an open problem.* •

In order to establish forward invariance of the set $\mathcal{J}_t$, and thus of $\mathcal{J}$, we proceed using the contradiction arguments as in the proof of Proposition 3.1. Assume that there exists $T > 0$ such that for all $t \in [0, T)$, $z_t(t) \in \mathcal{J}_t$ and $z_t(T) \notin \mathcal{J}_t$. More precisely, we have $|z_k(t)| \to \Delta_k$ as $t \to T$ for at least one $k \leq M$. From the definition of $\tilde{W}$ and W_k, this implies that $\tilde{W}(z_t(t)) \to \infty$ as $t \to T$ which is in contradiction with (3.36) and (3.40). We conclude that $\tilde{W}(z_t(t))$ is bounded for all initial conditions in $\mathcal{J}_t$, *i.e.*, $\tilde{W}(z_t(t)) \leq \tilde{W}(z_t(0)) < \infty$ for all $z_t(0) \in \mathcal{J}_t$ and all $t \geq 0$. Connectivity preservation follows from the forward invariance of $\mathcal{J}_t$.

It is left to show that the set $\mathcal{J}$ corresponds to the domain of attraction for the closed-loop system. This follows by showing that all solutions of (3.26) starting in $\mathcal{J}_t$ converge to the origin. To that end, for any $\varepsilon \in (0, \Delta_k)$, consider a subset $\mathcal{J}_{\varepsilon t} \subset \mathcal{J}_t$ defined as $\mathcal{J}_{\varepsilon t} := \{z_t \in \mathbb{R}^{n(N-1)} : |z_k| < \Delta_k - \varepsilon,\ \forall\, k \leq M\}$ and let $\bar{\mathcal{J}}_{\varepsilon t}$, denote the closure of $\mathcal{J}_{\varepsilon t}$. From (3.27) and akin to (3.11), it follows that $\tilde{W}(z_t)$ is positive definite on $\bar{\mathcal{J}}_{\varepsilon t}$ and it satisfies the bounds

$$\frac{\kappa_1}{2}|z_t|^2 \leq \tilde{W}(z_t) \leq \tilde{h}(|z_t|),$$

where $\tilde{h}(\cdot)$ is defined and strictly increasing everywhere in $\bar{\mathcal{J}}_{\varepsilon t}$, $\tilde{h}(s) > 0$ for all $s > 0$, and $\tilde{h}(0) = 0$. This means that $\tilde{W}(z_t) \to 0$ as $z_t \to 0$. Therefore, from (3.36), (3.40), and standard Lyapunov theory it follows that all trajectories of (3.26) starting in $\mathcal{J}_{\varepsilon t}$ converge to the origin. The previous arguments hold for any $\varepsilon \to 0$, so the origin is attractive for all trajectories $z_t(t)$ starting in $\mathcal{J}_t$, that is, for all trajectories $z(t)$ starting in $\mathcal{J}$. ■

We stress that a direct consequence of the proof of Propositions 3.1 and 3.2, which rely on the construction of strict Lyapunov functions, is that the origin $\{z_t = 0\}$ of (3.20) and (3.26), respectively for the case of undirected and directed graphs, is asymptotically stable with $\mathcal{J}_t$ as the domain of attraction. As we have explained, the importance of disposing of a strict Lyapunov function as opposed to merely guaranteeing a convergence property is to establish robustness of the system with respect to external disturbances, as we show next. Even though in this section we only address consensus of single integrators, the stability and robustness properties obtained for this case-study serve as basis for similar statements concerning more complex systems, as we present in subsequent chapters and, to the best of our knowledge are original contributions of [105], [106].

3.2.3 *Robustness analysis*

Using the explicit construction of the strict Lyapunov functions provided in Propositions 3.1 and 3.2, we are able to conduct a robustness analysis of the control laws (3.19) and (3.25) for first-order integrators interconnected over undirected and directed topologies, respectively.

Consider the case of a single-integrator system with an additive bounded disturbance $d_i \in \mathbb{R}^n$, that is,

$$\dot{p}_i = u_i + d_i. \tag{3.41}$$

Recalling the edge transformation (3.4) and the identity (2.50), the reduced-order system reads

$$\dot{z}_t = -c_1 \left[E_t^\top \otimes I_n\right] u + \left[E_t^\top \otimes I_n\right] d \tag{3.42}$$

where $d := \left[d_1^\top \cdots d_N^\top\right]^\top \in \mathbb{R}^{nN}$. Next, the robustness results are presented separately for undirected and directed topologies.

3.2.3.1 *Undirected topologies*

Implementing the control law (3.19), the reduced order system (3.42) in closed loop becomes

$$\dot{z}_t = -c_1 \left[E_t^\top E_t \otimes I_n\right] \nabla W(z_t) + \left[E_t^\top \otimes I_n\right] d. \tag{3.43}$$

The result is stated in the following Proposition.

Proposition 3.3 ([105]). *The closed-loop multi-agent system (3.43), with a communication topology given by an undirected graph satisfying Assumption 3.1, is input-to-state stable*[4] *with respect to an essentially bounded, locally integrable external disturbance d. Furthermore, the graph remains connected for all $t \geq 0$.* □

4 See Appendix A.1 for a definition.

Proof. The proof uses the strict Lyapunov function defined in (3.15) and (3.10). Differentiating (3.15) with respect to time and recalling (3.18) we obtain

$$\dot{W}(z_t) = -c_1 \nabla W(z_t)^\top \left[E_t^\top E_t \otimes I_n\right] \nabla W(z_t) + \nabla W(z_t)^\top \left[E_t^\top \otimes I_n\right] d. \tag{3.44}$$

Now, given c_1 let $\delta > 0$ be such that $c_1' := \left(c_1 - \frac{1}{2\delta}\right) \lambda_{min}(E_t^\top E_t) > 0$. Then, using Young's inequality on the second term of the right-hand side of (3.44) we have

$$\dot{W}(z_t) \leq -c_1' \left|\nabla W(z_t)\right|^2 + \frac{\delta}{2}|d|^2 \tag{3.45}$$

Thus, the system (3.43) is input-to-state stable with respect to bounded external input d.

In order to show connectivity maintenance it suffices to show that in the proximity of the limits of the connectivity region, that is, as $|z_k| \to \Delta_k$ for any $k \leq M$, the first term on the right-hand side of Inequality (3.45) dominates over the second term, which is bounded by assumption. More precisely, let $\bar{d} := ||d(t)||_\infty$ and $\varepsilon \in (0, \Delta_k)$ be an arbitrarily small constant. Let z_t be such that, there exists at least one $k \leq M$ such that $|z_k| \geq (\Delta_k - \varepsilon)$. Then, $|z_t| \geq \Delta_k - \varepsilon$. From (3.45), the definition of $W(z_t)$ in (3.15) and (3.11), we have

$$\begin{aligned}
\dot{W}(z_t) \leq & - c_1 \left|\nabla W_k(z_k)\right|^2 + \frac{\delta}{2}|d|^2 \\
\leq & - \frac{c_1}{\kappa_2} h_k(\Delta_k - \varepsilon) + \frac{\delta}{2}|d|^2
\end{aligned}$$

In turn, from Definition 3.1 and Assumption 3.3 we have that $h_k(\cdot)$ is continuous, non-decreasing, and $h_k(s) \to \infty$ as $|s| \to \Delta_k^2$ for at least one $k \leq M$. Then, there exists $\varepsilon^*(\bar{d}) > 0$ such that for all $\varepsilon < \varepsilon^*$, $\dot{W}(z_t) \leq 0$. Hence, connectivity maintenance follows from the same arguments used in the proof of Proposition 3.1. ■

3.2.3.2 *Directed topologies*

Replacing the constrained-consensus protocol (3.25) into (3.42), the closed-loop reduced-order edge system reads

$$\dot{z}_t = -c_1 \left[E_t^\top E_\odot \otimes I_n\right] \nabla W(z) + \left[E_t^\top \otimes I_n\right] d. \tag{3.46}$$

Proposition 3.4 ([106])**.** *If the directed communication topology satisfies Assumption 3.2, the closed-loop multi-agent system (3.46) is input-to-state stable with respect to a bounded locally integrable disturbance d. Furthermore, the graph remains connected for all $t \geq 0$.* □

Proof. Consider the barrier Lyapunov function (3.27). Under the standing assumption that the graph is either a directed spanning tree or a directed cycle, using (3.36) and (3.40), the total derivative of (3.27) along (3.46) satisfies

$$\dot{\tilde{W}}(z_t) \leq -c_1'' \left|\nabla W(z_t)\right|^2 + \frac{\delta}{2}|d|^2. \tag{3.47}$$

where we used Young's inequality to obtain the right-hand side of (3.47) with $\delta > 0$ and $c_1'' := \left(c_1' - \frac{\gamma_{min}^2}{2\delta}\right) > 0$. Thus, the system (3.46) is input-to-state stable with respect to bounded external input d.

Now, for the two considered classes of directed graphs, modulo a constant gain, the bound (3.47) is equivalent to that obtained for undirected graphs in (3.44). Therefore, the proof of connectivity maintenance follows after similar arguments as in the proof of Proposition 3.3. ■

3.3 SECOND-ORDER SYSTEMS

We now extend the previous results for first-order systems to second-order systems. More precisely we show how a gradient-based consensus control achieves position-consensus with connectivity maintenance for second-order systems. For second-order systems, the position-consensus problem under connectivity constraints, may be formulated as follows.

Consider that each agent composing the system is described by a second-order integrator of the form

$$\dot{p}_i = v_i \tag{3.48a}$$
$$\dot{v}_i = u_i \tag{3.48b}$$

where $p_i \in \mathbb{R}^n$ and $v_i \in \mathbb{R}^n$ are respectively, the position and the velocity of agent $i \leq N$, and $u_i \in \mathbb{R}^n$ is the control input. Denoting $v = \begin{bmatrix} v_1^\top & \cdots & v_N^\top \end{bmatrix}^\top \in \mathbb{R}^{nN}$ and using again the edge transformation (3.4), the second-order multi-agent system (3.48), becomes

$$\dot{z} = \left[E^\top \otimes I_n\right] v \tag{3.49a}$$
$$\dot{v} = u. \tag{3.49b}$$

In these coordinates, the position-consensus objective is that

$$\lim_{t\to\infty} z(t) = 0 \tag{3.50a}$$
$$\lim_{t\to\infty} v(t) = 0. \tag{3.50b}$$

Then, as for the first-order systems, in addition to (3.50), the connectivity maintenance objective is to render the constraints set (3.7) forward invariant.

Now, recalling again the reduced-order edge representation in Section 2.3.2, we know that the position-consensus objective (3.50) for second-order systems is achieved if it is achieved for the reduced-order system given by

$$\dot{z}_t = \left[E_t^\top \otimes I_n\right] v \tag{3.51a}$$
$$\dot{v} = u, \tag{3.51b}$$

Hence, the objective is to render the reduced-order system (3.51) asymptotically stable at the origin and, in light of Assumptions 3.1 and 3.2, render the constraints set (3.7) forward invariant, *i.e.*, that $z(t_0) \in \mathcal{J}$ implies that $z(t) \in \mathcal{J}$ for all $t \geq 0$.

As for the first-order systems, we start by studying the systems interconnected over undirected topologies. Then, we present the results for directed graphs.

3.3.1 *Undirected graphs*

Let us consider the second-order system in the reduced-order edge representation (3.51). Recalling the barrier Lyapunov function for the multi-agent systems defined in (3.15), akin to (3.19), we introduce the control law

$$u := -c_1 \left[E_t \otimes I_n\right] \nabla W(z_t) - c_2\, v, \tag{3.52}$$

where c_1, $c_2 > 0$ are the control gains.

Replacing (3.52) into (3.51), the closed-loop system reads

$$\dot{z}_t = v \tag{3.53a}$$

$$\dot{v} = -\, c_1 \left[E_t^\top E_t \otimes I_n\right] \nabla W(z_t) - c_2\, v. \tag{3.53b}$$

Then, we have the following.

Proposition 3.5 ([105]). *Consider the closed-loop system (3.53). Under Assumption 3.1, the controller (3.19) guarantees consensus with connectivity maintenance, i.e., (3.50) holds and the constraints set $\mathcal{J}$ defined in (3.7) is rendered forward invariant. Furthermore, the function*

$$V(z_t, v) = c_1\, W(z_t) + \frac{1}{2}|v|^2 + c_3\, z_t^\top \left[(E_t^\top E_t)^{-1} E_t^\top \otimes I_n\right] v + \frac{c_2 c_3}{2} z_t^\top \left[(E_t^\top E_t)^{-1} \otimes I_n\right] z_t, \tag{3.54}$$

where $0 < c_3 < c_2$, is a strict Lyapunov function for the closed-loop system (3.53). □

Proof. First, note that V in (3.54) can also be written as

$$V(z_t, v) = c_1\, W(z_t) + \frac{1}{2} \begin{bmatrix} z_t \\ v \end{bmatrix}^\top \left[\begin{bmatrix} c_2 c_3 (E_t^\top E_t)^{-1} & c_3 (E_t^\top E_t)^{-1} E_t^\top \\ c_3 E_t (E_t^\top E_t)^{-1} & I_N \end{bmatrix} \otimes I_n \right] \begin{bmatrix} z_t \\ v \end{bmatrix}. \tag{3.55}$$

Now, recall that under Assumption 3.1, the matrix $E_t^\top E_t$ is the edge Laplacian of a spanning tree —see Remark 2.2. Hence, the matrix $(E_t^\top E_t)^{-1}$ exists and is positive definite. Then, positive-definiteness of V in z_t and v follows after computing the Schur complement on the second term of the right-hand side of (3.55).

Now, taking the time derivative of (3.55) we obtain

$$\begin{aligned} \dot{V}(z_t, v) = & c_1 \nabla W(z_t)^\top \left[E_t^\top \otimes I_n\right] v - c_1 \nabla W(z_t)^\top \left[E_t^\top \otimes I_n\right] v - c_2 v^\top v \\ & - c_1 c_3 z_t^\top \left[(E_t^\top E_t)^{-1} E_t^\top E_t \otimes I_n\right] \nabla W(z_t) - c_2 c_3 z_t^\top \left[(E_t^\top E_t)^{-1} E_t^\top \otimes I_n\right] v \\ & + c_3\, v^\top \left[E_t (E_t^\top E_t)^{-1} E_t^\top \otimes I_n\right] v + c_2 c_3\, z_t^\top \left[(E_t^\top E_t)^{-1} E_t^\top \otimes I_n\right] v \\ = & - c_1 c_3 z_t^\top W(z_t) - v^\top \left[(c_2 I - c_3 E_t (E_t^\top E_t)^{-1} E_t^\top) \otimes I_n\right] v. \end{aligned} \tag{3.56}$$

Remark 3.5. *For the barrier Lyapunov function encoding the proximity constraints as defined in* (3.10) *and satisfying Assumption 3.3, it holds that*

$$\nabla W_k(z_k) = \psi_k(z_k) z_k \tag{3.57}$$

where $\psi_k : \mathcal{J}_k \to \mathbb{R}_{>0}$ *is a non-decreasing function on* $\mathcal{J}_k$ *such that, there exists a positive constant* ψ_0 *such that* $\psi_k(z_k) \geq \psi_0 > 0$ *for all* $z_k \in \mathcal{J}_k$*, and* $\psi_k(z_k) \to \infty$ *as* $|z_k| \to \Delta_k$ *—cf.* [33], [34] *and the so-called connectivity potential in* [106]*. Furthermore, from the definition of* W *in* (3.15) *and using* (3.57)*, it holds that*

$$\nabla W(z_t) = \Psi(z_t) z_t \tag{3.58}$$

where $\Psi(z_t) := \text{diag}\{\psi_k\} \in \mathbb{R}^{(N-1)\times(N-1)}$. •

Now, since the non-zero eigenvalues of L and of L_{et} coincide, it holds that

$$\lambda_{max}(E_t(E_t^\top E_t)^{-1}E_t^\top) = \lambda_{max}(E_t^\top E_t(E_t^\top E_t)^{-1}) = 1.$$

Then, from Remark 3.5, letting $c_1' := c_1 c_3 \psi_0$ and $c_2' := (c_2 - c_3)$, we obtain

$$\dot{V}(z_t, v) = -c_1'|z_t|^2 - c_2'|v|^2. \tag{3.59}$$

It follows that $\dot{V}(z_t, v) < 0$ in $\mathcal{J}_t \times \mathbb{R}^{nN} \backslash \{0, 0\}$. Therefore, V as defined in (3.54) is a strict Lyapunov function for the system (3.53).

Forward invariance of $\mathcal{J}$ is inferred using the same arguments as in the proof of Proposition 3.1. Thus, connectivity is preserved for any initial conditions satisfying $(z(0), v(0)) \in \mathcal{J} \times \mathbb{R}^{nN}$. Finally, note that $V(z_t, v)$ is positive definite for all $v \in \mathbb{R}^{nN}$ and all $z_t \in \bar{\mathcal{J}}_{\varepsilon t}$ and satisfies

$$\kappa_1|z_t|^2 + \kappa_1'|v|^2 \leq V(z_t, v) \leq h(|z_t|) + \kappa_2'|v|^2, \tag{3.60}$$

where κ_1, κ_1', and κ_2' are positive constants and $h(\cdot)$ is a positive strictly increasing function defined everywhere in $\bar{\mathcal{J}}_{\varepsilon t}$ satisfying $h(0) = 0$. This means that $V(z_t, v) \to 0$ as $(z_t, v) \to (0, 0)$. Therefore, from (3.59) we have that for all trajectories of the closed-loop system starting in $\mathcal{J}_{\varepsilon t} \times \mathbb{R}^{nN}$, the origin is asymptotically stable, *i.e.*, $v_i(t) \to 0$ $\forall i \leq N$ and $z_k(t) \to 0$ $\forall k \leq M$. Moreover, since ε can be chosen arbitrarily small, taking the limit $\varepsilon \to 0$, we establish asymptotic stability of the origin of the closed-loop system for all trajectories starting in $\mathcal{J}_t \times \mathbb{R}^{nN}$. Thus, consensus is achieved with preserved connectivity. ■

3.3.2 *Directed graphs*

Relying on the strict Lyapunov function provided in Proposition 3.2, we use a backstepping approach for our proposed control design for constrained consensus of second-order integrators interconnected over directed graphs. This underlines another perk of the contribution in Proposition 3.2. Indeed, the strict Lyapunov function $\tilde{W}$ is herein used in a Lyapunov-based control design to achieve the position-consensus objective (3.50) with connectivity maintenance.

Let us consider the second-order system in the reduced-order edge representation (3.51). We follow a standard backstepping procedure [108]. First we consider a virtual input $z \mapsto v^*(z)$, satisfying $v^*(0) = 0$, that stabilizes the origin for the subsystem (3.51a). Next, the input u is designed so that $v(t) \to v^*(z(t))$ as $t \to \infty$.

Akin to (3.25), the virtual control v^* is defined as

$$v^*(z) := -c_1 \left[E_\odot \otimes I_n\right] \nabla W(z). \tag{3.61}$$

where $W(z)$ is the barrier Lyapunov function defined in (3.15). Then, defining the error variable $\tilde{v} := v - v^*$ and using (3.61) and (3.51), the error system reads

$$\dot{z}_t = -\, c_1 \left[E_t^\top E_\odot \otimes I_n\right] \nabla W(z) + \left[E_t^\top \otimes I_n\right] \tilde{v} \tag{3.62a}$$

$$\dot{\tilde{v}} = u + \dot{v}^*. \tag{3.62b}$$

Thus, using the feedback-linearizing control law

$$u := -c_2 \tilde{v} + \dot{v}^* \tag{3.63}$$

with $c_2 > 0$, we obtain the closed-loop system:

$$\dot{z}_t = -\, c_1 \left[E_t^\top E_\odot \otimes I_n\right] \nabla W(z) + \left[E_t^\top \otimes I_n\right] \tilde{v} \tag{3.64a}$$

$$\dot{\tilde{v}} = -\, c_2\, \tilde{v}, \tag{3.64b}$$

and we obtain the following.

Proposition 3.6 ([106]). *Consider the closed-loop system (3.64). If the initial directed graph satisfies Assumption 3.2, the controller (3.63) guarantees consensus with connectivity maintenance, i.e., (3.50) holds and the constraints set $\mathcal{J}$ defined in (3.7) is rendered forward invariant along closed-loop solutions. Furthermore, the function*

$$V(z_t, \tilde{v}) = \tilde{W}(z_t) + \frac{c_3}{2} |\tilde{v}|^2, \tag{3.65}$$

where $c_3 > 0$ and $\tilde{W}$ is given in (3.27), is a strict Lyapunov function for the closed-loop system (3.64). □

Proof. In view of (3.36) and (3.40), the total derivative of V along the trajectories of (3.64) satisfies

$$\begin{aligned} \dot{V}(z_t, \tilde{v}) &\leq -\, c_1' \left|\nabla W(z_t)\right|^2 - c_2 c_3 |\tilde{v}|^2 + \nabla \tilde{W}(z_t)^\top \left[E_t^\top \otimes I_n\right] \tilde{v} \\ &\leq -\, c_1' \left|\nabla W(z_t)\right|^2 - c_2 c_3 |\tilde{v}|^2 + \nabla W(z_t)^\top \left[\Gamma E_t^\top \otimes I_n\right] \tilde{v}. \end{aligned} \tag{3.66}$$

Note that this bound holds indistinctly for directed-cycle topologies and for directed-spanning-tree graphs.

Now, given c_1', c_3 and $\gamma_{max} := \max_{k\leq M}\{\gamma_k\}$, let $\delta > 0$ be such that $c_1'' := c_1' - \frac{1}{2}\delta\gamma_{max}^2\lambda_{max}(E_t^\top E_t)$ and $c_2' := c_2c_3 - \frac{1}{2\delta}$ are positive. Then, after applying Young's inequality to the third term in the right-hand side of (3.66), we obtain

$$\dot{V}(z_t,\tilde{v}) \leq -c_1''\left|\nabla W(z_t)\right|^2 - c_2'|\tilde{v}|^2. \tag{3.67}$$

Thus, $\dot{V}(z_t,v) < 0$ for all $(z_t,v) \in \{\mathcal{J}_t \times \mathbb{R}^{nN}\}\backslash\{(0,0)\}$ and V in (3.65) is a strict Lyapunov function for the closed-loop system (3.64).

Forward invariance of the set $\mathcal{J}_t$, hence of $\mathcal{J}$, follows from the same arguments as in the proof of Proposition 3.2. Consequently, the connectivity of $\mathcal{G}$ is preserved for any $z(0) \in \mathcal{J}$ and for any $v(0)$. Finally, note that

$$\kappa_1|z_t|^2 + \kappa_1'|\tilde{v}|^2 \leq V(z_t,\tilde{v}(t)) \leq \tilde{h}(|z_t|) + \kappa_2'|\tilde{v}|^2 \tag{3.68}$$

where κ_1, κ_1', κ_2' are positive constants and $\tilde{h}(\cdot)$ is defined and strictly increasing everywhere in $\bar{\mathcal{J}}_{\varepsilon t}$ and satisfies $\tilde{h}(0) = 0$. Thus, following the same arguments as in the proof of Proposition 3.5, we establish asymptotic stability of the origin for all trajectories of (3.64) starting in $\mathcal{J}$. ■

3.3.3 *Robustness analysis*

As for the first-order systems in this section we use such strict Lyapunov functions provided in order to establish robustness in the sense of input-to-state stability of the edge-based consensus with connectivity preservation over undirected and directed graphs.

Consider a second-order system with an bounded external input, *i.e.*,

$$\dot{p}_i = v_i \tag{3.69a}$$
$$\dot{v}_i = u_i + d_i, \tag{3.69b}$$

where $d_i : \mathbb{R}_{\geq 0} \to \mathbb{R}^n$ is a locally integrable function. Akin to (3.51), recalling the edge transformation (3.4) and the identity (2.50), the reduced-order edge system is given by

$$\dot{z}_t = \left[E_t^\top \otimes I_n\right]v \tag{3.70a}$$
$$\dot{v} = u + d \tag{3.70b}$$

where $d := \begin{bmatrix} d_1^\top & \cdots & d_N^\top \end{bmatrix}^\top \in \mathbb{R}^{nN}$. Next, we present the robustness results for undirected and directed topologies separately.

3.3.3.1 *Undirected graphs*

Applying control law (3.52), the reduced-order system (3.70) in closed loop becomes

$$\dot{z}_t = \left[E_t^\top \otimes I_n\right]v \tag{3.71a}$$
$$\dot{v} = -c_1\left[E_t \otimes I_n\right]\nabla W(z_t) - c_2\, v + d \tag{3.71b}$$

Then, we have the following.

Proposition 3.7 ([105]). *The closed-loop multi-agent system (3.71) with a communication topology given by an undirected graph satisfying Assumption 3.1, is input-to-state stable with respect to an essentially bounded, locally integrable external disturbance d. Furthermore, the graph remains connected for all $t \geq 0$.* □

Proof. Taking the Lyapunov function $V(z_t, v)$ defined in (3.54) and differentiating with respect to time we obtain

$$\begin{aligned}
\dot{V}(z_t, v) = & c_1 \nabla W(z_t)^\top \left[E_t^\top \otimes I_n\right] v - c_2 v^\top v - c_1 \nabla W(z_t)^\top \left[E_t^\top \otimes I_n\right] v \\
& - c_1 c_3 z_t^\top \left[(E_t^\top E_t)^{-1} E_t^\top E_t \otimes I_n\right] \nabla W(z_t) - c_2 c_3 z_t^\top \left[(E_t^\top E_t)^{-1} E_t^\top \otimes I_n\right] v + v^\top d \\
& + c_3 z_t^\top \left[(E_t^\top E_t)^{-1} E_t^\top \otimes I_n\right] d + c_3 v^\top \left[E_t (E_t^\top E_t)^{-1} E_t^\top \otimes I_n\right] v \\
& + c_2 c_3 z_t^\top \left[(E_t^\top E_t)^{-1} E_t^\top \otimes I_n\right] v \\
= & - c_1 c_3 z_t^\top \nabla W(z_t) - v^\top \left[(c_2 I - c_3 E_t (E_t^\top E_t)^{-1} E_t^\top) \otimes I_n\right] v \\
& + v^\top d + c_3 z_t^\top \left[(E_t^\top E_t)^{-1} E_t^\top \otimes I_n\right] d,
\end{aligned} \tag{3.72}$$

where we recall again that, under Assumption 3.1, the matrix $(E_t^\top E_t)^{-1}$ exists and is positive definite.

Given c_2 and c_3 satisfying $c_2 > c_3$, let $\delta > 0$ be such that $c_2' := \left(c_2 - c_3 - \frac{1}{2\delta}\right) > 0$ and using Young's inequality on the third and fourth terms of the right-hand side of (3.72), we obtain

$$\begin{aligned}
\dot{V}(z_t, v) \leq & - c_1 c_3 z_t^\top \nabla W(z_t) - v^\top \left[\left(\left(c_2 - \frac{1}{2\delta}\right) I - c_3 E_t (E_t^\top E_t)^{-1} E_t^\top\right) \otimes I_n\right] v \\
& + \frac{c_3^2}{2\delta} z_t^\top \left[(E_t^\top E_t)^{-1} \otimes I_n\right] z_t + \delta |d|^2 \\
\leq & - c_1 c_3 z_t^\top \nabla W(z_t) + \frac{c_3^2}{2\delta} \lambda_{max}((E_t^\top E_t)^{-1}) |z_t|^2 - c_2' |v|^2 + \delta |d|^2
\end{aligned} \tag{3.73}$$

Then, from Remark 3.5 and (3.73) we have

$$\dot{V}(z_t, v) \leq -c_1' |z_t|^2 - c_2' |v|^2 + \delta |d|^2 \tag{3.74}$$

where $c_1' := c_3 \left(c_1 \psi_0 - \frac{c_3^2}{2\delta} \lambda_{max}\left((E_t^\top E_t)^{-1}\right)\right)$. Note that c_1' can be made positive by choosing δ sufficiently large. Now, defining $\zeta := \left[z_t^\top \; v^\top\right]^\top$, the derivative of V becomes

$$\dot{V}(\zeta) \leq -c' |\zeta|^2 + \delta |d|^2 \tag{3.75}$$

where $c' := \min\{c_1', c_2'\}$. Thus, the system (3.71) is input-to-state stable with respect to the bounded disturbance d.

Similarly to the case of first-order systems we need to show that as $|z_k| \to \Delta_k$ for any $k \leq M$, $\dot{V}(z_t, v) \leq 0$. More precisely, let $\bar{d} := ||d(t)||_\infty$ and $\varepsilon \in (0, \Delta_k)$ be an arbitrarily

small constant. Let z_t be such that, for at least one $k \leq M$ such that $|z_k| \geq (\Delta_k - \varepsilon)$. Then, $|z_t| \geq (\Delta_k - \varepsilon)$, so from Remark 3.5 and (3.73), it holds that

$$\dot{V}(z_t, v) \leq -c_1 c_3 \psi_k(\Delta_k - \varepsilon)(\Delta_k - \varepsilon)^2 + \frac{c_3^2}{2\delta}\lambda_{max}((E_t^\top E_t)^{-1})(\Delta_k - \varepsilon)^2 - c_2'|v|^2 + \delta|d|^2 \quad (3.76)$$

Since $\psi_k(\cdot)$ is continuous, non-decreasing, and $\psi_k(s_k) \to \infty$ as $|s_k| \to \Delta_k^2$ for at least one $k \leq M$, there exists $\varepsilon^*(\bar{d}) > 0$ such that for all $\varepsilon < \varepsilon^*$, $\dot{V}(z_t, v) \leq 0$. Then, connectivity maintenance follows from the same arguments as in Proposition 3.5. ■

3.3.3.2 *Directed graphs*

Let a virtual control input v^* be defined as in (3.61) and take u as (3.63). Akin to (3.64), the closed-loop error system takes the form

$$\dot{z}_t = -c_1 \left[E_t^\top E_\odot \otimes I_n\right] \nabla W(z) + \left[E_t^\top \otimes I_n\right] \tilde{v} \quad (3.77a)$$

$$\dot{\tilde{v}} = -c_2 \tilde{v} + d. \quad (3.77b)$$

Proposition 3.8 ([106]). *If the directed communication topology satisfies Assumption 3.2, then the closed-loop multi-agent system (3.77) is input-to-state stable with respect to an essentially bounded, locally integrable disturbance d. Furthermore, the graph remains connected for all $t \geq 0$.* □

Proof. Consider the Lyapunov function defined in (3.65). Then, from (3.67) and (3.77), under the standing assumption that the graph is either a directed spanning tree or a directed cycle, the total derivative of (3.65) satisfies

$$\dot{V}(z_t, \tilde{v}) \leq -c_1'' \left|\nabla W(z_t)\right|^2 - c_2'|\tilde{v}|^2 + c_3 \tilde{v}^\top d. \quad (3.78)$$

Next, given c_2' and c_3 let $\delta' > 0$ be such that $c_2'' := c_2' - c_3/(2\delta') > 0$. Applying Young's inequality to the third term on the right-hand side of (3.78), and using (3.11), we obtain

$$\begin{aligned} \dot{V}(z_t, \tilde{v}) \leq & -c_1'' \left|\nabla W(z_t)\right|^2 - c_2''|\tilde{v}|^2 + \frac{c_3\delta'}{2}|d|^2 \\ \leq & -\frac{c_1''\kappa_1}{2\kappa_2}|z_t|^2 - c_2''|\tilde{v}|^2 + \frac{c_3\delta'}{2}|d|^2 \end{aligned} \quad (3.79)$$

where κ_1 and κ_2 are positive constants. Thus, the system (3.77) is input-to-state stable.

To assert connectivity preservation in presence of additive disturbances, we show that in the proximity of the limits of the connectivity region the first term on the right-hand side of (3.79) dominates over the bounded disturbance. To that end, let $\bar{d} := ||d(t)||_\infty$ and let $\varepsilon \in (0, \Delta_k)$ be a small constant to be determined. Let $z_t \in \mathbb{R}^{n(N-1)}$ be such that for some $k \leq M$ we have $|z_k| \geq \Delta_k - \varepsilon$. Then, $|z_t| \geq \Delta_k - \varepsilon$, so from (3.79), Definition 3.1, and Assumption 3.3, we have

$$\begin{aligned} \dot{V}(z_t, \tilde{v}) \leq & -c_1''|\nabla W_k(z_k)|^2 - c_2''|\tilde{v}|^2 + \frac{c_3\delta'}{2}\bar{d}^2 \\ \leq & -\frac{c_1''\kappa_1}{\kappa_2}h_k(\Delta_k - \varepsilon) - c_2''|\tilde{v}|^2 + \frac{c_3\delta'}{2}\bar{d}^2 \end{aligned}$$

Since $h_k(s)$ is continuous, non-decreasing, and $h_k(s) \to \infty$ as $s \to \Delta_k^2$ it follows that there exists $\varepsilon^*(\bar{d})$ such that for all $\varepsilon \leq \varepsilon^*$, $\dot{V}(z_t, \tilde{v}) < 0$. The latter holds along trajectories starting from any initial conditions $z(0) \in \mathcal{J}$ which implies that $z(t)$ cannot approach the boundary of $\mathcal{J}$ so connectivity is preserved for all $t \geq 0$. ■

3.4 NUMERICAL EXAMPLE

In this section, we present a numerical example that demonstrates the performance of the edge-based consensus algorithms with connectivity maintenance for multiple second-order integrators interconnected over directed graphs. Concretely, in the simulation scenario we consider a multi-agent system composed of six agents described by the double-integrator model (3.48). The initial conditions as well as the radii of the connectivity regions for each agent are presented in Table 3.1 —see also Figure 3.4.

Table 3.1: Initial conditions and range constraints

Index	x_i **[m]**	y_i **[m]**	$v_{x,i}$ **[m/s]**	$v_{y,i}$ **[m/s]**	Δ_i **[m]**
1	2.4	-0.5	-5.0	0.0	2.5
2	-0.58	-0.9	0.0	0.0	3.2
3	4.5	2.0	3.0	0.0	3.8
4	5.0	-2.0	2.0	0.0	3.5
5	-4.0	-0.45	0.0	0.0	3.7
6	-2.0	-4.2	0.0	0.0	4.0

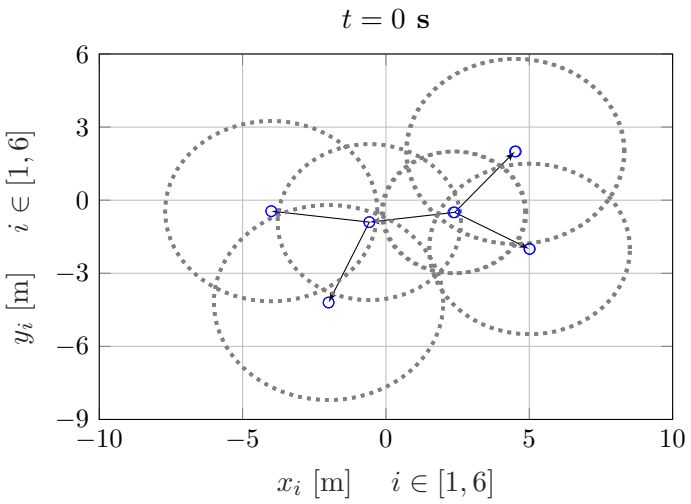

Figure 3.4: Initial configuration of the multi-agent system for the simulation scenario. The dotted gray circles represent the communication zones of each agent.

It is clear from Figure 3.4 that the initial proximity graph representing the available information to the agents of the system is a directed spanning tree. Indeed, the initial graph is represented in Figure 3.5.

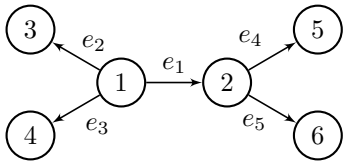

Figure 3.5: Example of a labeled directed spanning tree graph for six agents.

Note that the graph in Figure 3.5 has been labeled following the rules presented in Section 2.3.2. Using this labeling the incidence, in-incidence, and edge Laplacian matrices of the graph in Figure 3.5 are given by

$$E_t = \begin{bmatrix} 1 & 1 & 1 & 0 & 0 \\ -1 & 0 & 0 & 1 & 1 \\ 0 & -1 & 0 & 0 & 0 \\ 0 & 0 & -1 & 0 & 0 \\ 0 & 0 & 0 & -1 & 0 \\ 0 & 0 & 0 & 0 & -1 \end{bmatrix} \quad E_{\odot t} = \begin{bmatrix} 0_{1\times 5} \\ -I_5 \end{bmatrix} \quad L_{et} = \begin{bmatrix} 1 & 0 & 0 & 0 & 0 \\ 0 & 1 & 0 & 0 & 0 \\ 0 & 0 & 1 & 0 & 0 \\ -1 & 0 & 0 & 1 & 0 \\ -1 & 0 & 0 & 0 & 1 \end{bmatrix}.$$

It is clear that L_{et} is an *M-matrix*, *i.e.*, $[L_{et}]_{ii} > 0$, $[L_{et}]_{ij} \leq 0$ for $i \neq j$, and the real parts of the eigenvalues of L_{et} are strictly positive. Moreover, its symmetric part, $L_{es} = (1/2)\left[L_{et} + L_{et}^\top\right]$ is positive definite. In other words, the edge Laplacian, L_{et} satisfies (3.35) with Γ equal to the identity matrix.

As mentioned previously, one of the main advantages of providing a strict Lyapunov function is the possibility of directly establishing robustness properties for the closed-loop system. Therefore, in the simulation scenario we consider that systems are subject to a locally integrable disturbance given by the smooth inverted-step-like vanishing function

$$d_i(t) = -\sigma_i(t)\,[1\ 1\ 0]^\top$$
$$\sigma_i(t) = \begin{cases} -2.4\big[\tanh(2(t-15)) - 1\big] + [t+10]^{-1} & \text{if} \quad i \in \{3,5\} \\ 2.4\big[\tanh(2(t-15)) - 1\big] - [t+10]^{-1} & \text{if} \quad i = 2 \\ 0 & \text{if} \quad i \in \{1,4,6\}. \end{cases}$$

The disturbance d_i was designed so that it takes its maximal value at $t = 0$, when the agents are closer to the boundaries of the sensing zones. Then, the disturbance smoothly (but slowly) vanishes after $t = 15$s.

The barrier Lyapunov functions are defined as

$$W_k(z_k) = \frac{1}{2}\left[|z_k|^2 + \ln\left(\frac{\Delta_k^2}{\Delta_k^2 - |z_k|^2}\right)\right]. \tag{3.80}$$

Consequently, the gradient takes the form

$$\nabla W_k(z_k) = \left[1 + \frac{1}{\Delta_k^2 - |z_k|^2}\right] z_k, \tag{3.81}$$

and, akin to (3.63) and (3.61), the control input for each agent is given by

$$\begin{aligned} v_i^* &= -c_1 \sum_{k \le M} [E_\odot]_{ik} \nabla W_k(z_k) \\ u_i &= -c_2 \tilde{v}_i + \dot{v}_i^*, \end{aligned} \tag{3.82}$$

with $c_1 = 3$ and $c_2 = 2.5$.

The simulation results of our proposed control law (3.63) with (3.61) are depicted in Figures 3.6, 3.7 and 3.8. During the first 15s the perturbation $d(t)$ stymies the achievement of consensus; the systems reach a stable state with a steady-state error. However, the distance constraints (dashed lines) for all initially existing edges are always preserved as can be seen in Figure 3.7, implying that the initially connected (directed spanning tree) graph remains so. In consequence, as the perturbation vanishes after 15 seconds, the trajectories move from their previous steady state towards the consensus equilibrium.

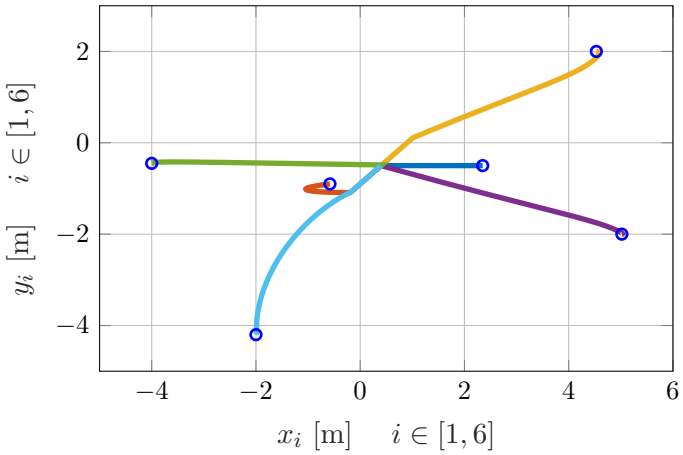

Figure 3.6: Paths described by the agents under the control law (3.82). The circles denote the initial positions.

For comparison, a second scenario was studied considering the same initial conditions satisfying $z(0) \in \mathcal{J}$, and the same disturbances acting on the system. For this comparison the controller is the standard linear consensus protocol —*cf.* (2.13). As it can be seen in Figure 3.9, a linear consensus protocol does not guarantee the respect of the range constraints, thus preventing the multi-agent system from reaching consensus.

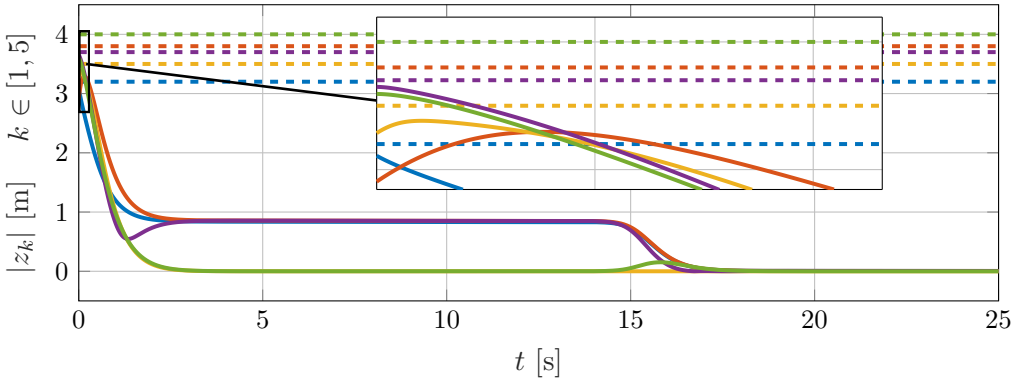

Figure 3.7: Trajectories of the norm of the edges' states. Dashed lines: distance constraints.

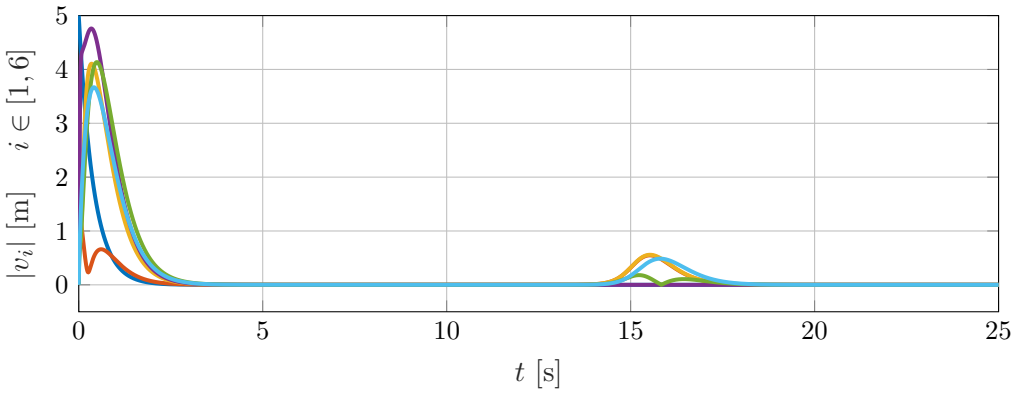

Figure 3.8: Trajectories of the norm of the nodes' velocities.

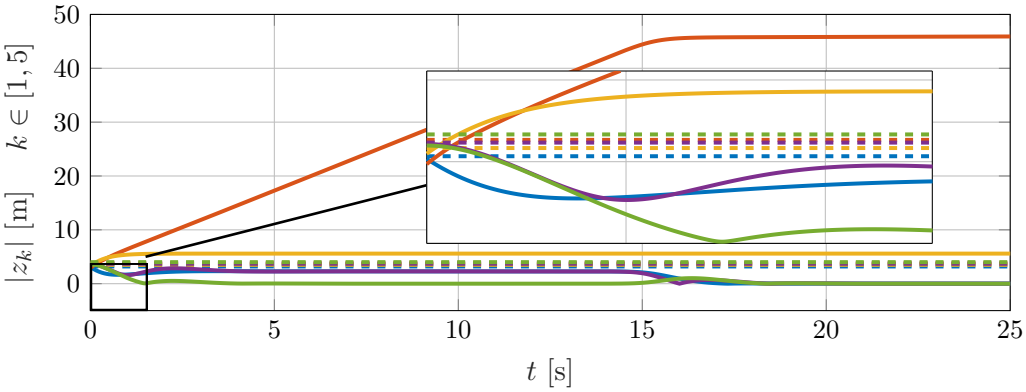

Figure 3.9: Trajectories of the norm of the edges' states for a linear controller without guarantee of connectivity. Dashed lines: distance constraints.

3.5 CONCLUSION

In this chapter we addressed the problem of consensus when the inter-agent information exchange is only reliable within a limited range, therefore imposing the need of guaranteeing the connectivity of the interaction topology via the control. For this purpose we designed the controllers and analyzed the behavior of the interconnected systems using the edge-based representation, rather than the more usual node-based approach, which has the technical advantage of naturally recasting the problem as that of stability of the origin, as opposed to a problem of stability of a manifold. This facilitates considerably the analysis and opens new perspectives for consensus control.

Indeed, as the edge-based representation allows us to rely on Lyapunov theory, we established asymptotic stability of the consensus manifold simultaneously with connectivity maintenance for first and second-order integrators interconnected over connected undirected graphs and two kinds of directed topologies, by means of the construction of strict Lyapunov functions. The latter, in particular, serves as basis to the solution of more complex control problems of nonlinear multi-agent systems and allows us to establish stronger properties in terms of stability and robustness. For instance, in this chapter, using the strict Lyapunov function for the first-order integrators intereconnected over directed graphs, we were able to use a Lyapunov-based design for the case of second-order integrators. Furthermore, through such strict Lyapunov functions we established robustness in the sense of input-to-state stability in all the considered cases.

In Chapter 5, the importance of having a strict Lyapunov function and establishing input-to-state stability for the constrained consensus protocols in the edge-based framework is emphasized further as we extend the results herein to a more general constrained-consensus problem, for systems of order higher than two.

4

LEADER-FOLLOWER CONSTRAINED FULL CONSENSUS OF NONHOLONOMIC VEHICLES

In Chapter 3 we addressed the constrained consensus problem for agents modeled by simple first- or second-order integrators. In order to study a more representative model for vehicle applications, we now address the full-consensus problem, that is, achieving consensus in position and in orientation, in the case of directed leader-follower topologies, using a nonlinear model.

Most often, autonomous vehicles are modeled using three variables, which correspond to two Cartesian coordinates and one orientation. The nonholonomic velocity constraints are captured by a non-integrable relation involving the orientation and the forward velocity. As evoked in Chapter 1, nonholonomic systems in such a representation have been studied abundantly in the control and robotics communities for several decades. However, a well-known fact is that such systems may not be stabilized to a constant pose (position and orientation) using smooth time-invariant feedback [54]. Consensus being inherently a set-point stabilization problem, this impediment also applies [55].

In this chapter we adopt an alternative model expressed in polar coordinates [57], [58], via a transformation that uses inter-agent distances and relative line-of-sight angles to describe the motion of pairs of vehicles. This representation is not only better suited for robotic applications since it uses only relative quantities, but it also transforms the consensus objective to the problem of stabilization of the origin. However, in contrast to the model based on Cartesian coordinates, the origin may be rendered attractive via smooth time-invariant feedback. Moreover, in a multi-agent setting, it lends itself naturally to use the edge-based representation of network graphs and Lyapunov-stability theory as described in previous chapters, including the barrier-Lyapunov-functions method.

It appears pertinent to emphasize at this point two distinct problems that go hand in hand with two control strategies for multiple autonomous vehicles. The first is the *position consensus* control, in which case the vehicles are summoned to a rendezvous position assuming, possibly, a formation pattern and, in the case of *full consensus*, a common orientation. The second is *formation-tracking* control, in which case, the robots are required to move in formation along a path. The former is a leaderless control problem while the second is a leader-follower problem. For nonholonomic systems these problems are different; formation tracking control laws, typically, are ineffective to achieve consensus. We acknowledge that the breadth of the literature of control on autonomous vehicles covers very well, also, multi-

agent settings. The leader-follower formation-tracking control problem is well-studied in the literature on robot control, but the full-consensus problem relatively less. In this chapter we address the latter.

We design smooth and time-invariant controllers that solve the leader-follower full-consensus problem for multiple vehicles with nonholonomic restrictions while guaranteeing connectivity maintenance. Using tools of cascade-systems theory, we establish asymptotic stability and robustness of the proposed full-consensus algorithms. Furthermore, we illustrate the results both in simulation and experimental setups.

4.1 PROBLEM FORMULATION

4.1.1 *The unicycle model in Cartesian coordinates*

We address the problem of full consensus for a group of N autonomous vehicles. That is, the objective is to design distributed control laws such that all agents converge to the same position with an agreement on the orientation. We consider that the agents interact in a leader-follower configuration, where each vehicle follows a single leader (except for one, which is called the root) and has one or multiple followers. Moreover, we consider that each vehicle is only able to measure or estimate information from its immediate leader. Therefore, the graph representing the interaction topology of the leader-follower system is modeled by an arbitrary directed spanning tree denoted $\mathcal{G} = (\mathcal{V}, \mathcal{E})$ —see Figure 4.4 below.

Now, a single autonomous ground vehicle is commonly modeled as a point on the plane with an orientation, with respect to a coordinate frame, that represents the direction of motion —see Figure 4.1. Such model is normally represented using the equations of a nonholonomic integrator, which, for an agent i, is given by

$$\dot{x}_i = v_i \cos\theta_i \tag{4.1a}$$

$$\dot{y}_i = v_i \sin\theta_i \tag{4.1b}$$

$$\dot{\theta}_i = \omega_i, \tag{4.1c}$$

where x_i, $y_i \in \mathbb{R}$ are the coordinates of the Cartesian position on the plane, $\theta_i \in (-\pi, \pi]$ is the orientation of the vehicle with respect to the coordinate frame, $v_i \in \mathbb{R}$ is the speed of the robot in the direction of motion, and $\omega_i \in \mathbb{R}$ is the angular velocity.

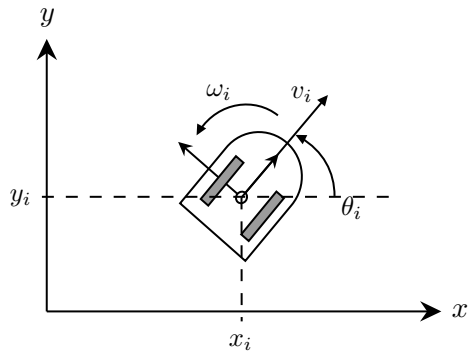

Figure 4.1: Diagram of a nonholonomic vehicle.

It is known from the seminal paper [54] that, for a system of the form (4.1), the origin is not stabilizable via time-invariant differentiable controls. The dual of such result for the problem of consensus, which is inherently a stabilization one, appeared in [55]. Indeed, for a leader-follower pair, where the leader is labeled i and the follower is labeled j, the full consensus objective is to drive the state of the follower (position and orientation) to that of its leader, *i.e.*, $x_j(t) \to x_i(t)$, $y_j(t) \to y_i(t)$, and $\theta_j(t) \to \theta_i(t)$. For that purpose, for the leader-follower pair i, j, denote the relative positions and orientations as

$$z_{xk} := x_i - x_j \tag{4.2a}$$
$$z_{yk} := y_i - y_j \tag{4.2b}$$
$$z_{\theta k} := \theta_i - \theta_j, \tag{4.2c}$$

where the index $k \leq M$ denotes the edges of the spanning tree $\mathcal{G}$. Then, we may transform the error state (4.2) from the local coordinates frame to the global coordinates frame in terms of the orientation of the follower as

$$\begin{bmatrix} e_{xk} \\ e_{yk} \\ e_{\theta k} \end{bmatrix} := \begin{bmatrix} \cos(\theta_j) & \sin(\theta_j) & 0 \\ -\sin(\theta_j) & \cos(\theta_j) & 0 \\ 0 & 0 & 1 \end{bmatrix} \begin{bmatrix} z_{xk} \\ z_{yk} \\ z_{\theta k} \end{bmatrix}. \tag{4.3}$$

Now, using (4.1), the new error coordinates (4.3) satisfy the dynamic equations

$$\dot{e}_{xk} = \omega_j e_{yk} - v_j + v_i \cos(e_{\theta k}) \tag{4.4a}$$
$$\dot{e}_{yk} = -\omega_j e_{xk} + v_i \sin(e_{\theta k}) \tag{4.4b}$$
$$\dot{e}_{\theta k} = \omega_i - \omega_j, \tag{4.4c}$$

in which we consider the velocities of the follower, v_j and ω_j, as inputs.

Note that the relative positions and orientations in (4.2) are similar to the edge transformation (2.27) exposed in Chapter 2. Hence, as in the edge-based perspective, using

the transformations (4.2) and (4.3), the leader-follower full-consensus problem (without constraints) reduces to steering the error variables in (4.4) to zero, that is, making

$$\lim_{t\to\infty} e_{xk}(t) = 0 \tag{4.5a}$$

$$\lim_{t\to\infty} e_{yk}(t) = 0 \tag{4.5b}$$

$$\lim_{t\to\infty} e_{\theta k}(t) = 0, \quad \forall k \leq M. \tag{4.5c}$$

However, due to the nonlinear nature of the system and to the nonholonomic constraints, some difficulties arise. Indeed, the error system (4.4), as the nonholonomic integrator (4.1), is also of the class of systems studied in the seminal paper [54]. Therefore, the origin is not reachable via smooth time-invariant controls from arbitrary initial conditions.

As an illustrative example consider the controller proposed in [109], which is given by

$$v_j = v_i \cos e_{\theta k} + c_1\, e_{xk} \tag{4.6}$$

$$\omega_j = \omega_i + c_2\, e_{\theta k} + c_3 F(t)\left[e_{xk}^2 + e_{yk}^2\right], \tag{4.7}$$

where c_1, c_2, $c_3 > 0$ and $F : \mathbb{R}_{\geq 0} \to [F_m, F_M]$, with $F_m > 0$ is a smooth bounded function. Then, replacing (4.6)-(4.7) into (4.4), we obtain that the closed-loop is given by

$$\begin{bmatrix} \dot{e}_{xk} \\ \dot{e}_{yk} \\ \dot{e}_{\theta k} \end{bmatrix} = \begin{bmatrix} -c_1 & \phi_k(t, e_{zk}) & 0 \\ -\phi_k(t, e_{zk}) & 0 & 0 \\ -c_3 F(t) e_{xk} & -c_3 F(t) e_{yk} & -c_2 \end{bmatrix} \begin{bmatrix} e_{xk} \\ e_{yk} \\ e_{\theta k} \end{bmatrix} + \begin{bmatrix} 0 \\ \omega_i e_{yk} \\ -\omega_1 e_{xk} + v_i \cos e_{\theta k} \end{bmatrix}, \tag{4.8}$$

where $e_{zk} := [e_{xk}\, e_{yk}\, e_{\theta k}]^\top$ and

$$\phi_k(t, e_{zk}) := c_2\, e_{\theta k} + c_3 F(t)\left[e_{xk}^2 + e_{yk}^2\right].$$

It is shown in [109] that, for the closed-loop system (4.8), the leader-follower full-consensus objective (4.5) is achieved provided that the function F and its derivative $\dot{F}$ are persistently exciting, *i.e.*, that there exist T, $\mu > 0$ such that $\dot{F}(t)$ satisfies

$$\int_t^{t+T} \dot{F}(\tau)^2 d\tau \geq \mu \quad \forall t \geq 0.$$

This result is obtained using the concept of δ-persistency of excitation from [110].

The previous δ-persistently exciting condition on the function F, and thereby on the angular velocities $\omega_i(t)$, $i \leq N$, is well-known in the literature of control of nonholonomic vehicles, including consensus-based control —see [111]–[113]. However, although time-varying controllers have been proved effective to stabilize nonholonomic systems and also to achieve consensus, they add a degree of complexity to the control design problem and to the stability analysis, and in the case of δ-persistency-of-excitation-based design, the controllers may induce oscillatory motions, which are undesirable in practice.

Despite, the geometric obstructions to asymptotically stabilize (4.1) that are described in [54], *smooth time-invariant* control of nonholonomic vehicles is not impossible. Indeed,

using an alternative representation of nonholonomic vehicles in terms of polar coordinates, as proposed in [57], the resulting dynamical system does not belong to the class of systems studied in [54], hence a smooth time-invariant control is not prevented. Moreover, the control design using the Cartesian-coordinates model (4.1) needs the knowledge of the position and orientation of the vehicles in a global coordinate framework, which may not be available in practice, *e.g.*, in indoor applications. On the contrary, a model in polar coordinates uses only distances and line-of-sight angles, which are easily obtained using embedded sensors that provide relative measurements. Therefore, in order to address the full-consensus problem with constraints for a group of nonholonomic vehicles, we use the alternative polar-coordinates-based representation.

4.1.2 *A polar-coordinates-based representation*

In this representation the motion of a unicycle is determined by the dynamic equations of its distance and its angular position with respect to a given goal, as well as those of the line-of-sight angle with respect to the line joining the agent and the goal. In a multi-agent setting, the definition of the polar variables is done for each pair of interconnected vehicles. Indeed, recalling the algorithms exposed in Chapter 2, the idea behind the consensus objective is to drive the state of each agent to that of its neighbors. In light of this, we may consider that for each vehicle the "goal" corresponds to the position (and the orientation) of its neighbors. Therefore, the multi-agent systems is described by the evolution of the inter-agent distances and of the relative line-of-sight angles for each pair of connected vehicles.

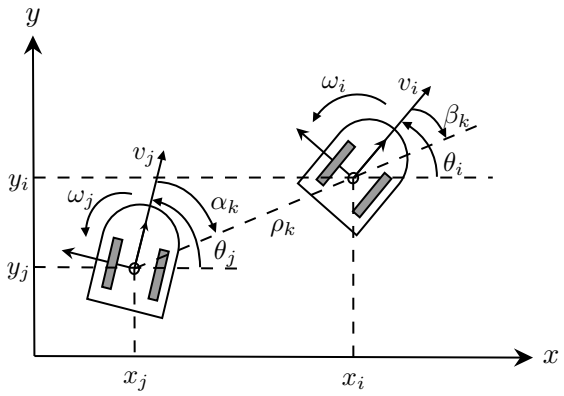

Figure 4.2: Polar coordinates representation for a pair of unicycles.

Then, after [57], for every pair of leader and follower vehicles, labeled i and j respectively, let ρ_k denote the distance separating them, let β_k denote the angle between the line of sight and the leader's direction of motion, and let α_k denote the angle between the line of sight

and the follower's direction of motion —see Figure 4.2 for an illustration. More precisely, for each $i \leq N$ denote $p_i^\top = [x_i \;\; y_i]$ and for each $k \leq M$ let

$$\rho_k := |p_i - p_j| \tag{4.9a}$$

$$\beta_k := \arctan\left(\frac{y_i - y_j}{x_i - x_j}\right) - \theta_i, \quad \forall \rho_k > 0 \tag{4.9b}$$

$$\alpha_k := \arctan\left(\frac{y_i - y_j}{x_i - x_j}\right) - \theta_j, \quad \forall \rho_k > 0. \tag{4.9c}$$

The triple $(\rho_k, \beta_k, \alpha_k)$ corresponds to the state of an edge e_k in the tree $\mathcal{G}$.

Now, differentiating the polar-coordinates variables defined in (4.9), using the equations of the nonholonomic integrator in (4.1), we have that the network of vehicles interacting in a leader-follower configuration corresponds to M interconnected dynamical systems of first order, but dimension three, defined as

$$\dot{\rho}_k = v_i \cos\beta_k - v_j \cos\alpha_k \tag{4.10a}$$

$$\dot{\beta}_k = \frac{1}{\rho_k}\left[-v_i \sin\beta_k + v_j \sin\alpha_k\right] - \omega_i \tag{4.10b}$$

$$\dot{\alpha}_k = \frac{1}{\rho_k}\left[-v_i \sin\beta_k + v_j \sin\alpha_k\right] - \omega_j. \tag{4.10c}$$

Since we assume that a "follower" can measure/estimate the distance and line-of-sight angles with respect to its leader but not the opposite, in the latter equations we consider that v_j and ω_j are the control inputs, and v_i and ω_i, which are respectively the leader's velocity and angular rate, are external signals. Note that the system (4.10), being singular at the origin, does not belong to the class of nonholonomic integrators characterized in [54], so, as evoked above, convergence to the origin using smooth time-invariant controllers is not prevented.

From a dynamical systems viewpoint, the solutions to equations (4.10) correspond to the leader-follower *relative* error trajectories for the pair of index k. Indeed, note that using the transformation (4.9) the three-dimensional space of (x_j, y_j, θ_j) is mapped into another space of dimension 3 $(\rho_k, \beta_k, \alpha_k) \in \mathbb{R}_{\geq 0} \times (-\pi, \pi]^2$. Moreover, $\rho_k = 0$ and $\beta_k = \alpha_k$ is equivalent to $q_i = q_j$ and $\theta_i = \theta_j$. Therefore, the full consensus control goal is reached if, for all $k \leq M$,

$$\lim_{t\to\infty} \rho_k(t) = 0 \tag{4.11a}$$

$$\lim_{t\to\infty} \beta_k(t) = 0 \tag{4.11b}$$

$$\lim_{t\to\infty} \alpha_k(t) = 0. \tag{4.11c}$$

Thus, in these coordinates, the problem of full consensus is also recast into that of rendering the origin for system (4.10) attractive. Furthermore, this model has the additional advantage of naturally leading to the design of controllers that rely only on local relative measurements.

Remark 4.1. *It is important to note, however, that neither the polar-coordinates transformation* (4.9) *nor the system* (4.10) *are defined at the origin (zero distance). Therefore, the*

regularity assumptions needed to apply Brockett's result [54] do not hold. The latter means that convergence to the origin is not prevented via smooth and time-invariant feedback laws. Indeed, although the system's variables are not defined at $\rho_k = 0$*, the origin* $(\rho_k, \beta_k, \alpha_k) = (0, 0, 0)$ *is a limiting point that is located at the frontier of the open set of validity of the system's equations* (4.10) *and can be reached using smooth time-invariant feedback [57].* •

As stated earlier we consider that the agents measure the relative variables with respect to their leader via embedded measurement devices. In turn, we consider that such devices have limited sensing capabilities in the form of a limited field-of-view, determined by an angle of view, and a limited range determined by a maximal detection distance. The field-of-view constraints are encoded by the set

$$\mathcal{J}_\alpha := \{\alpha_k \in (-\pi, \pi] \,:\, |\alpha_k| < \Delta_{\alpha,k},\ \forall\, k \leq M\}, \tag{4.12}$$

where, for each $k \leq M$, $\Delta_{\alpha,k} > 0$ denotes the maximum line-of-sight angle, corresponding to half the angle of view, such that for the leader-follower pair (i, j), *i.e.*, the edge e_k, the leader is inside the follower's field of view. Similarly, the distance constraints are encoded by the set

$$\mathcal{J}_\rho := \{\rho_k \in \mathbb{R}_{\geq 0} \,:\, \rho_k < \Delta_{\rho,k},\ \forall\, k \leq M\}, \tag{4.13}$$

where, for each $k \leq M$, $\Delta_{\rho,k} > 0$ denotes the maximum distance between the leader-follower pair (i, j), such that the measurements of the follower j are reliable.

Recall that, as we mentioned in Chapter 2, the existence of a directed spanning tree is a necessary condition to achieve consensus [6]. Under the constraints (4.12) and (4.13), however, the existence of the minimal tree topology cannot be assumed, but rather has to be enforced by the control law.

Thus, in accordance with the problem addressed in the previous chapter on consensus with connectivity maintenance, the problem considered herein is as follows.

Leader-follower full-consensus problem with connectivity maintenance. Define distributed smooth time-invariant control laws v_j and ω_j, $j \leq N$, such that, for all $k \leq M$, (4.11) holds and that the sets $\mathcal{J}_\alpha$ and $\mathcal{J}_\rho$ in (4.12) and (4.13) respectively, are rendered forward invariant. That is, $\alpha_k(0) \in \mathcal{J}_\alpha$ implies $\alpha_k(t) \in \mathcal{J}_\alpha$ and $\rho_k(0) \in \mathcal{J}_\rho$ implies $\rho_k(t) \in \mathcal{J}_\rho$, for all $t \geq 0$.

4.2 A SMOOTH TIME-INVARIANT CONTROLLER

In order to solve the full-consensus problem with connectivity maintenance defined above we follow a backstepping approach [17]. Hence, the control design exploits the natural cascaded structure of the systems. To explain this more clearly, consider a two-agent system, with a leader-follower interconnection denoted by the graph in Figure 4.3. For this system, the

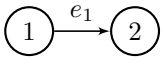

Figure 4.3: Directed tree for a two-agent system.

dynamic equations in polar coordinates are

$$\dot{\rho}_1 = v_1 \cos\beta_1 - v_2 \cos\alpha_1 \tag{4.14a}$$

$$\dot{\beta}_1 = \frac{1}{\rho_1}\left[-v_1 \sin\beta_1 + v_2 \sin\alpha_1\right] - \omega_1 \tag{4.14b}$$

$$\dot{\alpha}_1 = \frac{1}{\rho_1}\left[-v_1 \sin\beta_1 + v_2 \sin\alpha_1\right] - \omega_2. \tag{4.14c}$$

Now, for clarity, let us consider that the leader, *i.e.*, the agent labeled "1", is static. That is, we have $v_1 \equiv 0$ and $\omega_1 \equiv 0$. Then, the system (4.14) becomes

$$\dot{\rho}_1 = -v_2 \cos\alpha_1 \tag{4.15a}$$

$$\dot{\beta}_1 = \frac{v_2}{\rho_1}\sin\alpha_1 \tag{4.15b}$$

$$\dot{\alpha}_1 = \frac{v_2}{\rho_1}\sin\alpha_1 - \omega_2. \tag{4.15c}$$

The system (4.15) may be considered to be in cascaded form, where v_2 and α_1 are the control inputs for the subsystem (4.15a)-(4.15b), and ω_2 is the input for the subsystem (4.15c). Hence, we may apply a backstepping approach in which we first design the actual control input v_2 and a virtual control input $\alpha_1^* : \mathbb{R}_{\geq 0} \times \mathbb{R} \to (-\pi/2, \pi/2)$; $(\rho_1, \beta_1) \mapsto \alpha_1^*(\rho_1, \beta_1)$ such that $\alpha_1^*(0,0) = 0$, in order to make $\rho_1(t) \to 0$ and $\beta_1(t) \to 0$ asymptotically. Then, we design ω_2 so that α_1 tracks the desired virtual input α_1^*, *i.e.*, $\alpha_1(t) \to \alpha_1^*(t)$.

With that in perspective, for the sake of argument, consider that the two agents of the system in Figure 4.3 are not subject to the range and field-of-view constraints described above. In this setting, we define the virtual input

$$\alpha_1^* := \arctan(-c_3\beta_1), \quad c_3 > 0. \tag{4.16}$$

Then, let us denote the error variable $\tilde{\alpha}_1 := \alpha_1 - \alpha_1^*$, so that, using the identities

$$\sin(\arctan(s)) = \frac{s}{\sqrt{1+s^2}}, \quad \cos(\arctan(s)) = \frac{1}{\sqrt{1+s^2}},$$

the dynamical system (4.15) can be rewritten as

$$\dot{\rho}_1 = -\frac{v_2}{\sqrt{1+(c_3\beta_1)^2}} - \left[\cos(\alpha_1) - \cos(\alpha_1^*)\right] v_2 \tag{4.17a}$$

$$\dot{\beta}_1 = -c_3\frac{v_2}{\rho_1\sqrt{1+(c_3\beta_1)^2}}\beta_1 + \frac{1}{\rho_1}\left[\sin(\alpha_1) - \sin(\alpha_1^*)\right] v_2 \tag{4.17b}$$

$$\dot{\tilde{\alpha}}_1 = \frac{v_2}{\rho_1}\sin\alpha_1 - \dot{\alpha}_1^* - \omega_2. \tag{4.17c}$$

We show that the control inputs

$$v_2 = c_1\sqrt{1+(c_3\beta_1)^2}\,\rho_1 \tag{4.18}$$

$$\omega_2 = c_2\tilde{\alpha}_1 + \psi_1\, v_2 + \frac{v_2}{\rho_1}\sin\alpha_1 - \dot{\alpha}_1^*, \tag{4.19}$$

where c_1, $c_2 > 0$ and

$$\psi_1 = \rho_1\frac{[\cos(\alpha_1)-\cos(\alpha_1^*)]}{\tilde{\alpha}_1} + \frac{\beta_1}{\rho_1}\frac{[\sin(\alpha_1)-\sin(\alpha_1^*)]}{\tilde{\alpha}_1}, \tag{4.20}$$

render the origin for (4.17) attractive, thereby guaranteeing that the follower robot reaches the leader. To that end, let us define a quadratic Lyapunov function

$$V(\rho_1,\beta_1,\tilde{\alpha}_1) = \frac{1}{2}\left[\rho_1^2+\beta_1^2+\tilde{\alpha}_1^2\right]. \tag{4.21}$$

The total derivative of (4.21) along (4.17) reads

$$\begin{aligned}\dot{V}(\rho_1,\beta_1,\tilde{\alpha}_1) = &-\frac{\rho_1\, v_2}{\sqrt{1+(c_3\beta_1)^2}} - \rho_1\left[\cos(\alpha_1)-\cos(\alpha_1^*)\right]v_2 - c_3\frac{v_2}{\rho_1\sqrt{1+(c_3\beta_1)^2}}\beta_1^2\\ &+\frac{\beta_1}{\rho_1}\left[\sin(\alpha_1)-\sin(\alpha_1^*)\right]v_2 + \tilde{\alpha}_1\left[\frac{v_2}{\rho_1}\sin\alpha_1 - \dot{\alpha}_1^* - \omega_2\right].\end{aligned} \tag{4.22}$$

Now, replacing (4.18) and (4.19) into (4.23), we obtain

$$\dot{V}(\rho_1,\beta_1,\tilde{\alpha}_1) = -c_1\rho_1^2 - c_3c_1\beta_1^2 - c_2\tilde{\alpha}_1^2 < 0. \tag{4.23}$$

Therefore, from (4.23), asymptotic convergence to the origin $(\rho_1,\beta_1,\tilde{\alpha}_1) = (0,0,0)$ follows.

The previous control design is effective in stabilizing one robot to a point (static leader) without considering neither proximity nor field-of-view constraints. For the purpose of leader-follower consensus of multi-agent systems (4.10) we follow the previous ideas. However, as it was exposed for linear systems in Chapter 3, in order to account for the range and field-of-view constraints, for the solution to the full-consensus problem with connectivity maintenance defined above, we use the concept of barrier Lyapunov functions —see Definition 3.1. Indeed, the inputs v_j and ω_j shall not be simply chosen to be proportional to ρ_k and $\tilde{\alpha}_k$, respectively, but as functions of the gradient of a barrier Lyapunov function.

Hence, akin to (3.10), we encode the range constraints represented by the set $\mathcal{J}_\rho$ in (4.13) into the barrier Lyapunov function

$$W_{\rho,k}(\rho_k) = \frac{1}{2}\left[\rho_k^2 + B_{\rho,k}(\rho_k)\right], \tag{4.24}$$

where $B_{\rho,k}$ is a non-negative function satisfying $B_{\rho,k}(0)=0$, $\nabla B_{\rho,k}(0)=0$ and $B_{\rho,k}(\rho_k)\to\infty$ as $\rho_k\to\Delta_{\rho,k}$.

Correspondingly, for the field-of-view constraints represented by the set $\mathcal{J}_\alpha$ in (4.12) we define a barrier Lyapunov function of the form

$$W_{\alpha,k}(\alpha_k) = \frac{1}{2}\left[\alpha_k^2 + B_{\alpha,k}(\alpha_k)\right], \tag{4.25}$$

where $B_{\alpha,k}$ is a non-negative function satisfying $B_{\alpha,k}(0) = 0$, $\nabla B_{\alpha,k}(0) = 0$ and $B_{\alpha,k}(\alpha_k) \to \infty$ as $|\alpha_k| \to \Delta_{\alpha,k}$.

The functions (4.24) and (4.25) are barrier Lyapunov functions as per Definition 3.1. Moreover, they satisfy Assumption 3.3, that is,

$$\frac{\kappa_1}{2}\rho_k^2 \leq W_{\rho,k}(\rho_k) \leq \kappa_2 \left[\nabla W_{\rho,k}(\rho_k)\right]^2, \tag{4.26}$$

$$\frac{\bar{\kappa}_1}{2}\alpha_k^2 \leq W_{\alpha,k}(\alpha_k) \leq \bar{\kappa}_2 \left[\nabla W_{\alpha,k}(\alpha_k)\right]^2. \tag{4.27}$$

From a control theory viewpoint, as in Chapter 3, we want to use the barrier Lyapunov functions (4.24) and (4.25) for the analysis of the closed-loop system. However, in view of the backstepping method described above, the closed-loop system depends on the error variable $\tilde{\alpha}_k$ rather than on the constrained variable α_k. Therefore, in order to be able to use the barrier function encoding the field-of-view constraints as a Lyapunov function, $W_{\alpha,k}$ in (4.25) has to be modified so that it is made positive definite in terms of the error variable $\tilde{\alpha}_k$, that is, $W_{\alpha,k} = 0$ if $\tilde{\alpha}_k = 0$. For this purpose, we rely on the concept of *gradient recentered barrier function* introduced in [114], and exploited for multi-robot coordination in [32] among others. For consistency in the notation, let us redefine the field-of-view-constraints set as

$$\tilde{\mathcal{J}}_\alpha := \left\{\tilde{\alpha}_k \in (-\pi, \pi] \,:\, |\tilde{\alpha}_k + \alpha_k^*| < \Delta_{\alpha,k},\ \forall\, k \leq M\right\}, \tag{4.28}$$

Then, the gradient recentered barrier function $\tilde{W}_{\alpha,k} : \tilde{\mathcal{J}}_\alpha \to \mathbb{R}_{\geq 0}$ is defined as

$$\tilde{W}_{\alpha,k}(\tilde{\alpha}_k) := W_{\alpha,k}(\tilde{\alpha}_k + \alpha_k^*) - W_{\alpha,k}(\alpha_k^*) - \left.\frac{\partial W_{\alpha,k}(s)}{\partial s}\right|_{\tilde{\alpha}_k = 0} \tilde{\alpha}_k. \tag{4.29}$$

The recentered barrier function $\tilde{W}_{\alpha,k}$ is positive definite, that is, $\tilde{W}_{\alpha,k}(\tilde{\alpha}_k) > 0$ for all $\tilde{\alpha}_k \neq 0$ and $\tilde{W}_{\alpha,k}(0) = 0$. Moreover, it tends to $+\infty$ as $|\alpha_k| \to \Delta_{\alpha,k}$, or equivalently, as $|\tilde{\alpha}_k + \alpha_k^*| \to \Delta_{\alpha,k}$. Therefore it is a valid barrier Lyapunov function as per Definition 3.1. Moreover, $\tilde{W}_{\alpha,k}(\tilde{\alpha}_k)$ satisfies

$$\frac{\tilde{\kappa}_1}{2}\tilde{\alpha}_k^2 \leq \tilde{W}_{\alpha,k}(\tilde{\alpha}_k) \leq \tilde{\kappa}_2 \left[\nabla \tilde{W}_{\alpha,k}(\tilde{\alpha}_k)\right]^2. \tag{4.30}$$

Now, based on the backstepping approach exposed above, we design the constrained full-consensus control as follows. The virtual input is given by

$$\alpha_k^* := \arctan(-c_3 \beta_k), \tag{4.31}$$

with c_3 a design constant[1] satisfying

$$0 < c_3 < \min_{k \leq M} \left\{\frac{\Delta_{\alpha,k}}{\pi}\right\}. \tag{4.32}$$

1 For convenience we use a common gain c_3 for all the agents. This would require that all robots have knowledge of the upper bound (4.32), which is global parameter, albeit knwon *a priori* by design. However, it is important to note that it is equally possible to define $0 < c_{3k} < \frac{\Delta_{\alpha,k}}{\pi}$, for all $k \leq M$, so that the global bound (4.32) is not needed for the design.

Let the coefficients

$$a_{jk} := \begin{cases} 1 & \text{if edge } e_k \text{ is incident on node } j \\ 0 & \text{otherwise} \end{cases} \tag{4.33}$$

represent the available information for each agent j based on the interaction topology $\mathcal{G}$. Then, based on the latter, the distributed control inputs v_j and ω_j are taken proportional to the gradient of the barrier Lyapunov functions (4.24) and (4.29), respectively. More precisely, the control inputs are given as follows:

$$v_j := c_1 \sum_{k \leq M} a_{jk} \eta_k \, \nabla W_{\rho,k}(\rho_k), \quad \eta_k := \sqrt{1 + (c_3 \beta_k)^2} \tag{4.34}$$

$$\omega_j := \sum_{k \leq M} a_{jk} \left[c_2 \nabla \tilde{W}_{\alpha,k}(\tilde{\alpha}_k) + \left[\psi_k + \left[1 + \frac{c_3}{\eta_k^2} \tilde{\omega}_k \right] \frac{\sin(\alpha_k)}{\rho_k} \right] \sum_{i \leq N} a_{ik} v_i \right] \tag{4.35}$$

where c_1, $c_2 > 0$ are design constants. In turn, the term

$$\psi_k := -\nabla W_{\rho,k} \frac{[\cos(\alpha_k) - \cos(\alpha_k^*)]}{\nabla \tilde{W}_{\alpha,k}} + \frac{\beta_k}{\rho_k} \frac{[\sin(\alpha_k) - \sin(\alpha_k^*)]}{\nabla \tilde{W}_{\alpha,k}} \tag{4.36}$$

compensates for the error dynamics coming from the tracking problem of the backstepping method. The term

$$\frac{c_3}{\eta_k^2} \tilde{\omega}_k \frac{\sin(\alpha_k)}{\rho_k} \sum_{i \leq N} a_{ik} v_i,$$

where

$$\tilde{\omega}_k := \left[\frac{\partial^2 W_{\alpha,k}(s)}{\partial s^2} \bigg|_{\tilde{\alpha}_k = 0} \right] \frac{\tilde{\alpha}_k}{\nabla \tilde{W}_{\alpha,k}}, \tag{4.37}$$

is used to dominate the additional terms coming from the derivative of the recentered barrier Lyapunov function (4.25), as we will see below.

Note that, modulo the gradients of the barrier Lyapunov functions $W_{\rho,k}$ and $\tilde{W}_{\alpha,k}$, defined in (4.24) and (4.29), respectively, the control inputs (4.34)-(4.35) are defined in the same form as those given previously in (4.18)-(4.19) for the two-agent system without constraints considered above.

Remark 4.2. *The bound on c_3 in (4.32) comes from the design of the gradient recentered barrier Lyapunov function (4.29). Indeed, in order for the term $W_{\alpha,k}(\alpha_k^*)$ to be well-defined, we need to guarantee that the desired value of α_k also remains within the imposed bounds, i.e., that $|\alpha_k^*(t)| < \Delta_{\alpha,k}$, for all $t \geq 0$. Therefore, since $|\alpha_k^*| \leq c_3 |\beta_k|$ and $\beta_k \in (-\pi, \pi]$ by definition, choosing $c_3 < \min_{k \leq M} \{\Delta_{\alpha,k}/\pi\}$, the terms $W_{\alpha,k}(\alpha_k^*)$ and $\partial W_{\alpha,k}/\partial \alpha_k^*$ are well-defined and upper bounded in norm by positive constants.* •

Remark 4.3. *Note that the control law (4.35) is well posed for all $\rho_k \in \mathcal{J}_\rho \backslash \{0\}$ and all $\tilde{\alpha}_k \in \tilde{\mathcal{J}}_\alpha$. Indeed, note that using (4.26) and (4.30) in (4.37), we have*

$$\begin{aligned} |\tilde{\omega}_k| \leq & \left| \frac{\partial^2 W_{\alpha,k}(s)}{\partial s^2}\bigg|_{\tilde{\alpha}_k=0} \right| \frac{|\tilde{\alpha}_k|}{|\nabla \tilde{W}_{\alpha,k}|} \\ \leq & \frac{2\tilde{\kappa}_2}{\tilde{\kappa}_1} \left| \frac{\partial^2 W_{\alpha,k}(s)}{\partial s^2}\bigg|_{\tilde{\alpha}_k=0} \right|, \end{aligned} \tag{4.38}$$

and since $\alpha_k^*(t) \in \Delta_{\alpha,k}$ for all $t \geq 0$, the term in the right-hand side of inequality (4.38) is well defined and bounded. Moreover

$$\lim_{|\tilde{\alpha}_k| \to \Delta_{\alpha,k}} \frac{\tilde{\alpha}_k}{\nabla \tilde{W}_{\alpha,k}} = 0. \tag{4.39}$$

Furthermore, noting that $|\sin(\tilde{\alpha}_k + \alpha_k^*) - \sin(\alpha_k^*)| \leq |\tilde{\alpha}_k|$ and $|\cos(\tilde{\alpha}_k + \alpha_k^*) - \cos(\alpha_k^*)| \leq |\tilde{\alpha}_k|$, the previous statement holds also for (4.36). •

Remark 4.4. *In order to address the inter-agent connectivity constraints, the full-consensus control laws (4.34) and (4.35) are designed based on the gradients of the barrier Lyapunov functions (4.24) and (4.29), respectively. Note, however, that redefining $W_{\rho,k}$ in (4.24) and $W_{\alpha,k}$ in (4.25) to be quadratic Lyapunov functions, i.e., $B_{\rho,k}(\rho_k) = B_{\alpha,k}(\alpha_k) \equiv 0$, the control inputs (4.34) and (4.35) are still valid to address the full-consensus problem without constraints —cf. [115]. Indeed, considering quadratic Lyapunov functions, from (4.37) $\tilde{\omega}_k = 1$ and the control inputs (4.34)-(4.35) become*

$$v_j := c_1 \sum_{k \leq M} a_{jk} \eta_k \, \rho_k, \quad \eta_k := \sqrt{1 + (c_3 \beta_k)^2} \tag{4.40}$$

$$\omega_j := \sum_{k \leq M} a_{jk} \left[c_2 \tilde{\alpha}_k + \left[\psi_k + \left[1 + \frac{c_3}{\eta_k^2} \right] \frac{\sin(\alpha_k)}{\rho_k} \right] \sum_{i \leq N} a_{ik} v_i \right]. \tag{4.41}$$

•

4.3 CLOSED-LOOP ANALYSIS

So far, for the control design, we have considered the leader-follower pair (4.10) as an individual system. Let us consider now a multi-agent system composed of N unicycles communicating through an arbitrary directed spanning tree $\mathcal{G}$ represented in Figure 4.4. Recall that in leader-follower configuration, each robot has only one leader, but may have several followers. Hence, as it may be seen in Figure 4.4, we may divide the tree into $h \leq N-1$ levels based on the distance of the edges to the root node.

In light of this, let $\mathcal{E}_p \subset \mathcal{E}$ denote the set of edges such that the distance from its terminal node to the root of the tree, labeled "1", is equal to $p \leq h$, *i.e.*, $\mathcal{E}_p := \{e_k = (i,j) \in \mathcal{E} : d(1,j) = p\}$, where we recall that $d(i,j)$ is the distance between nodes i and j, that is, the

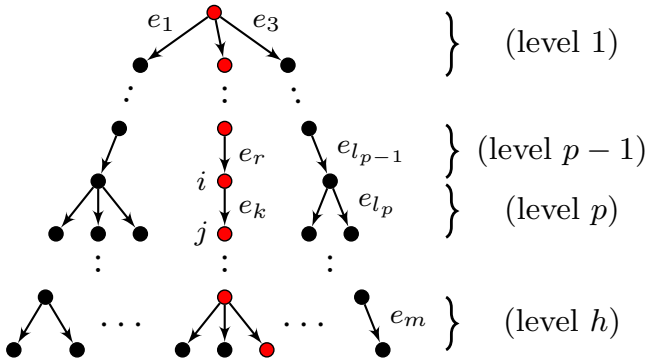

Figure 4.4: Directed spanning tree $\mathcal{G}$. Open directed chain illustrated in red.

number of edges in the shortest path from i to j. Without loss of generality, assume that each level p of the tree contains an l_p number of edges, such that $1 \leq l_p \leq M$, $\sum_{p=1}^{h} l_p = M$ —see Figure 4.4. Then, we define a multi-variable model containing the three states of all the edges belonging to a level of the tree. To that end, for each level p having l_p arcs labeled e_k with $k \in [l_{p-1}+1, l_p]$ we define the *closed-loop* state variables

$$\xi_p := \left[\xi_{p,1}^\top \cdots \xi_{p,l_p}^\top\right]^\top \in \mathbb{R}^{3l_p}, \quad \xi_{p,k} := [\rho_k\, \beta_k\, \tilde{\alpha}_k]^\top \in \mathbb{R}^3. \tag{4.42}$$

Using this notation, the equations corresponding to the closed-loop dynamics composed of the systems (4.10) with the inputs (4.34)-(4.35), with $k \leq M$ and for an arbitrary directed tree, may be written in the compact cascaded-system form,

$$\dot{\xi}_p = f_p(\xi_p) + g_p(\xi_p, \xi_{p-1}), \quad p \in [2, h] \tag{4.43a}$$
$$\dot{\xi}_1 = f_1(\xi_1) \tag{4.43b}$$

where, for each $p \leq h$,

$$f_p(\xi_p) := \left[f_{p,1}(\xi_{p,1})^\top \ldots\ f_{p,l_p}(\xi_{p,l_p})^\top\right]^\top,$$
$$g_p(\xi_p, \xi_{p-1}) := \left[g_{p,1}(\xi_{p,1},\, \xi_{p-1})^\top \ldots\ g_{p,l_p}(\xi_{p,l_p},\, \xi_{p-1})^\top\right]^\top.$$

In these equations, the nominal systems, $\dot{\xi}_{p,k} = f_{p,k}(\xi_{p,k})$, correspond to

$$\dot{\rho}_k = -\, c_1 \nabla W_{\rho,k} \Big[1 + [\cos(\alpha_k) - \cos(\alpha_k^*)]\eta_k\Big] \tag{4.44a}$$
$$\dot{\beta}_k = -\, 2c_1 \frac{\nabla W_{\rho,k}(\rho_k)}{\rho_k} \Big[\, c_3\beta_k - [\,\sin(\alpha_k) - \sin(\alpha_k^*)\,]\,\eta_k\,\Big] \tag{4.44b}$$
$$\dot{\tilde{\alpha}}_k = -\, c_2 \nabla \tilde{W}_{\alpha,k} - c_1 \left[\psi_k \eta_k - (1-\tilde{\omega}_k)\frac{c_3}{\eta_k}\frac{\sin(\alpha_k)}{\rho_k}\right] \nabla W_{\rho,k} \tag{4.44c}$$

where we recall that $\alpha_k = \tilde{\alpha}_k + \alpha_k^*$.

The interconnection terms $g_p(\xi_p, \xi_{p-1})$ depend on states relative to the p-th level in the tree and to the previous one in the following way. Fix $k \in [l_{p-1}+1, l_p]$ and $r \in [l_{p-2}+1, l_{p-1}]$ in a manner that the edge $e_r \in \mathcal{E}_{p-1}$ is incident on $e_k \in \mathcal{E}_p$, that is, so that the terminal node of e_r is the initial node of e_k —see the chain colored in red in Figure 4.4. Let $\xi_{p-1,r} := [\rho_r \ \beta_r \ \tilde{\alpha}_r]^\top$ be the state associated to e_r. Then,

$$g_{p,k}\left(\xi_{p,k}, \xi_{p-1}\right) = \begin{bmatrix} c_1 \cos(\beta_k)\eta_r \ \nabla W_{\rho,r} \\ \tilde{g}_\beta\left(\xi_{p,k}, \xi_{p-1,r}\right) \\ \tilde{g}_\alpha\left(\xi_{p,k}, \xi_{p-1,r}\right) \end{bmatrix}, \tag{4.45}$$

where $\eta_r := \sqrt{1 + (c_3\beta_r)^2}$,

$$\tilde{g}_\beta := -c_1\eta_r \nabla W_{\rho,r}\left[\frac{\sin(\beta_k)}{\rho_k} + \left[1 + \frac{c_3}{\eta_r^2}\tilde{\omega}_r\right]\frac{\sin(\alpha_r)}{\rho_r} + \psi_r\right] - c_2 \nabla \tilde{W}_{\alpha,r},$$

and

$$\tilde{g}_\alpha := -\frac{c_2 c_3}{\eta_k^2}\nabla \tilde{W}_{\alpha,r} - c_1\eta_r \nabla W_{\rho,r}\left[\left(1 + \frac{c_3}{\eta_k^2}\right)\frac{\sin(\beta_k)}{\rho_k} + \frac{c_3}{\eta_k^2}\left[\psi_r + \left(1 + \frac{c_3}{\eta_r^2}\tilde{\omega}_r\right)\frac{\sin(\alpha_r)}{\rho_r}\right]\right], \tag{4.46}$$

where $\alpha_r = \tilde{\alpha}_r + \alpha_r^*$.

The cascaded form of the closed-loop system (4.43), which is derived from the leader-follower structure of the interaction graph, is fundamental for the convergence and robustness analysis of the multi-agent system under the controls (4.34)-(4.35). Indeed, for the analyses presented below, we rely on standard arguments from cascaded-systems theory [116], [117], where convergence to the origin for a system of the form (4.43) is concluded by establishing asymptotic stability for each nominal system (4.44) and boundedness of the trajectories under the interconnections (4.45).

In what follows, before presenting the statements that constitute the original contributions of this chapter, with the purpose of clarity, we analyze a simple three-agent system under the action of the proposed inputs (4.34)-(4.35).

4.3.1 *Case-study*

Consider a system composed of three unicycle vehicles with a leader-follower interaction topology represented by the directed spanning tree in Figure 4.5. In polar coordinates, the system is described by (4.10) with $k \leq 2$.

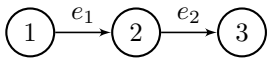

Figure 4.5: Directed tree for a three-agent system.

Recall the compact notation (4.42), where in this case $l_p = 1$ for all $p \leq 2$. Then, applying the control inputs (4.34)-(4.35), the closed-loop system reads

$$\dot{\xi}_2 = f_2(\xi_2) + g_2(\xi_2, \xi_1) \tag{4.47a}$$

$$\dot{\xi}_1 = f_1(\xi_1), \tag{4.47b}$$

where $\xi_1 = \xi_{1,1} = [\rho_1 \ \beta_1 \ \tilde{\alpha}_1]^\top$ and $\xi_2 = \xi_{2,2} = [\rho_2 \ \beta_2 \ \tilde{\alpha}_2]^\top$. The nominal systems $\dot{\xi}_p = f_p(\xi_p)$, $p \leq 2$, are given in (4.44) and the interconnection term is

$$g_2(\xi_2, \xi_1) = \begin{bmatrix} c_1 \cos(\beta_2)\eta_1 \ \nabla W_{\rho,1} \\ \tilde{g}_\beta(\xi_2, \xi_1) \\ \tilde{g}_\alpha(\xi_2, \xi_1) \end{bmatrix}, \tag{4.48}$$

where $\eta_1 := \sqrt{1 + (c_3\beta_1)^2}$,

$$\tilde{g}_\beta := -c_1\eta_1 \nabla W_{\rho,1} \left[\frac{\sin(\beta_2)}{\rho_2} + \left[1 + \frac{c_3}{\eta_1^2}\tilde{\omega}_1\right] \frac{\sin(\alpha_1)}{\rho_1} + \psi_1 \right] - c_2 \nabla \tilde{W}_{\alpha,1},$$

and

$$\tilde{g}_\alpha := -\frac{c_2 c_3}{\eta_2^2} \nabla \tilde{W}_{\alpha,1} - c_1\eta_1 \nabla W_{\rho,1} \left[\left(1 + \frac{c_3}{\eta_2^2}\right) \frac{\sin(\beta_2)}{\rho_2} + \frac{c_3}{\eta_2^2} \left[\psi_1 + \left(1 + \frac{c_3}{\eta_1^2}\tilde{\omega}_1\right) \frac{\sin(\alpha_1)}{\rho_1} \right] \right]. \tag{4.49}$$

The cascade structure of the system (4.47) captures well the fact that the dynamics of the edge e_1, with state ξ_1, is autonomous whereas the dynamics of the edge e_2, with state ξ_2, is driven by the former. Moreover, as we mentioned earlier, relying on well-known results for cascaded systems, asymptotic stability of the origin of a nonlinear cascaded system follows if the nominal systems $\dot{\xi}_1 = f_1(\xi_1)$ and $\dot{\xi}_2 = f_2(\xi_2)$ are asymptotically stable at their respective origins and the solutions of (4.47) are bounded.

The first condition may be asserted, for each $p \leq 2$ and for the edge $e_k \in \mathcal{E}_p$, using the barrier Lyapunov function

$$V_{p,k}(\xi_{p,k}) = W_{\rho,k}(\rho_k) + \tilde{W}_{\alpha,k}(\tilde{\alpha}_k) + \frac{1}{2}\beta_k^2, \tag{4.50}$$

with $W_{\rho,k}(\rho_k)$ and $\tilde{W}_{\alpha,k}(\tilde{\alpha}_k)$ given in (4.24) and (4.29), respectively. Assume, for the time-being (this assumption will be relaxed, and shown to hold, later), that the solutions of (4.47) are such that $\rho_k(t) \in \mathcal{J}_\rho$ and $\tilde{\alpha}_k(t) \in \tilde{\mathcal{J}}_\alpha$ for all $k \leq M$ and all $t \geq 0$. Then, the total derivative of (4.50) reads

$$\dot{V}_{p,k}(\xi_{p,k}) = \left[\frac{\partial W_{\rho,k}}{\partial \rho_k}\right] \dot{\rho}_k + \left[\frac{\partial \tilde{W}_{\alpha,k}}{\partial \tilde{\alpha}_k}\right] \dot{\tilde{\alpha}}_k + \left[\left.\frac{\partial \tilde{W}_{\alpha,k}(s)}{\partial s}\right|_{\tilde{\alpha}_k = 0}\right] \dot{\alpha}_k^* + \beta_k \dot{\beta}_k. \tag{4.51}$$

Now, notice that from (4.29), we have

$$\nabla\tilde{W}_{\alpha,k} = \frac{\partial\tilde{W}_{\alpha,k}}{\partial\tilde{\alpha}_k} = \frac{\partial W_{\alpha,k}(\tilde{\alpha}_k+\alpha_k^*)}{\partial\tilde{\alpha}_k} - \frac{\partial W_{\alpha,k}(\alpha_k^*)}{\partial\alpha_k^*}. \tag{4.52}$$

Moreover, since $\alpha_k = \tilde{\alpha}_k + \alpha_k^*$, from the definition of $W_{\alpha,k}$ in (4.25), the following holds

$$\frac{\partial W_{\alpha,k}(\tilde{\alpha}_k+\alpha_k^*)}{\partial\tilde{\alpha}_k} = \frac{\partial W_{\alpha,k}(\tilde{\alpha}_k+\alpha_k^*)}{\partial\alpha_k^*}.$$

Then, from (4.29), we have

$$\nabla_{\alpha^*}\tilde{W}_{\alpha,k} := \frac{\partial\tilde{W}_{\alpha,k}}{\partial\alpha_k^*} = \nabla\tilde{W}_{\alpha,k} - \left[\frac{\partial^2 W_{\alpha,k}s}{\partial s^*}\bigg|_{\tilde{\alpha}_k=0}\right]\tilde{\alpha}_k. \tag{4.53}$$

Hence, along the trajectories of the nominal system (4.44), (4.51) becomes

$$\begin{aligned}\dot{V}_{p,k}(\xi_{p,k}) =& -c_1\left[\nabla W_{\rho,k}\right]^2\left[1+\left[\cos(\alpha_k)-\cos(\alpha_k^*)\right]\eta_k\right] - 2c_1\frac{\nabla W_{\rho,k}}{\rho_k}\Big[c_3\beta_k\\ &-\left[\sin(\alpha_k)-\sin(\alpha_k^*)\right]\Big]\beta_k - c_2\left[\nabla\tilde{W}_{\alpha,k}\right]^2\\ &-c_1\left[\nabla\tilde{W}_{\alpha,k}\right]\left[\psi_k\eta_k-(1-\tilde{\omega}_k)\frac{c_3}{\eta_k}\frac{\sin(\alpha_k)}{\rho_k}\right]\nabla W_{\rho,k}\\ &-\nabla_{\alpha^*}\tilde{W}_{\alpha,k}\left[\frac{c_1c_3}{\eta_k}\frac{\sin(\alpha_k)}{\rho_k}\nabla W_{\rho,k}\right].\end{aligned} \tag{4.54}$$

Then, using (4.53), (4.36), (4.37), and the bounds (4.26) and (4.30), we have

$$\begin{aligned}\dot{V}_{p,k}(\xi_{p,k}) \leq& -c_1\left[\nabla W_{\rho,k}\right]^2 - \frac{4c_1c_3\kappa_2}{\kappa_1}\beta_k^2 - c_2\left[\nabla\tilde{W}_{\alpha,k}\right]^2\\ \leq& -c_1'\rho_k^2 - c_2'\tilde{\alpha}_k^2 - c_3'\beta_k^2\\ \leq& -c|\xi_{p,k}|^2,\end{aligned} \tag{4.55}$$

where $c_1' := 2c_1\kappa_2/\kappa_1$, $c_2' := 2c_2\tilde{\kappa}_2/\tilde{\kappa}_1$, $c_3' := 4c_1c_3\kappa_2/\kappa_1$, and $c := \min\{c_1', c_2', c_3'\}$. The inequality (4.55) implies that the origin is asymptotically stable for the nominal systems $\dot{\xi}_1 = f_1(\xi_1)$ and $\dot{\xi}_2 = f_2(\xi_2)$.

Next, we establish boundedness of the solutions of (4.47). For that purpose, we stress that the elements of the term $g_2(\xi_2,\xi_1)$ in (4.48) may be upper-bounded as

$$g_2(\xi_2,\xi_1) \leq \begin{bmatrix}\gamma_\rho(|\xi_{1,1}|)\\ \max\left\{1,\frac{1}{\rho_2}\right\}\gamma_\beta(|\xi_{1,1}|)\\ \max\left\{1,\frac{1}{\rho_2}\right\}\gamma_\alpha(|\xi_{1,1}|)\end{bmatrix} \tag{4.56}$$

where $\gamma_\rho(s)$, $\gamma_\beta(s)$, $\gamma_\alpha(s) \in \mathcal{K}_\infty$. Therefore, in view of (4.55) and (4.56), the total derivative of the barrier Lyapunov function in (4.50), with $p = k = 2$, along the trajectories of (4.47a) satisfies

$$\begin{aligned}\dot{V}_{2,2}(\xi_{2,2}) \leq & -c_1\left[\nabla W_{\rho,2}\right]^2 - c_3'\beta_2^2 - c_2\left[\nabla \tilde{W}_{\alpha,2}\right]^2 + |\nabla W_{\rho,2}|\gamma_\rho(|\xi_{1,1}|) \\ & + \max\left\{1, \frac{1}{\rho_2}\right\}\left[|\beta_2|\gamma_\beta(|\xi_{1,1}|) + 2|\nabla \tilde{W}_{\alpha,2}|\gamma_\alpha(|\xi_{1,1}|) + \left|\frac{\partial^2 W_{\alpha,2}(\alpha_2^*)}{\partial \alpha_2^{*2}}\right||\tilde{\alpha}_2|\gamma_\alpha(|\xi_{1,1}|)\right].\end{aligned} \tag{4.57}$$

Since α_k^* is bounded by definition —see (4.31), we have that $\left|\partial^2 W_{\alpha,2}(s)/\partial s^2\right|_{\tilde{\alpha}_2=0} \leq \mu$, where μ is a positive constant. Then, given a constant $\delta \in (0,1)$, using the bound (4.30), (4.57) is rewritten as

$$\begin{aligned}\dot{V}_{2,2}(\xi_{2,2}) \leq & -c_1\left[\nabla W_{\rho,2}\right]^2 - c_3'\beta_2^2 - \delta c_2\left[\nabla \tilde{W}_{\alpha,2}\right]^2 - (1-\delta)\frac{c_2\tilde{\kappa}_2}{\kappa_1}\tilde{\alpha}_2^2 + |\nabla W_{\rho,2}|\gamma_\rho(|\xi_{1,1}|) \\ & + \max\left\{1, \frac{1}{\rho_2}\right\}\left[|\beta_2|\gamma_\beta(|\xi_{1,1}|) + 2|\nabla \tilde{W}_{\alpha,2}|\gamma_\alpha(|\xi_{1,1}|) + \mu|\tilde{\alpha}_2|\gamma_\alpha(|\xi_{1,1}|)\right].\end{aligned} \tag{4.58}$$

Now, because of the max function in (4.58) we consider two scenarios. First, assume that $\rho_2 \gg 1$ so that $\max\{1, 1/\rho_2\} = 1$. Then, let $\lambda_1, \lambda_2, \lambda_3, \lambda_4 > 0$ be sufficiently large so that $\tilde{c}_1 := c_1 - \frac{1}{2\lambda_1} > 0$, $\tilde{c}_2 := \delta c_2 - \frac{1}{\lambda_2} > 0$, $\tilde{c}_3 := c_3' - \frac{1}{2\lambda_3} > 0$, and $\tilde{c}_4 := (1-\delta)\frac{c_2\tilde{\kappa}_2}{\kappa_1} - \frac{\mu}{2\lambda_4} > 0$. Applying Young's inequality to the last four terms of the right-hand side of (4.58) we obtain

$$\begin{aligned}\dot{V}_{2,2}(\xi_{2,2}) \leq & -\tilde{c}_1\left[\nabla W_{\rho,2}\right]^2 - \tilde{c}_2\left[\nabla \tilde{W}_{\alpha,2}\right]^2 - \tilde{c}_3\beta_2^2 - \tilde{c}_4\tilde{\alpha}_2^2 + \frac{\lambda_1}{2}\gamma_\rho(|\xi_{1,1}|)^2 + \lambda_2\gamma_\alpha(|\xi_{1,1}|)^2 \\ & + \frac{\lambda_3}{2}\gamma_\beta(|\xi_{1,1}|)^2 + \frac{\lambda_4\mu}{2}\gamma_\alpha(|\xi_{1,1}|)^2 \\ \leq & -\tilde{c}|\xi_{2,2}|^2 + \gamma_1(|\xi_{1,1}|)\end{aligned} \tag{4.59}$$

where $\tilde{c} := \min\{2\tilde{c}_1\kappa_2/\kappa_1, \tilde{c}_4 + 2\tilde{c}_2\tilde{\kappa}_2/\tilde{\kappa}_1, \tilde{c}_3\}$ and

$$\gamma_1(|\xi_{1,1}|) := \frac{\lambda_1}{2}\gamma_\rho(|\xi_{1,1}|)^2 + \frac{\lambda_3}{2}\gamma_\beta(|\xi_{1,1}|)^2 + \left(\frac{\lambda_3}{2} + \frac{\lambda_4\mu}{2}\right)\gamma_\alpha(|\xi_{1,1}|)^2. \tag{4.60}$$

Now, let $\max\{1, 1/\rho_2\} = 1/\rho_2$. For any $\epsilon > 0$ and for any $\rho_k \geq \epsilon$, we have $\max\{1, 1/\rho_2\} \leq 1/\epsilon$. Then, let $\lambda_1', \lambda_2', \lambda_3', \lambda_4' > 0$ be defined so that, with an abuse of notation, $\tilde{c}_1 := c_1 - \frac{1}{2\lambda_1'} > 0$, $\tilde{c}_2 := \delta c_2 - \frac{1}{\lambda_2'} > 0$, $\tilde{c}_3 := c_3' - \frac{1}{2\lambda_3'} > 0$, and $\tilde{c}_4 := (1-\delta)\frac{c_2\tilde{\kappa}_2}{\kappa_1} - \frac{\mu}{2\lambda_4'} > 0$. Applying Young's inequality on (4.58), again, we obtain

$$\dot{V}_{2,2}(\xi_{2,2}) \leq -\tilde{c}|\xi_{2,2}|^2 + \frac{1}{\epsilon}\gamma_1(|\xi_{1,1}|), \quad \forall\, \xi_{1,1},\, \xi_{2,2} \in \mathbb{R}^3. \tag{4.61}$$

From (4.59) and (4.61), we see that the function $V_{p,k}$ in (4.51) with $p = k = 2$, satisfies

$$\dot{V}_{2,2}(\xi_{2,2}) \leq -\tilde{c}|\xi_{2,2}|^2 + \bar{\gamma}_1(|\xi_{1,1}|) \tag{4.62}$$

where $\bar{\gamma}(|\xi_{1,1}|) := \max\{1, \frac{1}{\epsilon}\}\gamma_1(|\xi_{1,1}|)$. Assume now that the solutions $t \mapsto \xi_2(t)$ grow unbounded. We know from (4.55) that the solutions $t \mapsto \xi_1(t)$ are bounded. Hence, from the bound (4.62), there exists a time $t' > 0$ such that, as $\xi_2(t)$ grows, $\dot{V}_2(\xi_2(t)) \leq 0$ for all $t \geq t'$, which leads to a contradiction. That is, $\xi_2(t)$ is bounded. Furthermore, since we established that $\xi_1(t) \to 0$, it follows that, also, $\xi_2(t) \to 0$.

So far we have assumed that $\rho_k(t) \in \mathcal{J}_\rho$ and $\tilde{\alpha}_k(t) \in \tilde{\mathcal{J}}_\alpha$ for all $t \geq 0$. We show next that this holds under the assumption that $\rho_k(0) \in \mathcal{J}_\rho \backslash \{0\}$ and $\tilde{\alpha}_k(0) \in \tilde{\mathcal{J}}_\alpha$. We proceed by contradiction. Suppose that there exists $T > 0$ such that for all $t \in [0, T)$ and at least one $k \leq M$, $\tilde{\alpha}_k(t) \in \tilde{\mathcal{J}}_\alpha$ and $\tilde{\alpha}_k(T) \notin \tilde{\mathcal{J}}_\alpha$. Then, from the definition of the barrier Lyapunov function $\tilde{W}_{\alpha,k}$, we have that $\tilde{W}_{\alpha,k}(\tilde{\alpha}_k(t)) \to \infty$ as $t \to T$. This, however, is in contradiction with (4.55) and (4.62), which imply that $\tilde{W}_{\alpha,k}(\tilde{\alpha}_k(t))$ is bounded for all $t \geq 0$ and all $k \leq M$. The same analysis applies for the distance constraints, meaning that $W_{\rho,k}(\rho_k(t))$ is also bounded for all $t \geq 0$ and all $k \leq M$. Therefore, the constraints sets $\mathcal{J}_\rho$ and $\tilde{\mathcal{J}}_\alpha$ (equivalently $\mathcal{J}_\alpha$) are forward invariant and connectivity maintenance follows.

Thus, the three-agent system in Figure 4.5, in closed loop with the control input (4.34)-(4.35), achieves full consensus with connectivity maintenance.

4.3.2 *Static leader: stabilization*

Let us now return to N-agents system in closed loop (4.43). As in the case-study analyzed above, based on cascaded-systems theory [117], one can assert that if for every $p \in [2, h+1]$ the solution of $\dot{\xi}_{p-1} = f_{p-1}(\xi_{p-1})$ converges to zero and if, for every $p \in [2, h]$, the solutions of $\dot{\xi}_p = f_p(\xi_p) + g_p(\xi_p, \xi_{p-1})$, denoted $\xi_p(t)$, remain bounded, we also have $\xi_p(t) \to 0$. This is established in the following proposition which is an original contribution of this thesis and was presented in [118].

Proposition 4.1 ([118])**.** *Consider a multi-agent system composed of N unicycles, described by the M interconnected systems (4.10), interacting over a directed spanning tree $\mathcal{G}$ and subject to distance and field-of-view constraints as defined by the sets (4.12)-(4.13). Under the smooth time-invariant controller (4.34)-(4.35) the system asymptotically achieves full consensus with connectivity maintenance, i.e., $(\rho_k, \beta_k, \alpha_k) \to (0, 0, 0)$, and $\rho_k(t) \in \mathcal{J}_\rho$ and $\alpha_k(t) \in \mathcal{J}_\alpha$, for all $k \leq M$, all $t \geq 0$, and for all initial conditions $(\rho_k(0), \beta_k(0), \alpha_k(0))$ such that $\rho_k(0) \in \mathcal{J}_\rho \backslash \{0\}$ and $\alpha_k(0) \in \mathcal{J}_\alpha$.* □

Proof. First, let $k \leq M$ and $p \leq h$ be arbitrarily fixed and for the edge $e_k \in \mathcal{E}_p$, consider the barrier Lyapunov function

$$V_{p,k}(\xi_{p,k}) = W_{\rho,k}(\rho_k) + \tilde{W}_{\alpha,k}(\tilde{\alpha}_k) + \frac{1}{2}\beta_k^2, \tag{4.63}$$

with $W_{\rho,k}(\rho_k)$ and $\tilde{W}_{\alpha,k}(\tilde{\alpha}_k)$ given in (4.24) and (4.29), respectively. As before, assume for now that the solutions of (4.43) are such that $\rho_k(t) \in \mathcal{J}_\rho$ and $\tilde{\alpha}_k(t) \in \tilde{\mathcal{J}}_\alpha$ for all $k \leq M$ and

all $t \geq 0$. Then, the total derivative of (4.63) along the trajectories of the nominal systems (4.44) yields

$$\begin{aligned}\dot{V}_{p,k}(\xi_{p,k}) \leq & -c_1\left[\nabla W_{\rho,k}\right]^2 - \frac{4c_1c_3\kappa_2}{\kappa_1}\beta_k^2 - c_2\left[\nabla \tilde{W}_{\alpha,k}\right]^2 \\ \leq & -c_1'\rho_k^2 - c_2'\tilde{\alpha}_k^2 - c_3'\beta_k^2 \\ \leq & -c|\xi_{p,k}|^2, \end{aligned} \tag{4.64}$$

where we have used (4.53) and the bounds (4.26) and (4.30), and we defined $c_1' := 2c_1\kappa_2/\kappa_1$, $c_2' := 2c_2\tilde{\kappa}_2/\tilde{\kappa}_1$, $c_3' := 4c_1c_3\kappa_2/\kappa_1$, and $c := \min\{c_1', c_2', c_3'\}$.

Now, consider the function

$$V_p(\xi_p) = \sum_{k=1}^{l_p} V_{p,k}(\xi_{p,k}). \tag{4.65}$$

In view of (4.64), we have

$$\dot{V}_p(\xi_p) \leq -c|\xi_p|^2 < 0. \tag{4.66}$$

From (4.66) we establish asymptotic stability of the origin for the nominal systems (4.44).

Next, we establish boundedness of the solutions of (4.43). For that purpose, fix $p \leq h$ arbitrarily and consider the $(p-1)$-th and the p-th equations of the cascaded system (4.43).

In view of (4.45), for any r and k chosen above (such that the edge e_k is incident on e_r), the interconnection terms $g_{p,k}(\xi_{p,k}, \xi_{p-1})$, $p \in [2, h]$ satisfy, component-wise,

$$g_{p,k}(\xi_{p,k}, \xi_{p-1}) \leq \begin{bmatrix} \gamma_\rho(|\xi_{p-1,r}|) \\ \max\left\{1, \frac{1}{\rho_k}\right\}\gamma_\beta(|\xi_{p-1,r}|) \\ \max\left\{1, \frac{1}{\rho_k}\right\}\gamma_\alpha(|\xi_{p-1,r}|) \end{bmatrix}, \tag{4.67}$$

where $\gamma_\rho(s), \gamma_\beta(s), \gamma_\alpha(s) \in \mathcal{K}_\infty$ and we recall that $\xi_{p-1,r} = [\rho_r \ \beta_r \ \tilde{\alpha}_r]^\top$ is the r-th entry of ξ_{p-1}.

Now, consider the Lyapunov function in (4.63) with $p = 2$, $k \in [l_1 + 1, l_2]$, and $r \in [1, l_1]$. From (4.64) and (4.45), we have that the total derivative of $V_{2,k}$ satisfies

$$\begin{aligned}\dot{V}_{2,k}(\xi_{2,k}) \leq & -c_1\left[\nabla W_{\rho,k}\right]^2 - c_2\left[\nabla \tilde{W}_{\alpha,k}\right]^2 - \tilde{c}_3\beta_k^2 + |\nabla W_{\rho,k}|\,\gamma_\rho(|\xi_{1,r}|) \\ & + \max\left\{1, \frac{1}{\rho_k}\right\}\Big[\,|\beta_k|\gamma_\beta(|\xi_{1,r}|) + 2\left|\nabla \tilde{W}_{\alpha,k}\right|\gamma_\alpha(|\xi_{1,r}|) \\ & + \left|\frac{\partial^2 W_{\alpha,k}(s)}{\partial s^2}\right|_{\tilde{\alpha}_k=0}|\tilde{\alpha}_k|\,\gamma_\alpha(|\xi_{1,r}|)\Big]. \end{aligned} \tag{4.68}$$

Let $\epsilon > 0$ be an arbitrary positive constant. For any ϵ and any $\rho_k \geq \epsilon$, we have that $\max\{1, 1/\rho_k\} \leq \max\{1, 1/\epsilon\}$. Then, after some algebraic manipulations as in (4.58) and (4.59), we obtain

$$\dot{V}_{2,k}(\xi_{2,k}) \leq -c|\xi_{2,k}|^2 + \max\left\{1, \frac{1}{\epsilon}\right\}\gamma_r(|\xi_{1,r}|) \tag{4.69}$$

where c is a positive constant and γ_r is given as in (4.60), for each $r \in [1, l_1]$.

Now, considering again the function V_p in (4.65) with $p = 2$, we have

$$\dot{V}_2(\xi_2) \leq -c|\xi_2|^2 + \bar{\gamma}(|\xi_1|) \tag{4.70}$$

where $\bar{\gamma}(|\xi_1|) := \max\{1, \frac{1}{\epsilon}\} \sum_{r=1}^{l_1} \gamma_r(|\xi_{1,r}|)$, for any $\rho_k > \epsilon > 0$. Assume now that the solutions $t \mapsto \xi_2(t)$ grow unbounded. Since $\xi_1(t)$ is bounded, there exists $t' > 0$ such that $\dot{V}_2(\xi_2(t)) \leq 0$ for all $t \geq t'$, which leads to a contradiction. Therefore, $\xi_2(t)$ is bounded. Furthermore, since $\xi_1(t) \to 0$ it follows that, also, $\xi_2(t) \to 0$.

The previous arguments were stated for $p = 2$. However, given the cascaded nature of the system (4.43), proceeding recursively up to $p = h$ establishes the boundedness of $\xi_p(t)$, for each $\epsilon > 0$ such that $\rho_k \geq \epsilon$, and for all $2 \leq p \leq h$. Hence, from cascaded-systems arguments, we conclude that the origin of the system (4.43) is attractive for all initial conditions $\rho_k(0) \in \mathcal{J}_\rho$ and $\alpha_k(0) \in \mathcal{J}_\alpha$, which implies that full consensus is achieved.

Finally, we show next that, under the Proposition's assumption that $\rho_k(0) \in \mathcal{J}_\rho \backslash \{0\}$ and $\alpha_k(0) \in \mathcal{J}_\alpha$ the distance and field-of-view constraints are respected. As before, suppose that there exists $T > 0$ such that for all $t \in [0, T)$ and at least one $k \leq M$, $\alpha_k(t) \in \mathcal{J}_\alpha$ and $\alpha_k(T) \notin \mathcal{J}_\alpha$. Then, we have that $\tilde{W}_{\alpha,k}(\tilde{\alpha}_k(t)) \to \infty$ as $t \to T$. However, from (4.66) and (4.70), it follows that $\tilde{W}_{\alpha,k}(\tilde{\alpha}_k(t))$ is bounded for all $k \leq M$ and for all $t \geq 0$, which is a contradiction. The same analysis applies for the distance constraints, meaning that $W_{\rho,k}(\rho_k(t))$ is also bounded for all $t \geq 0$ and all $k \leq M$.

Thus, the control inputs (4.34)-(4.35) solve the leader-follower full-consensus problem with connectivity maintenance for the M interconnected systems (4.10). ■

4.3.3 *Non-static leader: robustness analysis*

Note that, after the definition of the coefficients a_{ij} (4.33) and the structure of the interaction topology in Figure 4.4, under the control laws (4.34)-(4.35), for the root node ($i = 1$) we have $v_1 = \omega_1 = 0$. However, it is not unlikely that in certain application scenarios, the root node, the "leader", follows a predefined trajectory. The latter implies that the root of the directed spanning tree, is subject to bounded non-zero velocities $v_1(t)$ and $\omega_1(t)$. Since we consider that there is no information exchange between the agents, the leader's velocities are assumed to be unknown to the followers. Therefore, $v_1(t)$ and $\omega_1(t)$ are considered as disturbances acting on the closed-loop system. Indeed, under such assumption, the multi-agent system (4.10) in closed-loop with the inputs (4.34)-(4.35) can be written in the form

$$\dot{\xi}_p = f_p(\xi_p) + g_p(\xi_p, \xi_{p-1}), \quad p \in [2, h] \tag{4.71a}$$

$$\dot{\xi}_1 = f_1(\xi_1) + \varphi(\xi_1, v_1, \omega_1) \tag{4.71b}$$

with

$$\varphi(\xi_1, v_1, \omega_1) := \left[\varphi_1(\xi_{1,1}, v_1, \omega_1)^\top \dots \varphi_{l_1}(\xi_{1,l_1}, v_1, \omega_1)^\top\right]^\top, \tag{4.72}$$

where

$$\varphi_k\left(\xi_{1,k}, v_1, \omega_1\right) = \begin{bmatrix} v_1 \cos(\beta_k) \\ -v_1 \frac{\sin(\beta_k)}{\rho_k} - \omega_1 \\ -v_1 \frac{\sin(\beta_k)}{\rho_k} \end{bmatrix}, \tag{4.73}$$

which comes from (4.10) when $v_1 \neq 0$ and $\omega_1 \neq 0$.

For system (4.71) we state the following.

Proposition 4.2 ([118]). *Consider a multi-agent system composed of N unicycles, described by the M interconnected systems (4.10), interacting over a directed spanning tree $\mathcal{G}$ and subject to distance and field-of-view constraints as defined by (4.13)-(4.12). Consider also that the leader agent, that is, the root of the directed spanning tree (labeled $i = 1$), is subject to bounded inputs $v_1(t)$ and $\omega_1(t)$ satisfying $|v_1(t)| \leq \bar{v}_1$ and $|\omega_1(t)| \leq \bar{\omega}_1$, respectively with $\bar{v}_1$ and $\bar{\omega}_1$ some positive constants. Then, under the controller (4.34)-(4.35), for all initial conditions $(\rho_k(0), \beta_k(0), \alpha_k(0))$ such that $\rho_k(0) \in \mathcal{J}_\rho \backslash \{0\}$ and $\alpha_k(0) \in \mathcal{J}_\alpha$, connectivity is maintained, i.e., $\rho_k(t) \in \mathcal{J}_\rho$ and $\alpha_k(t) \in \mathcal{J}_\alpha$, for all $k \leq M$ and $t \geq 0$.* □

Proof. The proof follows similar cascaded-systems' arguments as in the proof of Proposition 4.1. Consider first the subsystem (4.71b) and the barrier Lyapunov function

$$V_{1,k}(\xi_{1,k}) = W_{\rho,k}(\rho_k) + \tilde{W}_{\alpha,k}(\tilde{\alpha}_k) + \frac{1}{2}\beta_k^2, \tag{4.74}$$

with $k \leq l_1$ and $W_{\rho,k}$ and $\tilde{W}_{\alpha,k}$ given in (4.24) and (4.29), respectively. Differentiating $V_{1,k}$ with respect to time, akin to (4.68), using (4.72) and $|\partial^2 W_{\alpha,k}(s)/\partial s^2|_{\tilde{\alpha}_k=0} \leq \mu$, we have

$$\begin{aligned} \dot{V}_{1,k}(\xi_{1,k}) \leq & - c_1\left[\nabla W_{\rho,k}\right]^2 - c_2\left[\nabla \tilde{W}_{\alpha,k}\right]^2 - \tilde{c}_3\beta_k^2 + |\nabla W_{\rho,k}|\,|v_1| + |\beta_k||\omega_1| \\ & + \left|\nabla \tilde{W}_{\alpha,k}\right| \left[\frac{(1+c_3)}{\rho_k}|v_1| + c_3|\omega_1|\right] + |\tilde{\alpha}_k| \left[\frac{c_3\mu}{\rho_k}|v_1| + c_3\mu|\omega_1|\right]. \end{aligned} \tag{4.75}$$

After some algebraic manipulations, as in (4.58) and (4.59), for any $\epsilon > 0$ such that $\rho_k \geq \epsilon$, we obtain

$$\dot{V}_{1,k}(\xi_{1,k}) \leq -\tilde{c}|\xi_{1,k}|^2 + \frac{\tilde{\mu}}{\delta}\left[\bar{v}_1^2 + \bar{\omega}_1^2\right], \tag{4.76}$$

where $\tilde{c}$ and $\tilde{\mu}$ are positive constants. Next, for all the edges such that $p = 1$, we define the function

$$V_1(\xi_1) = \sum_{k=1}^{l_1} V_{1,k}(\xi_{1,k}). \tag{4.77}$$

From (4.76), the total derivative of V_1 satisfies

$$\dot{V}_1(\xi_1) \leq -\tilde{c}|\xi_1|^2 + \frac{\tilde{\mu} l_1}{\delta}\left[\bar{v}_1^2 + \bar{\omega}_1^2\right]. \tag{4.78}$$

From (4.76) we conclude boundedness of the solutions $\xi_1(t)$ of (4.71b). The latter follows by contradiction. Assume that the solutions $t \mapsto \xi_1(t)$ grow unbounded. From (4.76), there exists t' such that $\dot{V}_1(\xi_1(t)) \leq 0$ for all $t \geq t'$, which leads to a contradiction.

Finally, following recursively the same analysis as in the proof of Proposition 4.1 for the subsystems (4.71a), under the Proposition's assumption that $\rho_k(0) \in \mathcal{J}_\rho \backslash \{0\}$ and $\alpha_k(0) \in \mathcal{J}_\alpha$, we may conclude boundedness of $\xi_p(t)$, $p \in [1, h]$ as well as connectivity maintenance, for all $k \leq M$. ■

4.4 NUMERICAL EXAMPLES

To illustrate our theoretical results, the proposed control laws were validated in a realistic simulation scenario using the Gazebo simulator and the Robot Operating System (ROS) environment. Gazebo is an efficient 3D dynamic simulator of robotic systems in indoor and outdoor environments. In contrast to pure numerical-integration-based solvers of differential equations, in a Gazebo-ROS environment we can accurately emulate physical phenomena and dynamics otherwise neglected, such as friction, contact forces, actuator dynamics, slipping, *etc.* In addition, it offers high-fidelity robot and sensor models for simulation.

For the test scenario we employed the model of a velocity controlled Nexter Robotics' Wifibot Lab V4 to represent the agents. The necessary relative variables of distance and line-of-sight angles used in the controller are estimated from the ground truth data in Gazebo.

Concretely, in the simulation scenario we consider six Wifibots starting from an initial configuration defined in the 2nd-4th columns of Table 4.1. Moreover, we consider that each agent is equipped with a visual measurement device, fixed on the body of the robot, that has a limited range and a limited field of view. These constraint parameters are presented in the 5th-6th columns in Table 4.1, where Δ_ρ is the maximum distance so that the measurements are reliable and Δ_α is half of the maximum field-of-view angle.

Table 4.1: Initial conditions and constraint parameters

Index	x **[m]**	y **[m]**	θ **[rad]**	Δ_ρ **[m]**	Δ_α **[rad]**
1	-4.0	0.0	1.57	–	–
2	3.5	0.0	2.72	8.0	0.44
3	-11	5.0	-0.21	8.8	0.44
4	-11	-5.0	0.21	8.7	0.44
5	11	5.0	-2.16	9.3	0.44
6	11	-5.0	2.16	9.5	0.44

Under the initial conditions and the constraint parameters presented in Table 4.1, the initial interaction graph of the system is represented by the leader-follower topology (the directed spanning tree) illustrated in Figure 4.6.

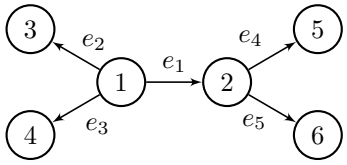

Figure 4.6: Initial leader-follower topology.

In order to test both the convergence and the robustness properties of the designed algorithm, in this simulation, we consider that the leader is subject to bounded vanishing inputs given by

$$v_1(t) = 0.2(\tanh(2(10-t))+1), \qquad \omega_1(t) = -0.1(\tanh(2(10-t))+1)\sin(0.5t),$$

satisfying $|v_1(t)| \leq 0.4$ m/s and $|\omega_1(t)| \leq 0.2$ rad/s. Furthermore, for all the simulations, the barrier Lyapunov functions $W_{\rho,k}$ and $W_{\alpha,k}$, for each $k \leq M$, were taken as

$$W_{\rho,k}(\rho_k) = \frac{1}{2}\left[\rho_k^2 + \ln\left(\frac{\Delta_{\rho,k}^2}{\Delta_{\rho,k}^2 - \rho_k^2}\right)\right] \tag{4.79}$$

$$W_{\alpha,k}(\alpha_k) = \frac{1}{2}\left[\alpha_k^2 + \ln\left(\frac{\Delta_{\alpha,k}^2}{\Delta_{\alpha,k}^2 - \alpha_k^2}\right)\right]. \tag{4.80}$$

The controller gains are fixed to $c_1 = 0.2$, $c_2 = 1$ and $c_3 = 0.2$. These values correspond to magnitudes comparable with the real Wifibot Lab V4 robots used for the experimental validation below.

The simulation results obtained in the Gazebo-ROS environment are presented in Figures 4.7-4.11. A video of the presented numerical simulations is also available at: https://tinyurl.com/distfullMultiRobFOVrange. It is important to remark that in the simulated scenario, in order to avoid collisions, the agents are forced to stop when the distance between pairs of robots is lower than a defined threshold. Hence, since the inter-agent distances cannot go to zero, full consensus is not achieved in this simulation —see Figure 4.7. The latter is the main limitation of the proposed control algorithm, which has yet to be addressed. Indeed, solving the full-consensus problem for nonholonomic vehicles under range and field-of-view limitations and with collision-avoidance guarantees via smooth time-invariant controllers is still an open problem.

For a more thorough numerical validation, the same scenario was simulated in MATLAB, where it is clear that, in the absence of collisions, full-consensus is achieved for the group of agents as soon as the leader's velocity disturbances vanish —see Figure 4.8. However, the interest of the Gazebo simulations is to show that in a realistic scenario, using the proposed controller, both the distance and field-of-view constraints are always respected, even when the leader has non-zero linear and angular velocities. The latter is evidenced on Figures 4.9 and 4.10. Moreover, from Figure 4.11 it can be seen that the inputs are smooth and time-invariant.

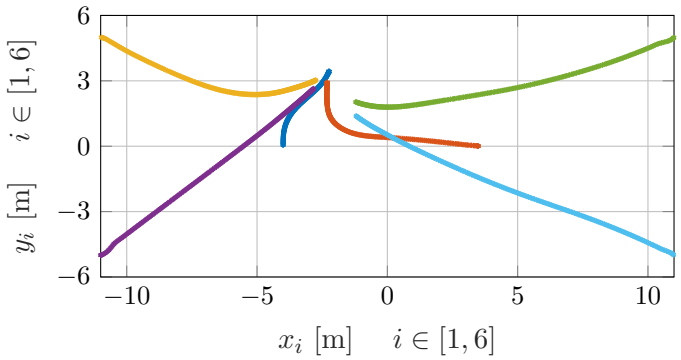

Figure 4.7: Paths followed by the Wifibots up to the stopping instant to prevent collisions —Gazebo simulation.

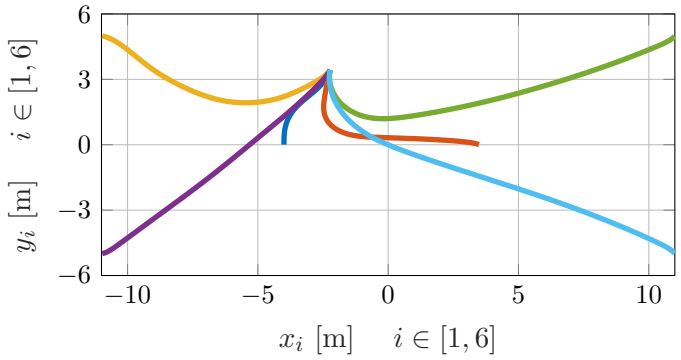

Figure 4.8: Paths followed by the Wifibots up to full consensus —MATLAB simulation.

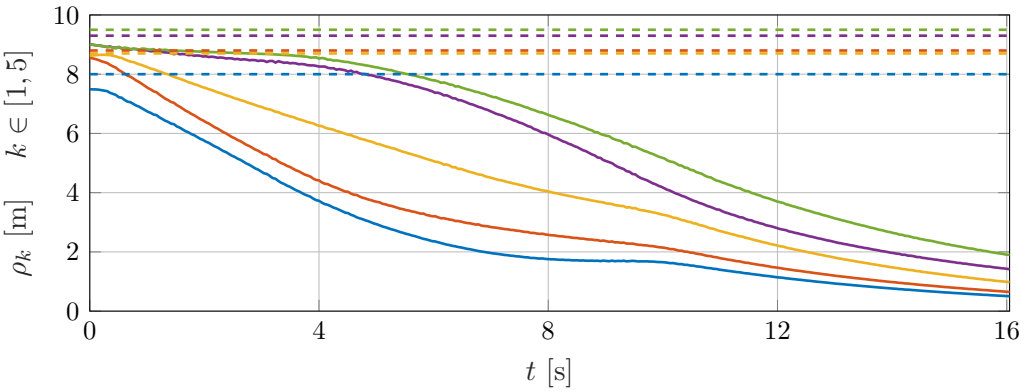

Figure 4.9: Inter-agent distances. The dashed lines represent the range limitations.

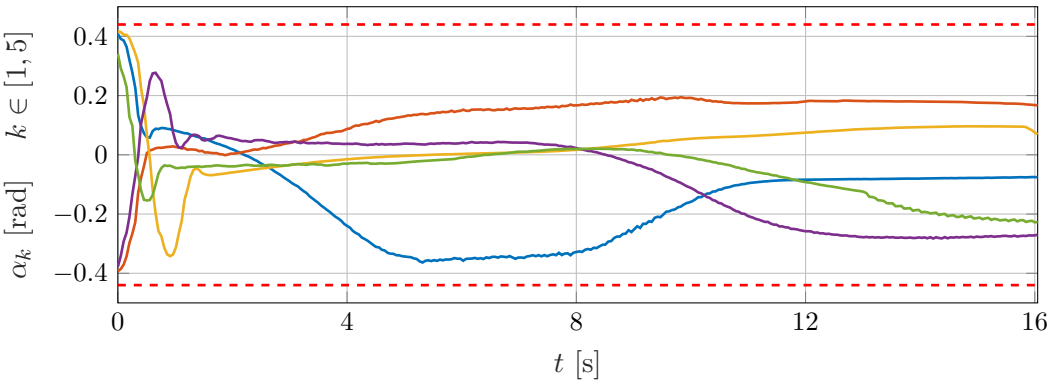

Figure 4.10: Line-of-sight angles. The dashed lines represent half of the maximal field-of-view limitations.

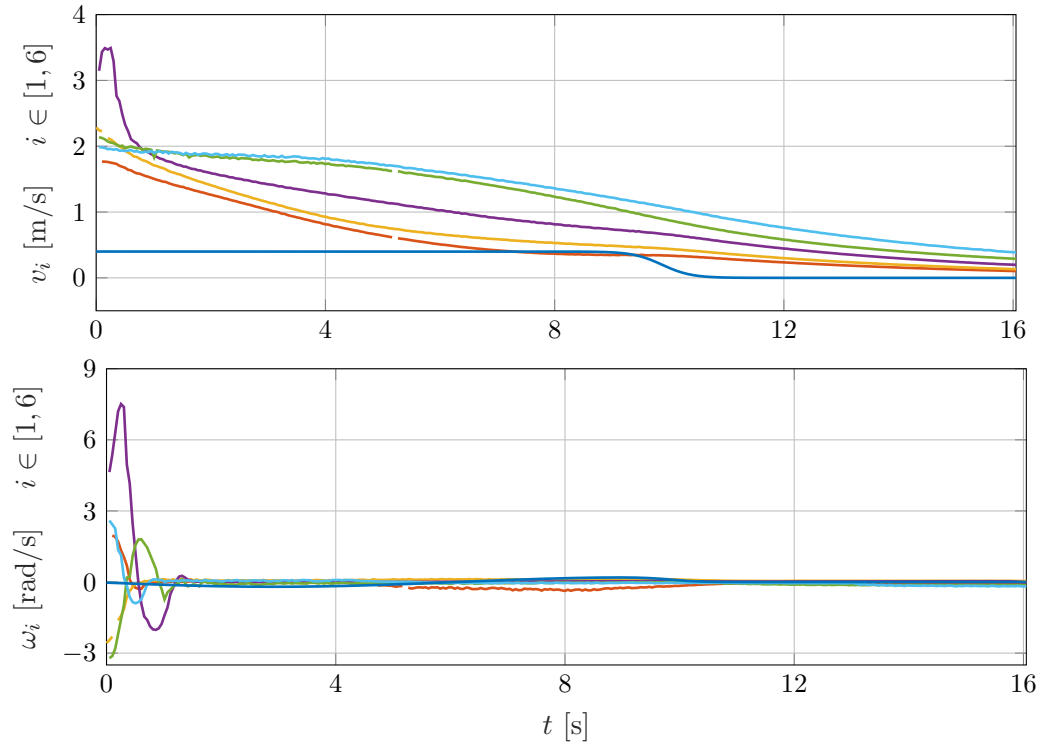

Figure 4.11: Smooth time-invariant inputs solving the full-consensus problem with connectivity maintenance. In the top figure are plotted the linear velocities while in the bottom one are plotted the angular rates.

As comparison, an additional Gazebo simulation was carried out using the full-consensus protocol (4.40)-(4.41) proposed in [119] where neither the distance nor the field-of-view

constraints were considered —see Remark 4.4. The results are presented in Figures 4.12 and 4.13, where it is clear that the constraints are not respected.

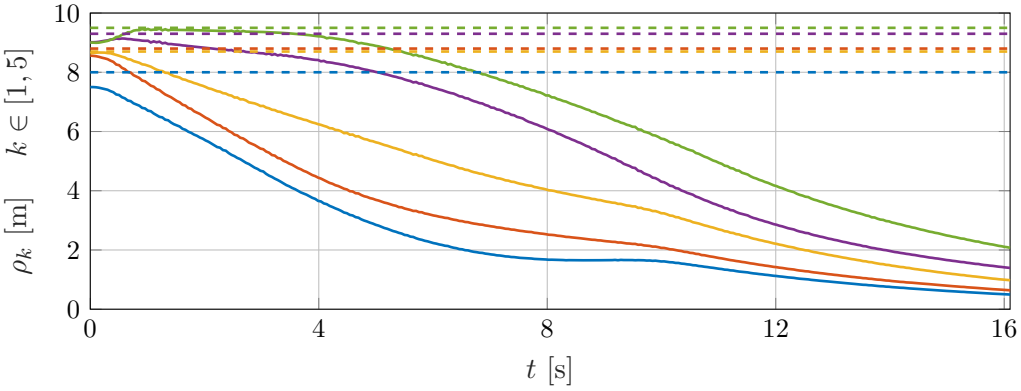

Figure 4.12: Inter-agent distances under the action of control laws (4.40)-(4.41). The dashed lines represent the range limitations.

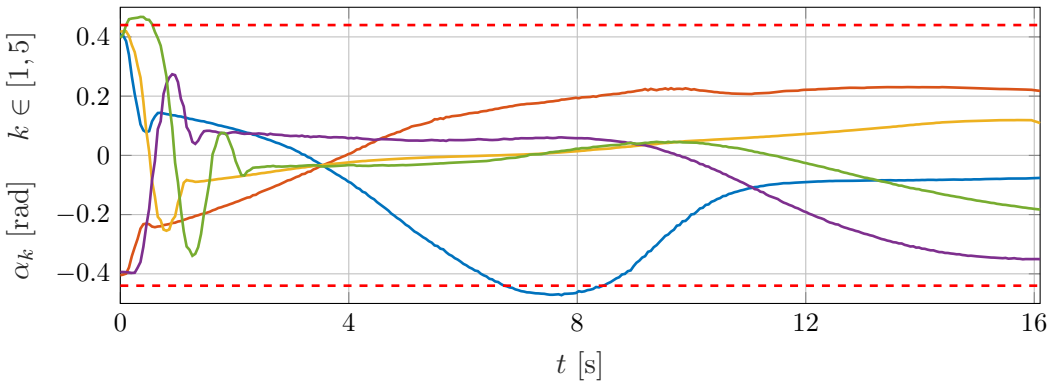

Figure 4.13: Line-of-sight angles under the action of control laws (4.40)-(4.41). The dashed lines represent half of the maximal field-of-view limitations.

Finally, in Figure 4.14 is presented a snapshot at around 7.5 seconds of both Gazebo simulations, visualized in Rviz. The Figure 4.14a corresponds to the controller without connectivity and visibility maintenance and the Figure 4.14b corresponds to the case where both constraints are considered in the control. The field of view of robot 2 is highlighted by the yellow dashed lines. It is clear from Figure 4.14a that the leader (in blue) is no longer inside the field of view of robot 2, whereas in Figure 4.14b the visibility constraint is satisfied. The latter corresponds to the constraint violation shown in Figure 4.13.

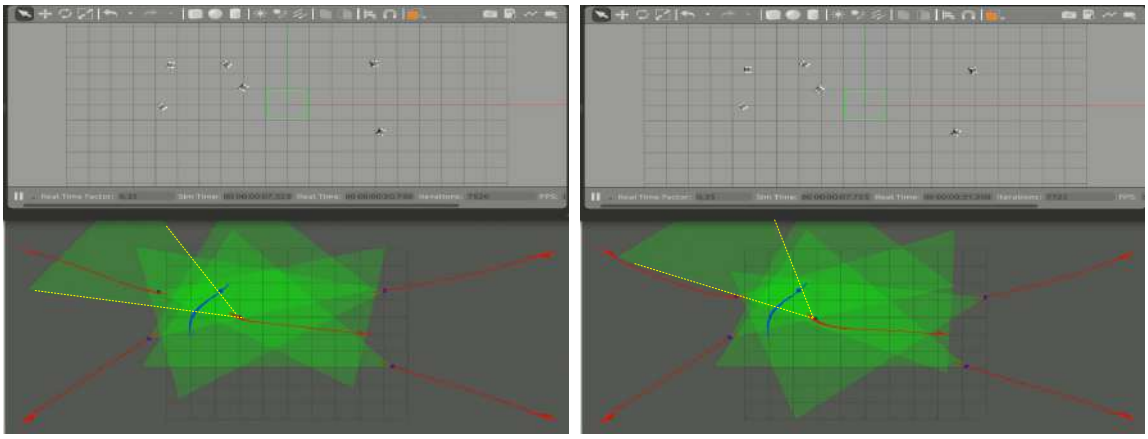

(a) Controller without connectivity maintenance (4.40)-(4.41).

(b) Controller with connectivity maintenance (4.34)-(4.35).

Figure 4.14: Snapshots of the Gazebo simulations. The field of view of robot 2 is highlighted by the dashed yellow lines.

4.5 EXPERIMENTAL VALIDATION

In addition to the numerical examples exposed above, some experiments were performed in order to illustrate the performance of the proposed control methodology in a real application setting. The experiments were performed using a group of four Nexter Robotics' Wifibots —see Figure 4.15. The latter correspond to the same models used in the Gazebo simulations. The implementation of the control law was done under the ROS interface. Moreover, an Optitrack motion capture system based on active IR cameras and markers was used which, coupled with odometry sensors, allowed us to obtain the ground-truth values of the positions and velocities of the robots. A video of the experimental test is also available at: https://tinyurl.com/SmoothConsensusUnicycles.

Figure 4.15: Snapshot of the experimental test using four Nexter Robotics' Wifibots.

In order to avoid potential collisions between the agents as they reach consensus, we consider a leader-follower full-consensus-based formation scenario, rather than a generic consensus one. For this purpose, instead of defining ρ_k as the distance between a pair of agents i and j (4.9a), we define it as the distance from a follower to the desired relative position with respect to its leader's position, *i.e.*,

$$\rho_k := |p_i - p_j - z_k^d|, \tag{4.81}$$

where z_k^d is the desired relative position determined by the formation. We stress that the definition (4.81) does not affect the methodology developed in this chapter as the system (4.10) remains unchanged for a constant z_k^d.

The initial configurations of the four Wifibots are defined in the 2nd-4th columns of Table 4.2. We consider that each robot has a limited interaction range given by the maximum distance Δ_ρ in the 5th column of Table 4.2. Note, however, that because the quantity (4.81) no longer represents the actual distances between agents, the values of Δ_ρ in Table 4.2 are the actual range limitations minus the distance between the desired position in the formation and the leader, $|z_k^d|$. Moreover, due to practical limitations, no constraints are imposed on the field of view. Therefore, for the control design we defined the barrier Lyapunov function $W_{\rho,k}$ encoding the range constraints as in (4.79), whereas the function $W_{\alpha,k}$ was taken as a quadratic function

$$W_{\alpha,k}(\alpha_k) = \frac{1}{2}\alpha_k^2. \tag{4.82}$$

We stress that, as evoked in Remark 4.4, using the function $W_{\alpha,k}$ in (4.82), the control methodology proposed above still holds —see also [120].

Table 4.2: Initial conditions and constraint parameters

Index	x **[m]**	y **[m]**	θ **[rad]**	Δ_ρ **[m]**
1	1.5	2.2	0.0	–
2	-1.3	2.2	-1.9	2.7
3	-1.5	-0.5	1.6	3.4
4	1.2	0.3	-2.8	4.2

Under the initial conditions and the range limitations in Table 4.2 the initial graph representing the interaction topology of the four robots is illustrated in Figure 4.16.

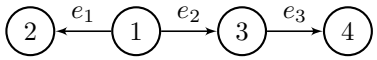

Figure 4.16: Initial leader-follower topology.

In Figure 4.17 are presented the trajectories of the vehicles up to the desired formation. The blue dot represents the position of the static leader and the red dots are the desired

positions of each agent with respect to its respective leader, as defined by the interaction graph showed in Figure 4.16. It is clear from Figures 4.18 and 4.19 that the group of agents successfully achieve the desired formation with consensus on the orientation, as expected. Additionally, in Figure 4.18 it can be appreciated that all distance constraints (dashed lines) are respected, thus guaranteeing connectivity maintenance.

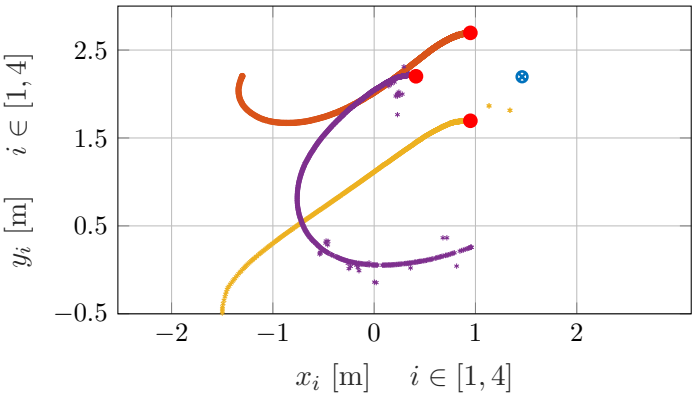

Figure 4.17: Paths followed by the Wifibots up to the desired formation.

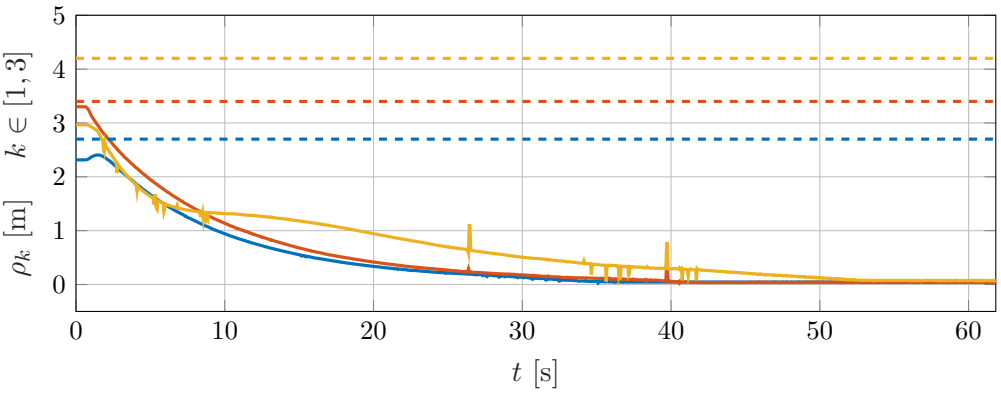

Figure 4.18: Inter-agent distances. The dashed lines represent the range limitations.

In Figure 4.20 are presented the control inputs for the four robots. It is evident from the figures that the control inputs are smooth, as claimed. We clarify that the apparent "dripping" in the curves on Figure 4.11 is due to position-measurements noise coming from the motion capture system of our *experimental* benchmark. The effect of such noise can also be appreciated in Figures 4.17 and 4.18.

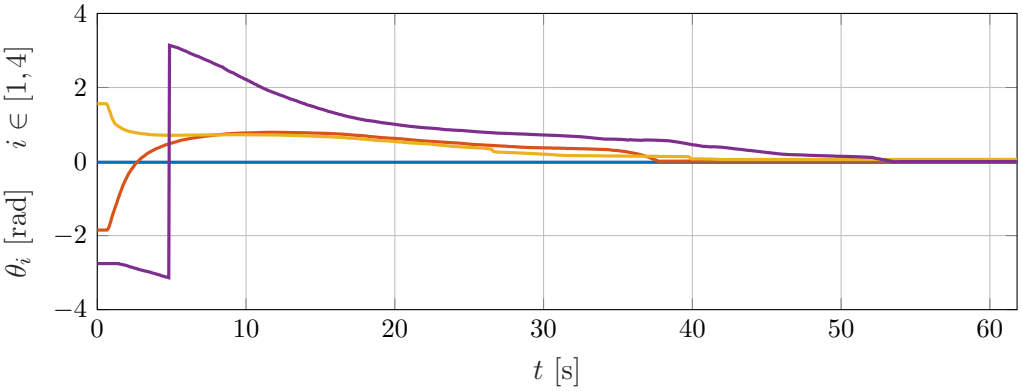

Figure 4.19: Orientations of the vehicles with respect to the coordinate frame.

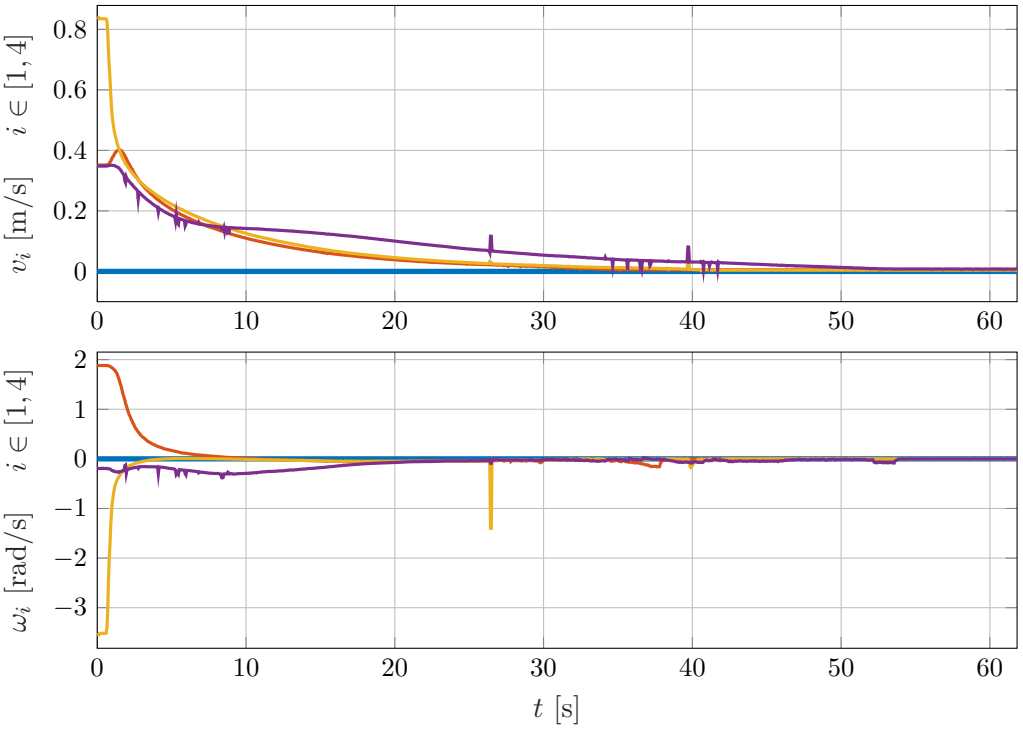

Figure 4.20: Smooth time-invariant inputs solving the full-consensus problem with range limitations. In the top figure are plotted the linear velocities while in the bottom one are plotted the angular rates.

4.6 CONCLUSION

We solved the leader-follower full-consensus problem with connectivity maintenance for a multi-vehicle nonholonomic system subject to range and field-of-view constraints, and interconnected through an arbitrary leader-follower (directed spanning tree) topology. Remarkably, using a polar-coordinates-based model, the proposed control law is smooth time-invariant and relies only on relative inter-agent variables. Our contributions are original in that most of the existing results either address only position consensus or design non-smooth or time invariant feedback laws, adding a degree of complexity to the control design problem and to the stability analysis. In contrast, smooth and time-invariant control laws are not prevented when considering the polar-coordinates model, as we do here. This renders the proposed controller more suited for practical implementation and facilitates the analysis through Lyapunov and cascaded systems' theory. Moreover, when considering the connectivity-maintenance problem, it is usually required that the agents communicate with their neighbors, ruling out the meaningful sensor-based coordination scenario. In such a scenario, we validated the performance of the proposed controllers via numerical examples and experimental setups.

With respect to the results exposed in Chapter 3, the contributions presented in this chapter are a natural next step for considering more realistic constrained-coordination problems for multi-robot systems. Indeed, the nonholonomic integrator represents well the motion of ground vehicles and of some types of aerial robots flying at constant altitudes. However, several kinds of systems fail to be represented via the low-order linear or nonlinear systems considered in this chapter and in the previous one. Therefore, in the next chapter we extend our results on constrained consensus to more complex high-order systems.

5

CONSENSUS OF HIGH-ORDER SYSTEMS UNDER OUTPUT CONSTRAINTS

In Chapter 3 we presented how the analysis of the consensus protocol using the edge-based representation is used to address scenarios where the (limited) interconnection between the agents is modeled via nonlinear functions of the state, and to establish strong stability and robustness properties. Then, in Chapter 4, the consensus problem with connectivity maintenance was studied for vehicles with nonholonomic restrictions, for which similar stability and robustness properties were also established. The previous results were established, respectively, for systems modeled as first- and second-order integrators and for the first-order nonholonomic integrator.

Although interesting on their own, such low-order models may fail to represent many meaningful and complex systems with a high relative degree with respect to an output of interest. Moreover, besides the connectivity problem addressed in previous chapters, in realistic settings, multi-agent systems are subject to other limitations imposed by the actuators or by the environment, such as input saturation or minimal safety distances. In addition, physical systems are constantly subject to disturbances in the form of external inputs, modeling uncertainties, delays, *etc.* Thus, in this chapter, we generalize the results previously obtained for first- and second-order systems. Indeed, the contributions presented hereafter pertain to the consensus-based formation control of high-order systems under inter-agent constraints, mainly connectivity maintenance and collision avoidance, and with robustness with respect to disturbances.

We propose a control-design methodology in order to solve partial- and full-state consensus problems under inter-agent constraints and disturbances for high-order systems in normal form, while guaranteeing strong stability and robustness properties. It applies to networks with undirected and directed topologies. The inter-agent constraints that guarantee the systems' safety as well as the integrity of the (initial) topology through the maintenance of connectivity, are encoded in the form of *output* constraints. Essentially, these take the mathematical form of a lower and an upper bound on the norm of relative-error states, which are more natural inter-agent constraints than those considered, *e.g.*, in [85] and [86].

For the control design we build upon the results on constrained-consensus for low-order integrators in Section 3.3 in order to propose a Lyapunov-based control design using the concept of *command filtered backstepping* [121], [122] with the barrier-Lyapunov-functions-based controllers for consensus of first-order systems. The command-filtered-backstepping

approach, which is not an original contribution of this thesis, replaces the successive derivatives of the gradient-based control law by approximations via linear strictly-positive-real filters, facilitating the implementation of the actual controllers.

In regards to the formal analysis, it is important to stress that since the inter-agent constraints may introduce undesired unstable equilibria within the edges' perspective, the closed-loop system is analyzed relying on the theory of multi-stable systems [123], [124]. Based on the latter we establish stronger results than the mere convergence property, commonly established in the literature —see, *e.g.*, [13]–[15], [28], [29]. Indeed, we establish asymptotic convergence of the multi-agent system to the consensus manifold, as well as robustness with respect to bounded disturbances in the sense of practical-input-to-state stability.

5.1 THE CONSENSUS-BASED FORMATION PROBLEM

5.1.1 *Problem formulation*

We consider now multi-agent nonlinear systems in feedback form with high relative degree with respect to an output of interest. The problem that we address here covers the one solved in Chapter 3 in that not only the systems studied in this chapter are of order higher than 2, but also in that we consider a broader class of constraints, beyond connectivity maintenance. For simplicity and clarity of exposition, in the theoretical development presented hereafter we consider that each agent is modeled as a high-order system in normal form subject to additive disturbances. More precisely, we consider N multi-variable systems in normal form and of relative degree ϱ as follows:

$$\dot{x}_{i,l} = x_{i,l+1} + \theta_{i,l}(t), \quad l \leq \varrho - 1 \tag{5.1a}$$

$$\dot{x}_{i,\varrho} = u_i + \theta_{i,\varrho}(t) \tag{5.1b}$$

where $x_{i,l} \in \mathbb{R}^n$, $l \leq \varrho$, $i \leq N$, denotes the components of the state of each agent, $u_i \in \mathbb{R}^n$ is the control input, $\theta_{i,l} : \mathbb{R}_{\geq 0} \to \mathbb{R}^n$ is an essentially bounded function that represents a disturbance, and $x_{i,1}$ is considered an output of interest.

There is little loss of generality in restricting our study to systems modeled as in (5.1) since many systems in feedback form can be transformed into (5.1) through different nonlinear control approaches, such as feedback linearization, input transformation, etc. [17], [108]. Plants that fit in this category include fully feedback-linearizable systems, but also a number of instances of physical systems, such as robot manipulators [125], spacecrafts [126], flexible-joint manipulators [127], [128], and, more relevant to this thesis, flying vehicles [129]. An extension to the case of underactuated UAVs is addressed in Chapter 6.

It is assumed that the local interaction between the agents is represented by a graph $\mathcal{G} = (\mathcal{V}, \mathcal{E})$. Similarly to Chapter 3 the topology is considered hereafter to be either an undirected graph, or the two classes of directed graphs: spanning-trees or cycles. Hence, akin to Assumptions 3.1 and 3.2, the following assumptions are used in this chapter.

Assumption 5.1. *The initial undirected graph contains a spanning tree.*

Assumption 5.2. *The initial directed graph is either a directed spanning tree or a directed cycle.*

As in Chapter 3, we consider that the inter-agent constraints are defined as a set of restrictions on the system's output. However, in this chapter we consider a more general set of constraints by setting both an upper and a lower bound on the inter-agent distances. In the case of autonomous vehicles, this apparently innocuous extension allows us to consider simultaneously connectivity maintenance and inter-agent collision avoidance. Mathematically, the constraints are defined as follows. For each $k \leq M$, let Δ_k and δ_k be, respectively, the upper and minimal distances, satisfying $0 \leq \delta_k < \Delta_k$. Then, akin to (3.7), the set of inter-agent output constraints is defined as

$$\mathcal{D} := \left\{ z \in \mathbb{R}^{nM} : \delta_k < |z_k| < \Delta_k, \ \forall\, k \leq M \right\}. \tag{5.2}$$

where

$$z_k := x_{i,1} - x_{j,1} \quad \forall k \leq M, \quad (i,j) \in \mathcal{E}, \tag{5.3}$$

are the components of the edge states for the multi-agent system. Hence, let $x_1^\top = \begin{bmatrix} x_{1,1}^\top \cdots x_{N,1}^\top \end{bmatrix} \in \mathbb{R}^{nN}$ be the collection of the first states, *i.e.*, $l = 1$, of all the agents of the system and let $z^\top = [z_1^\top \cdots z_M^\top]^\top \in \mathbb{R}^{nM}$. Then, recalling the edge transformation (2.28), in compact form, the edge states are given by

$$z := [E^\top \otimes I_n] x_1, \tag{5.4}$$

where E is the incidence matrix defined in (2.25).

In Chapters 3 and 4 we studied the (position) consensus problem in which the objective consists in all the agents converging to the same point, or, in other words, making $z \to 0$. The latter, however, is not possible when considering physical systems and safety constraints. In this chapter we generalize the previous results by setting the problem as one of consensus-based formation. In this setting, the new control goal is for the agents to achieve output consensus with a desired relative position, centered at a point of non-predefined coordinates in the presence of output constraints as given by the set $\mathcal{D}$ in (5.2). Mathematically, the consensus-based formation problem translates into making $x_{i,1} - x_{j,1} \to z_k^d$, or equivalently, $z_k \to z_k^d$ in the relative coordinates, where $z_k^d \in \mathbb{R}^n$ denotes the desired relative state between a pair of neighboring agents i and j.

Assumption 5.3. *The formation determined by the desired relative state z_k^d between a pair of neighbors i and j is compatible with the inter-agent constraints given by the set (5.2). That is, $z^d \in \mathcal{D}$, where $z^{d\top} = [z_1^{d\top} \cdots z_M^{d\top}] \in \mathbb{R}^{nM}$.*

For brevity, in the rest of this chapter we refer to the consensus-based formation problem as simply the consensus problem or the output-consensus problem according to the context.

Now, define the consensus error variable as

$$\tilde{z} := z - z^d. \tag{5.5}$$

Let each $x_l^\top = \begin{bmatrix} x_{1,l}^\top \cdots x_{N,l}^\top \end{bmatrix} \in \mathbb{R}^{nN}$, $l \in \{2, \dots, \varrho\}$, be the collection of each state of all the agents of the system. Then, in the error edge coordinates, the consensus objective is that

$$\lim_{t\to\infty} \tilde{z}(t) = 0 \tag{5.6a}$$

$$\lim_{t\to\infty} x_l(t) = 0, \quad \forall l \in \{2, \dots, \varrho\}. \tag{5.6b}$$

Remark 5.1. *Note that for $\varrho = 2$ the objective in (5.6) corresponds to that of position consensus of second-order integrators (3.50), addressed in Chapter 3.* •

Now, recalling the identities (2.48) and (2.50), denoting $z_t^d \in \mathbb{R}^{n(N-1)}$ as the vector of desired relative displacements corresponding to $\mathcal{G}_t$, and collecting the inputs of the multiple agents into the vector $u^\top = \begin{bmatrix} u_1^\top \cdots u_N^\top \end{bmatrix} \in \mathbb{R}^{nN}$ and the disturbances into $\theta_1^\top = \begin{bmatrix} \theta_{1,1}^\top \cdots \theta_{N,1}^\top \end{bmatrix} \in \mathbb{R}^{nN}$ and $\theta_l^\top = \begin{bmatrix} \theta_{1,l}^\top \cdots \theta_{N,l}^\top \end{bmatrix} \in \mathbb{R}^{nN}$, for $l \in \{2, \dots, \varrho\}$, the reduced-order system's equations read

$$\dot{\tilde{z}}_t = \begin{bmatrix} E_t^\top \otimes I_n \end{bmatrix} x_2 + \begin{bmatrix} E_t^\top \otimes I_n \end{bmatrix} \theta_1(t) \tag{5.7a}$$

$$\dot{x}_l = x_{l+1} + \theta_l(t), \quad l \in \{2, \dots, \varrho - 1\} \tag{5.7b}$$

$$\dot{x}_\varrho = u + \theta_\varrho(t), \tag{5.7c}$$

where we recall that E_t is the incidence matrix of an arbitrary spanning tree contained in the graph. In these coordinates, output-consensus as defined in (5.6) is achieved if the origin is asymptotically stabilized for the reduced-order system (5.7). More precisely, we consider the following problem.

Robust consensus problem with output constraints. Consider a multi-agent system of agents with high relative-degree dynamics given by (5.1), interacting over a connected undirected graph, a directed spanning tree or a directed cycle. Assume, in addition, that the systems are subject to inter-agent constraints that consist in the outputs being restricted to remain in the set defined in (5.2). Under these conditions, find a distributed dynamic controller with outputs u_i, $i \leq N$, which, in the absence of disturbances, *i.e.*, $\theta_{i,l} \equiv 0$, $l \leq \varrho$, $i \leq N$, achieves the objective (5.6) and renders the constraints set (5.2) forward invariant, *i.e.*, $z(0) \in \mathcal{D}$ implies that $z(t) \in \mathcal{D}$ for all $t \geq 0$. Furthermore, in the presence of essentially bounded disturbances, that is if $\theta_l \not\equiv 0$, u_i renders the origin of (5.7) practically input-to-state stable and the set $\mathcal{D}$ in (5.2) forward invariant. •

The solution to the robust consensus problem with output constraints stated above is the main contribution of this thesis. It was presented in [130]. We acknowledge that some works may be found in the literature that solve similar problems of consensus under constraints [28], [85], [86]. However, in the latter, the considered constraints weigh either on the synchronization errors or on the high-order variables, which may fail to capture meaningful inter-agent constraints as we do here. Furthermore, in regards to the formal analysis, as in Chapter 3, we establish stronger results than the mere convergence property, commonly established in the literature —see, *e.g.*, [13]–[15], [28], [29]. Indeed, we formally establish asymptotic convergence of the multi-agent system to the consensus manifold, as well as robustness with respect to bounded disturbances in the sense of practical-input-to-state stability.

5.1.2 *Barrier Lyapunov function with multiple singular points*

As in previous chapters, in order to account for the inter-agent constraints, the control design is based on the gradient of a barrier Lyapunov function —*cf.* [90], [91], [102] and Definition 3.1. Nonetheless, since in this chapter we address the problem of consensus-based formation, some particular considerations have to be made. Indeed, the edge state of our system (5.7) is the formation error $\tilde{z}_t$, but the output constraints encoded by the set (5.2) are in terms of the original edge states z. Therefore, with respect to the barrier Lyapunov functions recalled in Section 3.1.3, some modifications have to be applied.

First we introduce the set

$$\tilde{\mathcal{D}}_k := \{\tilde{z}_k \in \mathbb{R}^n \,:\, \delta_k < |\tilde{z}_k + z_k^d| < \Delta_k\}, \quad \forall k \leq M \tag{5.8}$$

as the set of inter-agent constraints for each edge in the graph. Then, for each $k \leq M$, we define a barrier Lyapunov function candidate $W_k : \tilde{\mathcal{D}}_k \to \mathbb{R}_{\geq 0}$, of the form

$$W_k(\tilde{z}_k) = \frac{1}{2}\left[|\tilde{z}_k|^2 + \tilde{B}_k(\tilde{z}_k + z_k^d)\right], \tag{5.9}$$

where $\tilde{B}_k$ is a non-negative function such that $\tilde{B}_k(z_k^d) = 0$ and $\nabla\tilde{B}_k(z_k^d) = 0$, while $\tilde{B}_k(\tilde{z}_k + z_k^d) \to \infty$ as either $|\tilde{z}_k + z_k^d| \to \Delta_k$ or $|\tilde{z}_k + z_k^d| \to \delta_k$. Therefore, the barrier Lyapunov function candidate (5.9) satisfies: $W_k(0) = 0$, $\nabla W_k(0) = 0$, and $W_k(\tilde{z}_k) \to \infty$ as either $|\tilde{z}_k + z_k^d| \to \Delta_k$ or $|\tilde{z}_k + z_k^d| \to \delta_k$, or equivalently in the original edge coordinates, as either $|z_k| \to \Delta_k$ or $|z_k| \to \delta_k$. See Figure 5.1 for an illustration.

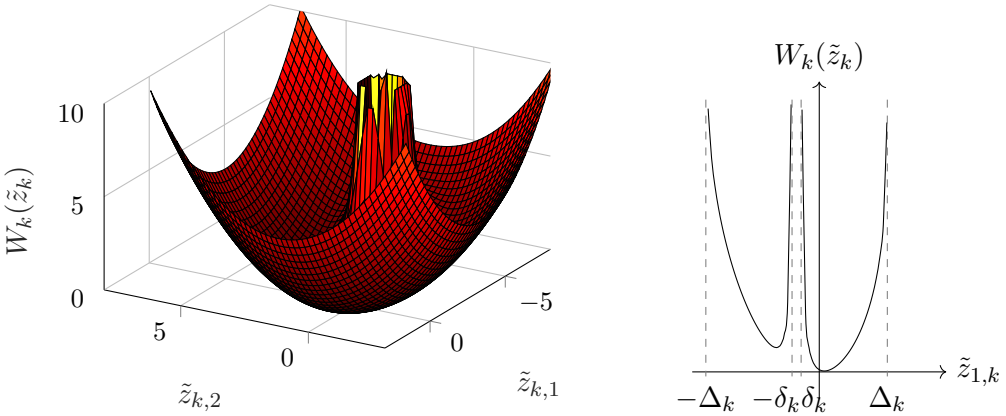

Figure 5.1: Example of a barrier Lyapunov function for a 2-dimensional state $\tilde{z}_k = [\tilde{z}_{k,1}\ \tilde{z}_{k,2}]^\top$ (left) and its level curve for $\tilde{z}_{k,2} = 0$ (right).

Remark 5.2. *The function $(\tilde{z}_k + z_k^d) \mapsto \tilde{B}_k(\tilde{z}_k + z_k^d)$ in (5.9) may seem equivalent to the function $z_k \mapsto B_k(z_k)$ in (3.10). Indeed, noting that $z_k \equiv \tilde{z}_k + z_k^d$, both functions satisfy $\tilde{B}_k(\tilde{z}_k + z_k^d) \to \infty$ and $B_k(z_k) \to \infty$ as $|z_k| \to \partial\tilde{\mathcal{D}}_k$ and $|z_k| \to \partial\mathcal{J}_k$, respectively, where $\tilde{\mathcal{D}}_k$ and $\mathcal{J}_k$ denote the respective inter-agent constraints, as defined in (5.8) and (3.9), respectively.*

However, under a close inspection we note that $\tilde{B}_k$ *is defined such that* $\tilde{B}_k(z_k^d) = 0$ *and* $\nabla\tilde{B}_k(z_k^d) = 0$*, whereas* B_k *in turn, is defined such that* $B_k(0) = 0$ *and* $\nabla B_k(0) = 0$*.*

The latter comes from the fact that the set $\mathcal{D}$ *in* (5.2) *encodes the constraints on the original edge coordinates* z_k *(as does* $\mathcal{J}$ *in* (3.7)*) and not in terms of the error variable* $\tilde{z}_k$*. For the consensus-based formation problem addressed in this chapter, defining a barrier Lyapunov function of the form* (3.10) *may lead to imposing conservative feasibility conditions in terms of the initial conditions* [131]*. Therefore, in this chapter we define* (5.9) *where* $(\tilde{z}_k + z_k^d) \mapsto \tilde{B}(\tilde{z}_k + z_k^d)$ *may be constructed as an integral barrier Lyapunov function* [131] *or as a weight recentered barrier function* [32], [132] *—see also Appendix A.2—, in order to satisfy the desired properties.* •

Remark 5.3. *The functions defined in* (5.9) *are reminiscent of scalar potential functions in constrained environments. Hence, the appearance of multiple critical points is inevitable* [30]*. Indeed, the gradient of the barrier Lyapunov function of the form* (5.9)*,* $\nabla W_k(\tilde{z}_k)$*, vanishes at the origin and at an isolated saddle point separated from the origin —see Appendix A.3 for an example. Therefore, when using the gradient of* (5.9) *for the control, the closed-loop system has multiple equilibria. This prevents us from using the classical stability tools for the analysis of the system, as used in Chapter 3. Such technical difficulty is addressed using tools tailored for so-called multi-stable systems —see* [123], [124]*, and Appendix A.4.* •

Now, as in Chapter 3, we define a barrier Lyapunov function for the whole multi-agent system as

$$W(\tilde{z}) = \sum_{k \leq M} W_k(\tilde{z}_k) \tag{5.10}$$

and, in light of Remark 5.3, let us denote by $\tilde{z}^* \in \mathbb{R}^{nM}$ the vector containing the saddle points of the barrier Lyapunov function for each edge (5.9). Then, define the disjoint set

$$\mathcal{W} := \{0\} \cup \{\tilde{z}^*\}, \tag{5.11}$$

which corresponds to the critical points of $\tilde{z} \mapsto W(\tilde{z})$ in (5.10). Then, we assume the following.

Assumption 5.4. *The gradient of the barrier Lyapunov function* W *in* (5.10) *satisfies the bound*

$$\frac{1}{2}|\tilde{z}|_{\mathcal{W}}^2 \leq \kappa|\nabla W(\tilde{z})|^2 \tag{5.12}$$

where κ *is a positive constant and* $|\tilde{z}|_{\mathcal{W}} := \min\left\{|\tilde{z}|, |\tilde{z} - \tilde{z}^*|\right\}$*.*

5.2 OUTPUT CONSENSUS

The robust consensus problem with output constraints previously formulated is solved using a distributed dynamic nonlinear controller. Akin to the controller proposed in Section 3.3 for

second-order integrators, the design follows a backstepping approach that naturally exploits the normal form of the system.

It is well-known, however, that the backstepping approach may lead to an increase of complexity of the control law due to the successive differentiation of the virtual controllers [108]. Indeed, note that, *e.g.*, in the constrained consensus control for second-order integrators interconnected over directed graphs designed in Section 3.3, the time derivative of the virtual input (3.61) is required. This problem is emphasized herein by the fact that we would need the high order derivatives of the gradient of a barrier Lyapunov function, which is defined only in open subsets of the state space and, in the context of this chapter, has multiple local minima —see Remark 5.3 above. Therefore, in order to bypass these technical obstacles, inspired by the *command filtered backstepping* approach [122], we approximate the virtual inputs and their derivatives in each step of the backstepping design by means of command filters. This is explained in detail farther below.

For simplicity, in the remainder of this chapter we only address the design in the case of directed graphs. Nonetheless we stress that, with appropriate modifications, the results in this section also hold for undirected connected topologies.

This backstepping-based control design is as follows. Consider, first, the edge subsystem (5.7a) with x_2 as an input. In order to cope with the output constraints, the control law is based on the gradient of the barrier Lyapunov function (5.10) and is given by[1]

$$x_2^* := -c_1 \left[E_\odot \otimes I_n\right] \nabla W(\tilde{z}), \tag{5.13}$$

where c_1 is a constant that is positive by design. Indeed, the right-hand side of (5.13) qualifies as a control law that solves the constrained consensus problem for first-order multi-agent systems interconnected over directed graphs —*cf.* Section 3.2. So, defining $\bar{x}_2 := x_2 - x_2^*$ and using (5.13), Equation (5.7a) becomes

$$\dot{\tilde{z}}_t = -c_1 [E_t^\top E_\odot \otimes I_n] \nabla W(\tilde{z}) + [E_t^\top \otimes I_n] \left[\bar{x}_2 + \theta_1\right]. \tag{5.14}$$

For the purpose of making $\bar{x}_2 \to 0$ in (5.13), following a backstepping-based design, we rewrite the second equation in (5.7b), *i.e.*, with $l = 2$, in error coordinates $\bar{x}_2$ and we consider x_3 as an input. We have

$$\dot{\bar{x}}_2 = x_3 - \dot{x}_2^* + \theta_2. \tag{5.15}$$

Hence, the natural virtual control law at this stage is

$$x_3^* = -c_2 \bar{x}_2 + \dot{x}_2^*, \quad c_2 > 0, \tag{5.16}$$

since it leads to the perturbed, otherwise exponentially stable, system

$$\dot{\bar{x}}_2 = -c_2 \bar{x}_2 + \theta_2. \tag{5.17}$$

However, applying such control requires the derivative of the right-hand side of (5.13). Furthermore, a recursive procedure requires up to $\varrho - 2$ successive derivatives of x_2^*, which

1 For undirected graphs this virtual control law takes the form $x_2^* = -c_1 [E \otimes I_n] \nabla W(\tilde{z})$ —*cf.* Chapter 3.

poses significant technical and numerical difficulties. Thus, to avoid the use of successive derivatives of $\nabla W(\tilde{z})$ we approximate the derivatives of the virtual controls x_l^*, with $l \in \{2, \dots, \varrho - 1\}$ by means of *command filters*. This modified form of backstepping control is known as *command-filtered* backstepping —see [122]. For simplicity, we use second-order systems defined as in the figure below:

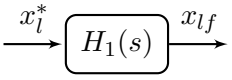

$$H_1(s) := \frac{\omega_n^2}{s^2 + 2\omega_n s + \omega_n^2}$$

Figure 5.2: Command filter used for implementation. The dirty derivative of x_l^* may be obtained using $\dot{x}_{lf} := sH_1(s)x_l^*$ which is equivalent to $\dot{x}_{lf} = H_1(s)\dot{x}_l^*$.

The virtual controls are considered as the inputs of a command filter, with the outputs corresponding to the approximated signals and their derivatives, denoted x_{lf} and $\dot{x}_{lf}$, respectively. The filters' natural frequency, $\omega_n > 0$, is a control parameter which is chosen large enough so that the approximation x_{lf} converges to the desired virtual control x_l^* in a faster time-scale than that of the system's dynamics —see Section 5.3.1 below for further details. Similarly, $\dot{x}_{lf} = H_1(s)\dot{x}_l^*$ approximates $\dot{x}_l^*$.

Remark 5.4. *For clarity, we use second-order command-filters as defined in Figures 5.2 above. However, the design is not restricted to this particular choice. Indeed, other possibilities include first-order low-pass filters* [133] *—see also* [134]*— or high-order Levant differentiators* [79]. •

For the purpose of stability analysis, we write the command filters' dynamics in state form. To that end, let the filters' variables be denoted as $\alpha_{l-1}^\top := \begin{bmatrix}\alpha_{l-1,1}^\top & \alpha_{l-1,2}^\top\end{bmatrix} \in \mathbb{R}^{2nN}$, for $l \in \{2, \dots, \varrho\}$. Then, in state-space representation, the command filters are written as

$$\dot{\alpha}_{l-1} = \omega_n \left[A \otimes I_{nN}\right] \alpha_{l-1} + \omega_n \left[B \otimes I_{nN}\right] x_l^* \tag{5.18a}$$

$$\begin{bmatrix} x_{lf}^\top & \dot{x}_{lf}^\top \end{bmatrix}^\top = \left[C \otimes I_{nN}\right] \alpha_{l-1}, \quad l \in \{2, \dots, \varrho\}, \tag{5.18b}$$

$$A := \begin{bmatrix} 0 & 1 \\ -1 & -2 \end{bmatrix}, \quad B := \begin{bmatrix} 0 \\ 1 \end{bmatrix}, \quad C := \begin{bmatrix} 1 & 0 \\ 0 & \omega_n \end{bmatrix} \tag{5.18c}$$

and the initial conditions are set to $\alpha_{l-1,1}(0) = x_l^*(0)$ and $\alpha_{l-1,2}(0) = 0$.

Remark 5.5. *Note that the second-order filters are designed with unit DC gain and critically damped so that the tracking of the virtual signals is guaranteed without overshoot. The latter, together with the initial conditions $\alpha_{l-1,1}(0) = x_l^*(0)$ and $\alpha_{l-1,2}(0) = 0$ ensures that, in the slower time-scale of the systems' dynamics, the "filtered forms" act as the desired virtual signals, corresponding to a classical backstepping control.* •

Thus, the virtual control input, starting with (5.16), are redefined using the filter variables as follows. First, we redefine

$$x_3^* := -c_2\tilde{x}_2 + \dot{x}_{2f}, \quad \dot{x}_{2f} = \omega_n \alpha_{1,2} \tag{5.19}$$

where $\tilde{x}_2 := x_2 - x_{2f}$ and $\dot{x}_{2f} = \omega_n \alpha_{1,2}$. Hence, in contrast to (5.15), from

$$\dot{x}_2 - \dot{x}_{2f} = x_3 - \dot{x}_{2f} + \theta_2 + x_3^* - x_3^* + \alpha_{2,1} - \alpha_{2,1},$$

defining $\tilde{x}_3 := x_3 - x_{3f}$ and using (5.19) and $\alpha_{2,1} = x_{3f}$, we obtain

$$\dot{\tilde{x}}_2 = -c_2 \tilde{x}_2 + \tilde{x}_3 + (\alpha_{2,1} - x_3^*) + \theta_2$$

— *cf.* Equation (5.17). Then, owing to the fact that the system is in feedback form, we define

$$x_l^* := -c_{l-1}\tilde{x}_{l-1} + \omega_n \alpha_{l-2,2} - \tilde{x}_{l-2}, \quad l \in \{4, \dots, \varrho\}, \tag{5.20}$$

where c_2, c_{l-1} are positive constants, and the tracking errors are given by

$$\tilde{x}_l := x_l - x_{lf} = x_l - \alpha_{l-1,1}, \quad l \in \{2, \dots, \varrho\} \tag{5.21}$$

—cf. Equation (5.19). That is, the virtual controls x_l^* starting from $l = 3$ are redesigned to steer x_{l-1} towards the *filtered* virtual input $x_{l-1\,f}$. Finally, the actual control input is set to

$$u = -c_\varrho \tilde{x}_\varrho + \omega_n \alpha_{\varrho-2,2} - \tilde{x}_{\varrho-1}. \tag{5.22}$$

Remark 5.6. *The system being in feedback form, the third term on the right-hand side of* (5.20) *and* (5.22) *are feedback passivation terms —cf.* [135]. *These terms, that come from the backstepping-as-recursive-feedback-passivation approach* [136] *are used to render the system* (5.7) *passive with respect to the output* $y_\varrho := x_\varrho - x_{\varrho f}$. •

Thus, taking the derivative of the backstepping error variables defined in (5.21) and using the input (5.22), with (5.18)-(5.20), we obtain the closed-loop system

$$\begin{aligned}
\dot{\tilde{z}}_t =& -c_1 [E_t^\top E_\odot \otimes I_n] \nabla W(\tilde{z}) + [E_t^\top \otimes I_n] [\tilde{x}_2 + (\alpha_{1,1} - x_2^*) + \theta_1] && \text{(5.23a)}\\
\dot{\tilde{x}}_2 =& -c_2 \tilde{x}_2 + \tilde{x}_3 + (\alpha_{2,1} - x_3^*) + \theta_2 && \text{(5.23b)}\\
\dot{\tilde{x}}_l =& -c_l \tilde{x}_l + \tilde{x}_{l+1} - \tilde{x}_{l-1} + (\alpha_{l,1} - x_{l+1}^*) + \theta_l, \quad \forall\, l \in \{3, \dots, \varrho - 1\} && \text{(5.23c)}\\
\dot{\tilde{x}}_\varrho =& -c_\varrho \tilde{x}_\varrho - \tilde{x}_{\varrho-1} + \theta_\varrho && \text{(5.23d)}\\
\dot{\alpha}_l =& \omega_n [A \otimes I_{nN}] \alpha_l + \omega_n [B \otimes I_{nN}] x_{l+1}^*, \quad \forall\, l \in \{1, \dots, \varrho - 1\}. && \text{(5.23e)}
\end{aligned}$$

Now, denoting $\bar{x}^\top := \begin{bmatrix} \tilde{x}_2^\top & \cdots & \tilde{x}_\varrho^\top \end{bmatrix}$, $\bar{\theta}^\top := \begin{bmatrix} \theta_2^\top & \cdots & \theta_\varrho^\top \end{bmatrix}$, $\bar{\alpha}^\top := \begin{bmatrix} \alpha_{2,1}^\top & \cdots & \alpha_{\varrho-1,1}^\top & 0^\top \end{bmatrix}$, and $\bar{x}^{*\top} := \begin{bmatrix} x_3^{*\top} & \cdots & x_\varrho^{*\top} & 0^\top \end{bmatrix}$, the closed-loop system (5.23) may be rewritten in the compact form

$$\begin{aligned}
\dot{\tilde{z}}_t =& -c_1 [E_t^\top E_\odot \otimes I_n] \nabla W(\tilde{z}) + [E_t^\top \otimes I_n] [\tilde{x}_2 + (\alpha_{1,1} - x_2^*) + \theta_1] && \text{(5.24a)}\\
\dot{\bar{x}} =& -[H \otimes I_{nN}] \bar{x} + \bar{\theta} + (\bar{\alpha} - \bar{x}^*), && \text{(5.24b)}\\
\dot{\alpha}_l =& \omega_n [A \otimes I_{nN}] \alpha_l + \omega_n [B \otimes I_{nN}] x_{l+1}^*, \quad \forall\, l \in \{1, \dots, \varrho - 1\}. && \text{(5.24c)}
\end{aligned}$$

where

$$H := \begin{bmatrix} c_2 & -1 & 0 & \cdots & 0 \\ 1 & c_3 & -1 & \cdots & 0 \\ \vdots & \ddots & \ddots & \ddots & \vdots \\ 0 & \dots & 1 & c_{\varrho-1} & -1 \\ 0 & \dots & 0 & 1 & c_\varrho \end{bmatrix}. \tag{5.25}$$

Roughly speaking, Equation (5.24c) corresponds to that of a stable first-order linear system (recall that A is Hurwitz) which tends to follow the input x^*_{l+1}. Therefore, for each $l \in \{1, \dots, \varrho-1\}$ we have $\alpha_l \to x^*_{l+1}$. In light of this, (5.24b) may be regarded as an ordinary feedback-interconnected strictly-positive-real system (note that H is also Hurwitz —see (5.25)) perturbed by the vanishing terms $(\bar{\alpha} - \bar{x}^*)$, and the non-vanishing disturbances $\bar{\theta}(t)$. Finally, (5.24a) corresponds to the reduced-order system (3.26), considered in Chapter 3, also under the vanishing disturbance $(\alpha_{1,1} - x^*_2)$ and the non-vanishing one $\theta_1(t)$.

Consequently, solving the robust consensus problem with output constraints boils down to guaranteeing that $\tilde{z}_t(t)$, as part of the solution to (5.24), tends to zero. More precisely, that the control law (5.22), with (5.13) and (5.18)-(5.20), solves the robust consensus problem with output constraints for system (5.1) is a fact established by the following statement.

Theorem 5.1 ([130]). *Consider the system (5.1) in closed loop with the dynamic controller defined by (5.22), together with (5.13) and (5.18)-(5.20). Then, there exists ϵ^*, such that, for $\epsilon \in (0, \epsilon^*]$ where $\epsilon := 1/\omega_n$, if the directed graph satisfies Assumption 5.2, and if $\theta_{i,l} \equiv 0$, $l \leq \varrho$, $i \leq N$, the objective (5.6) is achieved for almost all initial conditions satisfying $z(0) \in \mathcal{D}$. Otherwise, if $\theta_l \not\equiv 0$, the closed-loop system is almost-everywhere practically input-to-state stable with respect to $\theta := [\theta_1^\top \cdots \theta_\varrho^\top]^\top$. Moreover, the constraints set (5.2) is rendered forward invariant along the closed-loop solutions.* □

For clarity of exposition, the proof of Theorem 5.1 is presented in Section 5.3, but in anticipation of the latter we underline the following. As mentioned earlier, part of the control approach consists in choosing ω_n sufficiently large, so that $\alpha_{l-1,1} \to x^*_l$ faster than the dynamics of the system. To show this, we use singular-perturbation theory. Note that, setting $\epsilon := 1/\omega_n$ as a *singular* parameter in (5.24c), the closed-loop system (5.24) may be separated into two time scales, where the fast system corresponds to the command filters. Hence, when $\alpha_{l-1,1} = x^*_l$ and $\alpha_{l-1,2} = 0$, the reduced slow system, corresponding to the actual system with the backstepping control, effectively achieves consensus while respecting the output constraints.

Here we remark that using the reduction of the edge system presented in Chapter 2, we are able to analyze the system using Lyapunov and input-to-state stability. However, because the function W in (5.24) has multiple critical points, we rely on refinements of the latter, called multi-stability theory [123], [124]. The latter is significant since the reduced slow system corresponds to a high-order system in closed-loop with a classical backstepping controller solving the output-constrained consensus problem. On the other hand, the strict Lyapunov functions provided in Chapter 3 and the robustness properties of the proposed

constrained-consensus protocols are made relevant when considering the multi-stability framework for singularly perturbed systems, as we do in this chapter.

5.3 QUALITATIVE ANALYSIS AND PROOFS

The proof of Theorem 5.1 is organized in two main parts. In the first part, we show how the closed-loop system (5.24) can be written as a singularly-perturbed system with singular parameter $\epsilon := 1/\omega_n$ and in which the fast systems correspond to the dynamics of the command filters and the slow system corresponds to the high-order dynamics of the original multi-agent system. Second, we analyze the stability and the robustness of the singularly perturbed system, using analysis tools from multi-stable systems theory [123], [124].

5.3.1 *Analysis of the singular perturbation model*

Define $\alpha^\top := \begin{bmatrix}\alpha_1^\top & \cdots & \alpha_{\varrho-1}^\top\end{bmatrix} \in \mathbb{R}^{2nN(\varrho-1)}$, $\xi^\top := \begin{bmatrix}\tilde{z}_t^\top & \tilde{x}_2^\top & \cdots & \tilde{x}_\varrho\end{bmatrix}^\top \in \mathbb{R}^{n(\varrho N-1)}$, and $\theta^\top := [\theta_1 \ \cdots \ \theta_\varrho] \in \mathbb{R}^{n\varrho N}$. Then, the filter subsystem (5.23e) can be rewritten as

$$\begin{aligned}\dot{\alpha} &= \omega_n \tilde{A}\big[\alpha - \chi(\xi,\alpha)\big], \quad \tilde{A} := \text{blockdiag}\{[A \otimes I_{nN}]\}, \\ \chi(\xi,\alpha) &:= \begin{bmatrix} x_2^{*\top} & 0^\top & x_3^{*\top} & 0^\top & \cdots & x_\varrho^{*\top} & 0^\top \end{bmatrix}^\top.\end{aligned} \tag{5.26}$$

Now, as mentioned above, with $\epsilon := 1/\omega_n$ as the singular parameter, the closed-loop system (5.23) may be written in the singular-perturbation form [17]

$$\dot{\xi} = f(\xi,\alpha,\theta,\epsilon) \tag{5.27a}$$
$$\epsilon\dot{\alpha} = g(\xi,\alpha,\theta,\epsilon). \tag{5.27b}$$

Setting $\epsilon = 0$ in (5.27) we obtain the so-called quasi-state model

$$\dot{\xi} = f(\xi,\alpha,\theta,0) \tag{5.28a}$$
$$0 = g(\xi,\alpha,\theta,0) \tag{5.28b}$$

in which (5.28b) becomes an algebraic equation. Hence, the analysis of the singular perturbation model (5.27) is normally conducted studying its dynamic properties in different time scales [17].

Denote $\alpha_s = \varphi(\xi)$ the unique root of the algebraic equation (5.28b),

$$\begin{aligned}\varphi(\xi) = \Big[&(-c_1[E_\odot \otimes I_n]\nabla W(\tilde{z}))^\top \quad 0^\top \quad -c_2\tilde{x}_2^\top \quad 0^\top \quad -(c_3\tilde{x}_3^\top + \tilde{x}_2^\top) \quad 0^\top \quad \cdots \\ &-(c_{\varrho-1}\tilde{x}_{\varrho-1}^\top + \tilde{x}_{\varrho-2}^\top) \quad 0^\top\Big]^\top.\end{aligned} \tag{5.29}$$

Then, defining the coordinate transformation

$$\tilde{\alpha} := \begin{bmatrix}\tilde{\alpha}_{1,1}^\top & \tilde{\alpha}_{1,2}^\top & \cdots & \tilde{\alpha}_{\varrho-1,1}^\top & \tilde{\alpha}_{\varrho-1,2}^\top\end{bmatrix}^\top = \alpha - \varphi(\xi), \tag{5.30}$$

and using (5.23), we obtain the singularly perturbed system

$$\dot{\tilde{z}}_t = -\, c_1[E_t^\top E_\odot \otimes I_n]\nabla W(\tilde{z}) + [E_t^\top \otimes I_n]\,[\tilde{x}_2 + \tilde{\alpha}_{1,1} + \theta_1] \tag{5.31a}$$

$$\dot{\tilde{x}} = -\,[H \otimes I_{nN}]\bar{x} + \tilde{\bar{\alpha}} + \bar{\theta}, \tag{5.31b}$$

$$\epsilon\dot{\tilde{\alpha}} = \tilde{A}\tilde{\alpha} - \epsilon\frac{\partial\varphi(\xi)}{\partial\xi}\dot{\xi}. \tag{5.31c}$$

where, $\tilde{\bar{\alpha}}^\top := \begin{bmatrix}\tilde{\alpha}_{2,1}^\top & \cdots & \tilde{\alpha}_{\varrho-1,1}^\top & 0^\top\end{bmatrix}$. In turn, the reduced system $\dot{\xi} = f(\xi, \varphi(\xi), \theta, 0)$ takes the form

$$\dot{\tilde{z}}_t = -\, c_1[E_t^\top E_\odot \otimes I_n]\nabla W(\tilde{z}) + [E_t^\top \otimes I_n]\,[\tilde{x}_2 + \theta_1] \tag{5.32a}$$

$$\dot{\tilde{x}} = -\,[H \otimes I_{nN}]\bar{x} + \bar{\theta}, \tag{5.32b}$$

where H is defined in (5.25). On the other hand, the boundary layer system, $(d\tilde{\alpha}/d\tau) = g(\xi, \tilde{\alpha} + \varphi(\xi), \theta, 0)$, with $\tau = t/\epsilon$ and with ξ considered as fixed, is

$$\frac{d\tilde{\alpha}}{d\tau} = \tilde{A}\tilde{\alpha}, \tag{5.33}$$

where $\tilde{A}$ is Hurwitz —see Equations (5.26) and (5.18c).

5.3.2 *Stability and robustness analysis*

Even though the system (5.31) appears to be in the familiar form (5.27), its analysis is stymied by the fact that the gradient ∇W vanishes at multiple separate equilibria. Therefore, we rely on perturbation theory for multi-stable systems, taken from [124]. For convenience, some definitions and statements from [123], [124] are recalled in Appendix A.4.

First, recall the set $\mathcal{W}$ defined in (5.11) that contains the critical points of the barrier Lyapunov function in (5.10). From (5.31a), setting $\tilde{x}_2 = 0$, $\tilde{\alpha}_{1,1} = 0$, and $\theta_1 = 0$, the set $\mathcal{W}$ corresponds to an invariant set of isolated equilibria in Euclidean space. Then, the set (5.11) is an acyclic $\mathcal{W}$-limit set of (5.31a) as per the definition stated in [124]. This means that asymptotic stability of the origin of (5.31a) may be guaranteed, at best, almost everywhere in $\mathcal{D}$, that is, for all initial conditions in $\mathcal{D}$ except for a set of measure zero corresponding to the domain of attraction of the unstable critical point.

In light of the above, we first analyze the stability of the closed-loop system (5.31) from a multi-stability perspective. For this purpose we use Theorem A.1 in Appendix A.4, which is essentially a reformulation of [124, Theorem 2] adapted to the contents of this thesis. Theorem A.1 in Appendix A.4 establishes sufficient conditions for a practical input-to-state multi-stability property to hold for a singularly perturbed system with respect to a bounded external input θ, granted that the reduced system (5.32) is input-to-state stable with respect to the input θ and the set

$$\mathcal{W}_\Theta := \mathcal{W} \times \{0\}^{\varrho-1} \tag{5.34}$$

which consists in the singular values of the barrier Lyapunov function W and the origin for the subsystem (5.32b), and that the origin for (5.33) is globally asymptotically stable. Therefore, the stability and robustness analysis is conducted in the following steps:

1) remark that the origin is asymptotically stable for the boundary layer system (5.33);
2) relying on the results on cascaded multi-stable systems in [123], we show that the reduced system (5.32) is input-to-state stable with respect to the set $\mathcal{W}_\Theta$ and the input θ;
3) using Theorem A.1 in Appendix A.4, we prove that, for a sufficiently small ϵ, the singularly perturbed system (5.31) is practically input-to-state stable with respect to the set $(\mathcal{W}_\Theta \times \{0\}^{2nN(\varrho-1)})$[2] and a bounded external input θ; Moreover, using [124, Theorem 3], in the absence of disturbances, we show convergence to the set of equilibria;
4) using the practical input-to-state multi-stability property, we establish almost-everywhere-practical-input-to-state stability of (5.31). Similarly, if $\theta \equiv 0$, we establish convergence to the origin;
5) finally, we show that the output-constraints set defined in (5.2) is forward invariant.

Step 1) Since $\tilde{A}$ is Hurwitz by design, the origin $\tilde{\alpha} = 0$ is exponentially stable for the boundary-layer system (5.33).

Step 2) Consider the reduced system (5.32). Note that it has the form of a cascaded system, in which (5.32b) is the "driving" system and the "driven" system

$$\dot{\tilde{z}}_t = -c_1[E_t^\top E_\odot \otimes I_n]\nabla W(\tilde{z})$$

has multiple equilibria given by the set $\mathcal{W}$ in (5.11). In order to prove input-to-state stability of (5.32) with respect to set $\mathcal{W}_\Theta$ and input θ, as per in [123], we need to show that (5.32a) is input-to-state stable with respect to the set $\mathcal{W}$ and the inputs $\tilde{x}_2$ and θ_1, whereas the system (5.32b) is input-to-state stable with respect to $\bar{\theta}$. We start with the latter.

Input-to-state stability with respect to $\bar{\theta}$ for the system (5.32b) follows directly from Lyapunov theory since (5.32b) is a linear time-invariant system and $-[H \otimes I_{nN}]$ is Hurwitz, since so is $-H$.

Consider, in turn, the reduced subsystem (5.32a). Note that this subsystem corresponds to the first-order integrator with disturbances under a constrained-consensus protocol as studied in Section 3.2.2 of Chapter 3. Therefore, akin to (3.27), for this system we use the barrier Lyapunov function given by

$$\tilde{W}(\tilde{z}) = \sum_{k \leq M} \gamma_k W_k(\tilde{z}_k), \quad \gamma_k > 0 \quad \forall k \leq M, \tag{5.35}$$

where $W_k(\tilde{z}_k)$ is given in (5.9). Now, recall that the edges of the graph are linearly dependent on the edges of a tree, that is, $z = \left[R^\top \otimes I_n\right] z_t$. Therefore, as in Chapter 3, akin to (3.28), with an abuse of notation, we write

$$\tilde{W}\left(\left[R^\top \otimes I_n\right] \tilde{z}_t\right) \equiv \tilde{W}(\tilde{z}_t) \tag{5.36}$$

2 The set $\mathcal{W}_\Theta \times \{0\}^{2nN(\varrho-1)}$ corresponds to the equilibria of the closed-loop system (5.24)

and we have

$$\nabla\tilde{W}(z_t) = [R \otimes I_n]\, \nabla\tilde{W}(z). \tag{5.37}$$

Moreover, defining $\Gamma := \mathrm{diag}\{\gamma_k\} \in \mathbb{R}^{M\times M}$, the following identity holds

$$\nabla\tilde{W}(\tilde{z}) = [\Gamma \otimes I_n]\, \nabla W(\tilde{z}), \tag{5.38}$$

where ∇W is the gradient of W defined in (5.10) and used in the control.

On the other hand, for consistency in the notation, we define the constraint set (5.2) in terms of the edges of the spanning tree z_t as

$$\mathcal{D}_t := \left\{ z_t \in \mathbb{R}^{n(N-1)} : \left| \left[r_k^\top \otimes I_n \right] z_k \right| \in (\delta_k, \Delta_k),\ \forall\, k \le M \right\}$$

where r_k is the kth column of R in (2.47). Then, for all $\tilde{z}_t \in \mathcal{D}_t$, $\tilde{W}(\tilde{z}_t)$ satisfies

$$\frac{\gamma_{min}}{2} |\tilde{z}_t|_{\mathcal{W}}^2 \le \tilde{W}(\tilde{z}_t), \tag{5.39}$$

where $\gamma_{min} := \min_{k\le M}\{\gamma_k\}$ and $|\tilde{z}_t|_{\mathcal{W}} = \min\{|\tilde{z}_t|, |\tilde{z}_t - \tilde{z}_t^*|\}$, $\tilde{z}_t^*$ denoting the saddle points of $\tilde{W}$ in terms of the edges of a spanning tree.

For the time-being, we assume that $\mathcal{D}$ (equivalently $\mathcal{D}_t$) is forward invariant; this hypothesis is relaxed below.

Now, the derivative of $\tilde{W}$ along the trajectories of the subsystem (5.32a) is given by

$$\begin{aligned}
\dot{\tilde{W}} =& - c_1 \nabla\tilde{W}(\tilde{z}_t) \left[E_t^\top E_\odot \otimes I_n \right] \nabla W(\tilde{z}) + \nabla\tilde{W}(\tilde{z}_t)^\top \left[E_t^\top \otimes I_n \right] [\tilde{x}_2 + \theta_1] \\
=& - c_1 \nabla W(\tilde{z}) \left[\Gamma R^\top E_t^\top E_\odot \otimes I_n \right] \nabla W(\tilde{z}) + \nabla W(\tilde{z}_t)^\top \left[\Gamma R^\top E_t^\top \otimes I_n \right] [\tilde{x}_2 + \theta_1] \\
=& - c_1 \nabla W(\tilde{z}) \left[\Gamma E^\top E_\odot \otimes I_n \right] \nabla W(\tilde{z}) + \nabla W(\tilde{z}_t)^\top \left[\Gamma E^\top \otimes I_n \right] [\tilde{x}_2 + \theta_1],
\end{aligned} \tag{5.40}$$

where we used the identities (5.37), (5.38), and (2.48). Recalling the proof of Proposition 3.4, under Assumption 5.2, (5.40) satisfies

$$\dot{\tilde{W}} \le -c_1'' |\nabla W(\tilde{z}_t)|^2 + \frac{\delta}{2} \left[|\tilde{x}_2|^2 + |\theta_1|^2 \right], \tag{5.41}$$

where, for a sufficiently large $\delta > 0$, $c_1'' := \left(\frac{c_1'}{2} - \frac{\gamma_{min}^2}{2\delta} \right) > 0$ with $c_1' := c_1 \lambda_{min}(E_t^\top E_t)$ if the graph is a directed cycle and $c_1' := c_1 \lambda_{min}(Q)$, for Q as in (3.35), if the graph is a directed spanning tree.

Then, under Assumption 5.4, for either the spanning tree or the cycle case, the derivative of $\tilde{W}(z_t)$ satisfies

$$\dot{\tilde{W}} \le -\frac{c_1''}{2\beta_1} |\tilde{z}_t|_{\mathcal{W}}^2 + \frac{\delta}{2} \left[|\tilde{x}_2|^2 + |\theta_1|^2 \right]. \tag{5.42}$$

It follows from (5.39), (5.42), and Theorem A.2 in Appendix A.4, that the subsystem (5.32a) is input-to-state stable with respect to the set of equilibria $\mathcal{W}$, and the inputs $\tilde{x}_2$ and θ_1.

Thus, since (5.32b) is input-to-state stable with respect to $\bar{\theta}$ and (5.32a) is input-to-state stable with respect to the set of equilibria $\mathcal{W}$ and the inputs $\tilde{x}_2$ and θ_1, after [123, Theorem 3.1], the reduced system (5.32) is input-to-state stable with respect to $\mathcal{W}_\Theta$, defined in (5.34), and to the input θ. Furthermore, $\mathcal{W}_\Theta$ qualifies as a $\mathcal{W}$-limit set for (5.32).

Step 3) Since the reduced system (5.32) is input-to-state stable with respect to $\mathcal{W}_\Theta$ and θ, and the origin of (5.33) is asymptotically stable, it follows, after Theorem A.1 in Appendix A.4, that the singularly perturbed system (5.31) is practically input-to-state stable with respect to the set $\mathcal{W}_\Theta \times \{0\}^{2nN(\varrho-1)}$ and the input θ. More precisely, for any pair of constants d_1, $d_2 > 0$, there exists an $\epsilon^* > 0$ such that, for any $\epsilon \in (0, \epsilon^*]$, the solutions of (5.31) satisfy

$$\limsup_{t\to\infty} |\xi(t)|_{\mathcal{W}_\Theta} \leq \eta_\theta(\|\theta\|_\infty) + d_2 \tag{5.43a}$$

$$|\tilde{\alpha}(t)| \leq \beta_\alpha\left(|\tilde{\alpha}(0)|, \frac{t}{\epsilon}\right) + d_2, \quad \forall\, t \geq 0, \tag{5.43b}$$

provided that

$$\max\{|\xi(0)|_{\mathcal{W}_\Theta}, |\tilde{\alpha}(0)|, \|\theta\|_\infty, \|\dot{\theta}\|_\infty\} \leq d_1.$$

Now consider the case in which the disturbance $\theta \equiv 0$. From property (5.43a) we may conclude that the origin of the reduced system (5.32) is multi-stable with respect to $\mathcal{W}_\Theta$. Therefore, from the latter and the exponential stability of the boundary layer system (5.33) all the assumptions of [124, Theorem 3] are satisfied and the solutions of (5.31) satisfy

$$\lim_{t\to\infty} |\xi(t)|_{\mathcal{W}_\Theta} = 0 \tag{5.44a}$$

$$\lim_{t\to\infty} |\tilde{\alpha}(t)| = 0. \tag{5.44b}$$

Step 4) Since the critical point $\tilde{z}_t^*$ of the barrier function is a saddle point —see Appendix A.3, after [137, Proposition 11], it follows that the region of attraction of the unstable equilibrium $\tilde{z}_t^*$ has zero Lebesgue measure. Therefore, we conclude that the bound in (5.43a) and the limit in (5.44a) are satisfied for the origin $\{\xi = 0\}$. More precisely, we have

$$\limsup_{t\to\infty} |\xi(t)| \leq \eta_\theta(\|\theta\|_\infty) + d_2 \tag{5.45}$$

and, for $\theta \equiv 0$,

$$\lim_{t\to\infty} |\xi(t)| = 0. \tag{5.46}$$

Step 5) Up to this point we have assumed that the inter-agent constraints are satisfied for all time, that is, $z(t) \in \mathcal{D}$ for all $t \geq 0$. Then, in order to prove the forward invariance of the constraints set we proceed by contradiction as follows. Assume that the state constraints are not respected. Therefore, from continuity of the solutions, there exists a time $T > 0$ such that $z_t(T) \in \partial\mathcal{D}_t$. Now, from the previous analysis of the singularly perturbed system, we

have that in the interval $[0, T)$, condition (5.43b) holds. Moreover, since $\tilde{\alpha}(0) = 0$ by design, the solutions of the filter error satisfy $\tilde{\alpha}(t) \leq d_2$, for $t \in [0, T)$. Consider the derivative of the Lyapunov function (5.10) along the trajectories of (5.31a), which satisfies

$$\dot{\tilde{W}}(\tilde{z}_t) \leq -c_1''|\nabla\tilde{W}(\tilde{z}_t)|^2 + \frac{\delta}{2}\left[|\tilde{x}_2|^2 + |\theta_1|^2 + |\tilde{\alpha}|^2\right]$$

Therefore, since $\tilde{\alpha}(t) \leq d_2$, $\theta_1(t)$ is bounded and the system in (5.32b) is input-to-state stable, $\tilde{x}_2(t)$ is bounded, for all $t \in [0, T)$. Then, we have

$$\dot{\tilde{W}}(\tilde{z}_t(t)) \leq -c_1''|\nabla\tilde{W}(\tilde{z}_t(t))|^2 + d, \quad \forall t \in [0, T)$$

where d is a positive constant. By definition we know that $|\nabla\tilde{W}(\tilde{z}_t(t))| \to \infty$ as $z_t(t)$ approaches the border of the constraints set, $\partial\mathcal{D}_t$. Therefore, if $|\tilde{z}_t(t)|$ grows, there exists a time $0 < T^* < T$ such that $\dot{\tilde{W}}(\tilde{z}_t(T^*)) \leq 0$. The latter, in turn means that $\tilde{W}(\tilde{z}_t(t))$ is bounded for all $t \in [0, T)$, which contradicts the initial assumption that the constraints are not respected. By resetting the initial conditions, the previous reasoning can be repeated for $t \geq T$. Therefore, the interval where $\tilde{W}(\tilde{z}_t(t))$ is bounded can be extended to infinity. The boundedness of $\tilde{W}(\tilde{z}_t(t))$ means, based on the definition of the barrier Lyapunov function, that the constraints are always respected or, equivalently, that the set $\mathcal{D}_t$ is forward invariant.

5.4 PARTIAL- AND FULL-STATE CONSENSUS

The statement in Theorem 5.1 addresses the problem of robust *output* consensus under output constraints for high-order systems. This problem is relevant in a number of applications. For instance, the position-consensus problem under position constraints for autonomous aerial vehicles may be solved using Theorem 5.1 —see Chapter 6. However, in some scenarios it is required, that consensus be achieved for an additional number of high-order states. For instance, in the context of *flocking* in formation, besides achieving the desired formation, it is required that the velocities of all the agents converge to the same value.

Therefore, in this section we show how the control design methodology presented above can be directly extended to consider consensus for a part or all of the high-order states x_l.

Suppose that, besides achieving the output-consensus goal as defined in (5.6a), it is additionally required to achieve consensus of a number of states $r \leq \varrho$. For convenience, and without loss of generality, suppose that $3 < r < \varrho$. Then, akin to the edge transformation (5.4), we define the edge states

$$z_l := [E^\top \otimes I_n]x_l, \quad l \in \{2, \ldots, r\}. \tag{5.47}$$

and, accordingly, let the objectives in (5.6) be replaced with

$$\lim_{t\to\infty} \tilde{z}(t) = 0 \tag{5.48a}$$

$$\lim_{t\to\infty} z_l(t) = 0, \quad \forall l \in \{2, \ldots, r\} \tag{5.48b}$$

$$\lim_{t\to\infty} x_l(t) = 0, \quad \forall l \in \{r+1, \ldots, \varrho\}. \tag{5.48c}$$

Now, recalling the identities (2.48) and (2.50), let $z_{t,l} \in \mathbb{R}^{n(N-1)}$, $l \in \{2,\dots,r\}$, denote the edge states of the spanning tree contained in $\mathcal{G}$, satisfying $z_l = \left[R^\top \otimes I_n\right] z_{t,l}$. Then, the edge-based reduced-order system's equations read

$$\dot{\tilde{z}}_t = z_{t,2} + \left[E_t^\top \otimes I_n\right]\theta_1(t) \tag{5.49a}$$
$$\dot{z}_{t,l} = z_{t,l+1} + \left[E_t^\top \otimes I_n\right]\theta_l(t), \quad l \in \{2,\dots,r-1\} \tag{5.49b}$$
$$\dot{z}_{t,r} = \left[E_t^\top \otimes I_n\right]x_{r+1} + \left[E_t^\top \otimes I_n\right]\theta_r(t) \tag{5.49c}$$
$$\dot{x}_l = x_{l+1} + \theta_l(t), \quad l \in \{r+1,\dots,\varrho-1\} \tag{5.49d}$$
$$\dot{x}_\varrho = u + \theta_\varrho(t). \tag{5.49e}$$

Then, the objective in (5.48) is achieved if the origin is asymptotically stabilized for the system (5.49), via the control input u in (5.49e).

The control design follows the same command-filtered-backstepping-inspired method described in Section 5.2. Let

$$\tilde{z}_l := z_l - [E^\top \otimes I_n]x_{lf} \quad \forall\, l \in \{2,\dots,r\} \tag{5.50}$$
$$\tilde{x}_l := x_l - x_{lf} \quad \forall\, l \in \{r+1,\dots,\varrho\} \tag{5.51}$$

and recall that $x_{lf} = \alpha_{l-1,1}$. Then, to achieve the new consensus objectives (5.48) we consider the virtual control inputs x_2^* as in (5.13),

$$x_3^* := -c_2[E_\odot \otimes I_n]\tilde{z}_2 + \omega_n\alpha_{1,2}, \tag{5.52}$$
$$x_l^* := -c_{l-1}[E_\odot \otimes I_n]\tilde{z}_{l-1} + \omega_n\alpha_{l-2,2} - \tilde{x}_{l-2} \tag{5.53}$$

for all $l \in \{4,\dots,r\}$,

$$x_{r+1}^* := -c_r[E_\odot \otimes I_n]\tilde{z}_r + \omega_n\alpha_{r-1,2} - [E_\odot \otimes I_n]\tilde{z}_{r-1}, \tag{5.54}$$

and

$$x_l^* := -c_{l-1}\tilde{x}_{l-1} + \omega_n\alpha_{l-2,2} - \tilde{x}_{l-2}, \quad l \in \{r+2,\dots,\varrho\}. \tag{5.55}$$

Finally, the actual control input is set to

$$u := -c_\varrho\tilde{x}_\varrho + \omega_n\alpha_{\varrho-2,2} - \tilde{x}_{\varrho-1}. \tag{5.56}$$

Thus, taking the derivative of the error variables (5.50) and (5.51) and using the input (5.56), with the command filters (5.18) and (5.52)-(5.55), we obtain the closed-loop system

$$\dot{\tilde{z}}_t = -c_1[E_t^\top E_\odot \otimes I_n]\nabla W(\tilde{z}) + \tilde{z}_{t,2} + [E_t^\top \otimes I_n]\left[(\alpha_{1,1} - x_2^*) + \theta_1\right] \tag{5.57a}$$
$$\dot{\tilde{z}}_{t,2} = -c_2[E_t^\top E_\odot R^\top \otimes I_n]\tilde{z}_{t,2} + \tilde{z}_{t,3} + [E_t^\top \otimes I_n]\left[(\alpha_{2,1} - x_3^*) + \theta_2\right] \tag{5.57b}$$
$$\dot{\tilde{z}}_{t,l} = -c_l[E_t^\top E_\odot R^\top \otimes I_n]\tilde{z}_{t,l} + \tilde{z}_{t,l+1} - \tilde{z}_{t,l-1} + [E_t^\top \otimes I_n]\left[(\alpha_{l,1} - x_{l+1}^*) + \theta_l\right], \quad \forall l \in \{3,\dots,r-1\} \tag{5.57c}$$
$$\dot{\tilde{z}}_{t,r} = -c_r[E_t^\top E_\odot R^\top \otimes I_n]\tilde{z}_{t,r} + [E_t^\top \otimes I_n]\left[\tilde{x}_{r+1} - \tilde{x}_{r-1} + (\alpha_{r,1} - x_{r+1}^*) + \theta_r\right] \tag{5.57d}$$
$$\dot{\tilde{x}}_l = -c_l\tilde{x}_l + \tilde{x}_{l+1} - \tilde{x}_{l-1} + (\alpha_{l,1} - x_{l+1}^*) + \theta_l, \quad \forall\, l \in \{r+1,\dots,\varrho-1\} \tag{5.57e}$$
$$\dot{\tilde{x}}_\varrho = -c_\varrho\tilde{x}_\varrho - \tilde{x}_{\varrho-1} + \theta_\varrho \tag{5.57f}$$
$$\dot{\alpha}_l = \omega_n\left[A \otimes I_{nN}\right]\alpha_l + \omega_n\left[B \otimes I_{nN}\right]x_{l+1}^*, \quad \forall\, l \in \{1,\dots,\varrho-1\}. \tag{5.57g}$$

Now, denote $\bar{z}^\top := \begin{bmatrix}\tilde{z}_{t,2}^\top & \cdots & \tilde{z}_{t,r}^\top\end{bmatrix}$, $\bar{x}^\top := \begin{bmatrix}\tilde{x}_{r+1}^\top & \cdots & \tilde{x}_{\varrho}^\top\end{bmatrix}$, $\hat{\theta}^\top := \begin{bmatrix}\theta_2^\top & \cdots & \theta_r^\top\end{bmatrix}$, $\bar{\theta}^\top := \begin{bmatrix}\theta_{r+1}^\top & \cdots & \theta_{\varrho}^\top\end{bmatrix}$, $\hat{\alpha}^\top := \begin{bmatrix}\alpha_{2,1}^\top & \cdots & \alpha_{r,1}^\top\end{bmatrix}$, $\bar{\alpha}^\top := \begin{bmatrix}\alpha_{r+1,1}^\top & \cdots & \alpha_{\varrho-1,1}^\top & 0^\top\end{bmatrix}$, $\hat{x}^{*\top} := \begin{bmatrix}x_3^{*\top} & \cdots & x_{r+1}^{*\top}\end{bmatrix}$, and $\bar{x}^{*\top} := \begin{bmatrix}x_{r+2}^{*\top} & \cdots & x_{\varrho}^{*\top} & 0^\top\end{bmatrix}$, and define the matrices

$$H_z := \begin{bmatrix} c_2 E_t^\top E_\odot R^\top & -I_{N-1} & 0 & \cdots & 0 \\ I_{N-1} & c_3 E_t^\top E_\odot R^\top & -I_{N-1} & \cdots & 0 \\ \vdots & \ddots & \ddots & \ddots & \vdots \\ 0 & \cdots & I_{N-1} & c_{r-1} E_t^\top E_\odot R^\top & -I_{N-1} \\ 0 & \cdots & 0 & I_{N-1} & c_r E_t^\top E_\odot R^\top \end{bmatrix}, \tag{5.58}$$

$$H_x := \begin{bmatrix} c_r & -1 & 0 & \cdots & 0 \\ 1 & c_{r+1} & -1 & \cdots & 0 \\ \vdots & \ddots & \ddots & \ddots & \vdots \\ 0 & \cdots & 1 & c_{\varrho-1} & -1 \\ 0 & \cdots & 0 & 1 & c_\varrho \end{bmatrix}, \quad F_1 := \begin{bmatrix} 0_{(N-1)\times N} & 0_{(N-1)\times N} & \cdots & 0_{(N-1)\times N} \\ \vdots & \vdots & \ddots & \vdots \\ 0_{(N-1)\times N} & 0_{(N-1)\times N} & \cdots & 0_{(N-1)\times N} \\ E_t^\top & 0_{(N-1)\times N} & \cdots & 0_{(N-1)\times N} \end{bmatrix} \tag{5.59}$$

and

$$F_2 := \begin{bmatrix} E_t^\top & \cdots & 0_{(N-1)\times N} \\ \vdots & \ddots & \vdots \\ 0_{(N-1)\times N} & \cdots & E_t^\top \end{bmatrix}. \tag{5.60}$$

Then, the closed-loop system (5.57) is rewritten in the compact form

$$\dot{\tilde{z}}_t = -c_1 [E_t^\top E_\odot \otimes I_n] \nabla W(\tilde{z}) + \tilde{z}_{t,2} + [E_t^\top \otimes I_n] [(\alpha_{1,1} - x_2^*) + \theta_1] \tag{5.61a}$$

$$\dot{\bar{z}} = -[H_z \otimes I_n]\bar{z} + [F_1 \otimes I_n]\bar{x} + [F_2 \otimes I_n] \left[(\hat{\alpha} - \hat{x}^*) + \hat{\theta}\right] \tag{5.61b}$$

$$\dot{\bar{x}} = -[H_x \otimes I_{nN}]\bar{x} + (\bar{\alpha} - \bar{x}^*) + \bar{\theta} \tag{5.61c}$$

$$\dot{\alpha}_l = \omega_n [A \otimes I_{nN}] \alpha_l + \omega_n [B \otimes I_{nN}] x_{l+1}^*, \quad \forall l \in \{1, \ldots, \varrho - 1\}. \tag{5.61d}$$

which has similar structural properties as the closed-loop system (5.24). Then, we have the following.

Theorem 5.2 ([130]). *Consider the system (5.1) in closed loop with the dynamic controller defined by (5.56), together with (5.53)-(5.55) and (5.18). Then, there exists ϵ^*, such that, for $\epsilon \in (0, \epsilon^*]$ where $\epsilon := 1/\omega_n$, if the directed graph satisfies Assumption 5.2, and if $\theta_{i,l} \equiv 0$, $l \leq \varrho$, $i \leq N$, the limits in (5.48) hold for almost all initial conditions satisfying $z(0) \in \mathcal{D}$. Otherwise, if $\theta_l \not\equiv 0$, the closed-loop system is almost-everywhere practically input-to-state stable with respect to $\theta := [\theta_1^\top \cdots \theta_\varrho^\top]^\top$. Moreover, the constraints set (5.2) is rendered forward invariant along closed-loop solutions.* □

Proof. Modulo some consideration for the additional higher-order edge states, the proof is identical to the proof of Theorem 5.1. Indeed, recalling that the command filters can be represented by a system of the form (5.26), with (5.53)-(5.55), we can redefine

$$\tilde{\alpha} := \alpha - \tilde{\varphi}(\xi),$$

where

$$\begin{aligned}\tilde{\varphi}(\xi) = \Big[&(-c_1 \left[E_\odot \otimes I_n\right] \nabla W(\tilde{z}))^\top \;\; 0^\top \;\; (-c_2 \left[E_\odot \otimes I_n\right] \tilde{z}_2)^\top \;\; 0^\top \;\; (-c_3 \left[E_\odot \otimes I_n\right] \tilde{z}_3 - \tilde{z}_2)^\top \;\; 0^\top \\ &\cdots \; (-c_r \left[E_\odot \otimes I_n\right] \tilde{z}_r - \tilde{z}_{r-1})^\top \quad 0^\top \quad -(c_{r+1}\tilde{x}_{r+1}^\top + \tilde{x}_r^\top) \quad 0^\top \;\; \cdots \\ &-(c_{\varrho-1}\tilde{x}_{\varrho-1}^\top + \tilde{x}_{\varrho-2}^\top) \quad 0^\top\Big]^\top.\end{aligned} \tag{5.62}$$

Then, the closed-loop system (5.61) may be rewritten in singular-perturbation form as

$$\dot{\tilde{z}}_t = -\, c_1[E_t^\top E_\odot \otimes I_n]\nabla W(\tilde{z}) + \tilde{z}_{t,2} + [E_t^\top \otimes I_n]\,[\tilde{\alpha}_{1,1} + \theta_1] \tag{5.63a}$$

$$\dot{\tilde{z}} = -\,[H_z \otimes I_n]\bar{z} + [F_1 \otimes I_n]\bar{x} + [F_2 \otimes I_n]\left[\tilde{\hat{\alpha}} + \hat{\theta}\right] \tag{5.63b}$$

$$\dot{\bar{x}} = -\,[H_x \otimes I_{nN}]\bar{x} + \tilde{\bar{\alpha}} + \bar{\theta} \tag{5.63c}$$

$$\epsilon\dot{\tilde{\alpha}} = \tilde{A}\tilde{\alpha} - \epsilon\frac{\partial\tilde{\varphi}(\xi)}{\partial\xi}\dot{\xi}, \tag{5.63d}$$

where $\tilde{\hat{\alpha}}^\top := \left[\tilde{\alpha}_{2,1}^\top \;\cdots\; \tilde{\alpha}_{r,1}^\top\right]$ and $\tilde{\bar{\alpha}}^\top := \left[\tilde{\alpha}_{r+1,1}^\top \;\cdots\; \tilde{\alpha}_{\varrho-1,1}^\top \; 0^\top\right]$.

In turn, the reduced system $\dot{\xi} = f(\xi, \tilde{\varphi}(\xi), \theta, 0)$ takes the form

$$\dot{\tilde{z}}_t = -\, c_1[E_t^\top E_\odot \otimes I_n]\nabla W(\tilde{z}) + \tilde{z}_{t,2} + [E_t^\top \otimes I_n]\theta_1 \tag{5.64a}$$

$$\dot{\tilde{z}} = -\,[H_z \otimes I_n]\bar{z} + [F_1 \otimes I_n]\bar{x} + [F_2 \otimes I_n]\tilde{\theta} \tag{5.64b}$$

$$\dot{\bar{x}} = -\,[H_x \otimes I_{nN}]\bar{x} + \bar{\theta}. \tag{5.64c}$$

On the other hand, the boundary layer system, $(d\tilde{\alpha}/d\tau) = g(\xi, \tilde{\alpha} + \tilde{\varphi}(\xi), \theta, 0)$, with $\tau = t/\epsilon$ and with ξ considered as fixed, is

$$\frac{d\tilde{\alpha}}{d\tau} = \tilde{A}\tilde{\alpha} \tag{5.65}$$

where $\tilde{A}$ is Hurwitz —see Equations (5.26) and (5.18c).

Now, we follow the same steps evoked in Section 5.3. In light of this, note that, as before, the origin $\{\tilde{\alpha} = 0\}$ of the boundary layer system (5.65) is exponentially stable since $\tilde{A}$ is Hurwitz by design.

Next, we need to show that the reduced system (5.64) is input-to-state multi-stable with respect to θ. Note that, using the same arguments as in Section 5.3 and the Lyapunov function given in (5.35), the subsystem (5.64a) is input-to-state stable with respect to the

set $\mathcal{W}$ and the inputs θ_1 and $\tilde{z}_{t,2}$. Then, note that since the matrix $-[H_z \otimes I_n]$ is Hurwitz —*cf.* Lemma 2.2—, using standard Lyapunov theory, the linear time-invariant subsystem (5.64b) is input-to-state stable with respect to $\bar{x}$, $\bar{\theta}$ and $\tilde{\theta}$. Therefore, input-to-state stability of the subsystem (5.64c) follows from Lyapunov theory since (5.64c) is a linear time-invariant system and $-[H_x \otimes I_{nN}]$ is Hurwitz by design.

Thus, after [123, Theorem 3.1], the reduced system (5.64) is input-to-state stable with respect to the $\mathcal{W}$-limit set $\mathcal{W}_\Theta$ and the input θ.

The rest of the proof follows from the same arguments as in the proof of Theorem 5.1 —see Section 5.3. ■

Remark 5.7. *It is important to observe that Theorems 5.1 and 5.2 only state the existence of an upper bound ϵ^* on ϵ, or equivalently a lower bound on ω_n for almost all initial conditions satisfying $z(0) \in \mathcal{D}$. In order to obtain an approximate (albeit conservative) value of ϵ^* based on Lyapunov's theory, one would need to establish exponential stability of the reduced slow systems (5.7) and (5.49), which is still an open problem.* •

5.5 CONCLUSION

In this chapter we solved the consensus problem under output constraints (connectivity maintenance and collision avoidance) for high-order systems in normal form. This original contribution builds on our previous results presented in Chapter 3, where the consensus-with-connectivity-maintenance problem is addressed using the edge-based perspective. Indeed, we saw how input-to-state stability properties established in Chapter 3 via the provided strict Lyapunov functions are fundamental in order to establish stability and robustness of the consensus controller proposed in this chapter.

The practical-input-to-state stability property established in Theorems 5.1 and 5.2, respectively for the output- and partial-state-consensus problem under output constraints, cannot be underestimated; input-to-state stability implies boundedness of the systems' state trajectories and the satisfaction of the inter-agent output constraints may also be assessed, even in the presence of external disturbances. The same cannot be ascertained if in the absence of disturbances it is only known that the errors converge, as is more commonly established in the literature.

The contributions presented in this chapter for high-order systems are the culmination of all the theoretical results presented in this thesis. We believe that they represent a significant step forward in the study of multi-agent systems since the proposed methodology may be used for the control design of consensus protocols under multiple inter-agent constraints for complex nonlinear systems. Moreover, by providing explicit robustness properties, we open the way for its adaptation to more complex and meaningful scenarios of cooperative control for multi-agent systems. For instance, the results of Theorems 5.1 and 5.2 may apply to a number of relevant systems in engineering applications, such as the rendezvous problem of underactuated UAVs subject to inter-agent constraints. A solution to this problem, consisting in a non-trivial adaptation of the previous results is presented in the next chapter.

6

RENDEZVOUS OF UNDERACTUATED UAVS UNDER INTER-AGENT CONSTRAINTS

In this chapter we address the rendezvous problem for underactuated UAVs. In order to study the rendezvous in a realistic application setting, we consider that the vehicles are subject to inter-agent constraints and disturbances coming from the on-board measurement devices and from the dynamic environment.

To address the rendezvous problem for UAVs a starting point is to use the nonholonomic integrator model used in Chapter 4 which represents well, both, autonomous ground vehicles and aerial vehicles flying at constant altitude. However, the motion of thrust propelled UAVs is best represented by an underactuated nonlinear system with a strong coupling between the translational and the rotational dynamics. Therefore, in order to study a more relevant representation of aerial vehicles, we consider the motion of the UAV described by a second-order Cartesian dynamics equation and a first-order attitude kinematics equation, where the inputs correspond to the magnitude and the direction of the thrust force, highlighting the coupling between the translational and the rotational dynamics. For systems modeled in such a way, the controllers tailored for linear systems do not directly apply.

We also emphasize that, besides being highly nonlinear, the dynamic model that we employ is underactuated. To deal with this difficulty, we apply a preliminary feedback that allows us to transform the underactuated model into a third-order integrator. That is, the resulting system is of relative degree three with respect to the output of interest (the position). Therefore, the system is converted into a high-order multi-agent system under constraints, which belongs to the class of systems addressed in Chapter 6. For such a system, modulo some minor modifications, the methodology presented in the previous chapter can be used to solve the problem at hand. Hence, employing a barrier-Lyapunov-functions-based consensus protocol we establish asymptotic convergence to the consensus manifold and robustness with respect to bounded disturbances in the sense of practical-input-to-state stability, while guaranteeing the respect of the constraints. Furthermore, we illustrate the performance of our controller via numerical simulations and we present experimental validation.

We stress that, in contrast to nonholonomic systems, relatively few works in the literature consider the rendezvous problem for multiple thrust-propelled UAVs under inter-agent constraints and disturbances. Moreover, in general, the existing results address only undirected interaction topologies and provide weak stability results such as non-uniform convergence to the consensus manifold. In light of this, our contributions are important in that we establish

strong stability and robustness properties for the problem of rendezvous of multiple UAVs interconnected over both undirected and directed topologies, and under realistic conditions, mainly connectivity maintenance, collision avoidance and external disturbances.

6.1 PROBLEM FORMULATION

We address the problem of position-consensus-based formation of multiple thrust-propelled UAVs under a set of realistic assumptions. More precisely, for the multi-agent system composed of N UAVs evolving in a 3-dimensional environment we study the rendezvous problem under inter-agent constraints —see Figure 6.1. The control goal is for the robots, interconnected over a graph $\mathcal{G} = (\mathcal{V}, \mathcal{E})$, to achieve a predetermined three-dimensional formation while guaranteeing the respect of inter-agent connectivity and collision-avoidance constraints as well as robustness with respect to disturbances.

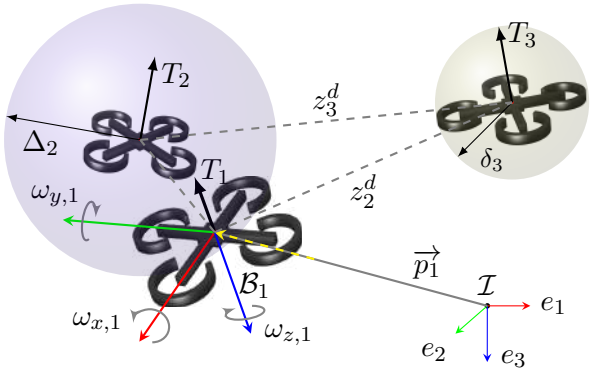

Figure 6.1: Group of thrust propelled vehicles and Inertial frame.

Consider first a single UAV. We choose to represent each vehicle's motion using a so-called "mixed" model that consists in a second-order Cartesian dynamics equation on E(3) and a first-order attitude kinematics equation on SO(3) —see, *e.g.*, [70], [138], and [71]. This *underactuated* model is justified by the fact that it describes well some commercial UAVs, which accept only thrust and angular rates as control inputs. Moreover, given the fully-actuated and passive nature of the attitude dynamics, angular torques can be easily defined in order to track the angular rates proposed hereafter.

The model for the ith agent is given by the equations

$$\dot{p}_i = v_i \tag{6.1a}$$

$$\dot{v}_i = -\frac{T_i}{m_i}\mathfrak{R}_i e_3 + g e_3 + \theta_i(t) \tag{6.1b}$$

$$\dot{\mathfrak{R}}_i = \mathfrak{R}_i S(\omega_i), \tag{6.2}$$

where m_i is the mass of the quadrotor, $e_3 = [0\ 0\ 1]^\top$ is the unitary vector in the vertical direction of the inertial frame $\mathcal{I}$, $p_i \in \mathbb{R}^3$ and $v_i \in \mathbb{R}^3$ are respectively the inertial position and

inertial velocity, $\mathfrak{R}_i \in \mathrm{SO}(3)$ is the rotation matrix of the body-fixed frame $\mathcal{B}_i$ with respect to $\mathcal{I}$, g is gravitational acceleration, $\theta_i : \mathbb{R}_{\geq 0} \to \mathbb{R}^3$ is an essentially bounded disturbance, and the matrix $S(x)$ is a skew-symmetric matrix such that $S(x)y = x \times y$ for any vectors $x \in \mathbb{R}^3$ and $y \in \mathbb{R}^3$. The inputs are the thrust force produced by the propellers, $T_i \in \mathbb{R}$, and the angular rate of the vehicle $\omega_i = [\omega_{xi}\ \omega_{yi}\ \omega_{zi}]^\top \in \mathbb{R}^3$ in the body-fixed frame $\mathcal{B}_i$ —see Figure 6.1 for an illustration.

Now, consider the N agents modeled by (6.1) interacting over the graph $\mathcal{G}$. Recalling the edge transformation (2.28), let the relative position between pairs of connected agents, in compact form, be given by

$$z := [E^\top \otimes I_3]p, \tag{6.3}$$

where $p^\top = [p_1^\top \ \cdots \ p_N^\top] \in \mathbb{R}^{3N}$ and E is the incidence matrix of the graph defined in (2.25). Then, denoting $z^{d\top} = [z_1^{d\top} \ \cdots \ z_M^{d\top}] \in \mathbb{R}^{3M}$ the relative displacements of the desired formation, the formation error is given by

$$\tilde{z} = z - z^d. \tag{6.4}$$

Therefore, in these coordinates, the rendezvous objective is that

$$\lim_{t\to\infty} \tilde{z}_k(t) = 0, \quad \forall k \leq M \tag{6.5a}$$

$$\lim_{t\to\infty} v_i(t) = 0, \quad \forall i \leq N. \tag{6.5b}$$

Now, considering the coordination of multiple vehicles in a realistic setting, it is assumed that the interactions between robots are executed only via embedded relative-measurements sensors. On the one hand, this naturally leads to considering directed-topology graphs. Therefore, we assume that the following holds.

Assumption 6.1. *The initial directed graph is either a directed spanning tree or a directed cycle.*

Hereafter, the controllers are designed only in the case of directed-spanning-tree and directed-cycle topologies; we stress, however, that the following results also apply to connected undirected graphs —*cf.* Chapter 5. Furthermore, we assume that the system is subject to inter-agent constraints in the form of bounds on the distances between initially connected agents. These constraints come, for one part, from the embedded measurements devices, which are reliable only if used within a limited range. Hence, in order to maintain the connectivity of the graph, the UAVs must remain within a limited distance from their neighbors. On the other hand, in order to guarantee the safety of the systems, inter-agent collision avoidance must also be ensured. Finally, we assume that the agents are subject to bounded time-varying disturbances generated by, *e.g.*, wind gusts, aerodynamic effects or unmodeled dynamics, which are common in applications involving cooperative UAVs.

In light of this, let Δ_k denote the maximal distance between the agents i and j, such that the agent j has access to information from the agent i through the arc $e_k = (i, j)$. Similarly,

let δ_k denote the minimal distance among neighbors such that collisions are avoided. Then, the connectivity and collision-avoidance constraints are encoded by the constraints set $\mathcal{D}$ introduced in (5.2). For the convenience of the reader we recall that the set $\mathcal{D}$ is defined as

$$\mathcal{D} := \left\{ z \in \mathbb{R}^{3M} : \delta_k < |z_k| < \Delta_k, \ \forall\, k \leq M \right\}. \tag{6.6}$$

Under the constriants in (6.6), the problem that we address herein is defined as follows.

Robust rendezvous problem with output constraints. Consider a multi-agent system composed of N quadrotor UAVs with underactuated dynamics described by (6.1)-(6.2). Let the interactions of the vehicles be modeled by a directed graph satisfying Assumption 6.1. Moreover, let the agents be subject to output inter-agent constraints given by the set (6.6). Find distributed controllers T_i and ω_i, with $i \leq N$, such that, in the absence of disturbances they achieve the objective (6.5), for a given desired formation z^d, and render the constraints set (6.6) forward invariant. That is, such that if $\theta_{i,2} \equiv 0$ for all $i \leq N$ the objective (6.5) holds and we have that $z(0) \in \mathcal{D}$ implies that $z(t) \in \mathcal{D}$ for all $t \geq 0$. Furthermore, in the presence of disturbances, that is $\theta_{i,2} \not\equiv 0$, the control law must render the formation practically input-to-state stable with respect to the disturbances and the set $\mathcal{D}$ in (6.6) forward invariant. •

The robust rendezvous problem of UAVs subject to inter-agent constraints stated above is a relevant problem to the aerospace industry that is motivated by the increasing interest for safety-aware fleet deployment. The solution to this problem, presented hereafter, is an original contribution of this thesis. It is fitting to mention that similar problems have been studied in the literature, as for instance in [78], [79], but only for systems interconnected over undirected graphs.

Beyond the proposed control laws for this particular problem of rendezvous for UAVs, the importance of this contribution is also to show how the framework for output-constrained consensus-based control developed in Chapter 5 may be adapted in a non-trivial way to address more complex systems, demonstrating both the applicability and the versatility of our results. This is presented hereafter.

6.2 CONTROL DESIGN AND STABILITY ANALYSIS

The controller that we propose to solve the robust formation problem with output constraints defined above builds upon the recursive design for output-constrained consensus described in the previous chapter. However, the dynamic model of a UAV (6.1) does not, *a priori*, fit in the class of systems characterized by the equations (5.1), which correspond to a chain of integrators. Therefore, the dynamic underactuated model first has to be transformed. To this end, using a change of variables we design a preliminary control loop inspired by the hierarchical backstepping approach of [71], so that the closed-loop system behaves as the kind of high-order systems addressed in Chapter 5. Indeed, the underactuated dynamical system is transformed into one with relative degree $\varrho = 3$. Thus, modulo some minor modifications explained further below, the control laws designed using the methodology in the previous chapter, can be used to solve the robust rendezvous problem with output

constraints considered in this chapter. A diagram of the control architecture is presented in Figure 6.2.

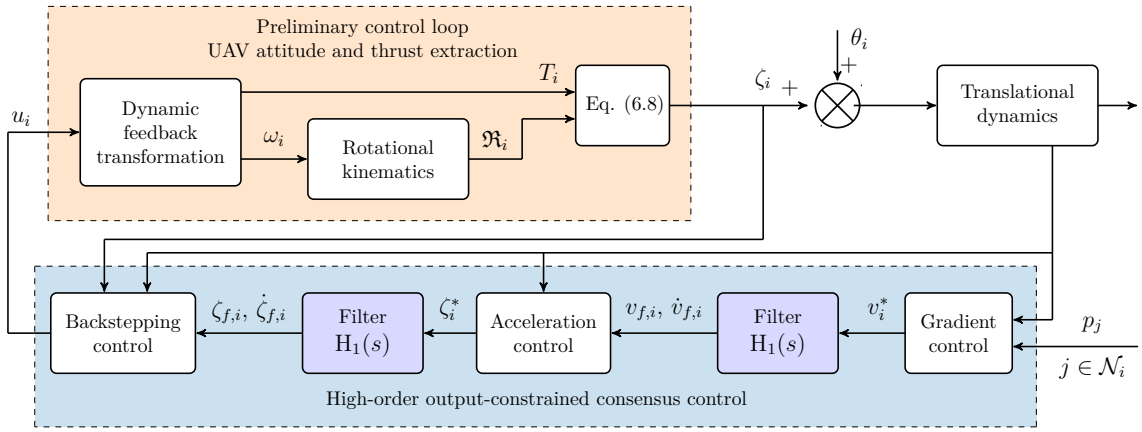

Figure 6.2: Block diagram of the control architecture for an underactuated UAV.

The first part of the control architecture follows a hierarchical approach that exploits the natural cascaded interconnection between the translational dynamics (6.1) and the rotational kinematics (6.2). We apply a dynamic feedback transformation to represent the system (6.1) in the form (5.1). To that end, first note that the second-order system defined by Equations (6.1) may be assimilated to a second-order integrator

$$\dot{p}_i = v_i \tag{6.7a}$$
$$\dot{v}_i = \zeta_i + \theta_i, \tag{6.7b}$$

with

$$\zeta_i := -\frac{T_i}{m_i}\mathfrak{R}_i e_3 + g e_3. \tag{6.8}$$

Nonetheless, the implementation of a virtual controller for (6.7), through the input ζ_i, is subject to the possibility of solving (6.8) for T_i, which is the actual control input. Because of the underactuation of (6.1), however, this is far from acquired. Indeed, note from (6.8) that the virtual input $\zeta_i \in \mathbb{R}^3$ cannot take an arbitrary value since $T_i \in \mathbb{R}$ and its direction is determined by the vehicle's attitude, $\mathfrak{R}_i$. In order to overcome the underactuation, we solve equation (6.8) dynamically, inspired by the distributed-backstepping approach in [71]. More precisely, we design the angular rates ω_i and an update law for the thrust T_i, so that ζ_i in (6.8) satisfies the dynamic equation

$$\dot{\zeta}_i = u_i, \quad i \leq N, \tag{6.9}$$

where $u_i \in \mathbb{R}^3$ is a new input. Note that, now, the system defined by (6.7) and (6.9) has the form of a high-order system (5.1) with $\varrho = 3$. Hence, the input u_i in (6.9) can be taken as the output-constrained consensus control law designed in Chapter 5.

On the other hand, to obtain (6.9) from (6.8) we proceed as follows. First we differentiate (6.8) with respect to time and use (6.2) to obtain

$$-\frac{\dot{T}_i}{m_i}\mathfrak{R}_i e_3 - \frac{T_i}{m_i}\mathfrak{R}_i S(\omega_i) e_3 = \dot{\zeta}_i. \tag{6.10}$$

That is, for (6.9) to hold, it is necessary and sufficient that

$$-\frac{\dot{T}_i}{m_i}\mathfrak{R}_i e_3 - \frac{T_i}{m_i}\mathfrak{R}_i S(\omega_i) e_3 = u_i. \tag{6.11}$$

That is, we must define T_i so that (6.11) holds. To that end, for a given u_i, we define $\nu_i \in \mathbb{R}^3$ as

$$\nu_i := u_i - \frac{c_3}{m_i} T_i \mathfrak{R}_i e_3, \tag{6.12}$$

where c_3 is a positive control gain. Next, replacing (6.12) into (6.11), we obtain

$$\begin{aligned} & -\frac{1}{m_i}\left[\dot{T}_i \mathfrak{R}_i + T_i \mathfrak{R}_i S(\omega_i)\right] e_3 = \nu_i + \frac{c_3}{m_i} T_i \mathfrak{R}_i e_3 \\ \iff & \left[(\dot{T}_i + c_3\, T_i)\mathfrak{R}_i + T_i \mathfrak{R}_i S(\omega_i)\right] e_3 = -m_i \nu_i. \end{aligned} \tag{6.13}$$

Left-multiplying by (the full-rank rotation matrix) $\mathfrak{R}_i^\top$ and using the structure of the matrix $S(\omega_i)$, the dynamic equation (6.13) is equivalent to

$$\left[T_i \omega_{yi},\ -T_i \omega_{xi},\ \dot{T}_i + c_3\, T_i\right]^\top = -m_i \mathfrak{R}_i^\top \nu_i. \tag{6.14}$$

Now, let $\tilde{\nu}_i := [\tilde{\nu}_{i,x}\ \tilde{\nu}_{i,y}\ \tilde{\nu}_{i,z}]^\top = \mathfrak{R}_i^\top \nu_i$. Then, we see that (6.14) holds if the angular rates are set to

$$\omega_i = \begin{bmatrix} \dfrac{m_i \tilde{\nu}_{i,y}}{T_i} & -\dfrac{m_i \tilde{\nu}_{i,x}}{T_i} & \omega_{zi} \end{bmatrix}^\top, \tag{6.15}$$

and the thrust is given by the update law

$$\dot{T}_i = -c_3\, T_i - m_i \tilde{\nu}_{i,z}. \tag{6.16}$$

Remark 6.1. *Note that by transforming the UAV model (6.1) using (6.8)-(6.9), only the three translational dimensions are directly controlled. Therefore, only three of the four available inputs are needed to solve the formation problem. Indeed, note that from equation (6.14), the yaw component of the angular rate ω_{zi} is not needed for control. Hence it may be considered as an additional degree of freedom and may be designed so that the vehicle follows independently a desired yaw trajectory.* •

Thus, using (6.15)-(6.16) in (6.1) we obtain that the underactuated system (6.1) may be rewritten in the form (5.1), as desired, that is,

$$\dot{p}_i = v_i \tag{6.17a}$$
$$\dot{v}_i = \zeta_i + \theta_i \tag{6.17b}$$
$$\dot{\zeta}_i = u_i. \tag{6.17c}$$

Furthermore, denoting $v^\top = [v_1^\top \ \cdots \ v_N^\top] \in \mathbb{R}^{3N}$, $\zeta^\top = [\zeta_1^\top \ \cdots \ \zeta_N^\top] \in \mathbb{R}^{3N}$, $\theta^\top = [\theta_1^\top \ \cdots \ \theta_N^\top] \in \mathbb{R}^{3N}$, and using the edge transformation (6.4), the multi-agent system in the reduced error-edge coordinates becomes

$$\dot{\tilde{z}}_t = \left[E_t^\top \otimes I_3\right] v \tag{6.18a}$$
$$\dot{v} = \zeta + \theta \tag{6.18b}$$
$$\dot{\zeta} = u, \tag{6.18c}$$

which corresponds to a system in the form of (5.1) with $\varrho = 3$ as addressed in the previous chapter. Hence, as mentioned above, the control approach presented in Chapter 5 may now be applied to solve the rendezvous problem under output constraints for a nonlinear and under-actuated multi-UAV system by designing u_i as for a third-order system and using it in (6.12) and (6.15)-(6.16) for the purpose of implementation. Thus, to apply the control law (5.22), designed in the previous chapter for the output-consensus problem under output constraints for high-order systems, we define the backstepping error variables

$$\tilde{v} = v - v_f \quad \text{and} \quad \tilde{\zeta} = \zeta - \zeta_f. \tag{6.19}$$

The filtered signals v_f and ζ_f are the outputs of command filters given, in state-space representation, by

$$\dot{\alpha}_1 = \omega_n \left[A \otimes I_{3N}\right] \alpha_1 + \omega_n \left[B \otimes I_{3N}\right] v^* \tag{6.20a}$$
$$\left[v_f^\top \ \dot{v}_f^\top\right]^\top = \left[C \otimes I_{3N}\right] \alpha_1, \tag{6.20b}$$

and

$$\dot{\alpha}_2 = \omega_n \left[A \otimes I_{3N}\right] \alpha_2 + \omega_n \left[B \otimes I_{3N}\right] \zeta^* \tag{6.21a}$$
$$\left[\zeta_f^\top \ \dot{\zeta}_f^\top\right]^\top = \left[C \otimes I_{3N}\right] \alpha_2, \tag{6.21b}$$

respectively, where

$$A := \begin{bmatrix} 0 & 1 \\ -1 & -2 \end{bmatrix}, \quad B := \begin{bmatrix} 0 \\ 1 \end{bmatrix}, \quad C := \begin{bmatrix} 1 & 0 \\ 0 & \omega_n \end{bmatrix} \tag{6.22}$$

and the initial conditions are set to $\alpha_{1,1}(0) = v^*(0)$, $\alpha_{2,1}(0) = \zeta^*(0)$, and $\alpha_{1,2}(0) = \alpha_{2,2}(0) = 0$. The inputs v^* and ζ^* in (6.20) and (6.21), correspond to the desired virtual controllers given by

$$v^* := -c_1 [E_\odot \otimes I_3] \nabla W(\tilde{z}) \tag{6.23}$$

and

$$\zeta^* := -c_2\tilde{v} + \omega_n\alpha_{1,2}, \tag{6.24}$$

respectively. The term $\nabla W(\tilde{z})$ is the gradient of a barrier Lyapunov function encoding the connectivity and collision avoidance constraints. It is defined as

$$W(\tilde{z}) = \sum_{k\leq M} W_k(\tilde{z}_k), \tag{6.25}$$

where

$$W_k(\tilde{z}_k) = \frac{1}{2}\left[|\tilde{z}_k|^2 + \tilde{B}_k(\tilde{z}_k + z_k^d)\right], \tag{6.26}$$

and a *weight recentered barrier function* —see Remark 5.2 and Appendix A.2— is given by

$$\begin{aligned}\tilde{B}_k(\tilde{z}_k + z_k^d) =& \kappa_{1,k}\left[\ln\left(\frac{\Delta_k^2}{\Delta_k^2 - |\tilde{z}_k + z_k^d|^2}\right) - \ln\left(\frac{\Delta_k^2}{\Delta_k^2 - |\tilde{z}_k + z_k^d|^2}\right)\right] \\ &+ \kappa_{2,k}\left[\ln\left(\frac{|\tilde{z}_k + z_k^d|^2}{|\tilde{z}_k + z_k^d|^2 - \delta_k^2}\right) - \ln\left(\frac{|z_k^d|^2}{|z_k^d|^2 - \delta_k^2}\right)\right],\end{aligned} \tag{6.27}$$

with

$$\kappa_{1,k} := \frac{\delta_k^2}{|z_k^d|^2(|z_k^d|^2 - \delta_k^2)}, \quad \kappa_{2,k} := \frac{1}{\Delta_k^2 - |z_k^d|^2}. \tag{6.28}$$

Note that the recentered barrier function and its gradient are equal to zero at the desired formation configuration, *i.e.*, $\tilde{B}_k(z_k^d) = 0$, $\nabla\tilde{B}_k(z_k^d) = 0$. Furthermore, it directly encodes the constraints in terms of the original edge-state z_k, *i.e.*, $\tilde{B}_k(z_k) \to \infty$ as either $|z_k| \to \Delta_k$ or $|z_k| \to \delta_k$. Hence, the function (6.25) with (6.26) and (6.27) is a barrier Lyapunov function as per Definition 3.1. Moreover, it satisfies Assumption 5.4 where the additional critical point $\tilde{z}_k^*$ is an unstable saddle point —see Appendix A.3.

Thus, following the control design from Chapter 5 we may infer that the transformed controller

$$u := -c_3\tilde{\zeta} + \omega_n\alpha_{2,2} - \tilde{v}, \tag{6.29}$$

with (6.20)-(6.21) and (6.23)-(6.24), solves the robust formation problem with output constraints for system (6.17). However, a closer inspection shows that there is one more technical difficulty to circumvent. Indeed, note that from (6.15), the dynamic solution to the equation (6.8) is valid if and only if $T_i \neq 0$. Therefore, in order to address this additional constraint, we perform a control redesign which respects the control method and the stability analysis proposed in Chapter 5.

Note that, from (6.8), the condition $T_i \neq 0$ is satisfied if the desired virtual control ζ_i^* satisfies $\zeta_i^* \neq ge_3$, for all $i \leq N$. Therefore, the virtual control input ζ^* is modified to

$$\zeta^* := \text{sat}\left(-c_2\tilde{v} + \omega_n\alpha_{1,2}\right), \tag{6.30}$$

where $\mathrm{sat}(\cdot)$ is a saturation function mapping $\mathbb{R}^N \to \mathbb{R}^N$ defined element-wise, *i.e.*, $\mathrm{sat}(s) = \left[\sigma(s_1)^\top \ \cdots \ \sigma(s_N)^\top\right]^\top$, where, *e.g.*, $\sigma(s_i) = \mathrm{sign}(s_i)\min\{|s_i|, \bar{\zeta}_M\}$, with $\bar{\zeta}_M < g$, or any other odd monotonic function, bounded in absolute value.

Remark 6.2. *The virtual control ζ^* is saturated to ensure that the physical input, the thrust, $T_i \neq 0$. In addition, by a proper choice of the filters' initial conditions, $\zeta \approx \zeta^*$, so, in view of (6.8) and (6.30), the control design also guarantees that ζ and the thrust T_i, $i \leq N$, satisfy pre-imposed bounds. This is significant because it implies that even though controllers based on the gradient of a barrier Lyapunov functions are not primarily designed to guarantee control-input constraints, the satisfaction of the latter may be accomplished using a dynamic controller, as done above.* •

Proposition 6.1 ([130])**.** *Consider N UAVs modeled by the system (6.1) with the control law (6.15)-(6.16) and (6.29), with (6.20)-(6.21), (6.23) and (6.30). Then, there exists ϵ^*, such that, for $\epsilon \in (0, \epsilon^*]$ where $\epsilon := 1/\omega_n$, if the graph representing the communication topology satisfies Assumption 6.1, and if $\theta \equiv 0$ the rendezvous objective (6.5) is achieved for almost any initial conditions satisfying $z(0) \in \mathcal{D}$, except for a set of measure zero. Otherwise if $\theta \not\equiv 0$, the closed-loop system is almost-everywhere practically input-to-state stable with respect to θ. Moreover, the constraints set (6.6) is rendered forward invariant along closed-loop solutions.* □

Proof. The proof follows the same arguments as the proof of Theorem 5.1 in Chapter 5. First, note that the system (6.18) in closed-loop with (6.29) may be written in singular-perturbation form

$$\dot{\tilde{z}}_t = -c_1[E_t^\top E_\odot \otimes I_3]\nabla W(\tilde{z}) + [E_t^\top \otimes I_3]\,[\tilde{v} + \tilde{\alpha}_{1,1}] \tag{6.31a}$$

$$\dot{\tilde{v}} = \mathrm{sat}(-c_2\tilde{v} + \omega_n\tilde{\alpha}_{1,2}) + \tilde{\zeta} + \tilde{\alpha}_{2,1} - \omega_n\tilde{\alpha}_{1,2} + \theta_2 \tag{6.31b}$$

$$\dot{\tilde{\zeta}} = -c_3\,\tilde{\zeta} - \tilde{v} \tag{6.31c}$$

$$\epsilon\dot{\tilde{\alpha}} = \tilde{A}\tilde{\alpha} - \epsilon\frac{\partial\varphi(\xi)}{\partial\xi}\dot{\xi}, \quad \xi^\top = \begin{bmatrix}\tilde{z}_t^\top & \tilde{v}^\top & \tilde{\zeta}^\top\end{bmatrix}. \tag{6.31d}$$

where $\tilde{\alpha} = \alpha - \varphi(\xi)$, with

$$\varphi(\xi) = \left[(-c_1[E_\odot \otimes I_3]\nabla W(\tilde{z}))^\top \ 0^\top \ -\mathrm{sat}(c_2\tilde{v})\ 0^\top\right]^\top, \tag{6.32}$$

and $\tilde{A} := \mathrm{blockdiag}\{[A \otimes I_{3N}]\}$.

Note that by setting $\mathrm{sat}(s) = s$ we recover (5.31) with $\varrho = 3$ so the analysis of the trajectories for (6.31) follows similar guidelines as for the system (5.31). Therefore, as for Theorem 5.1, first, we use the singular-perturbation theory for multi-stable systems; more precisely [124, Theorem 2]. To that end, we need to show that the boundary layer system is asymptotically stable and that the reduced slow system is input-to-state stable with respect to the set $\mathcal{W} \times \{0\}^2$ and input $\theta_{i,2}$, $i \leq N$.

Exponential stability of the origin for the boundary-layer system

$$\frac{d\tilde{\alpha}}{d\tau} = \tilde{A}\tilde{\alpha}, \quad \tau = \frac{t}{\epsilon} \tag{6.33}$$

follows from the fact that $\tilde{A}$ is Hurwitz by design.

Now, setting $\tilde{\alpha} = 0$ in (6.31a)-(6.31c), the reduced system reads

$$\dot{\tilde{z}}_t = -c_1[E_t^\top E_\odot \otimes I_3]\nabla W(\tilde{z}) + [E_t^\top \otimes I_3]\tilde{v} \tag{6.34a}$$

$$\dot{\tilde{v}} = -\mathrm{sat}(c_2\tilde{v}) + \tilde{\zeta} + \theta_2 \tag{6.34b}$$

$$\dot{\tilde{\zeta}} = -c_3\,\tilde{\zeta} - \tilde{v}. \tag{6.34c}$$

Note that, the subsystem (6.34a) is equivalent to (5.32a) in the proof of Theorem 5.1 in Chapter 5. Therefore, as before, we may conclude that under Assumption 6.1 it is input-to-state stable with respect to the set $\mathcal{W}$ and to the input $\tilde{v}$.

Next, consider the subsystem (6.34b)-(6.34c). Let $\varepsilon_u \in (0, 1)$ and define the Lyapunov function

$$V_2(\tilde{v}, \tilde{\zeta}) = \frac{(1 + c_3\,\varepsilon_u)}{2}|\tilde{v}|^2 + \frac{1}{2}|\tilde{\zeta}|^2 + \varepsilon_u\,\tilde{\zeta}^\top\tilde{v}, \tag{6.35}$$

which is positive definite. Its derivative along (6.34b)-(6.34c) satisfies

$$\dot{V}_2(\tilde{v}, \tilde{\zeta}) \leq -(1 + \varepsilon_u c_3 - \gamma_v)|\tilde{v}|\mathrm{sat}(c_2|\tilde{v}|) - \left(c_3 - \varepsilon_u - \frac{\varepsilon_u^2}{1 + c_3\,\varepsilon_u}\right)|\tilde{\zeta}|^2 + \frac{2\varepsilon_u}{1 + c_3\,\varepsilon_u}|\theta|^2. \tag{6.36}$$

Hence, choosing $\delta_v > 0$ and $\varepsilon_u > 0$ small enough so that

$$\delta_2 := c_3 - \varepsilon_u - \frac{\varepsilon_u^2}{1 + c_3\,\varepsilon_u} > 0$$

and $\delta_1 := 1 + \varepsilon_u c_3 - \delta_v > 0$, we have

$$\dot{V}_2(\tilde{v}, \tilde{\zeta}) \leq -\delta_1|\tilde{v}|\mathrm{sat}(c_2|\tilde{v}|) - \delta_2|\tilde{\zeta}|^2 + \delta_3|\theta_2|^2 \tag{6.37}$$

where $\delta_3 := 2\varepsilon_u/(1 + c_3\,\varepsilon_u)$. The inequality (6.37) implies that the subsystem (6.34b)-(6.34c) is input-to-state stable with respect to θ_2. Hence, invoking [123, Theorem 3.1] we conclude that, for all initial conditions $\xi(0)$ such that $z_t(0) \in \mathcal{D}_t$ and all essentially bounded inputs θ_2, the reduced system (6.34) is input-to-state stable with respect to $\mathcal{W}_\Theta$, defined in (5.34), and to the input θ_2. Furthermore, $\mathcal{W}_\Theta$ qualifies as a $\mathcal{W}$-limit set for (6.34).

Now, since the boundary layer system is exponentially stable and the reduced system is input-to-state stable with respect to $\mathcal{W}_\Theta$ and θ_2, using Theorem 5.1, we conclude that the controller (6.29), with (6.20)-(6.21), (6.23), and (6.30) solves the robust consensus problem with output constraints for system (6.18). This, in turn, implies that the actual controllers (6.15)-(6.16) solve the robust formation problem with output constraints for multi-agent system (6.1). ■

6.3 NUMERICAL EXAMPLES

To illustrate the performance of the controller proposed in this chapter, we present some numerical examples consisting in the rendezvous of six quadrotors under limited-range restrictions. More precisely, the objective is for the group of UAVs to reach a hexagonal formation while maintaining the connectivity of the initial interaction graph and avoiding potential collisions between connected agents. Two scenarios are considered. In the first, the range limitations are considered to be equal for all the agents, so that the initial interaction graph with seven edges is undirected. In the second scenario, each agent has a different range of interaction, which naturally leads to a directed graph topology with five edges.

In both considered scenarios, the desired formation is determined by the desired relative position vector $z_{dk} = (z_{dk,x}, z_{dk,y}, z_{dk,z})$, for each $k \leq 7$, set to $(1, 0.5, 0)$, $(-1, 1.5, 0)$, $(-1, 0.5, 0)$, $(-2, 1, 0)$, $(-1, 0.5, 0)$, $(0, -1, 0)$, $(1, -0.5, 0)$. The saturation limit for the desired controller of the translational dynamics is set to $\bar{\zeta}_M = 7$ m/s^2, the controller gains to $c_1 = 1$, $c_2 = 0.8$, $c_3 = 3$, and the filter natural frequency is set to $\omega_n = 350$ rad/s. We consider the mass of each drone to be $m_i = 0.4$ kg. Furthermore, it is also assumed that the agents are subject to a locally integrable and vanishing disturbance defined as follows:

$$\begin{aligned} \theta_i(t) &= -\sigma(t)\,[1\ 1\ 0]^\top \\ \sigma(t) &= \begin{cases} -0.6\big[\tanh(2(t-15)) - 1\big], & i \in \{3, 5\} \\ 0.6\big[\tanh(2(t-15)) - 1\big], & i = 2 \\ 0, & i \in \{1, 4, 6\}. \end{cases} \end{aligned} \tag{6.38}$$

The results of the first scenario are presented in Figures 6.4-6.8. The maximal and minimal distances of the inter-agent constraint set (6.6) are, respectively, $\Delta_k = 4.3$ m and $\delta = 0.2$ m, $\forall k \leq M$. The initial positions and velocities of the vehicles are presented in Table 6.1. Moreover, the initial poses are $\mathfrak{R}_i = I_3$ for all $i \leq 6$. In light of the initial conditions and the range limits Δ_k, at the initial time, the interconnections between the vehicles are represented by an initial undirected connected graph as in Figure 6.3.

Table 6.1: Initial conditions for the simulation in the undirected-graph scenario

Index	p_x	p_y	p_z	v_x	v_y	v_z
1	1.9	0	-1	0.6	-0.8	0
2	-2	0	0	-0.3	0	0
3	5.2	2	0	1.3	0.3	0
4	5.2	-2	0	0.1	0	0
5	-5.5	2	0	0	0	0
6	-4.5	2	2	-0.8	0	0

In Figure 6.4 are illustrated the paths of each agent as well as the final desired formation for the multi-agent system. Individual vehicles are represented by coordinate axes to illustrate

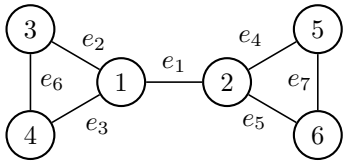

Figure 6.3: Undirected connected graph at the initial time.

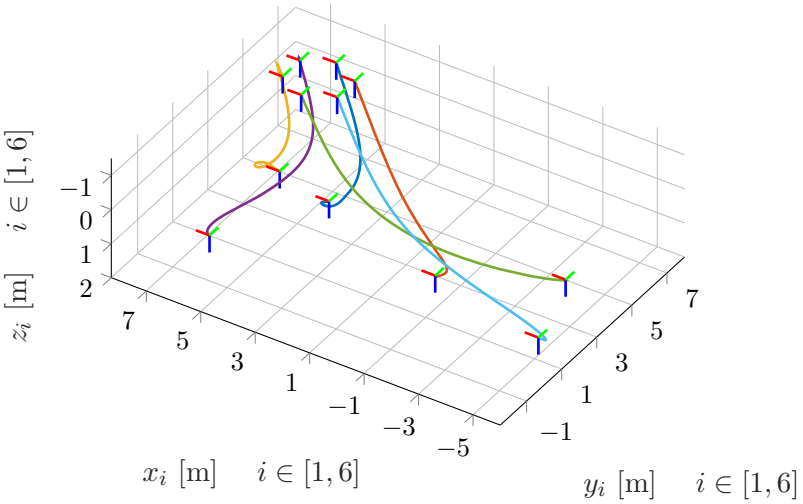

Figure 6.4: Paths of the agents in the undirected scenario.

their orientation as well —*cf.* Figure 6.1. In Figures 6.5 and 6.6 are depicted, respectively, the inter-agent distances and the velocities in the inertial frame. At first, under the action of the disturbances, the agents converge to a steady state. Then, as soon as the disturbances vanish, after 15 seconds, the agents converge to the desired static formation, as expected. Moreover, note that both connectivity and collision avoidance constraints, represented by the dashed lines in Figure 6.5, are respected, even in the presence of the additive disturbance.

The thrust and angular-rate control inputs are shown in Figures 6.7 and 6.8, respectively. One may appreciate that the non-crossing of zero condition for the thrust is respected.

The results of the second scenario are presented in Figures 6.10-6.14. The initial positions and velocities of the vehicles, as well as the range limits and the safety distances are presented in Table 6.1. The initial poses are $\mathfrak{R}_i = I_3$ for all $i \leq 6$. Since in this scenario the range limits Δ_k are different for each agent, with the given initial conditions, the initial graph is given by a directed spanning tree as in Figure 6.9.

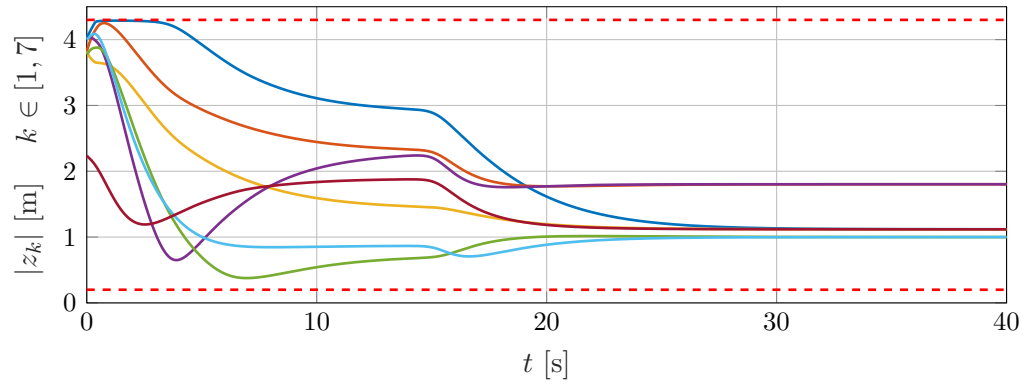

Figure 6.5: Distances between neighbor UAVs in the undirected case. The dashed lines represent the connectivity and collision avoidance constraints.

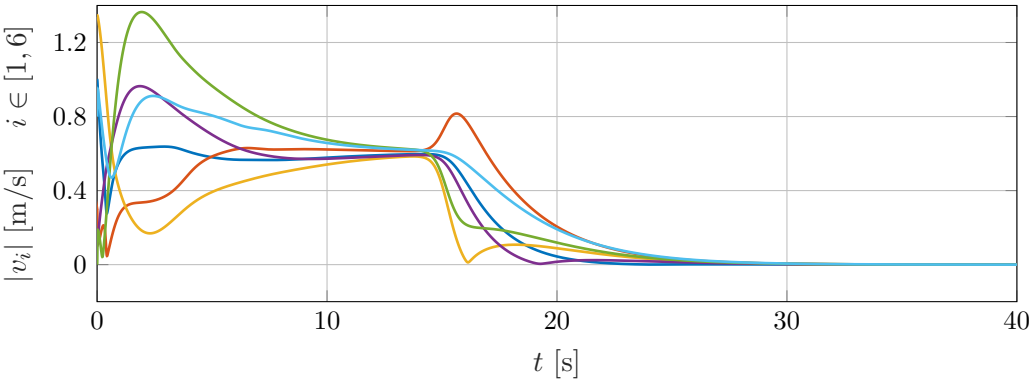

Figure 6.6: Inertial velocities of the UAVs in the undirected case.

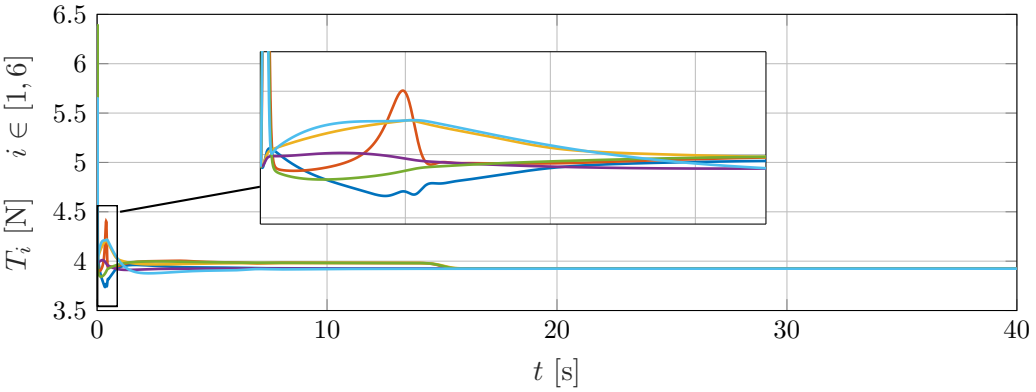

Figure 6.7: Thrusts of the UAVs in the undirected scenario.

Table 6.2: Initial conditions and constraint parameters for the directed scenario

Index	p_x	p_y	p_z	v_x	v_y	v_z	Δ_k	δ_k
1	2.4	0	-1	0.6	-0.8	0	2.5	0.2
2	-0.58	-0.9	0	-0.3	0	0	3.4	0.2
3	4	1.8	0	1.1	0.3	0	3.8	0.2
4	5	-2	0	0.1	0	0	3.5	0.2
5	-4.2	-0.45	0	0	0	0	3.7	0.2
6	-2	-4.2	2	-0.8	0	0	4.2	0.2

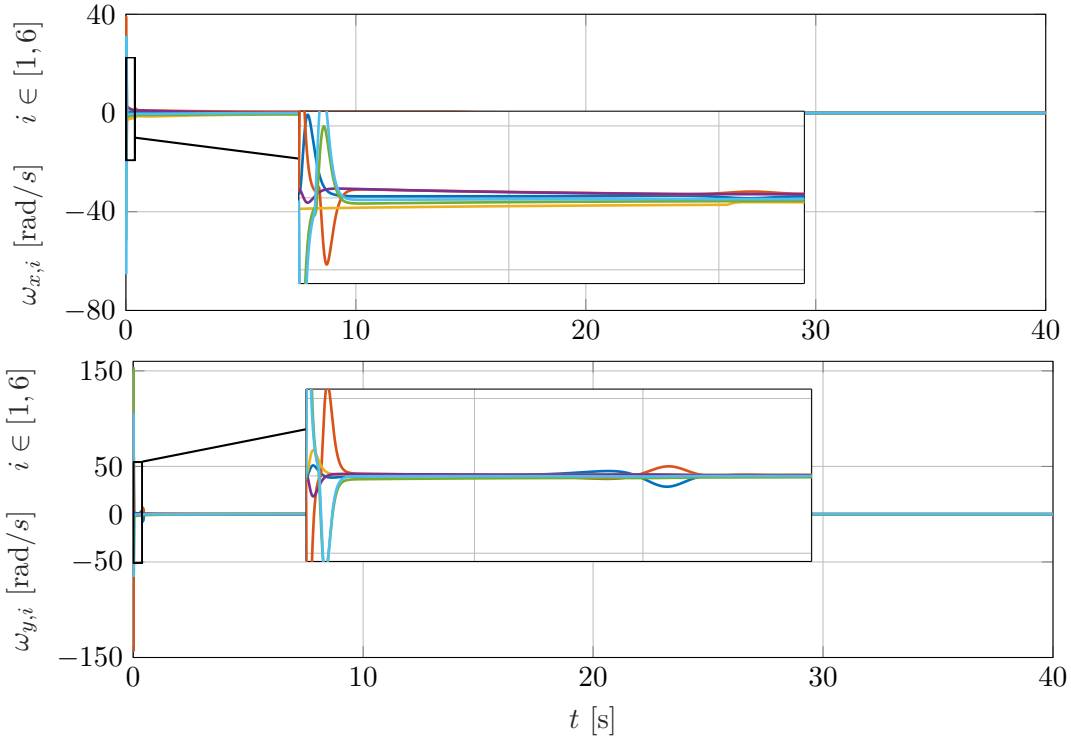

Figure 6.8: Angular rates of the UAVs in the undirected scenario.

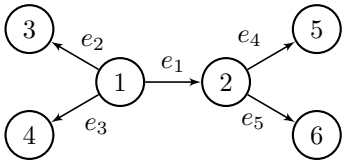

Figure 6.9: Directed-spanning-tree graph at the initial time.

The paths of each agent are shown in Figure 6.10. In Figures 6.11 and 6.12 are depicted, respectively, the inter-agent distances and the velocities in the inertial frame. As in the undirected case, it can be seen from Figures 6.11 and 6.12 that the connectivity and collision avoidance constraints are respected and, as soon as the disturbances vanish, the agents converge to the desired static formation. The thrust and angular-rate control inputs are shown in Figures 6.13 and 6.14, respectively.

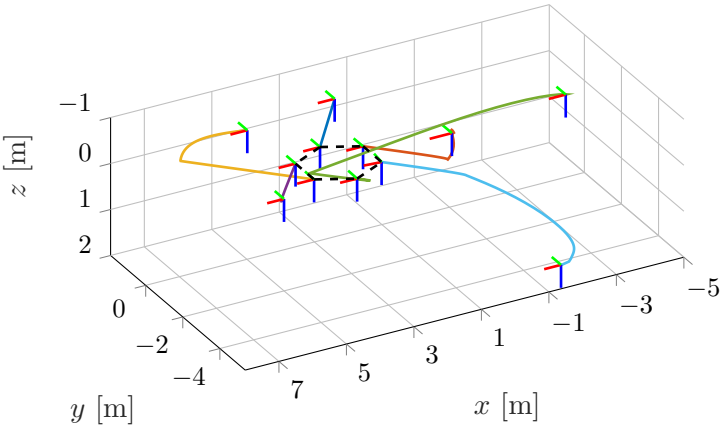

Figure 6.10: Paths of the agents in the directed scenario.

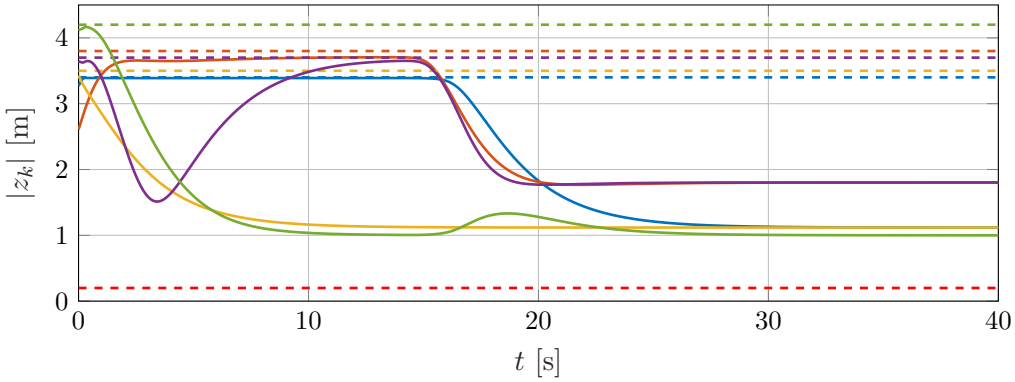

[Distances between neighbor UAVs in the directed case]

Figure 6.11: Distances between neighbor UAVs in the directed case. The dashed lines represent the connectivity and collision avoidance constraints.

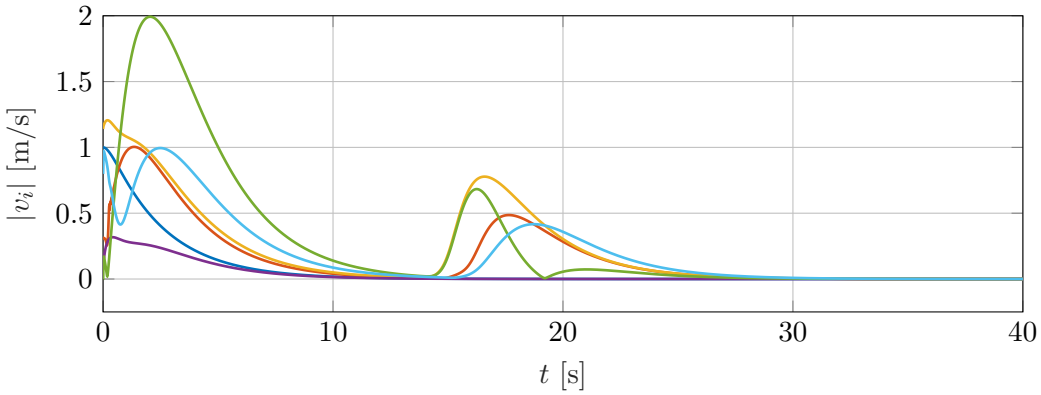

Figure 6.12: Inertial velocities of the UAVs in the directed case.

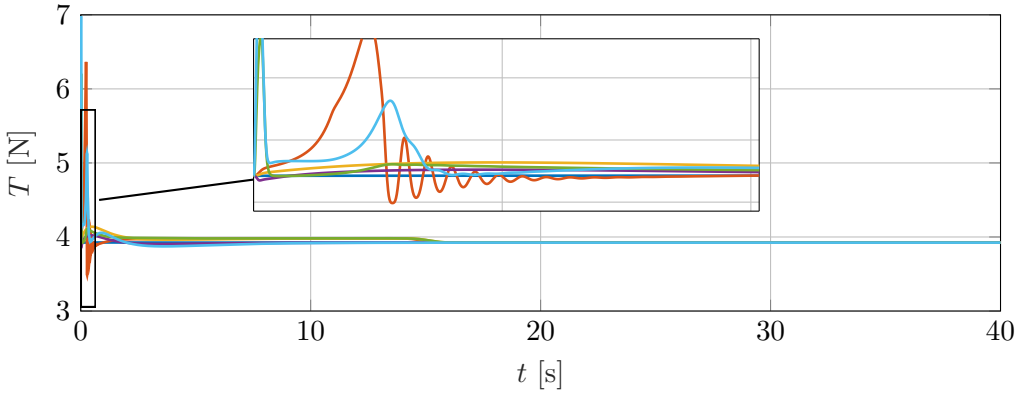

Figure 6.13: Thrusts of the UAVs in the directed scenario.

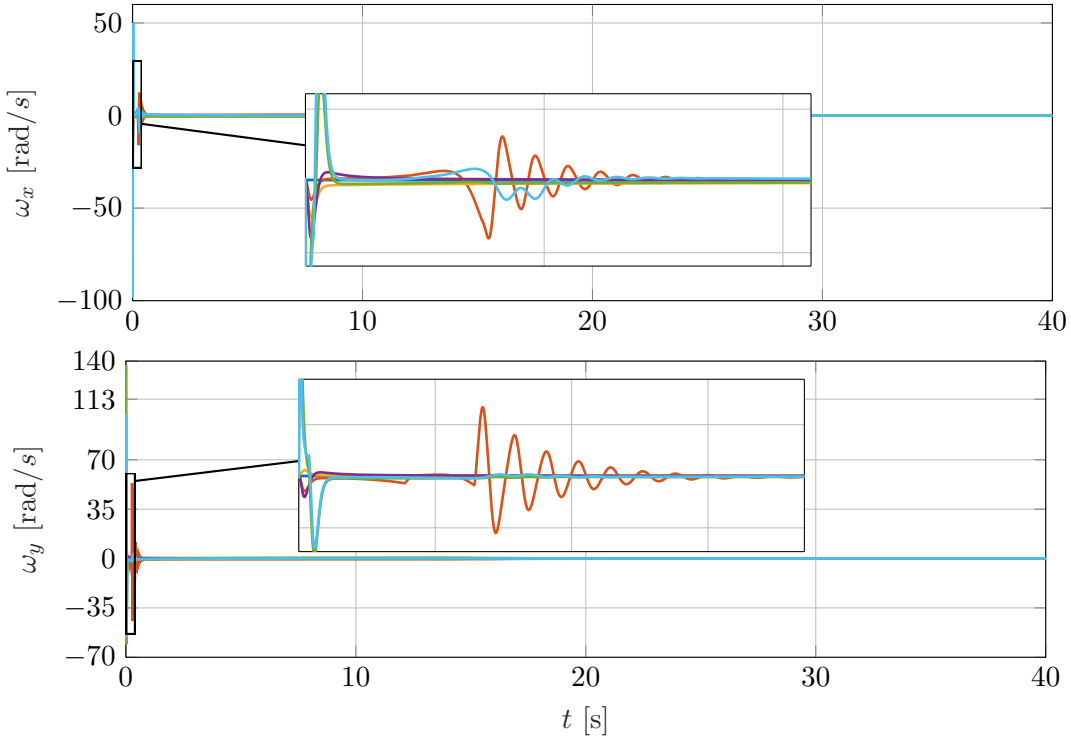

Figure 6.14: Angular rates of the UAVs in the directed scenario.

6.4 EXPERIMENTAL VALIDATION

In this section we illustrate the performance of the proposed controller via an experimental setup. The experiments were performed using a group of five DJI Tello EDU® drones —see Figures 6.15 and 6.16. The control law and the interactions among the agents were implemented via the Robot Operating System (ROS) interface. The ground truth of the positions, poses, and velocities of each robot was obtained using an Optitrack motion-capture system, based on active IR cameras and markers. However, we stress that each agent has access only to the relative positions of its neighbors, as given by an initial graph. Indeed, it is also assumed that the information of the neighbors' positions are only available within a limited range determined by a circle of radius Δ_k centered at each agent. The latter represents the scenario where the agents are not able to communicate with each other and rely solely on the measurements obtained using the embedded sensors.

Specifications	
Mass (g)	80
Length (mm)	98
Width (mm)	92.5
Height (mm)	41
Max. velocity (m/s)	8

Figure 6.15: DJI Tello EDU®. Source: adapted from [139]

The control objective in the experimental setup is for the group of drones to distributedly achieve a desired formation. Furthermore, since the information exchange among agents is range-limited, as we have mentioned earlier the connectedness of the initial topology is not guaranteed *a priori* and must be preserved by the controller. Finally, collision avoidance among neighboring agents, determined by a minimal safety distance δ, must be guaranteed.

Figure 6.16: Snapshot of the experimental test using five DJI Tello EDU® drones.

It is important to remark, however, that due to technical constraints in this setup only the "high-order output-constrained consensus control" corresponding to the outer-loop of the proposed methodology —*cf.* Figure 6.2— is experimentally validated. Indeed, the DJI Tello EDU® drones used in the experiments have an internal attitude controller which is not directly accessible to modification. Therefore, in practice, the drones are only controllable in the Cartesian coordinates. In other words, each agent may be assimilated to a second-order integrator system of the form

$$\dot{p}_i = v_i \tag{6.39a}$$
$$\dot{v}_i = \zeta_i + \theta_i(t) \tag{6.39b}$$

where ζ_i is the effective control input and θ_i represents additive disturbances.

In light of this, for the experiments, the rendezvous control law was set to $\zeta_f^\top = \begin{bmatrix}\zeta_{f,1}^\top & \cdots & \zeta_{f,5}^\top\end{bmatrix}$, corresponding to the output of the command filter (6.21) with input

$$\zeta^* = \text{sat}\left(-c_2\tilde{v} + \omega_n\alpha_{1,2}\right), \tag{6.40}$$

together with (6.23), (6.19), and (6.20).

Four different scenarios are presented. In Section 6.4.1, the initial interconnection topology is given by a directed spanning tree. Next, a connected undirected graph and a complete graph are considered in Sections 6.4.2 and 6.4.3, respectively. Finally, in Section 6.4.4 we consider that the agent labeled as "1" has access to information from a virtual leader with a given trajectory; this desired trajectory of the virtual leader is regarded as a disturbance affecting the group of agents. A video of the four experimental scenarios is available at: https://tinyurl.com/rdvUAVsConnectivity.

6.4.1 *Directed spanning tree*

For this setup, the initial conditions and the maximal and minimal inter-agent distances, Δ and δ respectively, representing the constraints, are presented in Table 6.3. Under these conditions and constraints, it is assumed that the initial interaction graph of the system is given by the directed spanning tree shown in Figure 6.17. The desired formation corresponds to a pentagon and is determined by the desired relative position vector $z_{dk} = (z_{dk,x}, z_{dk,y}, z_{dk,z})$, for each $k \leq 4$, set to $(0.9, 0.66, 0)$, $(-0.6, 1.7, 0)$, $(-0.3, -1.04, 0)$, $(1.2, 0, 0)$. The control gains were set to $c_1 = 0.8$, $c_2 = 0.4$, the natural frequency of the command filters was set to $\omega_n = 350$ rad/s, and the saturation limit was set to $\bar{\zeta}_M = 3$ m/s^2.

Table 6.3: Initial conditions and constraint parameter

Index	p_x **[m]**	p_y **[m]**	p_z **[m]**	v_x **[m/s]**	v_y **[m/s]**	v_z **[m/s]**	Δ **[m]**	δ **[m]**
1	-0.5	2.0	1.3	0.0	0.0	0.0	2.1	0.3
2	-0.9	3.0	1.8	0.0	0.0	0.0	2.1	0.3
3	0.9	1.5	1.8	0.0	0.0	0.0	2.1	0.3
4	2.1	2.2	1.8	0.0	0.0	0.0	2.1	0.3
5	2.1	0.8	1.5	0.0	0.0	0.0	2.1	0.3

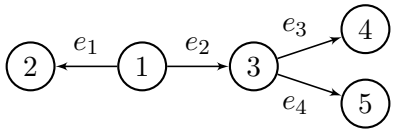

Figure 6.17: Initial interaction topology: directed spanning tree.

The experimental results are presented in Figures 6.18-6.22. As evidenced in Figure 6.18, the agents appear to reach the desired static formation. Moreover, from Figure 6.19 we see that the distances between the initially interconnected agents remains within the imposed bounds guaranteeing the maintenance of the connectivity and the avoidance of collisions. In Figure 6.22 are presented the control inputs $\zeta_{f,i}$, $i \leq 5$, which are the outputs of the command filters with input (6.40).

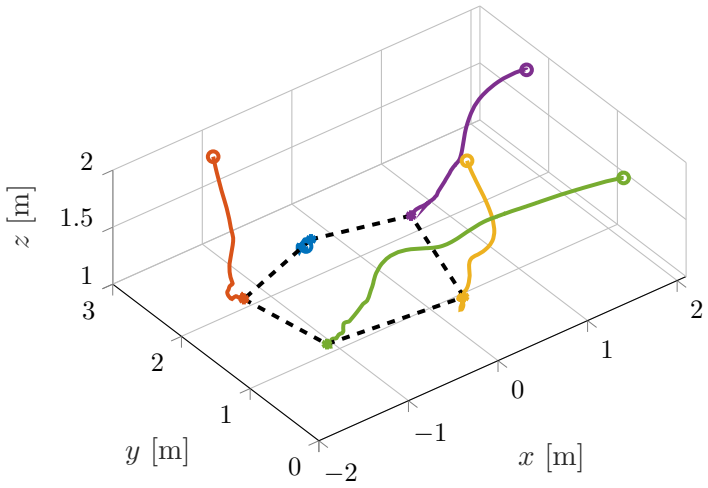

Figure 6.18: Paths followed by the DJI Tello drones up to the desired pentagonal formation.

In Figure 6.20 one can appreciate that the formation errors do not actually converge to zero but to a steady-state error. This, however is not in contradiction with the theoretical results. Indeed, in Proposition 6.1 we stated that, in the presence of disturbances, the desired formation is practically-input-to-state stable. The latter means that the trajectories of the state of the system satisfy the bound (5.45), which is determined by the supremum norm of the disturbances. So, since in practice the drones are constantly subject to, *e.g.*, aerodynamic disturbances, the formation errors do not converge exactly to zero, but satisfy the bound (5.45). Moreover, it seems fitting to say at this point that the results of Proposition 6.1 apply for drones controlled in thrust and angular rates, given by (6.16) and (6.15), respectively. Yet, as we mentioned earlier, neither the thrust nor the attitude dynamics are accessible for control. Therefore, part of the steady-state error may also be induced from the latter.

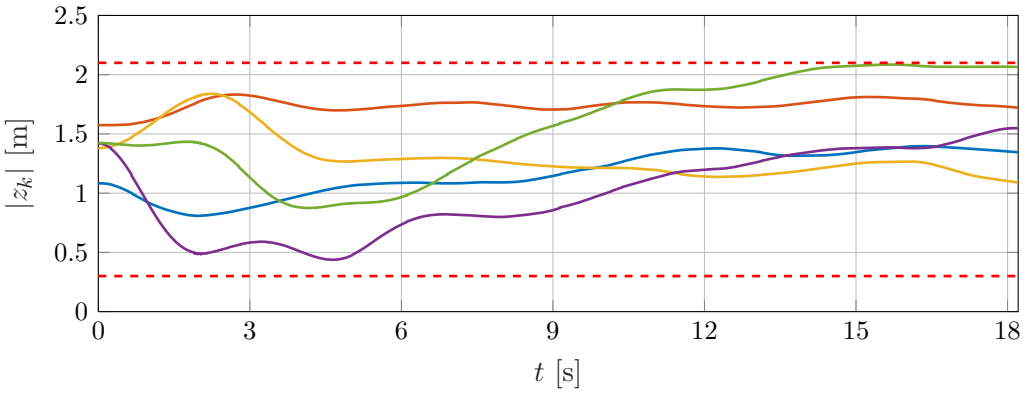

Figure 6.19: Inter-agent distances. The dashed lines represent the maximal and minimal distances guaranteeing connectivity maintenance and collision avoidance.

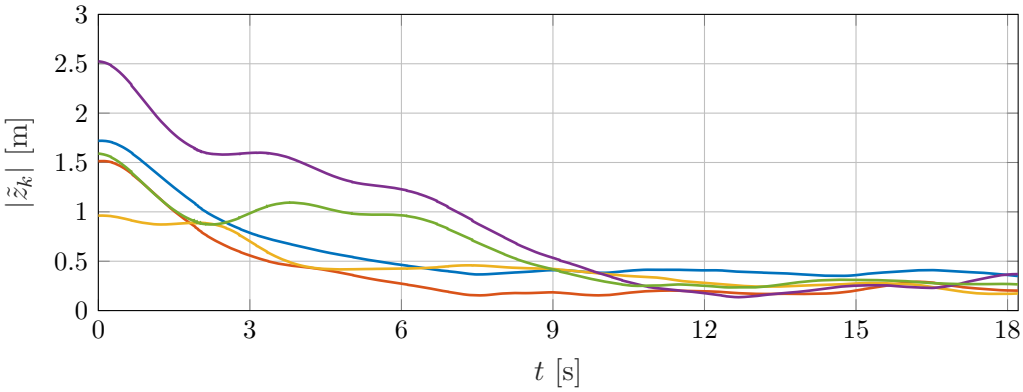

Figure 6.20: Norms of the formation errors.

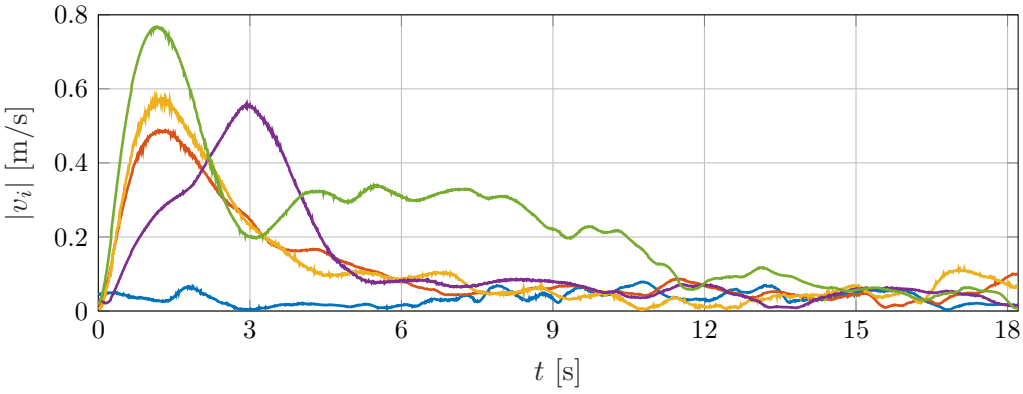

Figure 6.21: Norms of the velocities in the inertial frame.

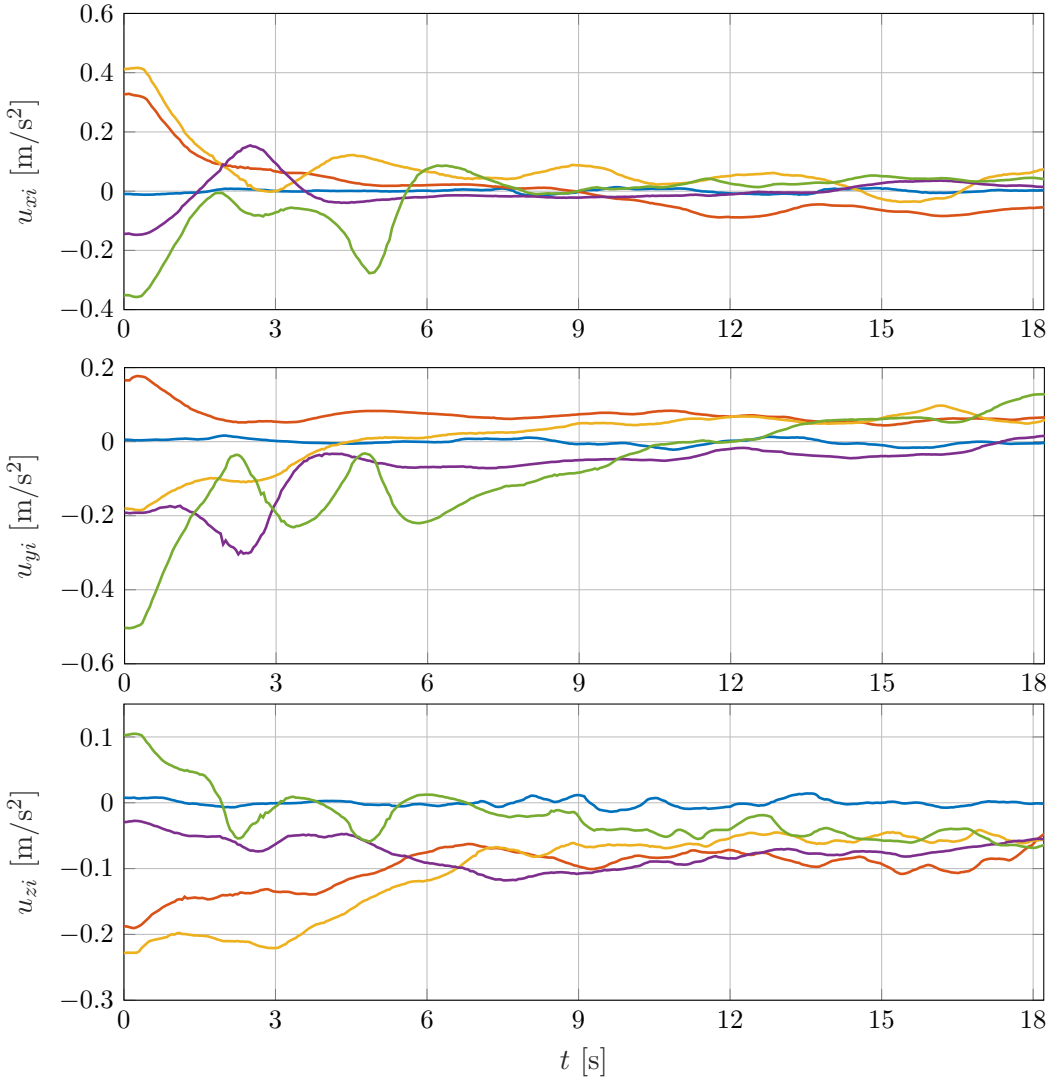

Figure 6.22: Control inputs.

6.4.2 *Undirected graph*

The initial conditions and the parameters Δ and δ denoting the inter-agent distance constraints are presented in Table 6.4. In this setting, the initial graph is given by the undirected connected graph in Figure 6.23. The desired relative position vector $z_{dk} = (z_{dk,x}, z_{dk,y}, z_{dk,z})$, for each $k \leq 5$, is set to $(0.9, 0.66, 0)$, $(-0.6, 1.7, 0)$, $(-0.3, -1.04, 0)$, $(1.2, 0, 0)$, $(1.5, 1.04, 0)$. The latter determines a pentagonal formation. The control gains were set to $c_1 = 0.6$, $c_2 = 0.3$, the natural frequency of the command filters was set to $\omega_n = 350$ rad/s, and the saturation limit was set to $\bar{\zeta}_M = 3$ m/s^2.

Table 6.4: Initial conditions and constraint parameters

Index	p_x **[m]**	p_y **[m]**	p_z **[m]**	v_x **[m/s]**	v_y **[m/s]**	v_z **[m/s]**	Δ **[m]**	δ **[m]**
1	-0.3	1.5	1.5	0.0	0.0	0.0	2.6	0.3
2	-0.7	2.8	2.0	0.0	0.0	0.0	2.6	0.3
3	0.9	1.5	1.8	0.0	0.0	0.0	2.6	0.3
4	2.1	2.2	1.8	0.0	0.0	0.0	2.6	0.3
5	2	1.2	1.5	0.0	0.0	0.0	2.6	0.3

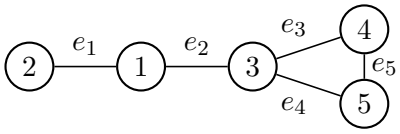

Figure 6.23: Interaction topology: undirected graph

The results are presented in Figures 6.24-6.28. As in the directed-topology case, it can be seen in Figure 6.24 that the agents reach the desired static formation. Moreover, the connectivity and inter-agent collision-avoidance constraints are satisfied —see Figure 6.25. Note, however, that as in the directed case, due to the disturbances encountered in practice, the desired formation is reached in a practical sense. In Figure 6.28 are presented the control inputs. It is clear from Figure 6.28 that the controllers stay within the desired saturation limits.

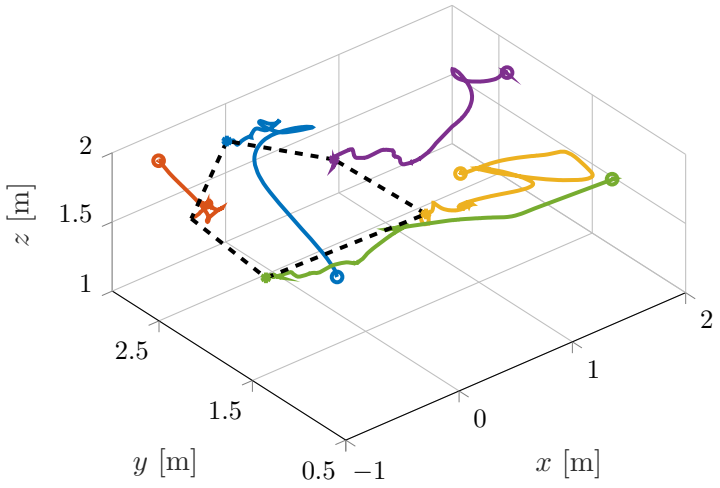

Figure 6.24: Paths followed by the DJI Tello drones up to the desired pentagonal formation.

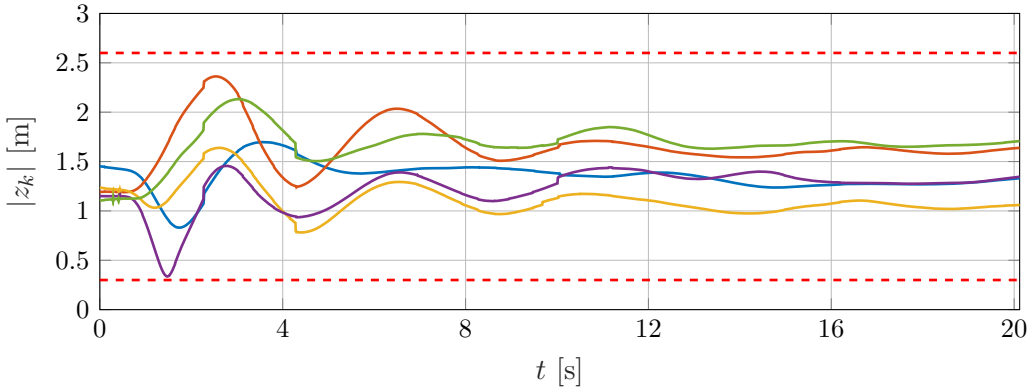

Figure 6.25: Inter-agent distances. The dashed lines represent the maximal and minimal distances guaranteeing connectivity maintenance and collision avoidance.

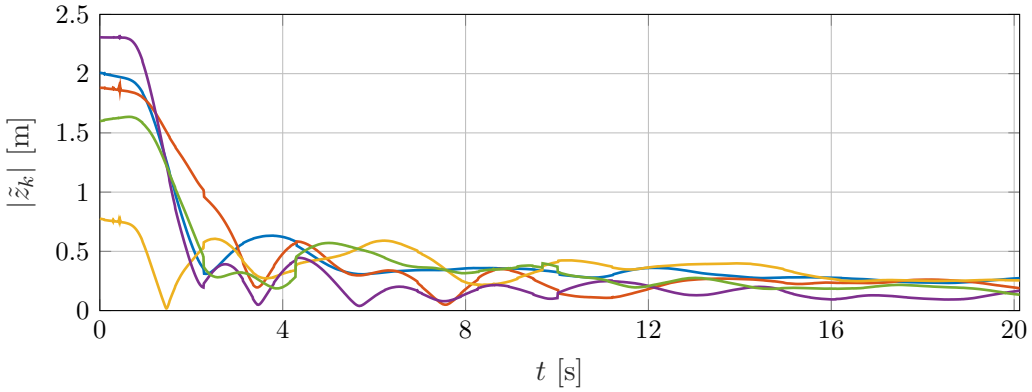

Figure 6.26: Norms of the formation errors.

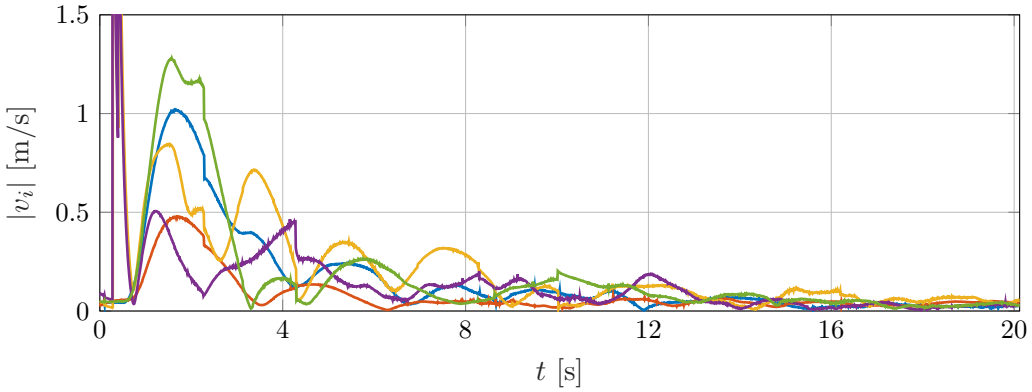

Figure 6.27: Norms of the velocities in the inertial frame.

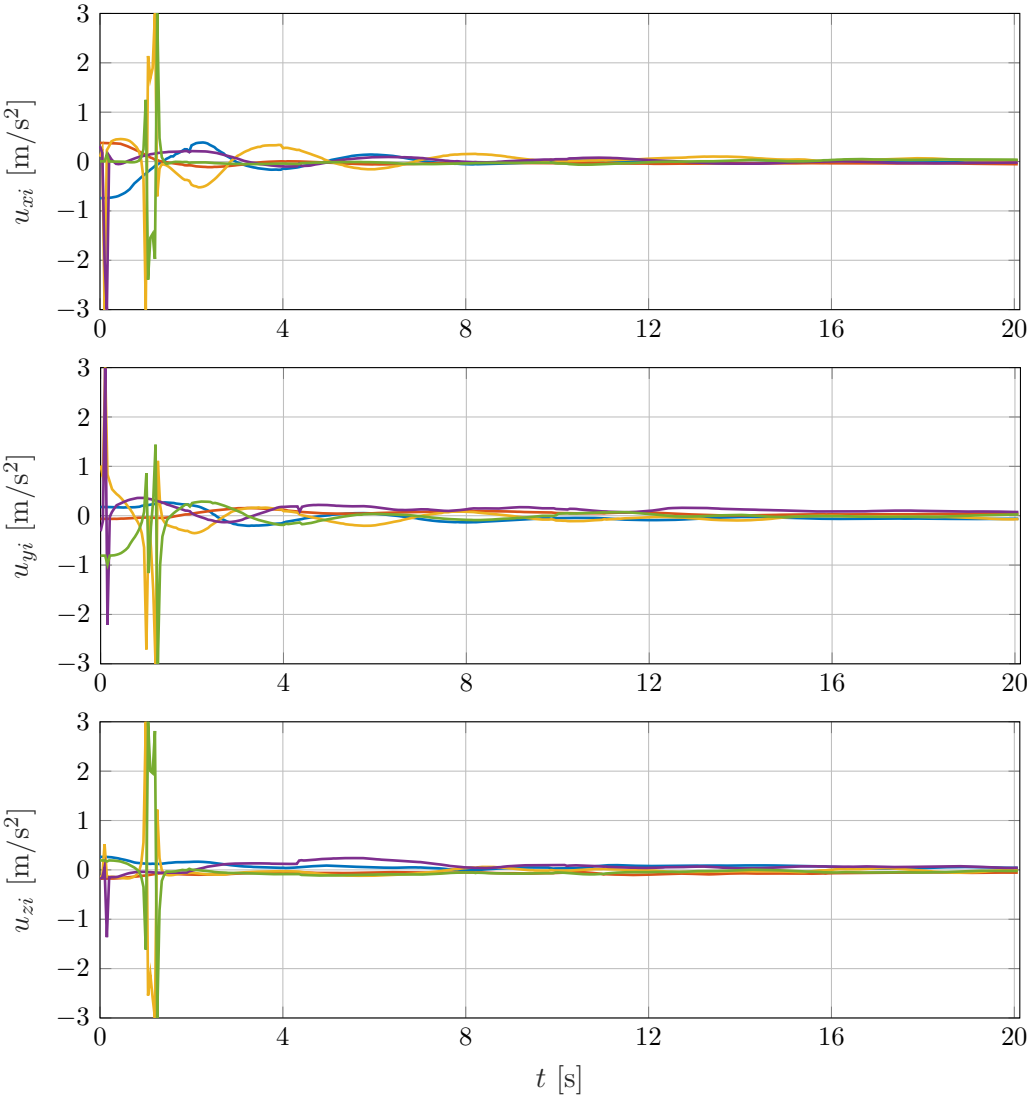

Figure 6.28: Control inputs.

6.4.3 *Complete graph*

For this setting, we assume that the radius Δ of the sensing zone of each agent is large enough so that it can interact with all the other agents in the systems. Therefore, the initial interaction topology is represented by the complete undirected graph in Figure 6.29. The radius of the sensing zones, as well as the minimal safety distances and the initial conditions are presented in Table 6.5. The desired pentagonal formation is described by the relative position vector $z_{dk} = (z_{dk,x}, z_{dk,y}, z_{dk,z})$, for each $k \leq 10$, set to $(0.9, 0.66, 0)$, $(-0.6, 1.7, 0)$, $(-0.3, -1.04, 0)$, $(1.2, 0, 0)$, $(1.5, 1.04, 0)$, $(-0.9, 0.66, 0)$, $(0.6, 1.7, 0)$, $(-0.3, 1.04, 0)$, $(-1.8, 0, 0)$, $(-1.5, 1.04, 0)$.

The control gains were set to $c_1 = 0.8$, $c_2 = 0.4$, the natural frequency of the command filters was set to $\omega_n = 350$ rad/s, and the saturation limit was set to $\bar{\zeta}_M = 3$ m/s^2.

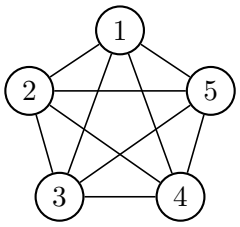

Figure 6.29: Interaction topology: complete undirected graph

Table 6.5: Initial conditions and constraint parameters

Index	p_x **[m]**	p_y **[m]**	p_z **[m]**	v_x **[m/s]**	v_y **[m/s]**	v_z **[m/s]**	Δ **[m]**	δ **[m]**
1	-0.5	1.5	1.3	0.0	0.0	0.0	4.0	0.3
2	-0.9	2.8	1.8	0.0	0.0	0.0	4.0	0.3
3	0.9	1.5	1.8	0.0	0.0	0.0	4.0	0.3
4	2.1	2.2	1.8	0.0	0.0	0.0	4.0	0.3
5	2.1	1.2	1.5	0.0	0.0	0.0	4.0	0.3

The results of this experimental setup are presented in Figures 6.30-6.34. As in the previous two cases, the agents (practically) reach the desired static formation, while guaranteeing the respect of the connectivity and inter-agent collision-avoidance constraints —see Figures 6.30, 6.31 and 6.32. The control inputs, shown in Figure 6.34, also remain within the imposed saturation limits.

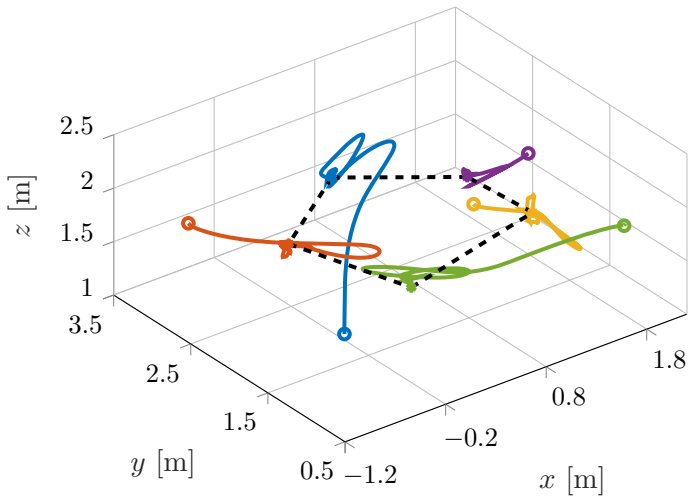

Figure 6.30: Paths followed by the DJI Tello drones up to the desired pentagonal formation.

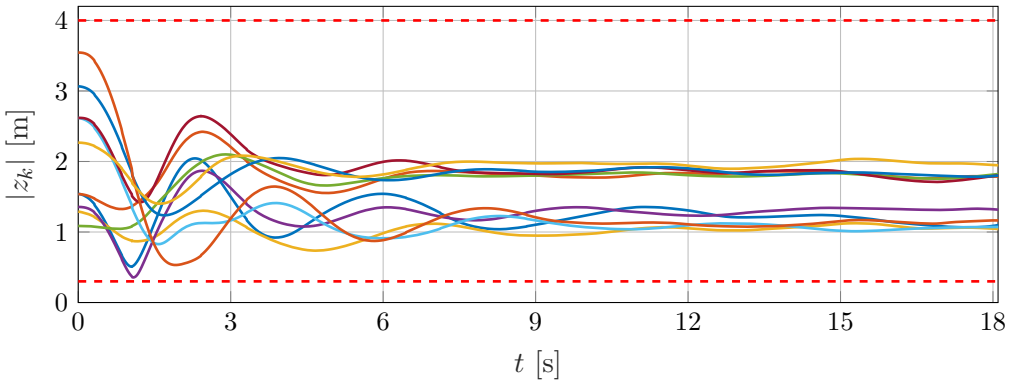

Figure 6.31: Inter-agent distances. The dashed lines represent the maximal and minimal distances guaranteeing connectivity maintenance and collision avoidance.

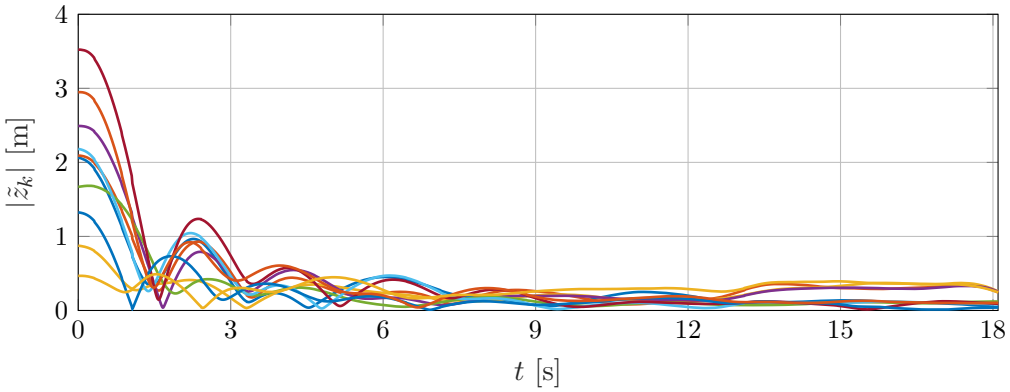

Figure 6.32: Norms of the formation errors.

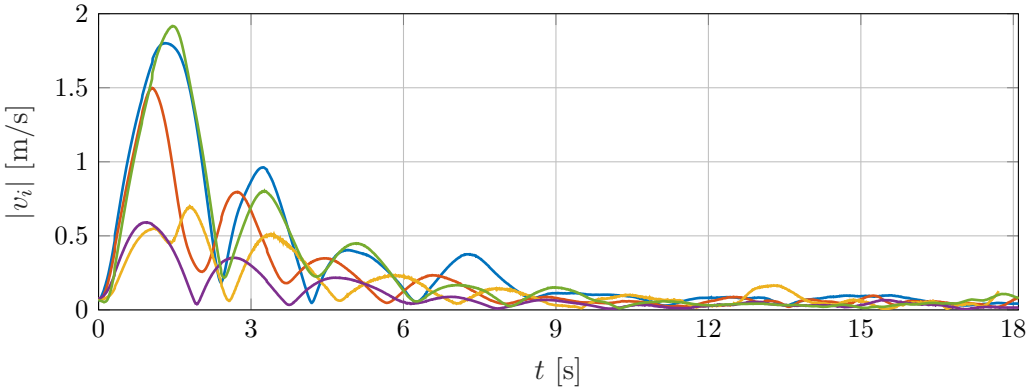

Figure 6.33: Norms of the velocities in the inertial frame.

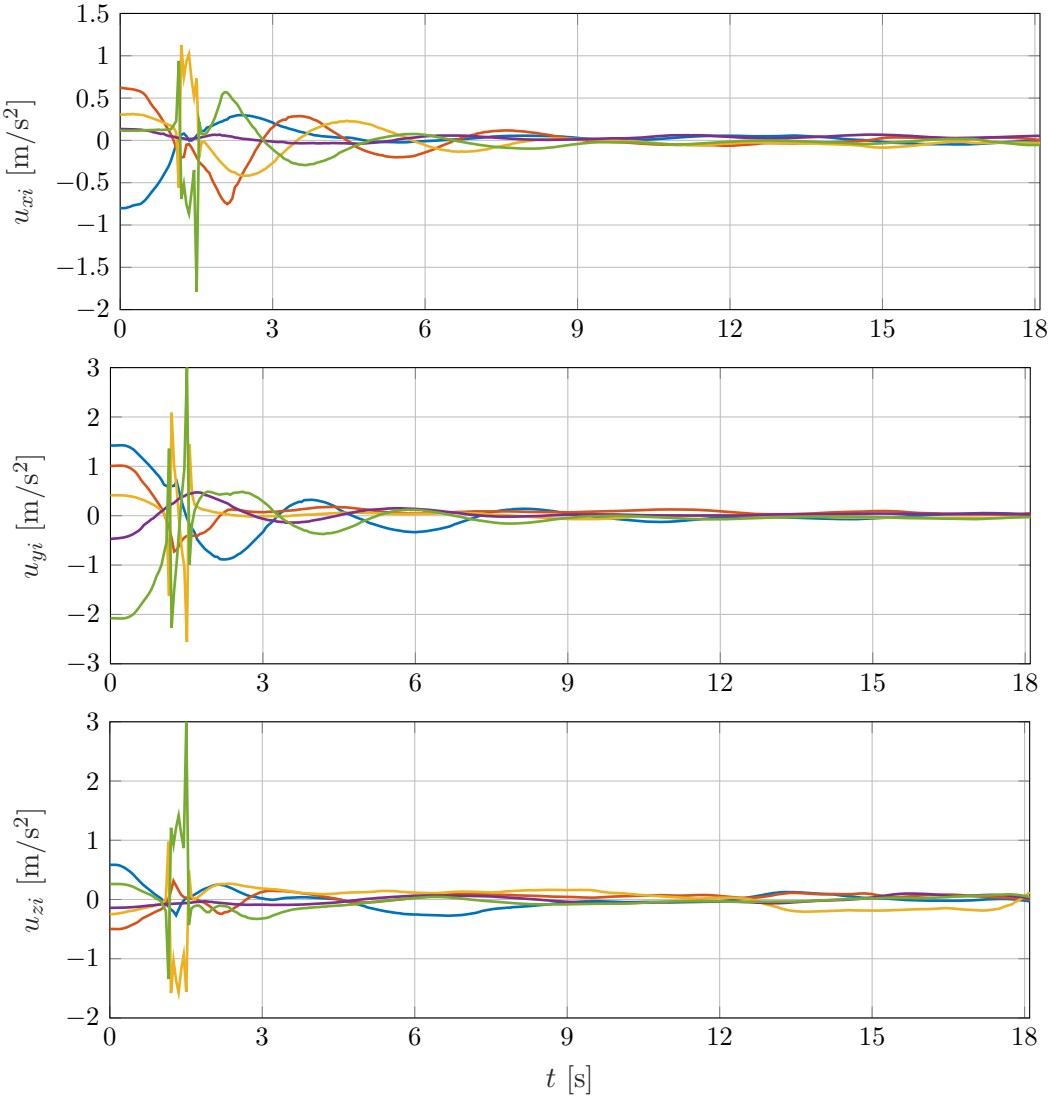

Figure 6.34: Control inputs.

6.4.4 *Virtual leader*

We now consider a three-agent system where an agent of the group, labeled ”1” (the root of a spanning tree), follows a virtual agent, labelled ”0”, describing a predefined trajectory. The initial conditions are given in Table 6.6 and the initial topology is represented by the directed spanning tree in Figure 6.35. The virtual agent follows an inclined 8-shaped trajectory described by the equations

$$x(t) = 0.5\sin(0.25\,t), \quad y(t) = 2 + \cos(0.5\,t), \quad z(t) = 1.8 + 0.5\cos(0.25\,t). \tag{6.41}$$

The control gains were set to $c_1 = 0.6$, $c_2 = 0.3$, the natural frequency of the command filters was set to $\omega_n = 350$ rad/s, and the saturation limit was set to $\bar{\zeta}_M = 3$ m/s^2.

Table 6.6: Initial conditions and constraint parameters

Index	p_x **[m]**	p_y **[m]**	p_z **[m]**	v_x **[m/s]**	v_y **[m/s]**	v_z **[m/s]**	Δ **[m]**	δ **[m]**
1	-0.3	1.5	1.5	0.0	0.0	0.0	2.1	0.3
2	-0.9	2.8	1.8	0.0	0.0	0.0	2.1	0.3
3	0.9	1.5	1.8	0.0	0.0	0.0	2.1	0.3

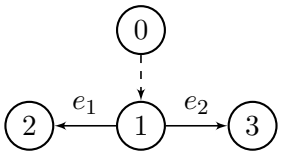

Figure 6.35: Interaction topology: directed spanning tree with virtual agent.

In this setting, the velocities of this virtual leader may be considered as additive disturbances for the other UAVs of the system. Since the proposed controllers deal only with the problem of consensus-based formation, and not target tracking, it is evident that the multi-agent system will not achieve the desired formation in this case. However, the importance of this experiment is to illustrate the performance of the proposed control law, and especially the respect of the inter-agent constraints, when the agents follow a virtual leader. Indeed, although the desired formation is not achieved, the connectivity and collision-avoidance constraints are always guaranteed.

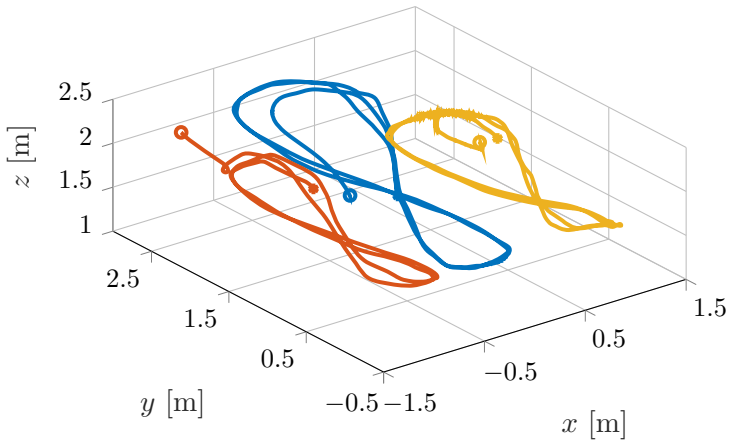

Figure 6.36: 8-shaped paths followed by the DJI Tello drones under the influence of the virtual agent.

These results are presented in Figures 6.36-6.38. It can be seen in Figure 6.37 that despite being subject to an important additive disturbance, both the connectivity and the collision-avoidance constraints are respected. The latter is in accordance to the theoretical results.

Indeed, since the desired formation is practically-input-to-state stable and the constraints set is forward invariant, the trajectories of the system remain bounded and the constraints are satisfied even in the presence of disturbances. Under these properties, some well-known results such as, *e.g.*, passivity-based [140] or disturbance rejection [141] strategies, may be used in order to modify the rendezvous control laws proposed in this chapter, so that the multi-agent system exactly follows a desired trajectory.

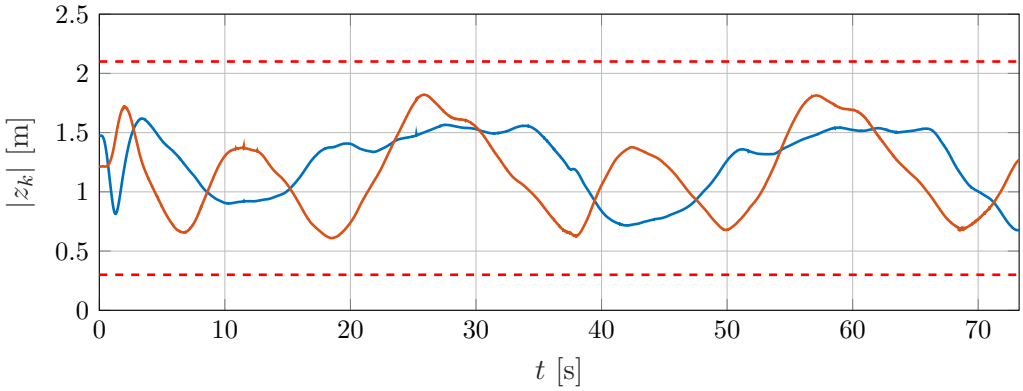

Figure 6.37: Inter-agent distances. The dashed lines represent the maximal and minimal distances guaranteeing connectivity maintenance and collision avoidance.

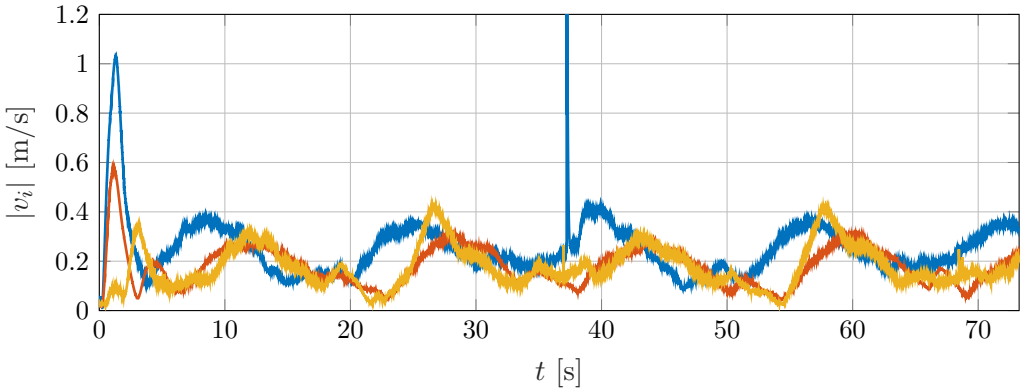

Figure 6.38: Norms of the velocities in the inertial frame.

6.5 CONCLUSION

The original contribution presented in this chapter consists in solving a relevant problem to the aerospace industry that is motivated by the increasing interest for safety-aware fleet deployment. In particular, we presented a solution to the robust rendezvous control problem of cooperative thrust-propelled UAVs under a set of realistic assumptions and not at the expense of formal analysis.

Building upon the contributions presented in Chapter 5 and based on a feedback transformation design, we proposed a distributed controller, using the gradient of a barrier Lyapunov function and the framework of command-filtered backstepping, that achieves the desired formation with guaranteed connectivity maintenance and inter-agent collision avoidance even in the presence of disturbances. From a theoretical point of view, we established almost-everywhere practical input-to-state stability of the desired formation with respect to bounded disturbances. Moreover, the results apply for networks interacting over undirected and some directed topologies. From a practical point of view, we validated the performance of the proposed controllers via numerical examples and experimental setups. We believe that the control methodology presented in this chapter constitutes an important step towards addressing more complex consensus-based tasks for groups of UAVs in realistic settings from the perspective of automatic control.

CONCLUSIONS AND FURTHER RESEARCH

In this work we have addressed the robust consensus-based control of multi-agent systems under constraints. To this end, we have proposed multiple contributions in terms of control design and stability analysis for a variety of relevant systems. These contributions are summarized as follows.

On consensus with connectivity maintenance. We first address the problem of consensus for first- and second-order systems where the inter-agent information exchange is only reliable within a limited range, therefore imposing the need of guaranteeing the connectivity of the interaction topology via the control. The control design and the analysis of the closed-loop system is carried out relying on the edge-based representation recalled in Chapter 2. The original contribution is to establish strong stability and robustness properties, in terms of asymptotic stability and input-to-state stability, respectively, by providing strict (barrier) Lyapunov functions for the problem of consensus with preserved connectivity of low-order multi-agent systems over undirected and directed graphs. These properties are stronger than the mere convergence usually established in the literature for consensus with nonlinear interconnections relying on the dynamics of the nodes. Indeed, we show that on top of achieving asymptotic stability of the consensus manifold, in the presence of disturbances, the trajectories of the system remain bounded and converge to a neighborhood of the origin while maintaining connectivity. The latter cannot be ascertained if only convergence with a non-strict Lyapunov function is established.

Although the systems considered in this first part are seemingly simple low-order linear systems, we believe that the results obtained in Chapter 3 are of great importance. Indeed, they constitute the basis for the consensus control design of more complex systems, as presented in the subsequent chapters.

On nonholonomic systems. Based on a polar-coordinates transformation which, similarly to the edge transformation, uses relative quantities instead of the global states of the nodes, we address the full consensus problem under connectivity constraints for multiple nonholonomic vehicles in a leader-follower configuration. This is a step towards a more representative model for *sensor-based* vehicle applications. Although there is a vast literature addressing the problem of consensus of nonholonomic vehicles, even considering inter-agent constraints, the contributions presented in this thesis are original in that, compared to most of the existing results which either address only position consensus or design non-smooth or time invariant feedback laws, we provide smooth time-invariant feedback laws that achieve *full* consensus under distance and field-of-view connectivity constraints. All these results are illustrated via numerical simulations and experimental setups.

On high-order systems. We solve the consensus problem under connectivity and collision-avoidance constraints for high-order systems in normal form interconnected over undirected and directed graphs. For the control design we build upon the gradient-based

control in the edge-based perspective used for the consensus with connectivity maintenance for low-order linear systems. By using a command-filtered-backstepping methodology we are able to extend our results to the output- and partial-state-consensus problem under output constraints of high-order systems. The latter is made possible by the strong robustness properties and the strict Lyapunov functions provided in previous chapters for the consensus under inter-agent constraints of first-order systems. Hence, the importance of the latter. In terms of the stability analysis, we establish for the first-time in the literature practical-input-to-state stability for the consensus problem under output constraints. We believe that by providing explicit robustness properties, the proposed methodology may be used for the control design of consensus protocols for more complex and meaningful scenarios of cooperative multi-agent systems, such as the rendezvous problem of underactuated UAVs with inter-agent constraints.

On underactuated UAVs. Relying on the solution to the robust consensus problem under output constraints of high-order systems, we address a relevant problem to the aerospace industry, the robust rendezvous control problem of cooperative thrust-propelled UAVs. Much as in the cases of low- and high-order systems, the originality of our contributions is to establish strong stability and robustness properties for the problem of rendezvous of multiple UAVs interconnected over both undirected and directed topologies, and under realistic conditions, mainly external disturbances, connectivity maintenance, and collision avoidance. The latter conditions are more representative of the constraints most often encountered in realistic applications than those considered in the literature, where most of the works consider only undirected topologies or constraints in terms of the consensus errors and not in terms of the individual inter-agent distances. We validated the performance of the proposed controllers via numerical examples and experimental setups.

FURTHER RESEARCH

The contributions presented in this thesis successfully addressed some of the most relevant technical challenges in the cooperative control of multi-agent systems, mainly nonlinear agent dynamics and interconnections as well as robustness of the systems under the action of the proposed control algorithms. Nonetheless, there are still numerous open problems yet to be addressed that constitute directions in which further research may be carried out. Some of these problems that arise directly from the contributions presented in this thesis are as follows.

General directed topologies. One of the original contributions of our work, for some of the studied systems such as the underactuated UAVs, is to solve the consensus problem under constraints for systems interacting over directed topologies. However, we stress that the results obtained in this thesis only apply to two directed topologies: directed spanning trees and directed cycles —*cf.* Remark 3.4. Both of these directed topologies are interesting on their own since they represent, respectively, the relevant leader-follower and cyclic-pursuit problems encountered in practice. Nonetheless, in sensor-based applications, other more general topologies may naturally arise. Therefore, an interesting direction of research is to

study the consensus problem under inter-agent constraints in the edge-based perspective for general directed topologies. Although strong stability and robustness properties for consensus over general directed graphs have already been obtained in the literature —see [7] and Chapter 2— the same cannot be said in the case of nonlinear interconnections and inter-agent constraints. A possible start point for considering more general directed topologies may be the work of [7] where it is shown that the in-incidence matrix of an acyclic directed graph may be expressed using the in-incidence matrix of a directed spanning tree, as is the case for the incidence matrix —see the identity (2.48) in Chapter 2.

All-to-all collision and obstacle avoidance. We mentioned in Chapter 4 that for nonholonomic vehicles, the full consensus problem under range and field-of-view constraints with collision-avoidance guarantees via smooth time-invariant feedback is still an open problem. On the contrary, in the case of high-order systems and underactuated UAVs, in Chapters 5 and 6, respectively, we addressed consensus-based problems with inter-agent collision avoidance. However, since we adopt a local strategy for dealing with the inter-agent constraints, only the potential collisions with *connected* agents are avoided. Yet, in realistic scenarios collisions have to be avoided with *all* the agents composing the system in order to guarantee its safety. Moreover, the system may evolve in cluttered or dynamic environments, where the agents have to successfully avoid collisions with static and dynamic, uncooperative or even antagonistic, obstacles. There is a vast amount of literature addressing the problem of navigation with obstacle avoidance for robotic systems, however few works solve this problem in the multi-agent setting and even less considering, simultaneously, other constraints, nonlinear dynamics, or external disturbances. An interesting tool that may help to extend the results of this thesis to include obstacle avoidance and take advantage of the edge-based perspective is bipartite consensus over signed networks encoding antagonistic interactions —see *e.g.*, [142], [143]. Moreover, the multi-stability properties established in this thesis may be used ensure obstacle avoidance using strategies based on limit cycles as in [144]. From another perspective, instead of considering the non-connected agents as non-collaborative obstacles to avoid, the all-to-all collision-avoidance problem may be solved cooperatively using global strategies based on the algebraic properties of the graph —see *e.g.*, [101]— or using local approaches coupled with an edge-addition/removal strategy.

Impulsive topologies and open networks. In a sensor-based approach, where it is considered that the agents have no way of communicating with their neighbors but rely exclusively on the embedded sensors in order to interact with each other and achieve the cooperative tasks, it is natural to imagine that interconnections may be created or deleted as the agents enter or leave, respectively, the sensing zones of their neighbors. Moreover, in some cases, agents may leave the systems or new agents may be added to the topology, resulting, again, in the creation or deletion of interconnections. Such edge addition and removal, in the edge coordinates, leads to a switched system where the dimension of the state may vary at every switching instant. Hence, the system has to be studied from the approach of *hybrid* and *impulsive* systems. In this context, the edge-based perspective is well suited to the control of such hybrid systems where the stability analysis requires strict Lyapunov

functions for the continuous-time dynamics —see, *e.g.*, [145]. Hence, the importance of our contributions.

Tracking. Another meaningful extension of the work presented in this thesis is to address the problem of collaborative tracking in formation under inter-agent constraints. Indeed, it is natural to imagine that besides the rendezvous objective, the agents may need to follow a predetermined trajectory that may come, *e.g.*, from a planning algorithm, an optimization strategy, or the motion of a target of interest. In the case of nonholonomic vehicles, the set-point stabilization and the tracking problems are fundamentally different. Therefore, exploring the adaptation of the polar-coordinates-based system and of the proposed controllers to the problem of tracking in formation is an interesting research direction, based on the input-to-state stability properties established in Chapter 4. In the case of underactuated UAVs, the practical-input-to-state stability properties established in Chapter 6, coupled with some well-known results such as, *e.g.*, passivity-based [140] or disturbance rejection [141] strategies, may be used so that the multi-agent system exactly follows a desired trajectory. A preliminary result in this direction is presented in [146] where, based on the stability and robustness properties established in Chapter 3 for the constrained-consensus problem and on a disturbance rejection strategy, we solve the tracking-in-formation problem applied to a system of multiple underactuated Unmanned Marine Vehicles.

A

MATHEMATICAL APPENDICES

A.1 LYAPUNOV FUNCTIONS AND LYAPUNOV CHARACTERIZATION

Definition A.1. *Let $x = 0$ be an equilibrium point for $\dot{x} = f(x)$, where $f : \mathbb{R}^n \to \mathbb{R}^n$, and $\mathcal{A} \in \mathbb{R}^n$ be a domain containing $x = 0$. Then, a continuously differentiable function $V : \mathcal{A} \to \mathbb{R}_{\geq 0}$, such that*

$$V(0) = 0 \quad \text{and} \quad V(x) > 0 \quad \text{in} \quad \mathcal{A}\backslash\{0\} \tag{A.1}$$

$$\dot{V}(x) \leq 0 \quad \text{in} \quad \mathcal{A} \tag{A.2}$$

is called a Lyapunov function for the system $\dot{x} = f(x)$. Moreover, if

$$\dot{V}(x) < 0 \quad \text{in} \quad \mathcal{A} \tag{A.3}$$

we say that V is a strict Lyapunov function for the system $\dot{x} = f(x)$. □

Consider the general nonlinear system with inputs:

$$\dot{x} = f(x, u) \tag{A.4}$$

where $f : \mathbb{R}^n \times \mathbb{R}^m \to \mathbb{R}^n$ is continuously differentiable and satisfies $f(0, 0) = 0$.

Definition A.2 ([147])**.** *The system (A.4) is input-to-state-stable if there exist a class $\mathcal{KL}$ function β and a class $\mathcal{K}$ function γ such that, for each input $u \in \mathcal{L}_\infty$ and each $x_0 := x(0) \in \mathbb{R}^n$, it holds that*

$$|x(t, x_0, u)| \leq \beta(|x_0|, t) + \gamma(||u||) \tag{A.5}$$

for each $t \geq 0$. □

Definition A.3 ([147])**.** *A smooth function $V : \mathbb{R}^n \to \mathbb{R}_{\geq 0}$ is called an ISS-Lyapunov function for system (A.4) if there exists class $\mathcal{K}_\infty$ functions α_1, α_2, and class $\mathcal{K}$ functions α_3 and χ, such that*

$$\alpha_1(|x|) \leq V(x) \leq \alpha_2(|x|) \tag{A.6}$$

$$\frac{\partial V(x)}{\partial x}^\top f(x, u) \leq -\alpha_3(|x|) \tag{A.7}$$

for any $x \in \mathbb{R}^n$ and any $u \in \mathbb{R}^m$ so that $|x| \geq \chi(|u|)$. □

Lemma A.1 ([147])**.** *If system (A.4) admits an ISS-Lyapunov function, then it is input-to-state stable.* □

A.2 WEIGHT RECENTERED BARRIER FUNCTION

Definition A.4. *Let $B : \mathcal{P} \to \mathbb{R}$, $x \mapsto B$, be a convex function on an open convex set $\mathcal{P}$. The function B is called a barrier function if it holds that*

$$B(x) \to \infty \quad as \quad x \to \partial\mathcal{P}, \tag{A.8}$$

where $\partial\mathcal{P}$ denotes the boundary of $\mathcal{P}$. □

Definition A.5. *Let $B_i : \mathcal{P} \to \mathbb{R}$, $x \mapsto B_i$, be a convex barrier function on an open convex set $\mathcal{P}_i$ with $0 \in \mathcal{P}_i$, $i \leq q$. Let $\mathcal{P} := \bigcap_{i=1}^{q} \mathcal{P}_i$. Then, the strictly convex function $\tilde{B} : \mathcal{P} \to \mathbb{R}_{\geq 0}$ given as*

$$\tilde{B}(x) = \sum_{i=1}^{q} \kappa_i \left[B_i(x) - B_i(0)\right] \tag{A.9}$$

with $\kappa_i > 0$ such that $\nabla\tilde{B}(0) = \sum_{i=1}^{q} \kappa_i \nabla B_i(0) = 0$ defines a weight recentered barrier function around the origin. □

A.3 CRITICAL POINTS OF THE RECENTERED BARRIER LYAPUNOV FUNCTION

The gradient of the barrier Lyapunov function (6.27) may be written as

$$\nabla W_k(\tilde{z}_k) := \frac{\partial W_k(\tilde{z}_k)}{\partial \tilde{z}_k} = \phi_k(\tilde{z}_k + z_k^d)\left[\tilde{z}_k + z_k^d\right] - z_k^d, \tag{A.10}$$

where

$$\phi_k(s_k) = 1 + \frac{\kappa_{1,k}}{\Delta_k^2 - |s_k|^2} - \frac{\kappa_{2,k}\delta_k^2}{|s_k|^2(|s_k|^2 - \delta_k^2)}. \tag{A.11}$$

Then the Hessian of the barrier Lyapunov function reads

$$\begin{aligned} \mathcal{H}_k(\tilde{z}_k) :=& \frac{\partial}{\partial \tilde{z}_k}\left[\nabla W_k(\tilde{z}_k)\right] \\ =& \phi_k(\tilde{z}_k + z_k^d) I_N + 2\tilde{\phi}_k(\tilde{z}_k + z_k^d)\left[\tilde{z}_k + z_k^d\right]\left[\tilde{z}_k + z_k^d\right]^\top \end{aligned} \tag{A.12}$$

where

$$\tilde{\phi}_k(s_k) := \frac{\kappa_{1,k}}{\left(\Delta_k^2 - |s_k|^2\right)^2} + \frac{\kappa_{2,k}}{\left(|s_k|^2 - \delta_k^2\right)^2} - \frac{\kappa_{2,k}}{|s_k|^4}. \tag{A.13}$$

From a straightforward computation, we see that the eigenvalues of $\mathcal{H}_k(\tilde{z}_k)$ are

$$\lambda_{i,k}(\tilde{z}_k) = \phi_k(\tilde{z}_k + z_k^d), \quad i \in \{1, \ldots, n-1\} \tag{A.14a}$$

$$\lambda_{n,k}(\tilde{z}_k) = \phi_k(\tilde{z}_k + z_k^d) + 2\tilde{\phi}_k(\tilde{z}_k + z_k^d)|\tilde{z}_k + z_k^d|^2. \tag{A.14b}$$

To show that $\tilde{z}_k^*$ is a saddle point it suffices to prove that at least one of these eigenvalues is negative. From (A.11), (A.13), and (6.28), it follows that for all $\delta_k < |\tilde{z}_k + z_k^d| < \Delta_k$,

$$\phi_k(s_k) + 2\tilde{\phi}_k(s_k)|s_k|^2 = 1 + \frac{\kappa_{1,k}(\Delta_k^2 + |s_k|^2)}{(\Delta_k^2 - |s_k|^2)^2} + \frac{\kappa_{2,k}\delta_k^2(3|s_k|^2 - \delta_k^2)}{|s_k|^2(|s_k|^2 - \delta_k^2)^2} > 1. \tag{A.15}$$

Hence, we show that $\lambda_{i,k}(\tilde{z}_k^*) = \phi_k(\tilde{z}_k^* + z_k^d) < 0$. To that end, note that from (A.10), since $\tilde{z}_k^*$ is a singular point of W_k,

$$\phi_k(\tilde{z}_k^* + z_k^d)\left[\tilde{z}_k^* + z_k^d\right] = z_k^d. \tag{A.16}$$

Now, since $\delta_k < |\tilde{z}_k^* + z_k^d| < \Delta_k$, we have $\left[\tilde{z}_k^* + z_k^d\right] \neq 0$. Also, $z_k^d \neq 0$. Therefore, $\varrho_k(\tilde{z}_k^* + z_k^d) \neq 0$. It follows that $\left[\tilde{z}_k^* + z_k^d\right] =: z_k^*$, which is the critical point expressed in the original relative-position coordinates, is aligned with z_k^d. Furthermore, for each $k \leq M$ the barrier-Lyapunov function W_k may possess only two singular points belonging to $\{z_k \in \mathbb{R}^n : \delta_k < |z_k| < \Delta_k\}$, but these must have opposite sign. Consequently, there exists $a > 0$ such that $z_k^* = -a\, z_k^d$ or, equivalently,

$$\phi_k(z_k^*) = -\frac{1}{a} < 0, \tag{A.17}$$

as required.

On the other hand, we have from (A.11) that $\phi_k(z_k^d) = 1$, so from (A.14), we can conclude that z_k^d is a minimum.

A.4 STABILITY OF MULTIPLE INVARIANT SETS

The following result on practical input-to-state stability of multi-stable systems is adapted from [124, Theorem 2] to the notation used in this thesis.

Theorem A.1. *Consider a singularly perturbed system of the form (5.31). Assume that:*

1. *the reduced system (5.32) is input-to-state stable with respect to an acyclic $\mathcal{W}$-limit set $\mathcal{W}_\Theta$ and an input θ;*
2. *the equilibrium $\tilde{\alpha} = 0$ of the boundary layer system (5.33) is globally asymptotically stable.*

Then, there exist a class $\mathcal{KL}$ function β_α and a class $\mathcal{K}_\infty$ function η_θ and, for any pair d_1, $d_2 > 0$, there exists an $\epsilon^* > 0$ such that, for any $\epsilon \in (0, \epsilon^*]$, any essentially bounded function $\theta(t)$, and any initial condition $\xi(0) \in \mathcal{D}_t \times \mathbb{R}^{nN(\rho-1)}$, and $\max\{|\xi(0)|_{\mathcal{W}_\Theta}, |\tilde{\alpha}(0)|, \|\theta\|_\infty, \|\dot{\theta}\|_\infty\} \leq d_1$, it holds that

$$\limsup_{t \to +\infty} |\xi(t)|_{\mathcal{W}_\Theta} \leq \eta_\theta(\|\theta\|_\infty) + d_2 \tag{A.18a}$$

$$|\tilde{\alpha}(t)| \leq \beta_\alpha\left(|\tilde{\alpha}(0)|, \frac{t}{\epsilon}\right) + d_2. \quad \forall t \geq 0 \tag{A.18b}$$

□

For completeness we include the following elements on input-to-state multi-stability adapted, respectively, from [123, Definition 2.7] and [123, Theorem 2.8].

Definition A.6. *A $\mathcal{C}^1$ function $V : \mathcal{M} \to \mathbb{R}_{\geq 0}$ is a practical ISS-Lyapunov function for a system $\dot{x} = f(x, \theta)$ if there exist $\mathcal{K}_\infty$ functions η_1, η, γ and $q \geq 0$ such that, for all $x \in \mathcal{M}$ and all θ, the following holds:*

$$\begin{aligned} \eta_1(|x|_{\mathcal{W}}) \leq & V(x) \\ \nabla V(x)^\top f(x, \theta) \leq & -\eta(|x|_{\mathcal{W}}) + \gamma(|\theta|) + q. \end{aligned} \tag{A.19}$$

If (A.19) holds with $q = 0$, then V is said to be an ISS-Lyapunov function. □

Theorem A.2. *Consider a system $\dot{x} = f(x, \theta)$ and an acyclic $\mathcal{W}$-limit set $\mathcal{W}$. Then, system $\dot{x} = f(x, \theta)$ is input-to-state stable with respect to input θ and to the set $\mathcal{W}$ if and only if it admits an ISS-Lyapunov function.* □

BIBLIOGRAPHY

[1] M. Mesbahi and M. Egerstedt, *Graph theoretic methods in multiagent networks*, ser. Princeton series in applied mathematics. Princeton: Princeton University Press, 2010, OCLC: ocn466341412.

[2] Y. Guo, *Distributed cooperative control: emerging applications*. John Wiley & Sons, 2017.

[3] W. Ren and R. Beard, *Distributed Consensus in Multi-vehicle Cooperative Control: Theory and Applications*, 1st. Springer Publishing Company, Incorporated, 2010.

[4] F. Chen, W. Ren, *et al.*, "On the control of multi-agent systems: A survey," *Foundations and Trends® in Systems and Control*, vol. 6, no. 4, pp. 339–499, 2019.

[5] S. Zhao, "Affine formation maneuver control of multiagent systems," *IEEE Transactions on Automatic Control*, vol. 63, no. 12, pp. 4140–4155, 2018.

[6] R. Olfati-Saber, J. A. Fax, and R. M. Murray, "Consensus and cooperation in networked multi-agent systems," *Proc. IEEE*, vol. 95, no. 1, pp. 215–233, Jan. 2007.

[7] D. Mukherjee and D. Zelazo, "Robustness of consensus over weighted digraphs," *IEEE Transactions on Network Science and Engineering*, vol. 6, no. 4, pp. 657–670, 2019.

[8] D. Dimarogonas and K. Kyriakopoulos, "On the rendezvous problem for multiple nonholonomic agents," *IEEE Transactions Automatic Control*, vol. 52, no. 5, pp. 916–922, May 2007.

[9] A. Dong and J. A. Farrell, "Cooperative control of multiple nonholonomic mobile agents," *IEEE Transactions on Automatic Control*, vol. 53, no. 6, pp. 1434–1447, 2008.

[10] C. P. Bechlioulis and K. J. Kyriakopoulos, "Robust model-free formation control with prescribed performance and connectivity maintenance for nonlinear multi-agent systems," *53rd IEEE Conference on Decision and Control*, 2014, pp. 4509–4514.

[11] A. Nikou, C. K. Verginis, and D. V. Dimarogonas, "Robust distance-based formation control of multiple rigid bodies with orientation alignment," *IFAC-PapersOnLine*, vol. 50, no. 1, pp. 15458 –15 463, 2017, 20th IFAC World Congress.

[12] W. Ren and R. W. Beard, "Consensus seeking in multiagent systems under dynamically changing interaction topologies," *IEEE Transactions on Automatic Control*, vol. 50, no. 5, pp. 655–661, 2005.

[13] D. H. Nguyen, T. Narikiyo, and M. Kawanishi, "Robust consensus analysis and design under relative state constraints or uncertainties," *IEEE Transactions Automatic Control*, vol. 63, no. 6, pp. 1784–1790, 2018.

[14] V. T. Pham, N. Messai, D. H. Nguyen, and N. Manamanni, "Robust formation control under state constraints of multi-agent systems in clustered networks," *Systems & Control Letters*, vol. 140, p. 104 689, 2020.

[15] G. Wang, C. Wang, and X. Cai, "Consensus control of output-constrained multiagent systems with unknown control directions under a directed graph," *International Journal of Robust and Nonlinear Control*, vol. 30, no. 5, pp. 1802–1818, 2020.

[16] J. P. LaSalle, "Stability theory and invariance principles," *Dynamical systems*, Elsevier, 1976, pp. 211–222.

[17] H. K. Khalil, *Nonlinear systems; 2nd ed.* Upper Saddle River, NJ: Prentice-Hall, 1996.

[18] M. Malisoff and F. Mazenc, *Constructions of strict Lyapunov functions*. Springer Science & Business Media, 2009.

[19] K. Liu, G. Xie, W. Ren, and L. Wang, "Consensus for multi-agent systems with inherent nonlinear dynamics under directed topologies," *Systems & Control Letters*, vol. 62, no. 2, pp. 152–162, 2013.

[20] E. Panteley and A. Loría, "Synchronization and Dynamic Consensus of Heterogeneous Networked Systems," *IEEE Transactions Automatic Control*, vol. 62, no. 8, pp. 3758–3773, Aug. 2017.

[21] D. Zelazo, A. Rahmani, and M. Mesbahi, "Agreement via the edge Laplacian," *46th IEEE Conference on Decision and Control*, New Orleans, LA, USA, 2007, pp. 2309–2314.

[22] Z. Zeng, X. Wang, and Z. Zheng, "Nonlinear consensus under directed graph via the edge Laplacian," *The 26th Chinese Control and Decision Conference (2014 CCDC)*, Changsha, China: IEEE, May 2014, pp. 881–886.

[23] D. Zelazo and M. Mesbahi, "Edge Agreement: Graph-Theoretic Performance Bounds and Passivity Analysis," *IEEE Transactions Automatic Control*, vol. 56, no. 3, pp. 544–555, Mar. 2011.

[24] Z. Zeng, X. Wang, and Z. Zheng, "Convergence Analysis using the Edge Laplacian: Robust Consensus of Nonlinear Multi-agent Systems via ISS Method," *International Journal of Robust and Nonlinear Control*, vol. 26, no. 5, pp. 1051–1072, 2016.

[25] Z. Zeng, X. Wang, Z. Zheng, and L. Zhao, "Edge agreement of second-order multi-agent system with dynamic quantization via the directed edge Laplacian," *Nonlinear Analysis: Hybrid Systems*, vol. 23, pp. 1–10, Feb. 2017.

[26] Y. Zhao, Y. Liu, G. Wen, W. Ren, and G. Chen, "Edge-based finite-time protocol analysis with final consensus value and settling time estimations," *IEEE Transactions on Cybernetics*, vol. 50, no. 4, pp. 1450–1459, 2020.

[27] P. Mukherjee, A. Gasparri, and R. K. Williams, "Stable motion and distributed topology control for multi-agent systems with directed interactions," *2017 IEEE 56th Annual Conference on Decision and Control (CDC)*, Melbourne, VIC: IEEE, Dec. 2017, pp. 3455–3460.

[28] J. Fu, G. Wen, Y. Lv, and T. Huang, "Barrier function based consensus of high-order nonlinear multi-agent systems with state constraints," *International Conference on Neural Information Processing*, Springer, vol. 11954, 2019, pp. 492–503.

[29] Y.-H. Lim and H.-S. Ahn, "Consensus under saturation constraints in interconnection states," *IEEE Transactions on Automatic Control*, vol. 60, no. 11, pp. 3053–3058, 2015.

[30] E. Rimon and D. E. Koditschek, "Exact robot navigation using artificial potential functions," *IEEE Transactions on Robotics and Automation*, vol. 8, no. 5, pp. 501–518, Oct. 1992.

[31] C. K. Verginis, A. Nikou, and D. V. Dimarogonas, "Robust formation control in SE(3) for tree-graph structures with prescribed transient and steady state performance," *Automatica*, vol. 103, pp. 538 –548, 2019.

[32] D. Panagou, D. M. Stipanovic, and P. G. Voulgaris, "Distributed coordination control for multi-robot networks using Lyapunov-like barrier functions," *IEEE Transactions on Automatic Control*, vol. 61, no. 3, pp. 617–632, Mar. 2016.

[33] M. Ji and M. Egerstedt, "Distributed coordination control of multiagent systems while preserving connectedness," *IEEE Transactions Robot.*, vol. 23, no. 4, pp. 693–703, Aug. 2007.

[34] D. V. Dimarogonas and K. J. Kyriakopoulos, "Connectedness preserving distributed swarm aggregation for multiple kinematic robots," *IEEE Transactions Robot.*, vol. 24, no. 5, pp. 1213–1223, Oct. 2008.

[35] A. Gasparri, L. Sabattini, and G. Ulivi, "Bounded control law for global connectivity maintenance in cooperative multirobot systems," *IEEE Transactions Robot.*, vol. 33, no. 3, pp. 700–717, Jun. 2017.

[36] H. A. Poonawala and M. W. Spong, "Preserving strong connectivity in directed proximity graphs," *IEEE Transactions Automatic Control*, vol. 62, no. 9, pp. 4392–4404, Sep. 2017.

[37] S. J. Yoo, "Error-transformation-based consensus algorithms of multi-agent systems: Connectivity-preserving approach," *International Journal of Systems Science*, vol. 49, no. 4, pp. 692–700, 2018.

[38] C. K. Verginis and D. V. Dimarogonas, "Closed-form barrier functions for multi-agent ellipsoidal systems with uncertain Lagrangian dynamics," *IEEE Control Systems Letters*, vol. 3, no. 3, pp. 727–732, 2019.

[39] C. Sun, G. Hu, X. Lihua, and M. Egerstedt, "Robust finite-time connectivity preserving consensus tracking and formation control for multi-agent systems," *2017 American Control Conference (ACC)*, 2017, pp. 1990–1995.

[40] G. Wen, Z. Duan, H. Su, G. Chen, and W. Yu, "A connectivity-preserving flocking algorithm for multi-agent dynamical systems with bounded potential function," *IET Control Theory & Applications*, vol. 6, no. 6, pp. 813–821, 2012.

[41] Z. Zhou and X. Wang, "Constrained consensus in continuous-time multiagent systems under weighted graph," *IEEE Transactions on Automatic Control*, vol. 63, no. 6, pp. 1776–1783, 2017.

[42] Y. Shang, "Resilient consensus in multi-agent systems with state constraints," *Automatica*, vol. 122, p. 109 288, 2020.

[43] L. Sabattini, C. Secchi, and N. Chopra, "Decentralized Estimation and Control for Preserving the Strong Connectivity of Directed Graphs," *IEEE Transactions Cybern.*, vol. 45, no. 10, pp. 2273–2286, Oct. 2015.

[44] D. Cai, S. Wu, and J. Deng, "Distributed global connectivity maintenance and control of multi-robot networks," *IEEE Access*, vol. 5, pp. 9398–9414, 2017.

[45] D. H. Nguyen, "Reduced-order distributed consensus controller design via edge dynamics," *IEEE Transactions Automatic Control*, vol. 62, no. 1, pp. 475–480, 2017.

[46] Y. Zhao, Y. Liu, G. Wen, W. Ren, and G. Chen, "Edge-based finite-time protocol analysis with final consensus value and settling time estimations," *IEEE Transactions on Cybernetics*, pp. 1–10, 2018.

[47] N. Chowdhury, S. Sukumar, M. Maghenem, and A. Loría, "On the estimation of the consensus rate of convergence in graphs with persistent interconnections," *International Journal of Control*, vol. 91, no. 1, pp. 132–144, 2018.

[48] N. Alvarez-Jarquín and A. Loría, "Consensus under persistent interconnections in a ring topology: A small gain approach," *Proc. Math. Theory of Networks and Systems*, Groningen, The Netherlands, 2014, pp. 524–529.

[49] H. Chu, D. Yue, C. Dou, and L. Chu, "Consensus of multiagent systems with time-varying input delay and relative state saturation constraints," *IEEE Transactions on Systems, Man, and Cybernetics: Systems*, 2020.

[50] A. Bautista-Castillo, C. López-Franco, and E. Nuño, "Consensus-based formation control for multiple nonholonomic robots," *2016 IEEE International Autumn Meeting on Power, Electronics and Computing (ROPEC)*, 2016, pp. 1–6.

[51] K.-C. Cao, B. Jiang, and D. Yue, "Rendezvous of multiple nonholonomic unicycles-based on backstepping," *International Journal of Control*, vol. 91, no. 6, pp. 1271–1283, Jun. 2018.

[52] M. Maghenem, A. Loría, and E. Panteley, "Lyapunov-based formation-tracking control of nonholonomic systems under persistency of excitation," *IFAC-PapersOnLine*, vol. 49, no. 18, pp. 404–409, 2016.

[53] M. Maghenem, A. Bautista, E. Nuño, A. Loría, and E. Panteley, "Consensus of multiagent systems with nonholonomic restrictions via Lyapunov's direct method," *IEEE Control Syst. Lett.*, vol. 3, no. 2, pp. 344–349, Apr. 2019.

[54] R. W. Brockett, "Asymptotic stability and feedback stabilization," *Differential Geometric Control Theory*, Birkhauser, 1983, pp. 181–191.

[55] Z. Lin, B. Francis, and M. Maggiore, "Necessary and sufficient graphical conditions for formation control of unicycles," *IEEE Transactions on Automatic Control*, vol. 50, no. 1, pp. 121–127, 2005.

[56] J. Zhao and G.-P. Liu, "Time-Variant Consensus Tracking Control for Networked Planar Multi-Agent Systems with Non-Holonomic Constraints," *J Syst Sci Complex*, vol. 31, no. 2, pp. 396–418, Apr. 2018.

[57] M. Aicardi, G. Casalino, A. Bicchi, and A. Balestrino, "Closed loop steering of unicycle like vehicles via Lyapunov techniques," *IEEE Robotics and Automation Magazine*, vol. 2, no. 1, pp. 27–35, Mar. 1995.

[58] M. Aicardi, G. Cannata, and G. Casalino, "Cusp-Free, Time-Invariant, 3D Feedback Control Law for a Nonholonomic Floating Robot," *International Journal of Robotics Research*, vol. 20, no. 4, pp. 300–311, Apr. 2001.

[59] H. Tanner, G. Pappas, and V. Kumar, "Leader-to-Formation Stability," *IEEE Transactions Robotics and Automataion*, vol. 20, no. 3, pp. 443–455, Jun. 2004.

[60] A. González, R. Aragüés, G. López-Nicolás, and C. Sagüés, "Stability analysis of nonholonomic multiagent coordinate-free formation control subject to communication delays," *International Journal of Robust and Nonlinear Control*, vol. 28, no. 14, pp. 4121–4138, 2018.

[61] A. Roza, M. Maggiore, and L. Scardovi, "A Smooth Distributed Feedback for Global Rendezvous of Unicycles," *IEEE Transactions Control Netw. Syst.*, vol. 5, no. 1, pp. 640–652, Mar. 2018.

[62] H. A. Poonawala and M. W. Spong, "On maintaining visibility in multi-robot-networks with limited field-of-view sensors," *2017 American Control Conference (ACC)*, 2017, pp. 4983–4988.

[63] M. Santilli, P. Mukherjee, A. Gasparri, and R. K. Williams, "Distributed connectivity maintenance in multi-agent systems with field of view interactions," *2019 American Control Conference (ACC)*, 2019, pp. 766–771.

[64] T. Endo, R. Maeda, and F. Matsuno, "Stability analysis for heterogeneous swarm robots with limited field of view," *2019 12th International Conference on Developments in eSystems Engineering (DeSE)*, 2019, pp. 27–32.

[65] Z. Kan, J. R. Klotz, J. M. Shea, E. A. Doucette, and W. E. Dixon, "Decentralized Rendezvous of Nonholonomic Robots With Sensing and Connectivity Constraints," *Journal of Dynamic Systems, Measurement, and Control*, vol. 139, no. 2, Nov. 2016.

[66] J. Lian, Y. Meng, and L. Li, "Formation Control and Obstacle Avoidance for Multi-Agent Systems Using Barrier Lyapunov Functions," *2018 Eighth International Conference on Information Science and Technology (ICIST)*, 2018, pp. 15–20.

[67] H. Poonawala, A. C. Satici, H. Eckert, and M. W. Spong, "Collision-free formation control with decentralized connectivity preservation for nonholonomic-wheeled mobile robots," *IEEE Transactions on Control of Network Systems*, vol. 2, pp. 122–130, 2015.

[68] I. M. Delimpaltadakis, C. P. Bechlioulis, and K. J. Kyriakopoulos, "Decentralized platooning with obstacle avoidance for car-like vehicles with limited sensing," *IEEE Robotics and Automation Letters*, vol. 3, no. 2, pp. 835–840, 2018.

[69] S.-L. Dai, S. He, X. Chen, and X. Jin, "Adaptive leader–follower formation control of nonholonomic mobile robots with prescribed transient and steady-state performance," *IEEE Transactions on Industrial Informatics*, vol. 16, no. 6, pp. 3662–3671, 2020.

[70] M. Hua, T. Hamel, P. Morin, and C. Samson, "Introduction to feedback control of underactuated VTOL vehicles: A review of basic control design ideas and principles," *IEEE Control Systems Magazine*, vol. 33, no. 1, pp. 61–75, 2013.

[71] D. Lee, "Distributed backstepping control of multiple thrust-propelled vehicles on a balanced graph," *Automatica*, vol. 48, no. 11, pp. 2971 –2977, 2012.

[72] A. Abdessameud, "Formation control of VTOL-UAVs under directed and dynamically-changing topologies," *2019 American Control Conference (ACC)*, 2019, pp. 2042–2047.

[73] S. Bertrand, N. Guénard, T. Hamel, H. Piet-Lahanier, and L. Eck, "A hierarchical controller for miniature VTOL UAVs: Design and stability analysis using singular perturbation theory," *Control Engineering Practice*, vol. 19, no. 10, pp. 1099 –1108, 2011.

[74] Y. Zou and Z. Meng, "Coordinated trajectory tracking of multiple vertical take-off and landing UAVs," *Automatica*, vol. 99, pp. 33 –40, 2019.

[75] Y. Zou, Z. Zhou, X. Dong, and Z. Meng, "Distributed formation control for multiple vertical takeoff and landing UAVs with switching topologies," *IEEE/ASME Transactions on Mechatronics*, vol. 23, no. 4, pp. 1750–1761, 2018.

[76] A. Roza, M. Maggiore, and L. Scardovi, "Local and distributed rendezvous of underactuated rigid bodies," *IEEE Transactions on Automatic Control*, vol. 62, no. 8, pp. 3835–3847, 2017.

[77] H. Wang, "Second-order consensus of networked thrust-propelled vehicles on directed graphs," *IEEE Transactions on Automatic Control*, vol. 61, no. 1, pp. 222–227, 2016.

[78] J. Ghommam, L. F. Luque-Vega, and M. Saad, "Distance-based formation control for quadrotors with collision avoidance via Lyapunov barrier functions," *International Journal of Aerospace Engineering*, 2020.

[79] Y. Zou and Z. Meng, "Distributed hierarchical control for multiple vertical takeoff and landing UAVs with a distance-based network topology," *International Journal of Robust and Nonlinear Control*, vol. 29, no. 9, pp. 2573–2588, 2019.

[80] C. P. Bechlioulis and G. A. Rovithakis, "Prescribed performance adaptive control for multi-input multi-output affine in the control nonlinear systems," *IEEE Transactions on Automatic Control*, vol. 55, no. 5, pp. 1220–1226, 2010.

[81] X. Wang, G. Wang, S. Li, and K. Lu, "Composite sliding-mode consensus algorithms for higher-order multi-agent systems subject to disturbances," *IET Control Theory & Applications*, vol. 14, no. 2, pp. 291–303, 2019.

[82] C.-C. Hua, K. Li, and X.-P. Guan, "Leader-following output consensus for high-order nonlinear multiagent systems," *IEEE Transactions on Automatic Control*, vol. 64, no. 3, pp. 1156–1161, 2018.

[83] H. Rezaee and F. Abdollahi, "Average consensus over high-order multiagent systems," *IEEE Transactions on Automatic Control*, vol. 60, no. 11, pp. 3047–3052, 2015.

[84] Z. Zuo, B. Tian, M. Defoort, and Z. Ding, "Fixed-time consensus tracking for multiagent systems with high-order integrator dynamics," *IEEE Transactions on Automatic Control*, vol. 63, no. 2, pp. 563–570, 2017.

[85] J. Liu, C. Wang, and Y. Xu, "Distributed adaptive output consensus tracking for high-order nonlinear time-varying multi-agent systems with output constraints and actuator faults," *Journal of the Franklin Institute*, vol. 357, no. 2, pp. 1090–1117, 2020.

[86] C. P. Bechlioulis and G. A. Rovithakis, "Decentralized robust synchronization of unknown high order nonlinear multi-agent systems with prescribed transient and steady state performance," *IEEE Transactions on Automatic Control*, vol. 62, no. 1, pp. 123–134, 2016.

[87] R. Merris, "Laplacian matrices of graphs: A survey," *Linear Algebra and its Applications*, vol. 197-198, pp. 143–176, Jan. 1994.

[88] W. Wasow, "On holomorphically similar matrices," *Journal of Mathematical Analysis and Applications*, vol. 4, no. 2, pp. 202–206, 1962.

[89] W. Ren, "On consensus algorithms for double-integrator dynamics," *IEEE Transactions Automatic Control*, vol. 53, no. 6, pp. 1503–1509, Jul. 2008.

[90] K. P. Tee, S. S. Ge, and E. H. Tay, "Barrier Lyapunov functions for the control of output-constrained nonlinear systems," *Automatica*, vol. 45, no. 4, pp. 918–927, 2009.

[91] Z.-L. Tang, P. T. Keng, and W. He, "Tangent barrier Lyapunov functions for the control of output-constrained nonlinear systems," *IFAC Proceedings Volumes*, vol. 46, no. 20, pp. 449–455, 2013.

[92] M. Santilli, P. Mukherjee, A. Gasparri, and R. K. Williams, "Distributed connectivity maintenance in multi-agent systems with field of view interactions," *2019 American Control Conference (ACC)*, 2019, pp. 766–771.

[93] L. Wang, A. Ames, and M. Egerstedt, "Safety barrier certificates for heterogeneous multi-robot systems," *2016 American Control Conference (ACC)*, IEEE, 2016, pp. 5213–5218.

[94] J. Kim and P. K. Khosla, "Real-time obstacle avoidance using harmonic potential functions," *IEEE Transactions on Robotics and Automation*, vol. 8, no. 3, pp. 338–349, Jun. 1992.

[95] C. Vrohidis, P. Vlantis, C. P. Bechlioulis, and K. J. Kyriakopoulos, "Reconfigurable multi-robot coordination with guaranteed convergence in obstacle cluttered environments under local communication," *Autonomous Robots*, vol. 42, no. 4, pp. 853–873, 2018.

[96] L. Consolini, F. Morbidi, D. Prattichizzo, and M. Tosques, "Leader–follower formation control of nonholonomic mobile robots with input constraints," *Automatica*, vol. 44, no. 5, pp. 1343–1349, 2008.

[97] M. Maghenem, A. Loría, and E. Panteley, "Cascades-based leader-follower formation-tracking and stabilization of multiple nonholonomic vehicles," *IEEE Trans. on Automatic Control*, vol. 65, no. 8, pp. 3639–3646, 2020.

[98] J. A. Marshall, M. E. Broucke, and B. A. Francis, "Formations of vehicles in cyclic pursuit," *IEEE Transactions on Automatic Control*, vol. 49, no. 11, pp. 1963–1974, 2004.

[99] M. M. Zavlanos, M. B. Egerstedt, and G. J. Pappas, "Graph-theoretic connectivity control of mobile robot networks," *Proceedings of the IEEE*, vol. 99, no. 9, pp. 1525–1540, 2011.

[100] L. Sabattini, C. Secchi, N. Chopra, and A. Gasparri, "Distributed Control of Multirobot Systems With Global Connectivity Maintenance," *IEEE Transactions Robot.*, vol. 29, no. 5, pp. 1326–1332, Oct. 2013.

[101] P. Robuffo-Giordano, A. Franchi, C. Secchi, and H. H. Bülthoff, "A passivity-based decentralized strategy for generalized connectivity maintenance," *The International Journal of Robotics Research*, vol. 32, no. 3, pp. 299–323, 2013.

[102] K. P. Tee and S. S. Ge, "Control of nonlinear systems with partial state constraints using a barrier Lyapunov function," *International Journal of Control*, vol. 84, no. 12, pp. 2008–2023, 2011.

[103] C. K. Verginis, A. Nikou, and D. V. Dimarogonas, "Position and orientation based formation control of multiple rigid bodies with collision avoidance and connectivity maintenance," *2017 IEEE 56th Annual Conference on Decision and Control (CDC)*, 2017, pp. 411–416.

[104] D. Boskos and D. V. Dimarogonas, "Robustness and invariance of connectivity maintenance control for multiagent systems," *SIAM J. on Control and Optimization*, vol. 55, no. 3, pp. 1887–1914, 2017.

[105] E. Restrepo, A. Loría, I. Sarras, and J. Marzat, "Stability and robustness of edge-agreement-based consensus protocols for undirected proximity graphs," *International Journal of Control*, pp. 1–9, 2020.

[106] E. Restrepo, A. Loría, I. Sarras, and J. Marzat, "Edge-based strict Lyapunov functions for consensus with connectivity preservation over directed graphs," *Automatica*, vol. 132, p. 109 812, 2021.

[107] R. J. Plemmons, "M-matrix characterizations.I—nonsingular M-matrices," *Linear Algebra and its Applications*, vol. 18, no. 2, pp. 175–188, Jan. 1977.

[108] M. Krstic, P. V. Kokotovic, and I. Kanellakopoulos, *Nonlinear and adaptive control design*. John Wiley & Sons, Inc., 1995.

[109] M. Maghenem, A. Loria, and E. Panteley, "A robust δ-persistently exciting controller for formation-agreement stabilization of multiple mobile robots," *2017 American Control Conference (ACC)*, IEEE, 2017, pp. 869–874.

[110] A. Loría, E. Panteley, D. Popovic, and A. R. Teel, "δ-persistency of excitation: A necessary and sufficient condition for uniform attractivity," *Proceedings of the 41st IEEE Conference on Decision and Control, 2002.*, IEEE, vol. 3, 2002, pp. 3506–3511.

[111] T. Hernández, A. Loría, E. Nuño, and E. Panteley, "Consensus-based formation control of nonholonomic robots without velocity measurements," *2020 European Control Conference (ECC)*, IEEE, 2020, pp. 674–679.

[112] M. A. Maghenem, A. Loría, and E. Panteley, "Cascades-based leader–follower formation tracking and stabilization of multiple nonholonomic vehicles," *IEEE Transactions on Automatic Control*, vol. 65, no. 8, pp. 3639–3646, 2019.

[113] K.-C. Cao, B. Jiang, and D. Yue, "Consensus of multiple nonholonomic chained form systems," *Systems & Control Letters*, vol. 72, pp. 61–70, 2014.

[114] A. G. Wills and W. P. Heath, "A recentred barrier for constrained receding horizon control," *Proceedings of the 2002 American Control Conference (IEEE Cat. No.CH37301)*, vol. 5, 2002, pp. 4177–4182.

[115] E. Restrepo, I. Sarras, A. Loría, and J. Marzat, "Leader-follower consensus of unicycle-type vehicles via smooth time-invariant feedback," *2020 European Control Conference (ECC)*, 2020, pp. 917–922.

[116] A. Loría, "From feedback to cascade-interconnected systems: Breaking the loop," *Proc. 47th. IEEE Conf. Decision Contr.*, Cancun, Mex., 2008, pp. 4109–4114.

[117] E. Panteley and A. Loría, "Growth rate conditions for uniform asymptotic stability of cascaded time-varying systems," *Automatica*, vol. 37, no. 3, pp. 453–460, Mar. 2001.

[118] E. Restrepo, A. Loría, I. Sarras, and J. Marzat, "Distributed full-consensus control of multi-robot systems with range and field-of-view constraints," *In Proceedings of the IEEE International Conference on Robotics and Automation*, 2021, To appear.

[119] E. Restrepo, I. Sarras, A. Loría, and J. Marzat, "Leader-follower consensus of unicycle-type vehicles via smooth time-invariant feedback," *In Proceedings of the European Control Conference*, pp. 917–922, 2020.

[120] E. Restrepo, A. Loría, I. Sarras, and J. Marzat, "Leader-follower consensus of unicycles with communication range constraints via smooth time-invariant feedback," *IEEE Control Systems Letters*, vol. 5, no. 2, pp. 737–742, 2021.

[121] J. A. Farrell, M. Polycarpou, and M. Sharma, "Adaptive backstepping with magnitude, rate, and bandwidth constraints: Aircraft longitude control," *Proceedings of the 2003 American Control Conference*, vol. 5, 2003, pp. 3898 –3904.

[122] J. A. Farrell, M. Polycarpou, M. Sharma, and W. Dong, "Command filtered backstepping," *IEEE Transactions on Automatic Control*, vol. 54, no. 6, pp. 1391–1395, 2009.

[123] P. Forni and D. Angeli, "Input-to-state stability for cascade systems with multiple invariant sets," *Systems & Control Letters*, vol. 98, pp. 97–110, 2016.

[124] P. Forni and D. Angeli, "Perturbation theory and singular perturbations for input-to-state multistable systems on manifolds," *IEEE Transactions on Automatic Control*, vol. 64, no. 9, pp. 3555–3570, 2018.

[125] T.-S. Li, D. Wang, G. Feng, and S.-C. Tong, "A DSC approach to robust adaptive NN tracking control for strict-feedback nonlinear systems," *IEEE Transactions on Systems, Man, and Cybernetics, Part B (Cybernetics)*, vol. 40, no. 3, pp. 915–927, 2009.

[126] H. Du, M. Z. Chen, and G. Wen, "Leader–following attitude consensus for spacecraft formation with rigid and flexible spacecraft," *Journal of Guidance, Control, and Dynamics*, vol. 39, no. 4, pp. 944–951, 2016.

[127] E. Nuño, D. Valle, I. Sarras, and L. Basañez, "Leader–follower and leaderless consensus in networks of flexible-joint manipulators," *European Journal of Control*, vol. 20, no. 5, pp. 249–258, 2014.

[128] G. Duan, "High-order fully actuated system approaches: Part II. Generalized strict-feedback systems," *International Journal of Systems Science*, vol. 52, no. 3, pp. 437–454, 2021.

[129] B. Xu, D. Wang, Y. Zhang, and Z. Shi, "DOB-based neural control of flexible hypersonic flight vehicle considering wind effects," *IEEE Transactions on Industrial Electronics*, vol. 64, no. 11, pp. 8676–8685, 2017.

[130] E. Restrepo, A. Loría, I. Sarras, and J. Marzat, "Robust consensus of high-order systems under output constraints: Application to rendezvous of underactuated UAVs," *IEEE Transactions on Automatic Control*, 2021, Submitted as a regular paper in April 2021.

[131] K. P. Tee and S. S. Ge, "Control of state-constrained nonlinear systems using integral barrier Lyapunov functionals," *2012 IEEE 51st IEEE Conference on Decision and Control (CDC)*, IEEE, 2012, pp. 3239–3244.

[132] C. Feller and C. Ebenbauer, "Weight recentered barrier functions and smooth polytopic terminal set formulations for linear model predictive control," *2015 American Control Conference (ACC)*, IEEE, 2015, pp. 1647–1652.

[133] W. Dong, J. A. Farrell, M. M. Polycarpou, V. Djapic, and M. Sharma, "Command filtered adaptive backstepping," *IEEE Transactions on Control Systems Technology*, vol. 20, no. 3, pp. 566–580, 2011.

[134] A. Loría, "Observers are unnecessary for output-feedback control of Lagrangian systems," *IEEE Transactions on Automatic Control*, vol. 61, no. 4, pp. 905–920, 2015.

[135] P. V. Kokotović and H. J. Sussmann, "A positive real condition for global stabilization of nonlinear systems," *Syst. & Contr. Letters*, vol. 13, no. 4, pp. 125–133, 1989.

[136] R. Sepulchre, M. Janković, and P. V. Kokotović, "Recursive designs and feedback passivation," *Systems and control in the twenty-first century*, Springer, 1997, pp. 313–326.

[137] P. Monzón and R. Potrie, "Local and global aspects of almost global stability," *Proceedings of the 45th IEEE Conference on Decision and Control*, IEEE, 2006, pp. 5120–5125.

[138] M. Hua, T. Hamel, P. Morin, and C. Samson, "A control approach for thrust-propelled underactuated vehicles and its application to VTOL drones," *IEEE Transactions on Automatic Control*, vol. 54, no. 8, pp. 1837–1853, 2009.

[139] L. SZ DJI Technology Co. "DJI store." (2021), [Online]. Available: https://store.dji.com/fr/product/tello-edu?vid=47091 (visited on 04/08/2021).

[140] A. Loría, E. Panteley, and H. Nijmeijer, "A remark on passivity-based and discontinuous control of uncertain nonlinear systems," *Automatica*, vol. 37, no. 9, pp. 1481–1487, 2001.

[141] J. Sun, Z. Geng, Y. Lv, Z. Li, and Z. Ding, "Distributed adaptive consensus disturbance rejection for multi-agent systems on directed graphs," *IEEE Transactions on Control of Network Systems*, vol. 5, no. 1, pp. 629–639, 2016.

[142] M. Du, B. Ma, and D. Meng, "Edge convergence problems on signed networks," *IEEE Transactions on Cybernetics*, vol. 49, no. 11, pp. 4029–4041, 2018.

[143] M. E. Valcher and P. Misra, "On the consensus and bipartite consensus in high-order multi-agent dynamical systems with antagonistic interactions," *Systems & Control Letters*, vol. 66, pp. 94–103, 2014.

[144] M. Boldrer, M. Andreetto, S. Divan, L. Palopoli, and D. Fontanelli, "Socially-aware reactive obstacle avoidance strategy based on limit cycle," *IEEE Robotics and Automation Letters*, vol. 5, no. 2, pp. 3251–3258, 2020.

[145] M. Xue, Y. Tang, W. Ren, and F. Qian, "Stability of multi-dimensional switched systems with an application to open multi-agent systems," *arXiv preprint arXiv:2001.00435*, 2020.

[146] E. Restrepo, J. Matouš, and K. Y. Pettersen, "Tracking-in-formation of multiple autonomous marine vehicles under proximity and collision-avoidance constraints," *2022 European Control Conference (ECC)*, 2022, Submitted for presentation.

[147] E. D. Sontag and Y. Wang, "On characterizations of the input-to-state stability property," *Systems & Control Letters*, vol. 24, no. 5, pp. 351 –359, 1995.

université PARIS-SACLAY

ÉCOLE DOCTORALE
Sciences et technologies de l'information et de la communication (STIC)

Titre : Commande en coordination de systèmes multi-agents robotiques autonomes sous contraintes
Mots clés : Fonctions de Lyapunov strictes, systèmes multi-agent, consensus, véhicules autonomes, consensus basé sur les arêtes, contraintes inter-agents

Résumé : Dans cette thèse, nous abordons et résolvons plusieurs problèmes de commande de systèmes multi-agents sous des contraintes multiples. Une partie des contributions consiste à résoudre des problèmes de consensus pour des systèmes linéaires (principalement des intégrateurs de tout ordre) et une autre partie pour des modèles non-linéaires, tels que des véhicules non-holonomes ou des drones autonomes sous-actionnés, en considérant des interconnexions non-linéaires. Ainsi, les problèmes de commande que nous abordons et leur formulation relèvent du domaine de la robotique et plus particulièrement de la commande des véhicules autonomes coopératifs terrestres et aériens.

Concernant les intégrateurs de premier et de second ordre, l'originalité de ce travail consiste à développer une nouvelle analyse de stabilité pour des systèmes multi-agents sous l'action des lois de commande de consensus et avec des contraintes de proximité et des perturbations. En utilisant une représentation basée sur les arêtes nous établissons des propriétés fortes de stabilité et de robustesse, dans le sens de stabilité entrée-sortie, en construisant des fonctions de Lyapunov strictes. Ensuite, nous généralisons les résultats dans deux directions. D'abord, nous développons une méthodologie de commande qui résout le problème de consensus pour des systèmes multi-agents d'ordre élevé sous des contraintes non-linéaires et des perturbations. D'autre part, nous considérons des systèmes robotiques modélisés par des équations dynamiques non-linéaires, soumis à des multiples contraintes et à des perturbations. Dans les deux cas, la stabilité et la robustesse des systèmes en boucle fermée sont établies en utilisant des arguments de l'automatique comme les interconnexions en cascade, les perturbations singulières et la multi-stabilité.

Title : Coordination control of autonomous robotic multi-agent systems under constraints
Keywords : Strict Lyapunov functions, multi-agent systems, consensus, autonomous vehicles, edge-agreement, inter-agent constraints

Abstract : In this thesis we address and solve several concrete problems of control of multi-agent systems under multiple inter-agent constraints. Some of our contributions address problems of consensus for linear systems (primarily integrators of any order) and others solve concrete relevant problems involving nonlinear models, such as nonholonomic vehicles or thrust-propelled underactuated unmanned autonomous vehicles, and considering nonlinear interconnections. Thus, the control problems that we address and their formulation stem from the realm of robotics and more particularly, of control of cooperative autonomous vehicles, both terrestrial and aerial.

Concerning first- and second-order integrators, the originality of this work consists in developing a new stability analysis for multi-agent systems under the action of consensus control algorithms and with proximity constraints and disturbances. Using an edge-based representation of the multi-agent system we establish strong stability and robustness properties, in the sense of asymptotic and input-to-state stability, via the construction of strict Lyapunov functions. Then, we consider generalize these results in two directions. First, we develop a control methodology that solves the consensus problem for multi-agent systems of high-order systems under nonlinear interconnections and disturbances. On the other hand, we consider robotic systems modeled by nonlinear dynamic equations and subject to multiple inter-agent constraints and disturbances. In both cases we establish stability and robustness of the closed-loop systems using arguments from control systems' theory on cascaded interconnections, singular perturbations, and multi-stability.